The copyright of this thesis rests with the University of Cape Town. No quotation from it or information derived from it is to be published without full acknowledgement of the source. The thesis is to be used for private study or non-commercial research purposes only.

University of Cape Town

MOLECULAR BASIS OF INSULIN RESISTANCE INDUCED BY ANTIRETROVIRAL DRUGS

WAN IRYANI WAN ISMAIL

University Of Cape Town

Thesis Presented for the Degree of

DOCTOR OF PHILOSOPHY

in the Division of Chemical Pathology,

Department of Clinical Laboratory Sciences

UNIVERSITY OF CAPE TOWN

June 2010

DECLARATION

The work contained in this thesis is original, except where indicated and acknowledged. No portion of this work has been submitted for another degree at this or any other university.

The University of Cape Town may reproduce the contents in whole or part for the purpose of research.

Wan Iryani Wan Ismail
02 February 2010

University Of Cape Town

ACKNOWLEDGEMENTS

First of all, I would like to take this opportunity to convey my greatest appreciation to my supervisor, Prof. Tahir S. Pillay, and co-supervisor, Dr. Judy A. King, who have guided me throughout this project. I feel very honoured to be their student, and to have the opportunity to discuss and learn in an open but highly academic atmosphere throughout my studying and working with them.

My appreciation also goes to Ingrid, Dave, Abdu, Jeff (MetaboAnalyst, University of Alberta, Canada), Dr. Pete, Dr. Fierdoz, Dr. David, Dr. Chilu, Lisa, Patricia, Baddy, Baldwin, Rayhannah, Cylene, Felicity, Farhana, Assoc. Prof. Denver, Dr. Virna, Dr. Owen, Prof Henderson and Dr. Philip for all the technical help and scientific information while this project was under way. To Dr. George, a special thank you for helping with GC-MS analysis. My colleagues – Nadiaa, Jackson, Khawar, Lauren, Kristen, Gabriel, Nick and Vuyo – for the ups and downs we have shared since I arrived here, thank you so much. And to Luke, Nelusha, Jacque, Pauline, Nana, Adry, Salegha, Hajiera, Mara, Ebrahiem and Bernie, thank you for all your help.

Finally, my special thanks to my beloved husband, Izwandy Idris, and our 'alive and kicking' daughters, Nurul Iffah and Nurul Izzah Natheema (a Capetonian baby!), who make me laugh and give me encouragement. A great honour to my late father, who passed away just I arrived in Cape Town. Though I missed giving you a last kiss, your undying soul always inspires me to love knowledge, the most valuable legacy in my life. My mom, who prays for my success and happiness, my parents-in-law, who continuously support me, and all my family and friends for your help, thank you so much – I really love you all.

My education at the University of Cape Town was sponsored through the Young Lecturer Scheme under Universiti Teknologi MARA and the Ministry of Higher Education of Malaysia. Laboratory work was funded by the National Research Foundation and the National Health Laboratory Service of the Republic of South Africa.

Thank you, shukran, baie dankie and trimakassie…

Wan
2006-2010

University of Cape Town

TABLE OF CONTENTS

University Of Cape Town

University Of Cape Town

University Of Cape Town

University Of Cape Town

University Of Cape Town

LIST OF FIGURES

University of Cape Town

University Of Cape Town

University Of Cape Town

University of Cape Town

LIST OF TABLES

University of Cape Town

ABBREVIATIONS

aPKC	atypical PKC
AIDS	acquired immune deficiency syndrome
APS	adapter proteins with a pleckstrin homology domain and an SH2 domain
APS	ammonium persulphate
ARV	antiretroviral
BPB	bromophenol blue
BSA	bovine serum albumin
BSTFA	bis-(trimethylsilyl)trifluoroacetamide
cPKC	classical PKC
cAMP	cyclic adenosine monophosphate
CCR5	chemokine co-receptor 5
CIM	coefficient-based importance measure
CHO-IR	Chinese hamster ovary transfected with high levels of human insulin receptor
CO_2	carbon dioxide
CXCR4	CXC chemokine co-receptor 4
dH2O	deionised water
DMEM	Dulbecco's modified Eagle's medium
DMSO	dimethyl sulphoxide
DNA	deoxyribonucleic acid
ER	endoplasmic reticulum
FC	fold change
FCS	foetal calf serum
FDA	Food and Drug administration
FDR	false discovery rate
FFA	free fatty acid
FPDL	Dunning-type familial partial lipodystrophy
G418-sulphate	geneticin
GC-MS	gas chromatography mass spectrometry
GLUT4	glucose transporter 4
gp41	glycoprotein 41
gp120	glycoprotein 120
HAART	highly active antiretroviral therapy
HDL	high density lipoprotein

University Of Cape Town

HEPES	4-(2-hydroxyethyl)-1-piperazineethanesulfonic acid
HIV	human immunodeficiency virus
HRP	horseradish peroxidase
IBMX	3-isobutyl-1-methyl-xanthine
IC_{50}	50 % inhibition concentration
IGF	insulin growth factor
IκB	inhibitor κB
IKKβ	IκB kinase β
IRS-1	insulin receptor substrate-1
IRS-2	insulin receptor substrate-2
JNK	Jun kinase
JNK-1	Jun kinase 1
LPL	lipoprotein lipase
MAM	mitochondria-associated ER membrane
MAPK	mitogen-activated protein kinase (aka extracellular-signal regulated kinase or ERK)
mTOR	mammalian target of rapamycin
mTORC1	mTOR complex 1
nPKC	novel PKC
NaCl	sodium chloride
NCS	newborn calf serum
NFκB	nuclear factor kappa B
NNRTIs	non-nucleotide reverse transcriptase inhibitors
NP40	phenoxylpolyethoxylethanol or Nonidet
NRTIs	nucleoside reverse transcriptase inhibitors
pIRS	phosphorylated IRS
PAI-1	plasminogen activator inhibitor 1
PBS	phosphate buffered saline
PDA	pentadecanoate
PDK	PIP_3-dependent protein kinase
PI3K	phosphoinositide 3-kinase
PIP_2	phosphatidylinositol 4,5-biphosphate
PIP_3	phosphatidylinositol 3,4,5-triphosphate
PKB	protein kinase B
PKC	protein kinase C
PLS-DA	partial-least squares discriminant analysis
PMSF	phenylmethylsulphonyl fluoride

University Of Cape Town

PPAR-γ	peroxisome proliferator-activated receptor gamma
PTP1B	protein tyrosine phosphatase 1B
PY20	purified mouse anti-phosphotyrosine antibody
RNS	reactive nitrogen species
ROS	reactive oxygen species
RNA	ribonucleic acid
SAM	significance analysis of microarrays (and metabolites)
SDS	sodium dodecyl sulphate
SDS-PAGE	sodium dodecyl sulphate polyacrylamide gel electrophoresis
SH2B	Src homology 2B
SOCS-1	suppressor of cytokine signaling 1
SOCS-3	suppressor of cytokine signaling 3
SREBP-1	sterol regulatory element binding protein 1
TBST	tris buffered saline + 0.1% tween 20
TEMED	N, N, N', N',-tetra-methyl-ethylenediamine
TNF-α	tumour necrosis factor alpha
Tris	tris(hydroxymethyl)aminomethane
Tris-HCl	tris-hydrochloride
Trypsin-EDTA	trypsin-ethylenediaminetetraacetic acid
Tween 20	polyoxyethylenesorbitan monooleate
TZD	troglitazone
UPR	unfolded protein response
VIP	variable importance in projection
VLDL	very-low-density lipoprotein
*p*NPB	*para*-nitrophenyl butyrate

University of Cape Town

ABSTRACT

Protease inhibitors are thought to be the major antiretroviral drugs involved in various metabolic disorders in HIV-positive patients. The primary side-effect induced by protease inhibitors is insulin resistance. However, the mechanistic basis of this insulin resistance remains largely unknown. Thus, this study was undertaken to understand the molecular basis of insulin resistance induced by protease inhibitors in Chinese hamster ovary cells transfected with high levels of human insulin receptor (CHO-IR cells) and in differentiated 3T3-L1 murine adipocytes.

The most pronounced effect of insulin resistance induced by protease inhibitors is inhibition of insulin-stimulated glucose uptake (the final outcome in the insulin signalling pathway). This effect on glucose uptake may result from inhibition at a proximal level, i.e. insulin-stimulated tyrosine phosphorylation of the insulin receptor β-subunit and insulin receptor substrate 1 (IRS-1). CHO-IR cells and 3T3-L1 adipocytes were treated with the protease inhibitors saquinavir and indinavir, followed by insulin stimulation. Since saquinavir may be toxic to these cells, indinavir was used in further analysis.

It was found for the first time that indinavir significantly inhibited insulin-stimulated tyrosine phosphorylation of the insulin receptor β-subunit and IRS-1. Indinavir also significantly increased serine 307 phosphorylation of IRS-1 in both cell lines. The effects of indinavir were reduced when CHO-IR cells were pre-treated with sodium salicylate. This result suggests that protease inhibitors inhibit insulin receptor tyrosine phosphorylation indirectly, via the nuclear factor kappa B (NFκB) pathway. The NFκB pathway works as a secondary process involving a regulator of tyrosine phosphorylation, specifically the level of phosphorylation of IRS-1 at serine 307. The findings also showed that other phosphotyrosine regulatory proteins investigated in the insulin signalling pathway were not altered and not involved in insulin resistance induced by protease inhibitors.

Metabolomic analysis was performed on free fatty acids (FFAs), amino acids and organic acids in 3T3-L1 adipocytes treated with indinavir. Free fatty acid analysis indicated that the levels of FFAs were not significantly decreased in the treated cell culture supernatants versus the basal medium. Concomitantly, the level of FFA was higher (i.e. had accumulated) in the treated versus the untreated cell culture supernatants. Thus, the protease inhibitors appear to block FFA utilisation. A high

University Of Cape Town

level of FFA is known to induce insulin resistance. FFA may also play a role in inducing insulin resistance via the NFκB pathway, as observed above. Alterations recorded in the levels of amino acids and organic acids may be a secondary effect of insulin insensitivity induced by a high level of FFA. For example, insulin-induced hydroxylysine synthesis in cells pre-treated with indinavir.

A colourimetric assay was established to measure lipoprotein lipase (LPL) activity in supernatants of 3T3-L1 adipocytes after exposure to protease inhibitors. The assay revealed that protease inhibitors significantly decreased LPL activity in the cells and the inhibition profile differed among different drugs.

Taken together, the results of this study suggest that treatment with HIV protease inhibitors inhibits LPL activity and increases the level of FFA. The high level of FFA stimulates the NFκB pathway, which then increases serine 307 phosphorylation of IRS-1. The level of FFA also decreased insulin-stimulated tyrosine phosphorylation of IRS-1 and insulin receptor β-subunit, inducing insulin resistance. Low levels of hydroxylysine and succinate, and high levels of aspartate, butanoic acid acid 3-(trimethylsiloxy)-ethylester and isovalerate, were probably secondary effects found to induce insulin resistance.

University Of Cape Town

CHAPTER 1: GENERAL INTRODUCTION

1.1 Introduction

Twenty-seven years after the association between acquired immune deficiency syndrome (AIDS) and the human immunodeficiency virus (HIV) was first reported, HIV infection remains a major global challenge, especially in the southern part of sub-Saharan Africa. In South Africa, six million people were infected and more than 400 000 had died from AIDS by 2007 (Figure 1.1) (Beyrer, 2007; Larmarange, 2009; Weiss, 2008).

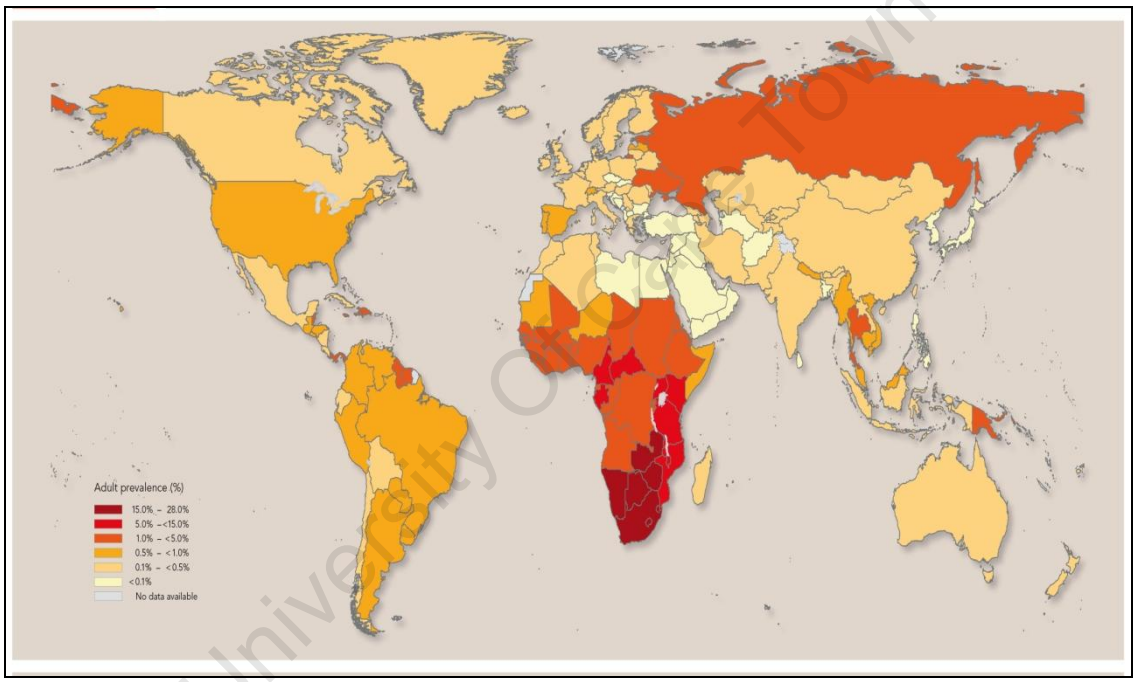

University of Cape Town

Figure 1.1: A global view of HIV infection in 2007 [http://data.unaids.org/pub/GlobalReport/2008/GR08_2007_HIVPrevWallMap_GR08_en.jpg]

Currently, the most potent treatment for AIDS is highly active antiretroviral therapy (HAART). This therapy uses a combination of three or more antiretroviral drugs. These drugs are inhibitors derived from five classes, namely entry inhibitors, nucleoside or nucleotide reverse transcriptase inhibitors (NRTIs), non-nucleotide reverse transcriptase inhibitors (NNRTIs), integrase inhibitors, and protease inhibitors. This treatment may extend the lifespan of HIV-infected patients by suppressing HIV viral load, increasing $CD4^+$ T-cell[1] count[2], and reducing

[1] T-cells or T-helper cells are a subgroup of lymphocytes; a T-cell is a type of white cell which functions to activate other immune cells and express surface protein CD4.

opportunistic infections associated with AIDS (Hammer et al., 1997; Piacenti, 2006). Unfortunately, in addition to improving patient prognosis, these drugs also result in metabolic abnormalities; in particular, insulin resistance accompanied by hyperglycaemia and lipodystrophy[3] (Bernasconi, 1999; Esser et al., 2007). Consequently, patients are also at high risk of developing premature cardiovascular morbidity and type 2 diabetes mellitus (Bozkurt, 2004; Florescu and Kotler, 2007; Friedl et al., 2000; Stein, 2007).

A substantial number of clinical and epidemiological studies have shown that protease inhibitors play a major role in inducing metabolic disorders in HAART-treated patients (Bernasconi, 1999; Carr, 2000; Hui, 2003). It appears that all protease inhibitor compounds induce insulin resistance and lipid abnormalities to various degrees (Young et al., 2005), but the mechanisms of these serious side-effects are largely unknown. In one study, it was found that protease inhibitors impaired insulin-regulated metabolism in adipose tissue to the extent of inducing metabolic disorders (Gougeon et al., 2004).

However, a systematic molecular evaluation of the effects of these drugs on metabolism in fully-differentiated adipocytes has not yet been performed. Only a few studies have reported alterations in insulin signalling and insulin-regulated metabolism caused by protease inhibitors at the cellular level (Ben-Romano et al., 2006; Rudich et al., 2005). It is important to understand the mechanistic basis for these side-effects, as their incidence is likely to increase as the rollout of antiretroviral drugs continues. For this reason, this study was undertaken to further understand the molecular basis of insulin resistance induced by protease inhibitors in a cell culture system.

University of Cape Town

1.2 Human immunodeficiency virus

HIV, particularly HIV-1, is the causative agent of AIDS in HIV-positive patients. This virus is a member of the retrovirus family (Gallo and Reitz, 1985). At present, HAART is the only treatment available for AIDS. In order to understand the mechanisms of action of these antiretroviral drugs, it is essential to know and understand the structure of HIV and its replication cycle (Temesgen et al., 2006).

[2] This figure may be used to detect HIV infection, as HIV targets cells that express $CD4^+$ T-cells and reduces the circulating levels of the cells.
[3] Lipodystrophy is an abnormal redistribution of fat.

1.2.1 HIV morphology

HIV is an enveloped virus that contains a single infectious strand of viral genomic ribonucleic acid (RNA), with some cellular factors and enzymes at its core. The enzymes required for HIV replication are reverse transcriptase, integrase, protease, Vpu, Vif, Vpr and Nef. An HIV virion has a spherical morphology of 100-120 nm diameter, and is surrounded by a lipid bilayer membrane with glycoprotein 120 (gp120). This is anchored to the viral envelope by glycoprotein 41 (gp41) molecules (Sierra et al., 2005; Turner and Summers, 1999) (Figure 1.2).

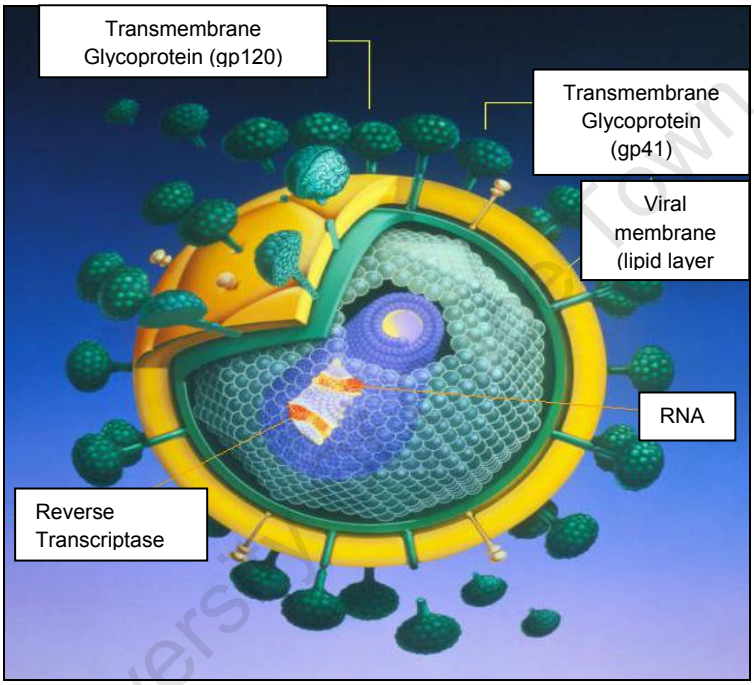

Figure 1.2: HIV structure [www.vircolab.com/.../hiv_virus.gif]

1.2.2 HIV life-cycle and pathogenesis

The initial step in the HIV replication cycle (Figure 1.3) is the interaction between the envelope proteins of the virus, HIV gp 120, and specific host-cell surface receptors such as CD4 receptors, with the presence of co-receptors such as chemokine co-receptor 5 (CCR5)[4] or CXC chemokine co-receptor 4 (CXCR4)[5].

[4] CCR5 is expressed on dendritic cells, macrophages and T-lymphocyte cells.
[5] CXCR4 is expressed on T-lymphocyte cells.

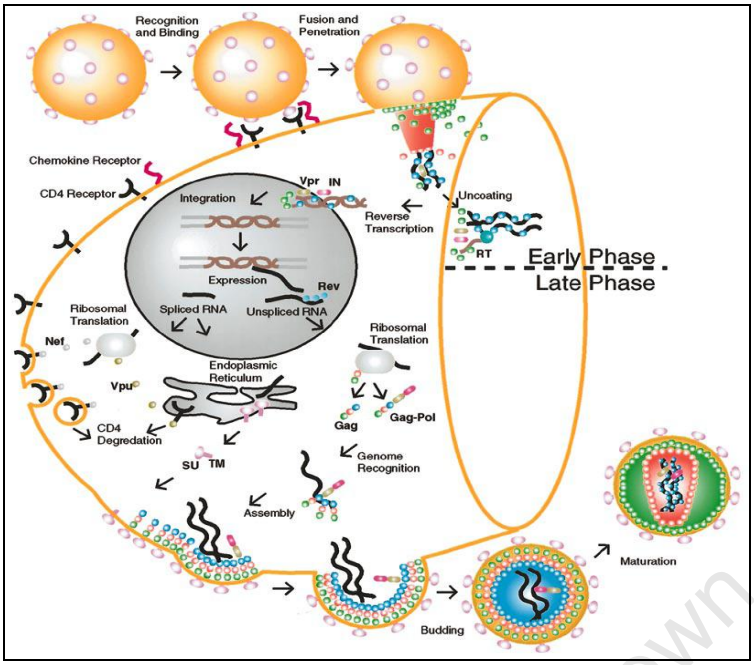

Figure 1.3: HIV-1 replication cycle (Turner and Summers, 1999)

Binding of the HIV to a co-receptor causes conformational changes in the envelope proteins. This leads to the fusion of the viral envelope and the host cytoplasmic membrane, creating a pore through which the viral capsid contents enter the cell. Within the cell, the viral reverse transcriptase enzyme catalyses the conversion of one single-stranded viral RNA into a double-stranded complementary viral deoxyribonucleic acid (DNA). The viral DNA enters the nucleus and integrates with the chromosomal DNA of the host cell, via integrase.

The integration between viral DNA and chromosomal DNA induces the HIV replication process. The $CD4^+$ T-lymphocyte cells produce strands of viral Gag (p55) and Gag-Pol (p160) polyproteins. New HIV virions are produced when a protease, aspartyl endopeptidase, cleaves viral Gag (p55) and Gag-Pol (p160) polyprotein strands. These virions are able to grow to become mature virions and infect other healthy human host cells within 1.5 days (Sierra et al., 2005; Turner and Summers, 1999).

1.3 Highly active antiretroviral therapy

Although HIV was identified in 1983, the use of HAART to treat HIV-positive patients was only introduced in 1996 (Weiss, 2008). This therapy is a combination of three or more antiretroviral drugs, as indicated in Table 1.1.

University Of Cape Town

Table 1.1: FDA-approved antiretroviral drugs in South Africa [http://www.hst.org.za/publications/625]

Antiretroviral drug	Generic name	Product	Manufacturer
Nucleoside/nucleotide reverse transcriptase inhibitors	1. Abacir	Ziagen	GlaxoSmithKline
	2. Didanosine	Videx	Bristol-Myers Squibb
	3. Lamivudine	Epivir	GlaxoSmithKline
	4. Stavudine	Zerit	Bristol-Myers Squibb
	5. Zidovudine	Retrovir	GlaxoSmithKline
	6. Zidovudine/Lamivudine	Combivir	GlaxoSmithKline
Non-nucleoside reverse transcriptase inhibitors	1. Efavirenz	Sustiva	Bristol-Myers Squibb
	2. Nevirapine	Viramune	Boehringer Ingelheim
Protease inhibitors	1. Indinavir	Crixivan	Merck
	2. Ritonavir	Norvir	Abbott Laboratories
	3. Saquinavir	Invirase	Roche
	4. Lopinavir/ritonavir	Kaletra	Abbott Laboratories

University Of Cape Town

1.3.1 HAART treatment

HAART acts to alter and impair the HIV life-cycle. This results in a reduction of the HIV viral load and an increase in $CD4^+$ T-cell counts, and consequently a decrease in opportunistic infections associated with AIDS (Hammer et al., 1997; Piacenti, 2006).

At the early stage of the HIV life-cycle, entry inhibitors (number 1 in Figure 1.4) block the binding of HIV gp 120 to human host CD4 receptors, and prevent the fusion of the viral envelope to the plasma membrane. NRTIs (number 2 in Figure 1.4) are designed to inhibit reverse transcriptase through competition with the natural substrate to decrease the synthesis of viral DNA. The function of NNRTIs (number 2 in Figure 1.4) is to block enzyme activity by binding the natural substrate directly. This causes a conformational change, and disrupts the catalytic site of the enzyme. Integrase inhibitors (number 3 in Figure 1.4) prevent integration of double-stranded

complementary viral DNA into the cell genome. In the final stages of the HIV life-cycle, protease inhibitors (number 6 in Figure 1.4) prevent HIV protease from producing infectious viral particles (Figure 1.4) (Bailey and Fisher, 2008).

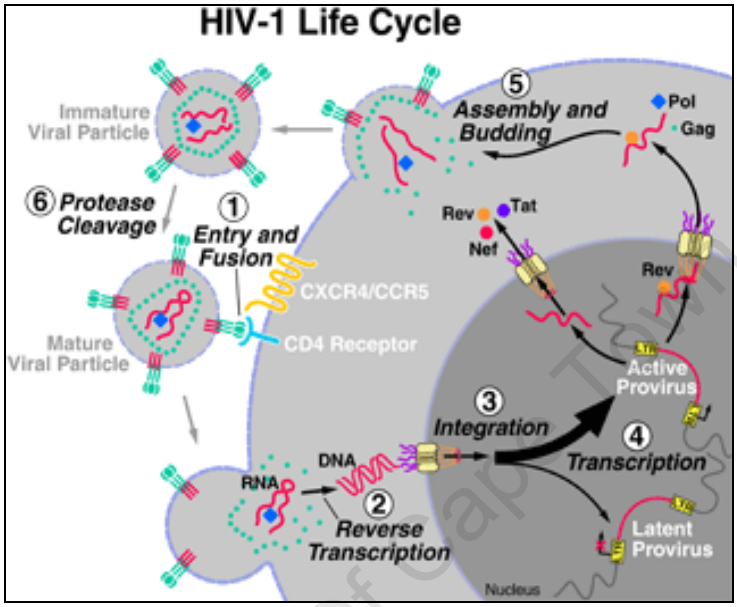

Figure 1.4: HAART targets in the HIV life-cycle
[www.gladstone.ucsf.edu/.../section.php?id=1707]

1.3.2 Effects of HAART

Following the introduction of HAART as a treatment for AIDS in 1996, HIV-associated morbidity and mortality have decreased significantly (Palella et al., 1998; Quinn, 2008). Unfortunately, though HAART lengthened the lifespan of HIV-positive patients, more than 60 % of patients treated using HAART developed various metabolic disorders, such as insulin resistance accompanied by lipodystrophy and atherosclerosis (Monier and Wilcox, 2004). Protease inhibitors play the major role in causing these adverse effects (Barbaro and Barbarini, 2006; Bernasconi, 1999; Carr, 2000; Hui, 2003).

1.4 Protease inhibitors

The management of AIDS underwent a dramatic change in 1996, when HIV-positive patients were first introduced to saquinavir, the first protease inhibitor (Palella et al., 1998; Quinn, 2008). Protease inhibitors are potent competitive inhibitors of HIV

University of Cape Town

aspartyl endopeptidase, an enzyme required for normal processing of the Gag and Gag-Pol HIV proteins (Flexner, 1998).

Protease inhibitors bind to the HIV protease active site which contains two flap domains, two core domains and a terminal domain. The domains accommodate the ligand binding as an induced fit mechanism (Rose *et al*., 1998). The protease inhibitor binding prevents interaction of the enzyme with its substrate. The substrate contains a recognition motif i.e. a polypeptide between phenylalanine, or tyrosine, and proline. The lack of cleavage produces immature virions (Figure 1.5) (Temesgen et al., 2006). This cleavage, specifically N-terminal of proline, is considered to be rare in mammals. Therefore, inhibition of the cleavage does not impact significantly on the mammalian host, as mammalian proteases do not display such cleavage preferences (Schmidtke et al., 1999).

Protease inhibitors are active against clinical isolates of HIV-1 *in vitro* with an IC_{50} ranging from 2 to 60 nM. Simultaneously, they are inactive or weakly active (IC_{50} > 10 000 nM) against the human aspartyl proteases, renin and pepsin (Flexner, 1998).

It has emerged that all protease inhibitors play a critical role in inducing various side-effects (Table 1.2) (Temesgen et al., 2006).

University Of Cape Town

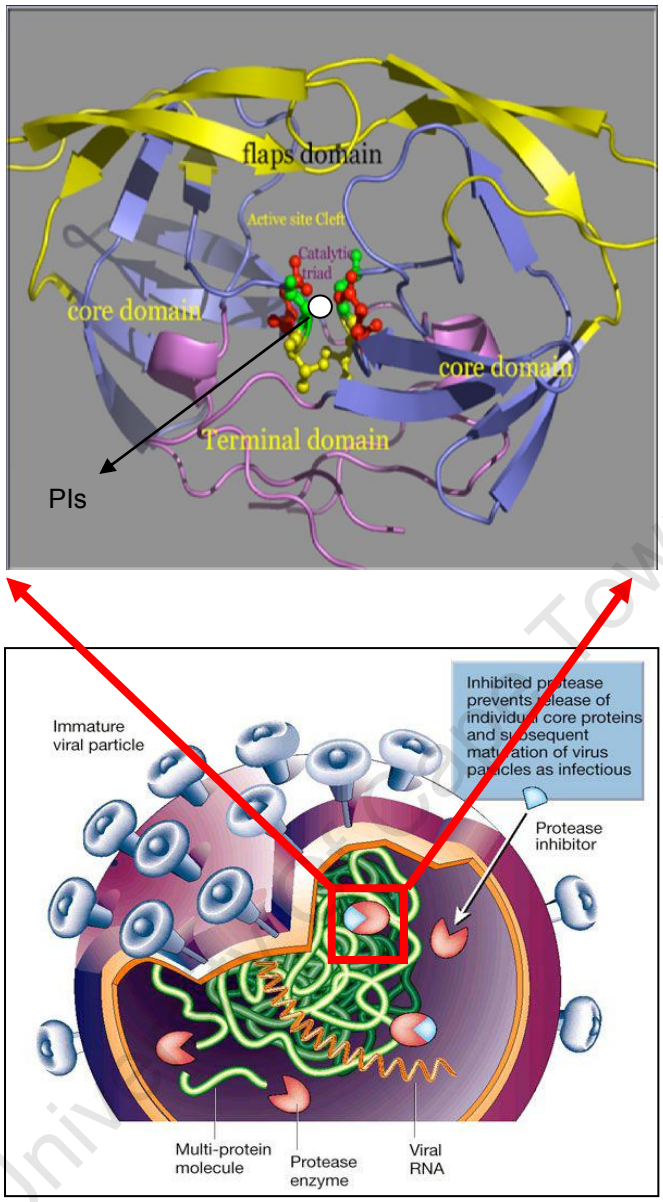

Figure 1.5: Protease inhibitors bind to the HIV protease active site to produce a non-infectious virus (Richman, 2001)

University of Cape Town

Table 1.2: Complications induced by protease inhibitors (Temesgen et al., 2006)

Protease inhibitors	Major side-effects
1. Amprenavir	Gastrointestinal, severe rash, hyperglycaemia, hypertriglyceridaemia and hypercholesterolaemia
2. Atazanavir	Indirect hyperbilirubinaemia, rash, gastrointestinal
3. Darunavir	Diarrhoea, nausea, hyperlipidaemia
4. Fosamprenavir	Rash, gastrointestinal, hyperglycaemia, hyperlipidaemia, headache, hepatotoxicity
5. Indinavir	Nephrolithiasis, hyperbilirubinaemia, gastrointestinal, insulin resistance, hyperglycaemia, hyperlipidaemia, hepatoxicity
6. Kaletra (lopinavir/ritonavir)	Gastrointestinal (particularly diarrhoea), hyperlipidaemia (especially hypertriglyceridaemia), elevated transaminases, hyperglycaemia, hepatotoxicity
7. Nelfinavir	Gastrointestinal (particularly diarrhoea), hyperglycaemia, hyperlipidaemia, hepatotoxicity
8. Ritonavir	Gastrointestinal, paresthesia, taste perversion, hyperlipidaemia, hyperglycaemia, hepatotoxicity
9. Saquinavir	Gastrointestinal, hepatotoxicity, hyperglycaemia
10. Tipranavir	Hepatotoxicity, rash, hyperlipidaemia (especially hypertriglyceridaemia), hyperglycaemia, gastrointestinal

University Of Cape Town

Clinical studies have demonstrated that both long-term and short-term protease inhibitor therapies are strongly associated with the development of metabolic abnormalities such as insulin resistance and lipodystrophy (Monier and Wilcox, 2004; Moyle, 2007). In addition, the incidence of insulin resistance in HIV-positive patients is significantly higher in protease-inhibitor-treated patients than in patients treated with NRTIs or NNRTIs (Woerle et al., 2003), even when one considers related factors such as demography and virology (Palella et al., 1998). Furthermore, protease inhibitors have been shown to induce insulin resistance in seronegative patients and in animal models (Hruz et al., 2002; Lee et al., 2007; Noor et al., 2001; Noor et al.,

2002), implying a clear link between protease inhibitor use and insulin resistance (Ismail et al., 2009).

With the rollout of these drugs and the increased longevity of patients, the side-effects have become more apparent. Currently, in South Africa, NRTIs (stavudine, lamivudine, zidovudine and didanosine), NNRTIs (efavirenz and nevirapine) and protease inhibitors (lopinavir/ritonavir) are used to treat AIDS; and the side-effects of protease inhibitors have also been observed in this country (Filippini et al., 2006; Wouters et al., 2009).

1.5 Insulin resistance

The primary metabolic disorder induced by protease inhibitors is insulin resistance (Carr et al., 1998). This occurs when normal insulin levels are inadequate to stimulate glucose uptake in the insulin signalling pathway in insulin-sensitive tissues such as liver, skeletal muscle and adipose tissue. Insulin resistance frequently manifests as dyslipidaemia (hypertriglyceridaemia) and lipodystrophy (Ismail et al., 2009).

1.5.1 The insulin signalling pathway

At a physiological level, signalling through the insulin receptor pathway is critical for the regulation of blood glucose levels by insulin (Youngren, 2007). In the post-prandial phase, the pancreas releases insulin into the bloodstream in response to glucose. Insulin then binds to its heterotetrameric (2 α- and 2 β-subunits) receptor, which is a ligand-activated tyrosine kinase.

This binding of insulin leads to autophosphorylation of the receptor β-subunit on tyrosine residues, which then activates the intrinsic tyrosine kinase domain and leads to tyrosine phosphorylation of its substrate, insulin receptor substrate 1 (IRS-1). Following autophosphorylation of the kinase domain, some regulatory proteins in the insulin signalling pathway – such as Src homology 2B (SH2B), and adapter proteins with a pleckstrin homology domain and an SH2 domain (APS) – bind to phosphorylated tyrosines on the kinase domain and lead to further activation of phosphorylation of the insulin receptor and IRS-1 (Ahmed and Pillay, 2001). The tyrosine-phosphorylated IRS-1 binds to the SH2 domain of phosphoinositide 3-kinase (PI3-K) with high specificity and affinity, leading to the activation of this enzyme and the conversion of phosphatidylinositol 4,5-biphosphate (PIP_2) into phosphatidylinositol 3,4,5-triphosphate (PIP_3).

University Of Cape Town

The bound PIP_3 causes translocation of both the PIP_3-dependent protein kinase (PDK) and protein kinase B (PKB), aka Akt. This allows the PDK to phosphorylate and then activate PKB/Akt. The activation of PKB/Akt is necessary for the final steps leading to glucose transport, and results in the migration of glucose transporter 4 (GLUT4) from the cytoplasm to the cell membrane, to facilitate the uptake of extracellular glucose (Figure 1.6).

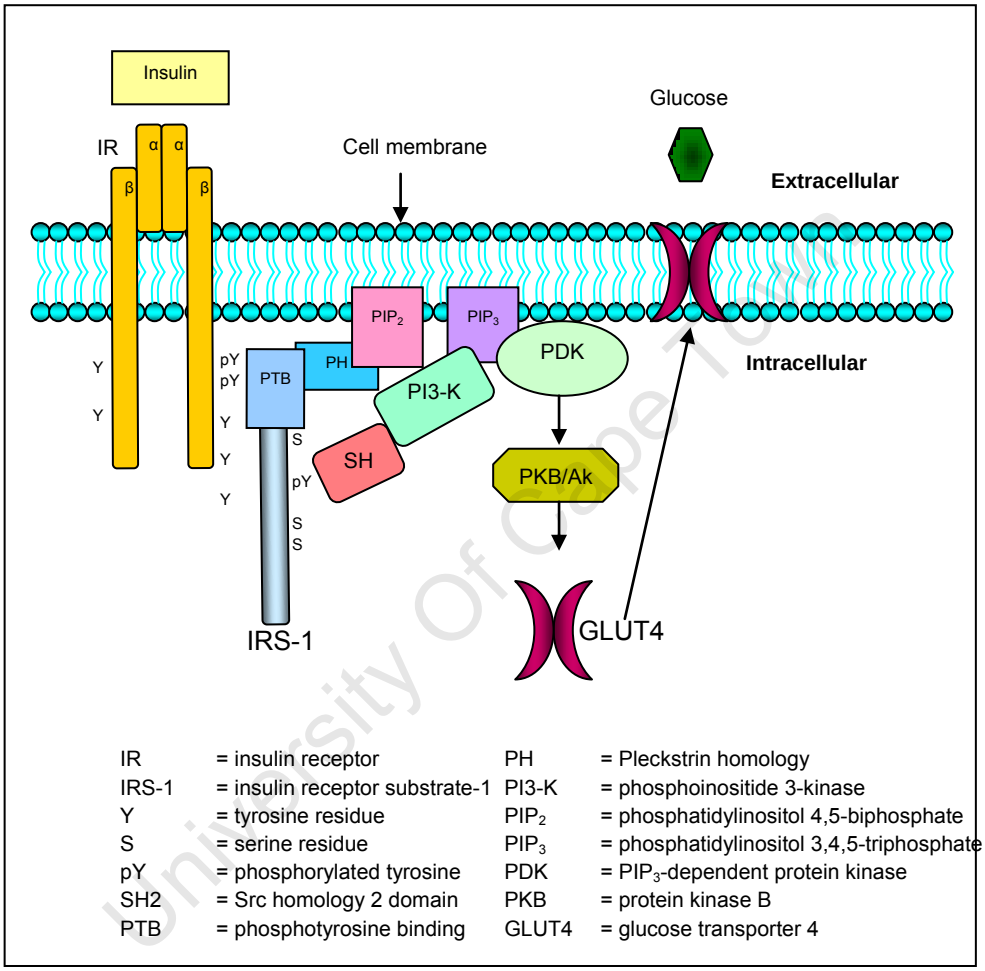

Figure 1.6: Insulin signalling pathway (Ismail et al., 2009)

After the blood glucose has reached the normal level (approximately 5-6.6 mmol/l), the insulin signalling pathway is deactivated by phosphotyrosine regulatory proteins. There are several known phosphotyrosine regulatory proteins in the insulin signalling pathway that act as inhibitors, such as serine 307 phosphorylated IRS-1; protein tyrosine phosphatase 1B (PTP1B); and suppressor of cytokine signaling-1 and -3 (SOCS-1 and -3) (Aguirre et al., 2002; Ueki et al., 2004; Youngren, 2007; Zhang et al., 2002). There is a possibility that protease inhibitors may also activate these phosphotyrosine regulatory proteins, and thereby induce insulin resistance.

University Of Cape Town

1.5.2 The mechanism of insulin resistance

The primary metabolic disorder induced by protease inhibitors is insulin resistance. This is also the primary metabolic disorder in type 2 diabetes, obesity, the metabolic syndrome and atherosclerotic cardiovascular disease (Meyer et al., 2002; Nolan et al., 1994; Savage et al., 2005). The most pronounced effect of insulin resistance is the inhibition of glucose uptake, the major outcome of the activation of the insulin signalling pathway (Murata et al., 2002; Rudich et al., 2005).

This effect on glucose uptake may result from inhibition at a proximal level. However, in the context of insulin resistance induced by protease inhibitors, there are relatively few studies that have examined proximal steps in the insulin signalling cascade. This includes insulin binding to the insulin receptor β-subunit, and activation of the intrinsic tyrosine kinase activity and subsequent tyrosine phosphorylation of the substrate, where direct or indirect protease inhibitor-induced inhibition may occur. Thus, an understanding of the effects of protease inhibitors on these proximal steps in the insulin signalling pathway may shed new light on the molecular basis of insulin resistance induced by antiretroviral drugs. In addition, other mechanisms such as activation of inflammatory pathways and mitochondrial dysfunction, as observed in type 2 diabetes and obesity, may also be involved in the insulin resistance induced by protease inhibitors.

1.5.2.1 Insulin receptor

The insulin signalling pathway is initiated by the activation of the insulin receptor, i.e. tyrosine kinase activity after binding with insulin. The insulin receptor, a receptor tyrosine kinase, plays an important role in the insulin regulation of glucose transport and oxidation, as well as in glycogen, lipid and protein synthesis. The insulin receptor is usually expressed at a very high level in insulin-sensitive tissues such as skeletal muscle, liver and adipose tissue (Youngren, 2007). Autophosphorylation of insulin receptor tyrosine residues stimulates the intrinsic catalytic activity of tyrosine kinase. Phosphorylation of the receptor results in the recruitment of IRS-1. This substrate initiates a cascade of cellular phosphorylation reactions that regulate protein interactions in the insulin signalling pathway to stimulate GLUT4 translocation and glucose uptake (Youngren, 2007).

In type 2 diabetes, tyrosine phosphorylation of the insulin receptor β-subunit is reduced *in vivo,* resulting in the inhibition of glucose uptake (Meyer et al., 2002; Nolan et al., 1994). This finding parallels those from studies of obesity with or without

University Of Cape Town

diabetes (Arner et al., 1987; Caro et al., 1987; Nolan et al., 1994), and obesity with insulin resistance and polycystic ovary syndrome (Dunaif et al., 1995). However, tyrosine phosphorylation of the insulin receptor β-subunit (in the context of insulin resistance induced by protease inhibitors) has not been investigated in depth. A few studies have shown that some protease inhibitors decreased tyrosine phosphorylation of IRS-1, e.g. in HepG2 hepatoma cells exposed to 100 μM indinavir for 48 h (Schutt et al., 2000), and in 3T3-L1 preadipocytes exposed to 10 μM ritonavir for 11 days (Cammalleri and Germinario, 2003). The findings from these studies show that protease inhibitors may also affect tyrosine phosphorylation of the insulin receptor β-subunit as a primary site of insulin resistance in HIV-positive patients, similar to the findings in type 2 diabetes patients.

In order to understand the effect of protease inhibitors on tyrosine phosphorylation of the insulin receptor β-subunit and IRS-1, a number of phosphotyrosine regulatory proteins also require further study. Previous work has revealed several phosphotyrosine regulatory proteins now known to be involved in the modulation of tyrosine phosphorylation of the insulin receptor β-subunit and of IRS-1, such as SH2B, APS, IRS-1 phosphorylated on serine 307 (phosphoIRS-1 Ser 307), PTP1B, and SOCS-1 and -3 (Aguirre et al., 2002; Ueki et al., 2004; Youngren, 2007; Zhang et al., 2002).

1.5.2.2 SH2B and APS

SH2B (aka SH2B1) is an adapter protein involved in the signalling pathways mediated by insulin tyrosine kinase and the Janus kinase (Kotani et al., 1998). Deletion of the adapter protein gene in mice results in severe obesity, infertility, and leptin and insulin resistance (Maures et al., 2007). This protein has also been shown to regulate the tyrosine phosphorylation state of the insulin receptor (Ahmed and Pillay, 2001).

Another adapter protein, APS (aka SH2B2) has a similar role to the SH2B1 protein in delaying the dephosphorylation of the insulin receptor kinase, and IRS-1 and -2, in the insulin signalling pathway (Ahmed and Pillay, 2001; Ahmed and Pillay, 2003). However, APS binds the insulin receptor with a higher affinity than SH2B (Ahmed and Pillay, 2001; Ahmed and Pillay, 2003). The role of these adapter proteins has not been investigated in the insulin resistance induced by protease inhibitors.

University Of Cape Town

1.5.2.3 Phosphorylation of serine 307 on IRS-1

Serine phosphorylation of IRS-1 (serine 307 in rat or serine 312 in human) is known to inhibit tyrosine phosphorylation of the insulin receptor β-subunit (Aguirre et al., 2002). This increase in serine phosphorylation in induced by means of several mechanisms (Figure 1.7), viz. elevation of circulating levels of several adipose-derived cytokines such as TNF-α (section 1.5.2.6) and metabolites (e.g. free fatty acids (FFAs)) (section 1.5.2.9), and activation of IκB kinase (IKK) (section 1.5.2.7), Jun kinase (JNK) (section 1.5.2.8), protein kinase Cs (PKCs) (section 1.5.2.10) and mammalian target of rapamycin (mTOR) (section 1.5.2.11) (Aguirre et al., 2002; Lee et al., 2009). The increased serine 307 phosphorylation of IRS-1, decreased tyrosine phosphorylation of IRS-1 and then reduced activation of PI3-K leads to an inhibition of translocation of GLUT4 from the cytoplasm to the cell membrane. This reduces glucose uptake and results in insulin resistance in adipocytes, hepatocytes and skeletal muscle cells (Figure 1.7).

1.5.2.4 PTP1B

Protein tyrosine phosphatase 1 B (PTP1B), a tyrosine phosphatase negatively regulates insulin signalling by binding to the tyrosine phosphorylated proteins, insulin receptor β-subunit and IRS-1 (Figure 1.7), and catalysing tyrosine dephosphorylation (Cheng et al., 2002; Zhang et al., 2002). Mice lacking functional PTP1B exhibit increased sensitivity toward insulin, and are resistant to obesity (Zhang et al., 2002). However, the effect of protease inhibitors on PTP1B expression *in vivo* and *in vitro* has not been investigated as yet.

University Of Cape Town

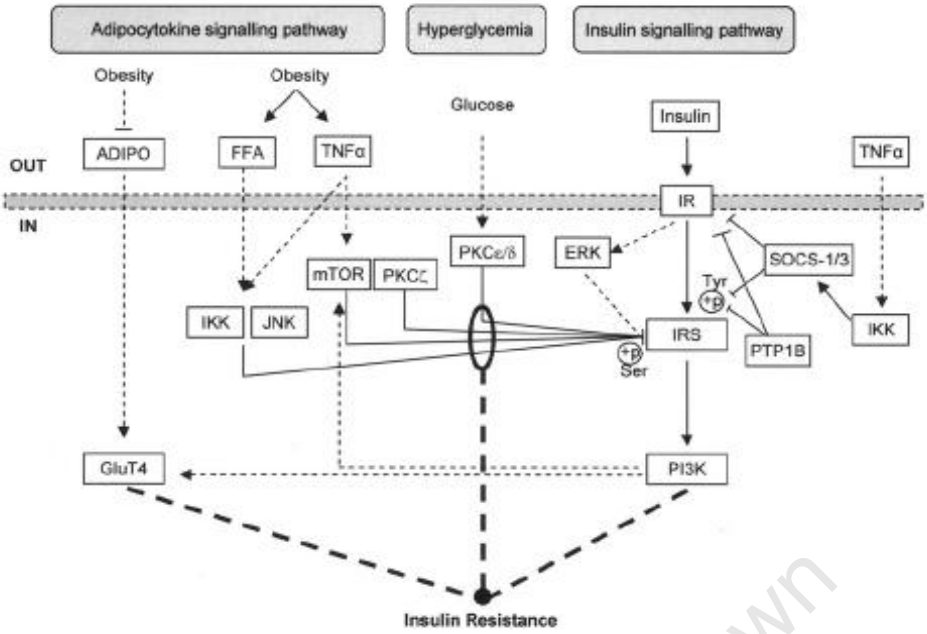

Figure 1.7: Pathways implicated in insulin resistance in adipocytes, hepatocytes and skeletal muscle cells (Vodenik et al., 2009). Adipo = adipocytes, FFA = free fatty acid, TNF-α = tumour necrosis factor alpha, IKK = IκB kinase, JNK = Jun kinase, mTOR = mammalian target of rapamycin, PKC = protein kinase C, ERK = extracellular-signal regulated kinase, IR = insulin receptor, IRS = insulin receptor substrate, Tyr = tyrosine, +p = phosphorylation, PTP1B = protein tyrosine phosphatase 1 B, SOCS-1/3 = suppressor of cytokine signaling-1 and -3, PI3-K = phosphoinositide 3-kinase and GLUT4 = glucose transporter 4.

University Of Cape Town

1.5.2.5 SOCS-1 and -3

SOCS-1 and -3 are adapter proteins that bind to the insulin receptor β-subunit or IRS-1 or IRS-2 to inhibit downstream signalling (Figure 1.7) (Emanuelli et al., 2000). The expression of these proteins can be induced by tumour necrosis factor alpha (TNF-α) (Emanuelli et al., 2001). Increased SOCS-1 and -3 expression has been reported to induce insulin resistance involved in obesity (Ueki et al., 2004; Youngren, 2007). In addition, knockout of SOCS expression in adipocytes prevented much of the impaired tyrosine phosphorylation of IRS-1 or IRS-2 induced by TNF-α (Youngren, 2007). Therefore, studies of SOCS-1 and -3 expressions in protease inhibitor-induced insulin resistance in cells may provide information regarding the molecular basis of this side-effect.

1.5.2.6 TNF-α

TNF-α is a multifunctional cytokine secreted largely by adipocytes (Hotamisligil et al., 1993). This cytokine is involved in inflammation, apoptosis, cytotoxicity, the production of other cytokines, such as interleukin 1 (IL-1) and interleukin 6 (IL-6), and also induces insulin resistance (Fonseca-Alaniz et al., 2007; White, 2002). The level

of TNF-α correlates negatively with the level of adiponectin (Lee et al., 2009). Adiponectin is another adipocytokine secreted by adipocytes. This protein hormone promotes insulin sensitivity by modulating a number of metabolic processes in adipose tissue and the whole body including decreasing blood glucose levels and stimulating fatty acid catabolism (Lee et al., 2009). Thus, a high level of adiponectin acting through endocrine mechanisms is able to increase insulin sensitivity (Guogeon *et al*., 2004). In contrast, plasma adiponectin was found to be low in insulin resistance induced by protease inhibitors, type 2 diabetes and obesity, *in vivo* and *in vitro* (Kadowaki et al., 2006; Kern et al., 2003).

Mice lacking TNF-α or TNF-α receptors show improved insulin sensitivity in both dietary and genetic models of obesity (Lee et al., 2009). Therefore, an understanding of the function of TNF-α may provide a therapeutic target for insulin resistance and type 2 diabetes. However, the signalling cascades regulated by TNF-α are complex and involve many pathways, including the activation of various serine kinases and transcription factors (White, 2002).

TNF-α activates the transcription factor of the IκB kinase β (IKKβ), the nuclear factor kappa B (NFκB) pathway, and increases phosphorylation of serine 307 on IRS-1 in the liver of obese Zucker rats (Cai et al., 2005). This activation then induces insulin insensitivity in both the liver and in skeletal muscle (Figure 1.7) (Cai et al., 2005). In a subsequent study, rats with high-fat-diet-induced insulin resistance do not develop the insulin resistance when IKKβ was lacking in the liver (Arkan et al., 2005).

Interestingly, high doses of salicylate have been shown to reverse obesity- and diet-induced insulin resistance in Zucker rats through disruption of IKKβ (Yuan et al., 2001). Adipose tissue biopsies from lipodystrophic HIV-positive patients undergoing treatment with protease inhibitors and NRTIs, showed an increased expression of TNF-α (Vigouroux et al., 2003). However, IKKβ expression and the NFκB pathway induced by TNF-α have not been investigated in insulin resistance induced by protease inhibitors in HIV-positive patients.

1.5.2.7 The NFκB pathway

It has been shown that IKKβ and the NFκB pathway become a target for TNF-α and SOCS-1/3 induced insulin resistance (Yuan et al., 2001). IKKβ is a serine kinase that regulates the activation of NFκB, a crucial activator of genes involved in inflammation and immunity. Prior to activation, NFκB is bound to the inhibitor κB (IκB). The activated IKKβ then phosphorylates the NFκB-IκB complex, which stimulates the

University of Cape Town

conjugation of IκB with ubiquitin and the subsequent degradation of IκB protein in the proteasome, leading to the nuclear translocation of NFκB (Tergaonkar, 2006). Activation of IKKβ also induces serine 307 phosphorylation of IRS-1, as IRS-1 is a substrate of IKKβ. This phosphorylation blocks interactions with the insulin receptor β-subunit, decreases tyrosine phosphorylation, and inhibits insulin action in cells (Figure 1.7) (Aguirre et al., 2002; Gao et al., 2003).

1.5.2.8 JNK-1

Jun kinase 1 (JNK-1) is another inflammatory serine kinase involved in insulin resistance via phosphorylation of serine 307 on IRS-1 (Lee et al., 2009; Perseghin et al., 2003). TNF-α and FFAs have been found to activate JNK-1 (Figure 1.7) (Lee et al., 2009). In both dietary and genetic (*ob/ob*) mice models of obesity, there was a significant increase in total JNK activity in liver, adipose tissue and skeletal muscle (Hirosumi et al., 2002). JNK-1 knockout mice show an increase in insulin sensitivity implying a role of JNK-1 in modulating insulin sensitivity (Hirosumi et al., 2002). Therefore, JNK-1 could potentially also be involved in the insulin resistance induced by protease inhibitors.

1.5.2.9 Free fatty acids (FFAs)

Increased lipolysis with decreased suppression of FFA levels by insulin suggests a state of insulin resistance at the adipose tissue level (Rudich et al., 2005). In addition, increased plasma FFA concentrations are also associated with obesity and type 2 diabetes (Lee et al., 2009). Prolonged treatment of adipocytes *in vitro* with TNF-α stimulates lipolysis – and thereby increases circulating FFA levels, promoting insulin resistance (Gougeon et al., 2004).

In addition, patients receiving treatment with protease inhibitors and who have insulin resistance and lipodystrophy show elevated TNF-α levels, and increased lipolysis and FFA flux (Lenhard et al., 2000; Meininger et al., 2002; Rudich et al., 2005). Moreover, it was found that the level of FFA was reduced by acipimox, a potent inhibitor of lipolysis, and insulin sensitivity was significantly increased in lipodystrophic HIV-positive patients under treatment with protease inhibitors and NRTIs (Hadigan et al., 2003). These findings show that TNF-α stimulates lipolysis, increases FFA levels and induces insulin resistance. It is interesting that salicylate has also been found to block lipolytic actions of TNF-α and increase insulin sensitivity in primary rat adipocytes (Zu et al., 2008).

University Of Cape Town

IRS-1 has been suggested as a molecular target of FFAs in the development of insulin resistance (Gao et al., 2004). Increased FFA concentrations led to phosphorylation of serine 307 directly on IRS-1, thus reducing the ability of the IRS-1 to activate PI3-K and GLUT4, and inducing insulin resistance (Gao et al., 2004; Lee et al., 2009; Meininger et al., 2002). Moreover, increased FFA levels play a similar role to TNF-α in activating inflammatory pathways such as IKKβ and JNK-1 (Figure 1.7), thereby inhibiting insulin signalling in rodents (Lee et al., 2009).

In addition to TNF-α, protease inhibitors were found to increase lipolysis via the inhibition of the activity of the insulin-regulated enzyme, lipoprotein lipase (LPL), to increase the level of FFA (Ranganathan and Kern, 2002). Alteration of LPL activity affects lipid metabolism, and induces metabolic disorders such as chylomicronaemia, atherosclerosis, cancer and lipodystrophy associated with insulin resistance, as well as diabetes mellitus. Triglyceride-rich lipoproteins such as chylomicrons and very low density lipoproteins are not stored in adipocytes without the LPL enzyme, which leads to hypertriglyceridaemia, lipodystrophy and increased coronary artery disease (Mead et al., 2002)

1.5.2.10 PKCs

FFAs may also induce insulin resistance through the overexpression of protein kinase C (PKC) isoforms. This overexpression of PKCs may stimulate IKKβ to increase serine 307 phosphorylation of IRS-1 or PKCs may phosphorylate IRS-1 directly, and decrease tyrosine phosphorylation of IRS-1, thus inducing insulin resistance (Figure 1.7) (Perseghin et al., 2003). PKC isoforms are divided into classical (cPKC-α, -βI, -βII and -γ), novel (nPKC-δ, -ε, -θ and –η) and atypical (aPKC-ζ and –λ) forms. nPKCs are known to play a role in insulin signalling (Bhattacharya et al., 2007).

Overexpression of PKC-δ due to stimulation with 12-*O*-tetradecanoyl 13-phorbol acetate (TPA), an activator of PKC, may induce insulin resistance in cultured myotubes and skeletal muscle cells (Bhattacharya et al., 2007; Waraich et al., 2008). This may occur via stimulation of serine phosphorylation of the insulin receptor, and reduction of tyrosine phosphorylation of the insulin receptor (Bhattacharya et al., 2007; Waraich et al., 2008). In addition, overexpression of PKC-ε in the skeletal muscle of diabetic animals and humans has also been reported to induce insulin resistance (Ikeda et al., 2001; Itani et al., 2002). The high levels of FFAs stimulate the PKC-ε to induce insulin resistance through PDK1-independent phosphorylation, and reduction of insulin receptor gene transcription (Itani et al., 2002). However,

University Of Cape Town

details of the precise mechanism causing PKC to inhibit the gene transcription are still unclear.

In a recent study, increased FFA concentrations have also been shown to activate PKC-θ in the skeletal muscle of rats with fat-induced insulin resistance. Subsequently, the activated PKC-θ was found to increase serine 307 phosphorylation, decrease tyrosine phosphorylation of IRS-1 and induce insulin resistance in the rats (Lee et al., 2009). In contrast, PKC-θ-deficient mice are protected from fat-induced insulin resistance (Kim et al., 2004). A few studies have also reported that the knock-out of PKC-α in mice and the inhibition of PKC-ε in rats enhanced insulin signalling (Kim et al., 2004; Leitges et al., 2002; Samuel et al., 2007). An evaluation of the role of PKCs in the insulin resistance induced by protease inhibitors may provide interesting findings.

1.5.2.11 mTOR

mTOR, a conserved serine/threonine kinase, plays a key role in the regulation of cellular response to nutrients (Vodenik et al., 2009). For this reason, it was suggested that mTOR is also involved in obesity and insulin resistance (Figure 1.7) (Um et al., 2006). In a model of nutrient overload presenting as obesity, constitutive and sustained activation of the mTORC1 (an mTOR complex) pathway led to insulin resistance (Um et al., 2006). mTORC1 was found to increase serine phosphorylation of IRS-1 on serine 632 in mice and serine 636 in humans; and it appears the effect was abrogated by sirolimus, the mTOR inhibitor (Um et al., 2006).

1.5.2.12 PAI-1

Recently, there has been growing evidence linking plasminogen activator inhibitor 1 (PAI-1) with obesity and insulin resistance (Lee et al., 2009). PAI-1 is a key regulatory protein of tissue fibrinolysis, cell migration, angiogenesis and tissue remodelling, and is mainly synthesised in adipose tissue (Lijnen, 2005). It has been found that PAI-1 can be induced by TNF-α and PKCs (Pandey et al., 2005). PKCs and TNF-α may induce PAI-1 mRNA by increasing the rate of transcription of the PAI-1 gene. The dramatic increase in PAI-1 results in insulin resistance (Pandey et al., 2005). Interestingly, the absence or inhibition of PAI-1 through genetic alteration in adipocytes was found to protect against insulin resistance, by promoting glucose uptake and adipocyte differentiation via increased peroxisome proliferator-activated receptor gamma (PPARγ) expression (Lee et al., 2009). However, the function of

University of Cape Town

PAI-1 in insulin resistance induced by protease inhibitors in HIV-positive patients has investigated as yet.

1.5.2.13 Oxidative stress

Oxidative stress – or chronic and/or increased production of reactive molecules such as reactive oxygen species (ROS) and reactive nitrogen species (RNS) – has also been associated with insulin resistance, type 2 diabetes, cardiovascular disease and cancer (Figure 1.8) (Evans et al., 2005). High levels of FFAs, inflammatory cytokines, hyperinsulinaemia and hyperglycaemia have been reported to induce oxidative stress, which later triggers the activation of the stress-sensitive serine/threonine kinase signalling pathway such as TNF-α, JNK, IKKβ, PKCs and mTOR. This stress-sensitive serine/threonine kinase increases phosphorylation of IRS-1 on serine 307 and induces insulin resistance (Evans et al., 2005). In animal models and patients with diabetes, treatment with the antioxidant α-lipoic acid or salicylate has been reported to improve insulin sensitivity (Evans et al., 2005; Fenkci et al., 2003).

1.5.2.14 Pre-lamin A

Lamin A is a nuclear laminar protein and is ubiquitously expressed in differentiated tissues (Capanni et al., 2005). However, the physiological function of lamin A is still unclear. Biogenesis of lamin A from pre-lamin A requires the ZMPST24 enzyme. The inhibition of ZMPST24 leads to the blockade of lamin A processing and the accumulation of pre-lamin A. Recently, pre-lamin A was found to be involved in lipodystrophy associated with insulin resistance in HIV-positive patients treated with protease inhibitors (Goulbourne and Vaux, 2010). Similar effects have also been observed in inherited lipodystrophy such as the Dunning-type familial partial lipodystrophy (FPDL) (Capanni et al., 2005). In the adipose tissue from these patients, the accumulated pre-lamin A was found to cause a reduction in the amount of the DNA-bound adipocyte transcription factor sterol regulatory element binding protein 1 (SREBP-1) and consequently a reduction of PPARγ expression. This resulted in an impairment of pre-adipocyte differentiation and induced lipodystrophy associated with insulin resistance (Maraldi et al., 2007). Interestingly, the treatment with the PPARγ ligand troglitazone (a thiazolidinedione) was found to improve adipocyte differentiation in these patients (Maraldi et al., 2007). These findings suggest that pre-lamin A is a possible therapeutic target in lipodystrophy associated with insulin resistance induced by protease inhibitors.

University of Cape Town

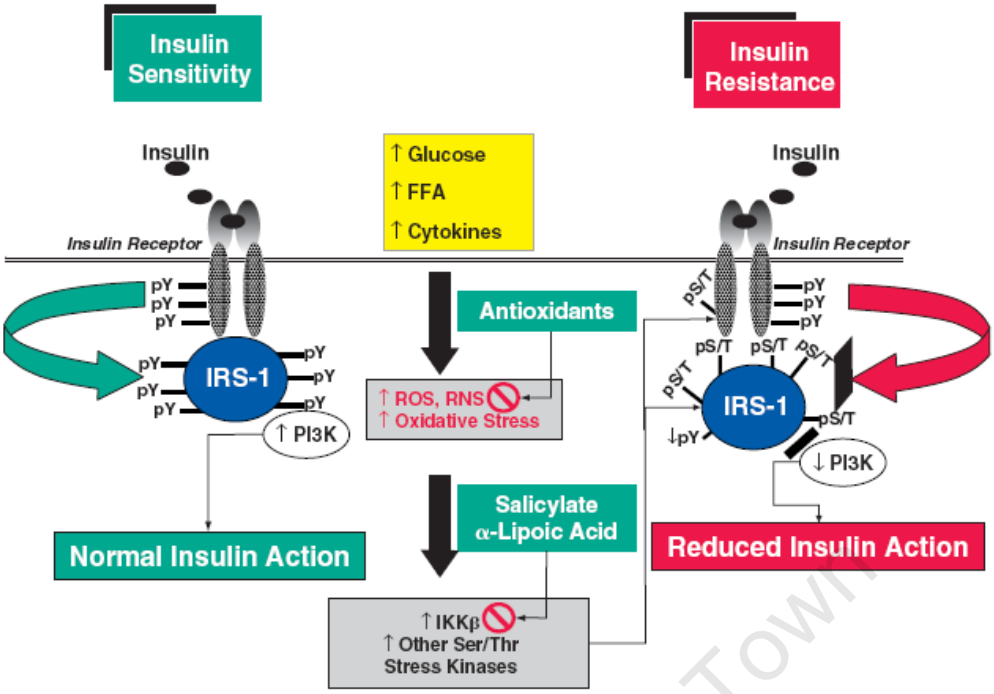

Figure 1.8: The role of serine kinase activation in oxidative stress-induced insulin resistance (Evans et al., 2005)

University Of Cape Town

1.5.2.15 Mitochondrial dysfunction and endoplasmic reticulum stress response

In addition to insulin signalling and inflammatory pathways, severe mitochondrial dysfunction has been known to cause type 2 diabetes (van den Ouweland et al., 1992). The mitochondrion is a membrane-enclosed organelle which plays an important role in cellular metabolism, via the Krebs cycle (van den Ouweland et al., 1992).

Mitochondrial dysfunction is known to elevate several kinase activities such as PKC and JNK. PKC and JNK are capable of increasing serine phosphorylation of IRS-1 and inducing insulin resistance (Lim et al., 2009). Using a magnetic resonance spectroscopy (MRS) approach, it was found that mitochondrial function was reduced in healthy lean insulin-resistant offspring of parents with type 2 diabetes. This finding was attributed to reductions in mitochondrial density (Morino et al., 2006).

Endoplasmic reticulum (ER) stress response (aka the unfolded protein response, UPR) has also been found to induce type 2 diabetes (Lim et al., 2009). ER stress response is triggered by the accumulation of unfolded proteins in the ER lumen (Lim et al., 2009).

Mitochondria and the ER are able to interact with each other both physically and functionally, and form an endomembrane network known as a mitochondria-associated ER membrane (MAM). In type 2 diabetes, mitochondrial dysfunction was found to induce ER stress response and form a MAM. The MAM then coordinated the increased levels of gluconeogenic enzyme, as observed in many insulin resistance states, through p38 mitogen-activated protein kinase (MAPK) and JNK, in a Ca^{2+}-dependent manner (Lim et al., 2009).

1.5.2.16 Adiponectin

Adiponection is also secreted by adipocytes, in addition to TNF-α (Lee et al., 2009). This adipokine contains a collagenous domain with four lysine residues (68, 71, 80 and 104) which are hydroxylated to hydroxylysine. The hydroxylysines are subsequently glycosylated to modulate the insulin sensitivity of cells (Fonseca-Alaniz et al., 2007; Wang et al., 2002).

Adiponectin exists as multiple isoforms, such as trimeric low molecular weight (LMW), albumin-binding LMW (Alb-LMW), hexameric middle molecular weight (MMW) and high molecular weight (HMW) forms (Hara et al., 2006). The biologically active form of adiponectin is the HMW form, and its ratio to total adiponectin is closely correlated with insulin sensitivity (Hara et al., 2006). A high level of adiponectin *in vivo* acting via endocrine mechanisms is able to increase insulin sensitivity and known as an insulin sensitising hormone (Guogeon *et al*., 2004). This is probably by acting through AMP kinase to increase fatty acid oxidation. In contrast, a low level of adiponectin is associated with several diseases, such as insulin resistance, type 2 diabetes, obesity and lipodystrophy (Kadowaki et al., 2006; Kern et al., 2003). Adiponectin also plays a major role to modulate a number of metabolic processes such as glucose regulation, fatty acid catabolism in adipose tissue, anti-atherosclerotic and anti-inflammatory actions in human and animal (Lee et al., 2009). Adiponection production is upregulated during adipogenesis which is enhanced by PPARγ (Guogeon *et al*., 2004).

HIV protease inhibitors have also been known to decrease the secretion of adiponectin in inducing insulin resistance and lipodystrophy (Jones et al., 2008). These findings show that adiponectin may play a leading role as a biomarker, in particular in insulin resistance induced by protease inhibitors. However, further study of adiponectin, in particular synthesis of hydroxylysine in type 2 diabetes, obesity and insulin resistance induced by protease inhibitors has not been undertaken.

University of Cape Town

1.5.3 Review of insulin resistance induced by protease inhibitors

The mechanism of insulin resistance is complex, and is the result of many factors. In the context of insulin resistance induced by protease inhibitors, the molecular basis is largely unknown. An understanding of the general mechanism of insulin resistance may provide ideas for investigating the possible pathway of insulin resistance induced by the antiretroviral drugs.

Briefly, the effects of protease inhibitors on the insulin signalling pathway have been reviewed in several types of cell lines and appear to occur via three major mechanisms (Ismail et al., 2009). The drugs impair either the distal steps, or the proximal steps in the insulin signalling pathway; or they involve other factors such as oxidative stress, adapter proteins and adiponectin (Table 1.3) (Ismail et al., 2009).

1.5.3.1 Protease inhibitors impair the distal steps in the insulin signalling pathway

An early study of insulin resistance induced by protease inhibitors demonstrated that the drug inhibits GLUT4 uptake *in vitro* (Murata et al., 2000). GLUT4 is the major transporter responsible for insulin-stimulated glucose disposal into adipose tissue, cardiac and skeletal muscle, and plays a critical role in whole-body glucose homeostasis (Mueckler, 2001). In this particular study, it was reported that 3T3-L1 adipocytes treated with indinavir, a protease inhibitor, at 100 μM for 4 h decreased GLUT4 uptake (Murata et al., 2000). However, there was no evidence for any effects from protease inhibitors on early insulin signalling events, such as insulin receptor β-subunit and IRS-1 tyrosine phosphorylation (Hertel et al., 2004; Murata et al., 2000; Murata et al., 2002). Similar effects on glucose uptake were reported in rats and in HIV-negative patients treated with protease inhibitors (Hruz et al., 2002; Lee et al., 2007; Noor et al., 2001).

University Of Cape Town

Table 1.3: Summary of the effects of protease inhibitors in the insulin signalling pathway (Ismail et al., 2009)

Protease inhibitor effects	References	Drug concentration used in the experiments	Experimental model	Observations
1. Distal steps in the insulin signalling pathway	(Murata et al., 2000)	Indinavir (100 μM) for 4 h	3T3-L1 adipocytes	Decreased glucose uptake
	(Rudich et al., 2001)	Nelfinavir (10 μM) for 18 h	3T3-L1 adipocytes	Impaired GLUT4 translocation and glucose uptake by inhibiting stimulation of PKB serine 473 phosphorylation
	(Ben-Romano et al., 2004) and (Rudich et al., 2005)	Nelfinavir (30 μM) for 18 h	3T3-L1 adipocytes	Inhibited recruitment and activation of PI3-K, impaired GLUT4 translocation and glucose uptake
	(Kachko et al., 2009)	Nelfinavir (30 μM) for 18 h	3T3-L1 adipocytes used a GLUT4-GFP chimeric construct	Interfered with the sensing of PIP_3 by PKB/Akt and inhibited GLUT4 translocation
2. Proximal steps in the insulin signalling pathway	(Schutt et al., 2000)	Indinavir (100 μM) for 48 h	HepG2 hepatoma cells	Decreased tyrosine phosphorylation of IRS-1 and PI3-K activation
	(Cammalleri and Germinario, 2003)	Ritonavir (10 μM) for 11 days	3T3-L1 pre-adipocytes	Decreased insulin receptor expression and tyrosine phosphorylation of IRS-1
	(Djedaini et al., 2009)	Lopinavir (10 μg/ml) for 48 h	Human adipocytes	Decreased tyrosine phosphorylation of IRS-1 and glucose uptake
3. Other factors	(Ben-Romano et al., 2006)	Nelfinavir (30 μM) for 18 h	3T3-L1 adipocytes	Induced oxidative stress
	(Lagathu et al., 2007)	Indinavir, amprenavir, lopinavir, ritonavir (10 μmol/l), atazanavir (4 μmol/l), nelfinavir (5 μmol/l) for 24 and 48 h	Human adipocytes and macrophages	Induced oxidative stress and altered chemokines, cytokines or adiponectin production
	(Carper et al., 2008)	Indinavir (20 μM) for 7 weeks	Rats	Increased SOCS-1, TNF-α and SREBP-1 expression
	(Chaparro et al., 2005)	Indinavir, nelfinavir, liponavir/ritonavir, ritonavir and saquinavir	Human adipose tissue biopsies	Altered adipose tissue gene expression

University of Cape Town

However, in a subsequent study, prolonged treatment (18 h) of 3T3-L1 adipocytes with another protease inhibitor, nelfinavir, at plasma concentrations (10 μM), impaired both GLUT4 translocation and glucose uptake (Rudich et al., 2001). Nelfinavir appeared to induce insulin resistance by inhibiting the stimulation of PKB/Akt serine 473 phosphorylation without any effect on the tyrosine phosphorylation of IRS-1. Nelfinavir also decreased expression of the lipolysis regulator, perilipin (Rudich et al., 2001). The ability of nelfinavir to impair PKB/Akt activation, GLUT4 translocation and glucose uptake was confirmed in a subsequent study (Ben-Romano et al., 2004; Rudich et al., 2005).

Nelfinavir concentration at 30 μM induced insulin resistance in 3T3-L1 adipocytes by inhibiting recruitment and activation of PI3-K, leading to impaired GLUT4 translocation and thus preventing insulin-stimulated glucose uptake (Ben-Romano et al., 2004; Rudich et al., 2005). These effects were not accompanied by changes in insulin receptor expression or insulin receptor tyrosine phosphorylation. A subsequent study using a similar model maintained that PKB/Akt activation was affected after insulin-stimulated generation of PIP_3, leading to impaired GLUT4 translocation (Kachko et al., 2009).

It has also been proposed that nelfinavir induces oxidative stress (Ben-Romano et al., 2006; Chandra et al., 2009). Oxidative stress induces insulin resistance by activating serine kinase, leading to serine phosphorylation of IRS-1, and also by disrupting the subcellular distribution of PI3-K (i.e. decreased membrane localisation). This in turn would lead to decreased tyrosine phosphorylation of IRS-1 and consequently reduced PKB/Akt activation, and hence decreased GLUT4 translocation.

1.5.3.2 Protease inhibitors impair the proximal steps in the insulin signalling pathway

On the other hand, a previous study proposed that indinavir interfered with the very early steps of the insulin signalling cascade in HepG2 hepatoma cells, (Schutt et al., 2000). The drug inhibited phosphorylation of IRS-1, activation of PI3-K and phosphorylation of PKB/Akt, without affecting the insulin binding. Ritonavir at 10 μM decreased insulin receptor numbers in 3T3-L1 pre-adipocytes without any effect on binding affinity. This was accompanied by decreased IRS-1 tyrosine phosphorylation in response to insulin (Cammalleri and Germinario, 2003). A more recent study suggested that lopinavir, a protease inhibitor, inhibited IRS-1 phosphorylation in human adipocytes and resulted in a concentration-dependent decrease in glucose uptake (Djedaini et al., 2009). It was suggested that lopinavir decreased the phosphorylation of IRS-1 directly since there was no effect observed on the phosphorylation of the insulin receptor β-subunit.

1.5.3.3 Protease inhibitors induce insulin resistance via other factors: oxidative stress, adapter proteins and adipokines

As indicated above (section 1.5.3.1), some of the protease inhibitors may increase oxidative stress (Ben-Romano et al., 2006; Chandra et al., 2009). Protease inhibitors may also alter chemokines, cytokines or adiponectin production in human adipocytes

University Of Cape Town

and macrophages (Lagathu et al., 2007). The induction of oxidative stress is known to cause insulin resistance. Changes in the expression of regulatory proteins in the insulin signalling pathway could also potentially explain the effects of protease inhibitors. SOCS-1 and -3 are examples of known inducers of insulin resistance. These proteins bind to the insulin receptor β-subunit following activation, and impair the ability of the insulin receptor β-subunit to phosphorylate downstream substrates.

It has also been shown that the expression of SOCS-1 was increased in indinavir-treated rats (Carper et al., 2008). In this study, chronic protease inhibitor exposure induced SOCS-1 expression in muscle, liver and adipose tissue. This was associated with an increase in the expression of TNF-α and the downstream target SREBP-1, along with decreased expression of IRS-2. IRS-2 is another major substrate that mediates insulin action in the insulin signalling pathway (Carper et al., 2008).

In relation to IRS-1, TNF-α induces the activation of several serine kinases (JNK and IKK) leading to increased serine 307 phosphorylation of IRS-1. Increasing the serine phosphorylation converts it into an inhibitory protein of the insulin receptor, leading to insulin resistance. Therefore, in summary, TNF-α can induce insulin resistance by affecting IRS-1 function directly or by inducing the expression of SOCS-1.

Protease inhibitors have also been found to alter adipose tissue gene expression *in vivo* (Chaparro et al., 2005). The mRNA expression levels of the CCAAT/enhancer-binding protein α, leptin, and adiponectin of HIV-positive patients treated with protease inhibitors have been found to be significantly lower than the levels measured in protease-inhibitor-naive patients (Chaparro et al., 2005). Since adiponectin levels are important in the whole body response to insulin such as glucose regulation and fatty acid catabolism, a lowering of adiponectin would affect glucose homeostasis adversely and oppose the actions of insulin.

Briefly, the differences in the protease inhibitor effects observed in the different studies may be attributed to the different protease inhibitor drugs used in the studies, and to differences in experimental design. Some studies report that protease inhibitors induce different effects on different cell lines (Ben-Romano et al., 2003; Kovsan et al., 2009). Additionally, several protease inhibitors demonstrate different results *in vitro* and *in vivo* (Noor et al., 2006). However, the most consistent phenomenon observed has been the effect on glucose uptake, the most obvious physiological end result of insulin.

University Of Cape Town

Whether these phenomena arise primarily from effects on early steps in the insulin signalling pathway or otherwise is not entirely clear. Recent studies (Djedaini et al., 2009; Kachko et al., 2009) support the idea that protease inhibitors affect a more proximal level of the insulin signalling pathway, in particular tyrosine phosphorylation of the insulin receptor and its substrate, IRS-1. This leads to the inhibition of downstream insulin signalling events; in particular, extracellular glucose uptake by GLUT4, similar to insulin resistance in type 2 diabetes and obesity (Meyer et al., 2002; Nolan et al., 1994).

1.6 Objectives

The general mechanism of insulin resistance in type 2 diabetes and obesity (section 1.5.2) has been extensively studied. The study of the insulin resistance induced by protease inhibitors is still in its infancy, and the information available does not precisely allude to the mechanisms of insulin resistance because the studies have been performed using different models and have produced divergent findings.

Therefore, this study was undertaken to clarify the molecular basis of the insulin resistance induced by protease inhibitors using several cell culture models.

The objectives were therefore to:

1. Analyse the effects of protease inhibitors on the insulin signalling pathway of cells transfected with the insulin receptor, and in 3T3-L1 adipocytes. Of particular interest were the proximal steps of the insulin signalling cascade, and the associated regulatory proteins.

2. Analyse the effects of protease inhibitors on metabolic pathways in 3T3-L1 adipocytes, by analysing metabolites in the cell culture medium, particularly amino acids, organic acids and free fatty acids.

3. Analyse and compare the effects of protease inhibitors on lipoprotein lipase activity, an important step in the insulin-activated anabolic functions of adipocytes. This would be achieved by establishing a rapid method for analysing LPL activity in supernatants from 3T3-L1 adipocytes.

University Of Cape Town

CHAPTER 2: GENERAL MATERIALS AND METHODS

2.1 Methods

This study was designed to investigate the molecular basis of insulin resistance induced by protease inhibitors *in vitro,* using a cell culture system. The full study is summarised by the flowchart in Figure 2.1.

The study of insulin signalling was performed using two cell lines: CHO-IR cells (Ahmed and Pillay, 2001) and differentiated 3T3-L1 murine adipocytes (Wilcox et al., 2004). The CHO-IR cell line is a useful cell culture model for the study of insulin signalling; the cells are easy to culture as they have a short doubling time, making the planning of experiments relatively simple. They also have high levels of insulin receptor protein expression, allowing sensitive detection of changes in signalling proteins involved in the insulin receptor signalling pathway.

This study also used 3T3-L1 adipocytes, as these cells are a well-known model for studying the insulin signalling pathway and lipid metabolism *in vitro* (Glenn et al., 1992). The cells have a similar morphology and physiology to human adipocytes (Glenn et al., 1992), and also express additional substrates that are not present in CHO-IR cells, such as the APS and the GLUT4 transporter (Ahn et al., 2004).

The cells were serum-starved and then stimulated with insulin, both in the presence and absence of protease inhibitors saquinavir and indinavir. The cells were serum-starved to obtain the highest impact of insulin stimulation in the cells and to provide a high level of phosphorylation of the insulin receptor β-subunit. It is also used to reduce the basal level of phosphorylation induced by growth factors present in serum such that a higher level of stimulation is facilitated. The level of insulin stimulation was compared with that of the basal unstimulated cells (the control). The cell lysates were then subjected to immunoblotting with the appropriate antibodies. The CHO-IR cells were also pre-treated with sodium salicylate (known to reduce blood glucose), prior to treatment with the protease inhibitor (indinavir). The results were analysed using realtime imaging (ChemiImager).

In addition, the cell culture supernatants of 3T3-L1 adipocytes treated with protease inhibitors were used to assay lipoprotein lipase activity and for metabolomic analysis.

University Of Cape Town

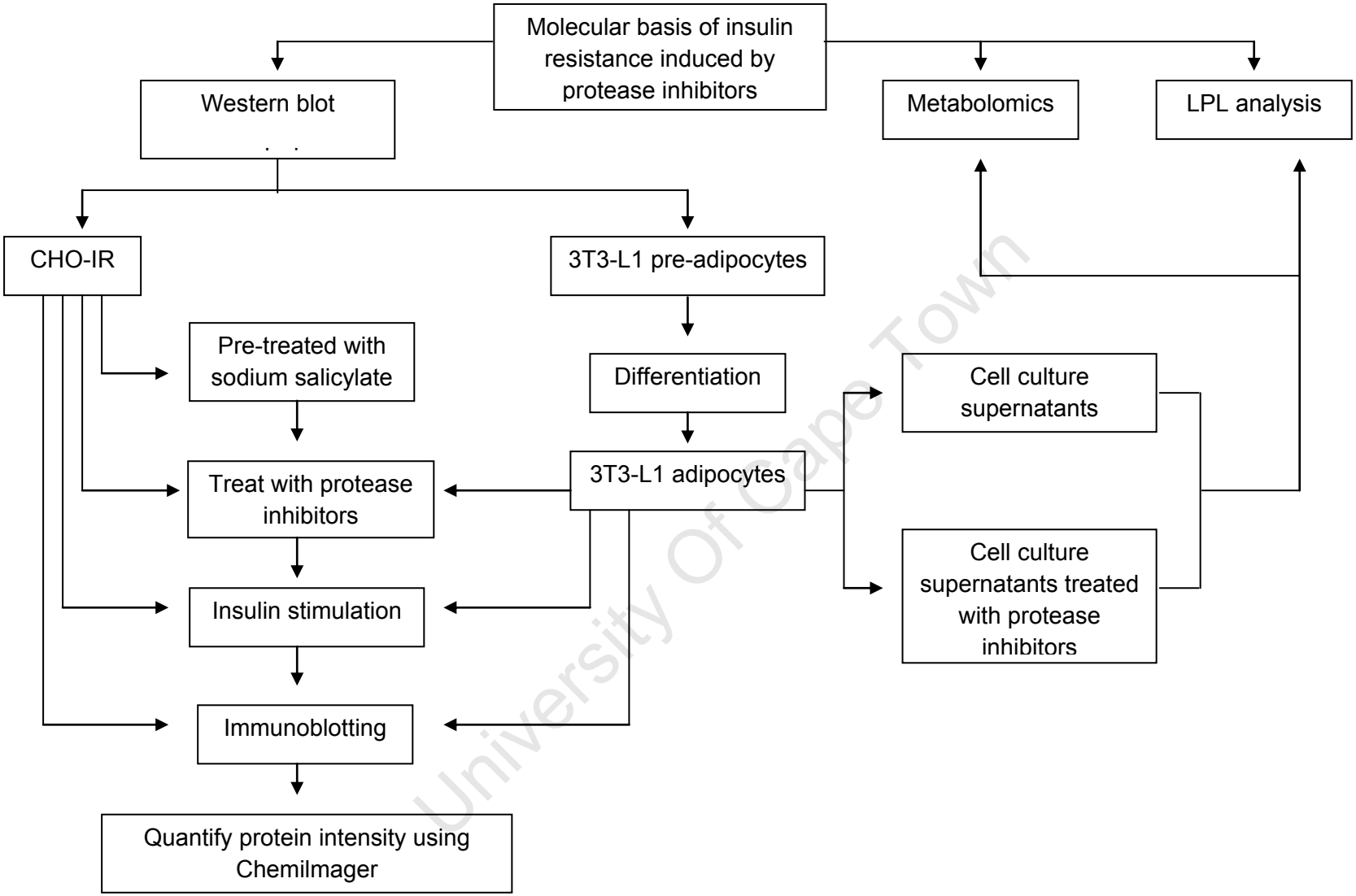

University Of Cape Town

Figure 2.1: Flowchart of study to understand molecular basis of insulin resistance induced by protease inhibitors in cell culture systems

2.1.1 Preparation of culture medium and maintenance of cell lines

The CHO-IR cells were cultured in Ham's F12 mixture culture medium in 75 cm^2 flasks, and incubated at 37 °C in a 5 % CO_2 incubator. The medium was supplemented with 10 % FCS, 2 mM L-glutamine, 1 % of 100 x antibiotic/antimycotic (combination of penicillin, streptomycin and amphotericin), 0.5 % gentamicin and 400 µg/ml G418-sulphate solution. Ham's F12 medium was used as a base medium for the CHO-IR cells as the cells require L-proline, which is supplied by the medium. FCS has a high level of insulin growth factor (IGF) to stimulate the growth of cells. L-glutamine is an essential amino acid for supporting the growth of cells, and is an alternative energy source for rapidly dividing cells and cells that use glucose inefficiently. Antibiotic/antimycotic solution is effective against the most common forms of cell culture contamination, including gram-positive and gram-negative bacteria, yeast and fungi. Gentamicin was used to prevent contamination of the mycoplasma in the cell culture medium. As mentioned earlier in this chapter, CHO-IR cells are transfected cells with insulin receptor. The transfected insulin receptor is on a plasmid that contains the G418 resistance gene. G418 is an antibiotic to ensure that only transfected cells are present in a flask while any cells that lose the plasmid will die.

Within 3-4 days, after the cells had reached semi-confluence, they were split for subculture in the following way: the culture medium was drained and the cells were rinsed, first with sterile phosphate buffered saline (PBS) (10 ml) and then with 1x trypsin-ethylenedinitrilotetraacetic acid (Trypsin-EDTA) (2 ml) solution. The flask was incubated at 37 °C for 2 min to allow the release of the cells from the flask. The trypsin reaction was terminated with 5 ml of culture medium, and 1 ml of the culture medium was then transferred to a new flask containing the fresh culture medium (20 ml).

The 3T3-L1 pre-adipocyte fibroblasts were cultured in four different culture media (named Medium 1, 2, 3 and 4) in 75 cm^2 flasks, and incubated at 37 °C in a 10 % CO_2 incubator during the process of maintenance culture and the induction of differentiation.

The 3T3-L1 pre-adipocytes were initially cultured in Medium 1 (Dulbecco's modified Eagle's medium (DMEM) with 10 % newborn calf serum (NCS), 2 mM L-glutamine, 1 % of 100 x antibiotic/antimycotic and 0.1 % gentamicin) to maintain 3T3-L1 fibroblast

University Of Cape Town

growth. DMEM was used as a base medium. NCS has a low level of IGF, which allows cells to grow as fibroblasts and prevents them from differentiating. After the cells had grown to 60-70 % confluence, they were split into a new flask, in order to maintain the fibroblasts for other experiments.

For the differentiation procedure, the pre-adipocytes were grown to confluence in Medium 1. Subsequently, the cells were induced to differentiate by placing them for two days in Medium 2 (DMEM with 10 % FCS, 2 mM L-glutamine, 1 % of 100 x antibiotic/antimycotic, 0.1 % gentamicin, 0.25 µM dexamethasone and 0.5 mM 3-isobutyl-1-methyl-xanthine (IBMX) and 166 nM insulin). FCS has a high level of IGF, which stimulates the differentiation of pre-adipocytes to adipocytes. Dexamethasone and IBMX were used to induce differentiation of 3T3-L1 pre-adipocytes through the activation of transcription factors, the CCAAT/echancer-binding proteins (C/EBPs) and the PPARγ. Insulin was added to the culture medium to facilitate the differentiation procedure in the cells. The differentiation of cells was continued for two days in Medium 3 (DMEM with 10 % FCS, 2 mM L- glutamine, 1 % of 100 x antibiotic/antimycotic, 0.1 % gentamicin and 166 nM insulin). The 3T3-L1 adipocytes were then cultured in Medium 4, which was prepared as for Medium 3, but without insulin to maintain the adipocyte differentiation.

Stocks of frozen CHO-IR cells and 3T3-L1 pre-adipocytes were routinely prepared for storage in liquid nitrogen. The freezing medium for CHO-IR cells was prepared using 20 % dimethyl sulfoxide (DMSO) in FCS solution. The freezing medium for 3T3-L1 adipocytes was prepared using 20 % DMSO in NCS solution. Following trypsinisation and suspension in culture medium, the cells were mixed in a cryotube, with a ratio of 1:1 to the freezing medium. The tube was then placed in an isopropanol cryo-freezing container at -80 °C. Isopropanol was added to the container to freeze the cells gradually in the liquid nitrogen. Isopropanol facilitated the temperature in the container to drop about 1°C per minute.

Cells were thawed by placing the cryotubes in 37 °C in an incubator for approximately 2 min, or until thawed. The cells/freezing medium solution was then added to 5 ml of the culture medium (i.e. Ham's F12 mixture culture medium, or Medium 1) in a 25 cm^2 flask, and resuspended. The culture medium was changed after 12 h, grown as above, and split into a 75 cm^2 flask when the cells were in a state of semi-confluence.

University Of Cape Town

2.1.2 Serum starvation procedure

1 x 10^5 cells/ml of CHO-IR cells were plated into 6-well plates until they were in a state of semi-confluence. In parallel, 3T3-L1 pre-adipocyte fibroblasts were subcultured in 3.5 cm dishes and then grown to full confluence, after which differentiation was induced (Mehra et al., 2007). Both CHO-IR cells and differentiated 3T3-L1 adipocytes were serum-starved for 16 h in a serum-free medium (2 mM L-glutamine, 1 % of 100 x antibiotic/antimycotic and 0.1 % gentamicin in DMEM). The cells were incubated at 37 ºC in an incubator, with 10 % CO_2.

Prior to aspirating the serum-free medium from the cells, the cells were stimulated with 10-100 ng/ml (1.7-17 nM) insulin for 5 min. The serum-free medium from the CHO-IR cells was discarded, and the medium from 3T3-L1 adipocytes was stored at -80 ºC for the subsequent analysis.

2.1.3 Preparation of cell lysates

After serum-starvation for 16 h, followed by insulin stimulation for 5 min, the serum-free medium was discarded. The 6-well plates were put on ice. Subsequently, 100 µl lysis buffer (consisting of 50 mM 4-(2-hydroxyethyl)-1-piperazineethanesulfonic acid (HEPES), pH 7.5, 1 % phenoxylpolyethoxyethanol (NP40), 10 % glycerol, 50 mM sodium chloride (NaCl), protease inhibitor and phosphatase inhibitor) was added evenly to the plates, which were left on ice for 10 min. Protease and phosphatase inhibitors were added to the lysis buffer to protect proteins of the cells against dephosphorylation. Specifically, protease inhibitor inhibits a broad spectrum of serine, cysteine, metalloproteases and calpains, while phosphatase inhibitor inhibits a broad spectrum of phosphatases such as acid, alkaline, serine/threonine and tyrosine protein phosphatase.

The cells were scraped with a scraper and transferred into a micro-centrifuge tube. They were then centrifuged at 4 °C and 10 000 rpm for 10 min. 60 µl of the cells were mixed with 15 µl of 5 x Laemmli buffer (25 nM Tris, pH 6.8, 2 % SDS, 0.002 % bromophenol blue, 10 % glycerol and 5 % 2-mercaptoethanol) prior to boiling at 100 ºC for 5 min, and brief spinning to settle all the evaporation from the lid of the micro-centrifuge tube. The cell lysate was stored at -20 °C prior to use, or at -80 °C for extended maintenance.

University of Cape Town

The experiment was repeated using cells treated with 0-100 µM protease inhibitors indinavir and saquinavir, left for 16 h in a serum-free medium followed by insulin stimulation.

2.1.4 Measurement of protein concentration

A Bradford protein assay was performed to measure the protein concentration of cell lysate (Bradford, 1976). This method is a colourimetric protein assay based on an absorbance shift in the dye Coomassie when bound to arginine and hydrophobic amino acid residues present in the protein. The colour of the dye is blue, and it has an absorption spectrum maximum of 595 nm. The increase in absorbance at 595 nm is proportional to the amount of bound dye, and thus to the amount (i.e. concentration) of protein present in the sample.

The concentrated dye reagent of Bio-Rad protein assay was added to dH_2O with ratio 1:5, to measure protein concentration in a sample. The reagent was then filtered using filter paper (110 mm diameter) prior to use.

Bovine serum albumin (BSA) (1 mg/ml) was prepared as a stock in dH_2O to generate a standard curve. The standard curve was designed with 5, 10 and 15 µl of BSA was added into the reagent to give final concentrations 5, 10 and 15 µg/ml. 5 µl of cell lysate was mixed with the reagent in another cuvette. The absorbance of the mixture in the cuvette was measured at 595 nm, with the reagent as a blank.

2.1.5 Preparation of protease inhibitors

5 mM indinavir and saquinavir, 1.2 mM tipranavir and 0.2 mM darunavir were prepared as a stock in dimethyl sulphoxide (DMSO) (final concentration 0.01 %) (Martin et al., 2009; Vernochet et al., 2005). DMSO was used as a solvent because the drugs are not water-soluble and furthermore, DMSO has minimal effects on the cells, in terms of the parameters under investigation (Martin et al., 2009; Vernochet et al., 2005).

2.1.6 Statistical analysis

Data are expressed as the mean ± S.E.M. of at least triplicate experiments. Statistical comparisons were made using Student's *t*-test or factorial-ANOVA using Microsoft Excel 2003, Statistica, GraphPad Prism and Sigma plotting software.

University of Cape Town

CHAPTER 3: THE EFFECT OF HIV PROTEASE INHIBITORS ON THE INSULIN SIGNALLING PATHWAY

3.1 Introduction

More than 60 % of HIV-positive patients treated with protease inhibitors suffer from various metabolic disorders; in particular, insulin resistance, which is associated with lipodystrophy, type 2 diabetes mellitus and cardiovascular disease (Barbaro, 2002; Esser et al., 2007; Florescu and Kotler, 2007; Stein, 2007).

Previous studies (Ismail et al., 2009) have suggested that the manifestation of insulin resistance due to treatment using protease inhibitors is likely to be a result of dysregulation of several cellular factors, specifically in the early steps in the pathway of insulin receptor signalling, in addition to alterations in GLUT4 transporter function.

In order to clarify the role of protease inhibitors in insulin resistance, the protease inhibitors saquinavir and indinavir were used in the present study. These drugs were obtained more readily than other protease inhibitors. Thus, the drugs were chosen for the study. CHO-IR cells and differentiated murine 3T3-L1 adipocytes were treated with various drug concentrations (0-100 μM) of saquinavir and indinavir for 16 h, followed by insulin stimulation (10-100 ng/ml) (1.7-17 nM).

CHO-IR cells were also pre-treated with a high dose of sodium salicylate (5 mM) for 1 h prior to indinavir treatment. These cells were selected as they have a short doubling time and a high level of insulin receptor expression than 3T3-L1 adipocytes. Sodium salicylate is known to reduce fasting blood glucose in diabetic patients (Yuan et al., 2001). The mechanism by which salicylates reduce blood glucose is well-understood (i.e. via IKKβ in the NFκB pathway) (Yuan et al., 2001). This may potentially explain the molecular basis of insulin resistance induced by protease inhibitors. Although sodium salicylate has been superseded by other oral hypoglycaemics such as metformin (Yuan et al., 2001), there has been a recent resurgence of interest in the use of salicylates as hypoglycaemic agents because of the role of IKKβ in mediating insulin resistance (Fleischman et al., 2008; Koska et al., 2009). In view of the above, the effects of sodium salicylate were also evaluated.

As mentioned previously, the precise mechanism by which protease inhibitors induce insulin resistance is not clear (Ismail et al., 2009). Therefore, the main objective of this study was to investigate possible mechanisms by which protease inhibitors

University Of Cape Town

induce insulin resistance in CHO-IR cells and 3T3-L1 adipocytes, by the analysis of signalling proteins in the insulin signalling cascade.

3.2 Methods

3.2.1 Preparation of acrylamide gels for sodium dodecyl sulphate polyacrylamide gel electrophoresis (SDS-PAGE)

An SDS polyacrylamide gel (8 cm x 7.3 cm) was prepared as a composite of two gels, following a standard protocol. The upper gel was a 4 % stacking gel (0.126 M Tris, pH 6.8, 4 % acrylamide/bis (19:1), 0.1 % SDS, 0.05 % ammonium persulphate (APS) and 0.1 % N, N, N', N',-tetramethylethylenediamine (TEMED)) and the lower gel was a 7.5 % resolving gel (0.375 M Tris, pH 8.8, 7.5 % acrylamide/bis (19:1), 0.1 % SDS, 0.05 % APS and 0.05 % TEMED) (Figure 3.1). The stacking gel contained the wells for loading the samples.

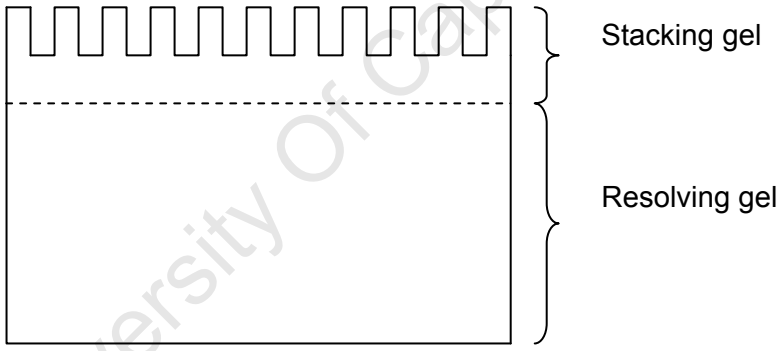

Figure 3.1: Acrylamide gel for SDS-PAGE

University Of Cape Town

3.2.2 Electrophoresis

Cell lysates (20 µl) (from section 2.2.3) and a marker (Precision Plus Protein Dual Colour Standard, Bio-Rad) (5 µl) were loaded into the wells of the gel. The gel was placed in a tank (Bio-Rad Mini Protean II apparatus) with a running buffer (0.025 M Tris, 0.192 M glycine and 0.1 % SDS). Electrophoresis was performed at 150 V and 0.06 A for 1 h.

3.2.3 Protein transfer

Following electrophoresis, the acrylamide gel was placed in a nitrocellulose membrane-filter paper transfer sandwich. The transfer sandwich was prepared as shown in Figure 3.2, and placed in a tank with a transfer buffer (0.025 M Tris, 0.192 M glycine and 20 % methanol), and an ice box and a bar stirrer to facilitate the dissipation of heat. The transfer procedure was performed at 100 V and 0.25 A for 2 h.

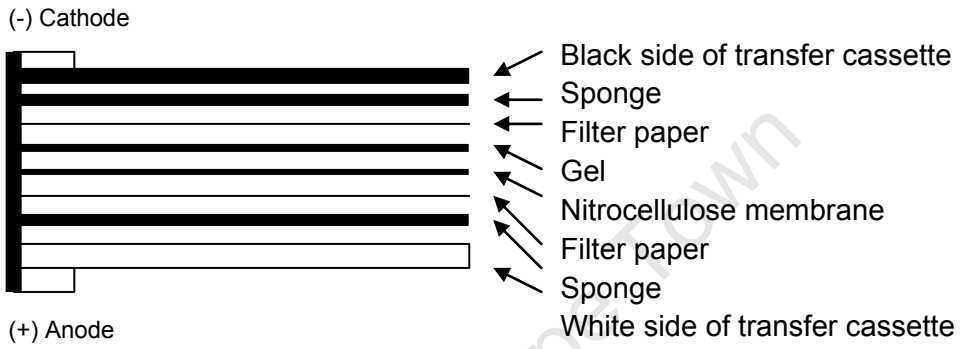

Figure 3.2: Transfer sandwich

3.2.4 Immunoblotting

The membrane was stained with 0.1 % Ponceau S in 5 % acetic acid, to confirm successful and even transfer of proteins to the membrane. The membrane was destained with deionised water and incubated in a blocking solution (3 % BSA or 5 % skimmed milk solution (Marvel) in Tris buffered saline (0.05 M Tris, 0.150 M NaCl, pH 7.4)) + 0.1% Tween 20 (TBST) for 1 h at room temperature (18-25 °C). The membrane was then incubated with a specific primary antibody (Table 3.2), and washed with 20 ml TBST for 15 min, 4 times.

The membrane was then incubated with a horseradish peroxidase (HRP)-labelled secondary antibody (Table 3.2) to detect the primary antibody bound to the protein of interest. It was rinsed once with TBST and then twice more with deionised water (20 ml). The membrane was then soaked in chemiluminescent reagent (Pierce) (4 ml) for 1 min, and excess reagent was drained using tissue paper. The membrane was covered with transparent plastic and exposed to X-ray film (Agfa) for a few sec to 1 h to capture a visual signal from the secondary antibody. The film was developed in developer (Ilford, Cheshire) for 1 min, washed with tap water, fixed with fixer (Ilford, Cheshire) for 1 min, washed again with tap water and then air-dried.

University Of Cape Town

Table 3.1: Incubation conditions for primary and secondary antibodies

<table>
<tr><th>Primary antibody</th><th>Concentration (antibody : blocking solution)</th><th>Incubation time</th><th>Temperature</th><th>Blocking solution</th><th>Secondary antibody</th><th>Concentration (antibody : blocking solution)</th><th>Incubation time</th><th>Temperature</th><th>Blocking solution</th></tr>
<tr><td>1) Mouse anti-PY20 (1 mg/ml)</td><td>1:2000</td><td rowspan="2">16 h (overnight) for 3T3-L1 adipocyte cell lysate and 1 h for CHO-IR cell lysate</td><td rowspan="2">4 °C for 16 h incubation and 18-25 °C (room temperature) for 1 h incubation</td><td>3% BSA</td><td>Goat anti-mouse (1 mg/ml)</td><td>1: 5000</td><td rowspan="11">1 h</td><td rowspan="11">18-25 °C</td><td>3% BSA</td></tr>
<tr><td>2) IR β-subunit rabbit polyclonal IgG (200 µg/ml)</td><td>1:1000</td><td rowspan="9">5% Milk solution</td><td>Goat anti-rabbit (400 µg/ml)</td><td rowspan="10">1: 1000</td><td rowspan="9">5% Milk solution</td></tr>
<tr><td>3) PTP1B rabbit polyclonal IgG (200 µg/ml)</td><td>1:200</td><td rowspan="3">16 h</td><td rowspan="3">4 °C</td><td rowspan="4">Goat anti- rabbit (400 µg/ml)</td></tr>
<tr><td>4)SOCS-1 rabbit polyclonal IgG (200 µg/ml)</td><td rowspan="6">1:1000</td></tr>
<tr><td>5)SOCS-3 rabbit polyclonal IgG (200 µg/ml)</td></tr>
<tr><td>6) SH2B rabbit polyclonal IgG (crude serum) (Kotani et al., 1998)</td><td rowspan="2">1 h</td><td rowspan="2">18-25 °C</td></tr>
<tr><td>7) Actin goat polyclonal IgG (200 µg/ml)</td><td>Mouse anti- goat (1 mg/ml)</td></tr>
<tr><td>8) Total IRS-1 rabbit polyclonal IgG (200 µg/ml)</td><td rowspan="3">16 h</td><td rowspan="3">4 °C</td><td rowspan="3">5% BSA</td><td rowspan="3">Goat anti- rabbit (400 µg/ml)</td></tr>
<tr><td>9) pIRS-1 (S307) rabbit polyclonal IgG (200 µg/ml)</td></tr>
<tr><td>10) APS (200 µg/ml) rabbit polyclonal IgG</td></tr>
</table>

PY20 = phosphotyrosine, IR = insulin receptor, PTP1B = protein tyrosine phosphatase 1 B, SOCS-1 = suppressor of cytokines signalling 1, SOCS-3 = suppressor of cytokines signalling 3, SH2B = Src homology 2 B, IRS-1 = insulin receptor substrate 1, pIRS-1 (S307) = phosphoIRS-1 at serine 307, APS = adapter protein with a pleckstrin homology domain and an SH2 domain.

University Of Cape Town

3.2.5 Stripping of membranes

The membrane was stripped with a stripping solution (0.063 M Tris, pH 6.8, 2 % SDS and 0.1 M 2-mercaptoethanol) for 30 min at 50 ºC, incubated in a blocking solution once more and then reprobed with a different primary antibody (Table 3.2) as indicated in Section 3.2.4.

3.2.6 Treatment with sodium salicylate

50 mM sodium salicylate was prepared freshly in 1 M Tris, pH 7.4 (Yuan et al., 2001). CHO-IR cells were pre-treated with sodium salicylate (0.5-5 mM) at 37 ºC for 1 h prior to treatment with indinavir (100 µM) for 16 h. The cell lysates were prepared as described in section 2.2.3.

3.2.7 Quantification of chemiluminescence

The membrane was analysed using a realtime imager, ChemiImager (Fluorchem 5500 Programme, Alpha Innotech Corporation, CA, USA) to quantify the chemiluminescent intensity.

3.3 Results

3.3.1 Pilot studies using different protease inhibitors in a range of concentrations

Initially, saquinavir was used to examine the effects of protease inhibitors in the insulin receptor signalling pathway in CHO-IR cells and 3T3-L1 adipocytes. The cells were pre-treated with saquinavir (20-50 µM) for 16 h followed by insulin stimulation (100 ng/ml) (17 nM) for 5 min. Saquinavir inhibited tyrosine phosphorylation of the insulin receptor β-subunit in both cell lines (Figure 3.3(a) and (b)). Saquinavir also decreased the expression levels of total insulin receptor β-subunit and actin (Figure 3.3(a) and (b)). These findings suggest that saquinavir was probably toxic to the cells.

University Of Cape Town

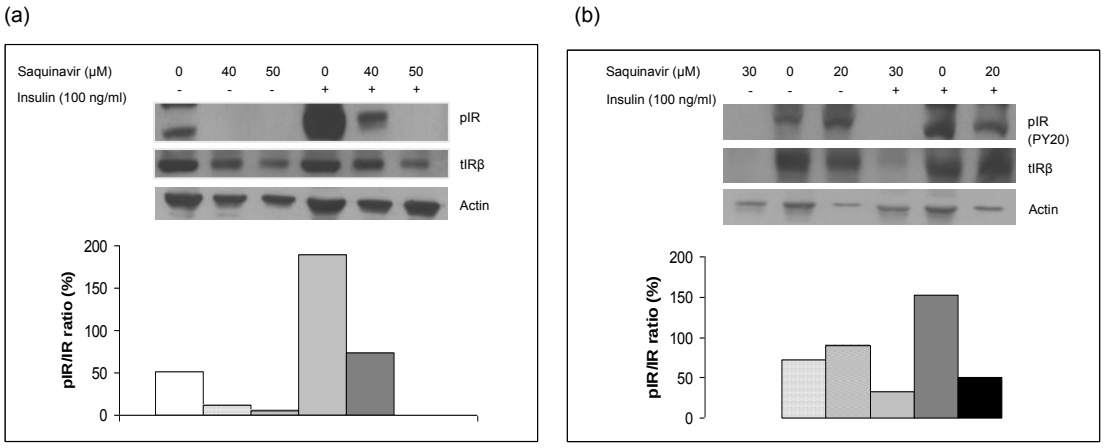

Figure 3.3: Effects of saquinavir on insulin-stimulated tyrosine phosphorylation in (a) CHO-IR cells and (b) 3T3-L1 adipocytes. CHO-IR cells and 3T3-L1 adipocytes were treated with different concentrations of saquinavir for 16 h followed by insulin stimulation. The cells were then lysed and the lysates subjected to immunoblotting with anti-phosphotyrosine PY20 antibody (upper panels). The blots were then stripped and reprobed with anti-IR β-subunit and anti-actin (lower panels). Bound antibodies were made visible by chemiluminescence. Chemiluminescence was quantified by realtime imaging. The band intensity of the proteins from one experiment was normalised to the band intensity of total IR protein. The discontinuity in saquinavir concentrations in Figure 3.3(b) was inadvertent. pIR (PY20) = tyrosine phosphorylation of IR, tIRβ = total insulin receptor β-subunit.

CHO-IR cells (Figure 3.4) and 3T3-L1 adipocytes (Figure 3.5) were pre-treated with indinavir (10-50 μM) for 16 h followed by insulin stimulation (10 ng/ml) (1.7 nM) for 5 min. In CHO-IR cells, 50 μM indinavir inhibited tyrosine phosphorylation of the insulin receptor β-subunit without showing any effects on the expression levels of total insulin receptor β-subunit and actin (Figure 3.4). No inhibition of tyrosine phosphorylation on the insulin receptor β-subunit was observed in CHO-IR cells treated with 10-40 μM indinavir (Figure 3.4).

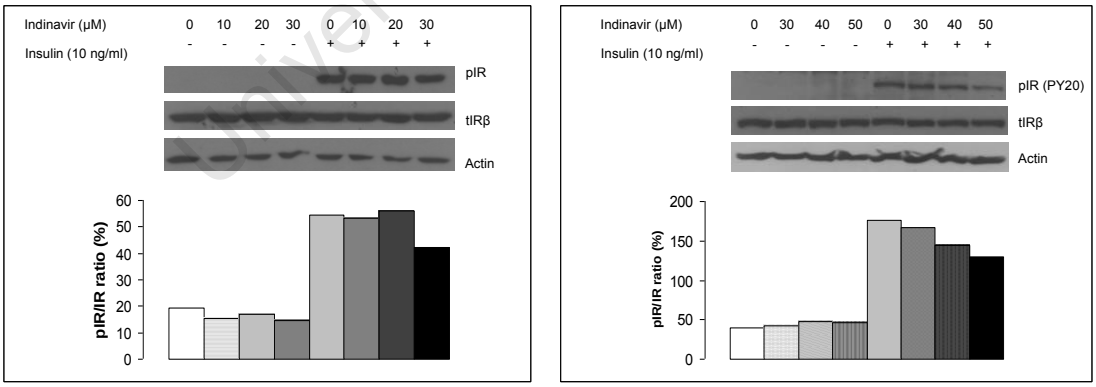

Figure 3.4: Effects of indinavir on insulin-stimulated tyrosine phosphorylation in CHO-IR cells. CHO-IR cells were treated with different concentrations of indinavir for 16 h followed by insulin stimulation. The cells were then lysed and the lysates subjected to immunoblotting with anti-phosphotyrosine PY20 antibody (upper panels). The blots were then stripped and reprobed with anti-IR β-subunit and anti-actin (lower panels). Bound antibodies were visualised by chemiluminescence. Chemiluminescence was quantified by realtime imaging. The band intensity of the proteins from one experiment was normalised to the band intensity of total IR protein. pIR (PY20) = tyrosine phosphorylation of IR, tIRβ = total insulin receptor β-subunit.

University Of Cape Town

In 3T3-L1 adipocytes, 50 μM indinavir significantly inhibited tyrosine phosphorylation of the insulin receptor β-subunit (p = 0.003) without having any effect on the expression levels of total insulin receptor β-subunit and actin (Figure 3.5).

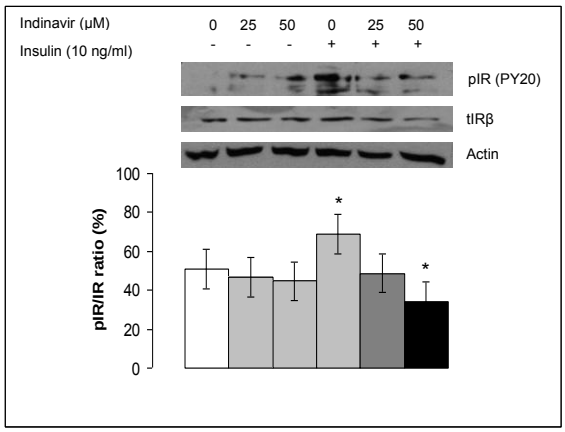

Figure 3.5: Effects of indinavir on insulin-stimulated tyrosine phosphorylation in 3T3-L1 adipocytes. 3T3-L1 adipocytes were treated with different concentrations of indinavir for 16 h followed by insulin stimulation. The cells were then lysed and the lysates subjected to immunoblotting with anti-phosphotyrosine PY20 antibody (upper panel). The blots were then stripped and reprobed with anti-IR β-subunit and anti-actin (lower panels). Bound antibodies were visualised by chemiluminescence. Chemiluminescence was quantified by realtime imaging. The band intensity of the proteins from six independent experiments for 3T3-L1 adipocytes was normalised to the band intensity of total IR protein. Data are shown as the mean ± S.E.M. (n=6). pIR (PY20) = tyrosine phosphorylation of IR, tIRβ = total insulin receptor β-subunit, *p < 0.05 versus cells stimulated with insulin without indinavir treatment, using Student's *t*-test.

3.3.2 Effect of protease inhibitors on tyrosine phosphorylation of insulin receptor β-subunit and IRS-1

Based on the previous results, indinavir was then used to study the molecular basis of the effects of protease inhibitors on the insulin signalling pathway in both cell lines. CHO-IR cells and 3T3-L1 adipocytes were pre-treated with indinavir for 16 h prior to stimulation with a submaximal insulin concentration (10 ng/ml) (1.7 nM) for 5 min. In CHO-IR cells, samples pre-treated with indinavir and stimulated with insulin showed a significant decrease in tyrosine phosphorylation of the insulin receptor β-subunit (p = 0.02) (Figure 3.6(a)) and in the phosphorylation of IRS-1 (p = 0.0002) (Figure 3.6(b)). In 3T3-L1 adipocytes under the same conditions, there was a significant decrease in tyrosine phosphorylation of the insulin receptor β-subunit (p = 0.003) (Figure 3.7(a)) and IRS-1 (p = 0.0002) (Figure 3.7(b)), compared to cells stimulated with insulin only. Based on chemiluminescence results and statistical analysis, indinavir itself did not increase basal pIR (3T3-L1 adipocytes) and pIRS (CHO-IR cells)

The expression levels of total insulin receptor β-subunit and IRS-1 were also examined to determine if the decreased tyrosine phosphorylation was due to

University Of Cape Town

changes in protein expression. There were no significant differences in expression levels of insulin receptor β-subunit and IRS-1 among the samples, indicating that the decreased signal observed (Figures 3.6 and 3.7) was due to a decrease in tyrosine phosphorylation rather than a decrease in total protein levels. In addition, the expression level of actin was examined as a loading control for cellular protein.

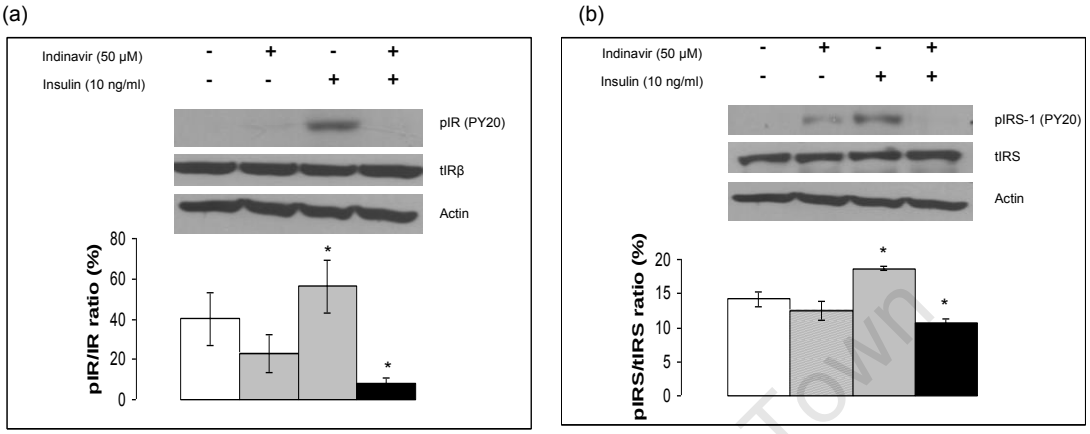

Figure 3.6: Effects of indinavir on insulin-stimulated tyrosine phosphorylation in CHO-IR cells. CHO-IR cells were treated with indinavir (50 μM) for 16 h, followed by insulin stimulation. The cells were then lysed and the lysates subjected to immunoblotting with anti-phosphotyrosine PY20 antibody (upper panels). The blots were then stripped and reprobed with anti-IR β-subunit, anti-IRS-1 and anti-actin (lower panels). Bound antibodies were visualised by chemiluminescence. Chemiluminescence was quantified by realtime imaging. The band intensity of the proteins from three independent experiments was normalised to the band intensity of total IR or IRS protein. Data are shown as the mean ± S.E.M. (n=3). pIR (PY20) = tyrosine phosphorylation of IR, tIRβ = total insulin receptor β-subunit, pIRS-1 (PY20) = tyrosine phosphorylation of IRS-1 and tIRS-1 = total IRS-1, *p < 0.05 versus cells with insulin stimulation only, using Student's *t*-test (Lord test).

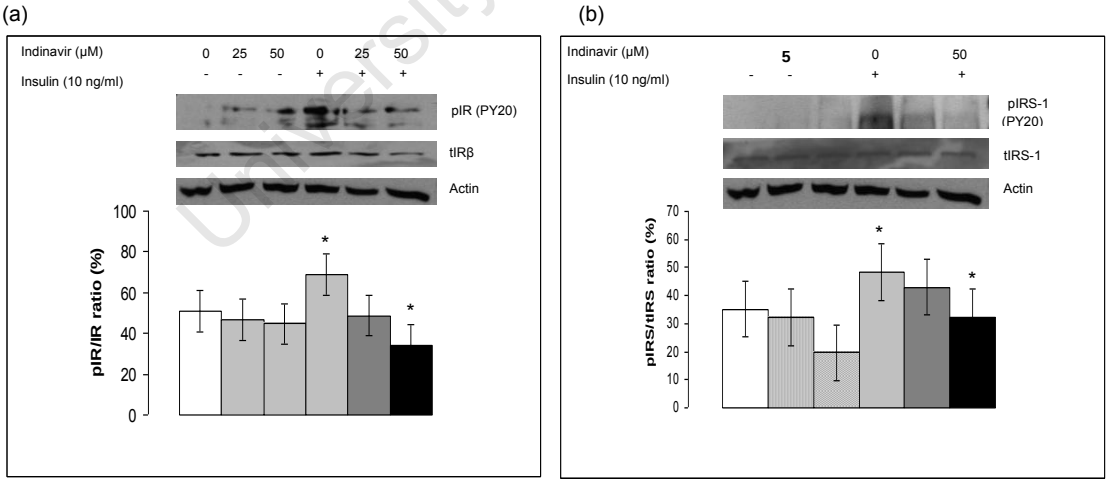

Figure 3.7: Effects of indinavir on insulin-stimulated tyrosine phosphorylation in 3T3-L1 adipocytes. 3T3-L1 adipocytes were treated with different concentrations of indinavir for 16 h, followed by insulin stimulation. The cells were then lysed and the lysates subjected to immunoblotting with anti-phosphotyrosine PY20 antibody (upper panels). The blots were then stripped and reprobed with anti-IR β-subunit, anti-IRS-1 and anti-actin (lower panels). Bound antibodies were visualised by chemiluminescence. Chemiluminescence was quantified by realtime imaging. The band intensity of the proteins from six independent experiments was normalised to the band intensity of total IR or IRS protein. Data are shown as the mean ± S.E.M. (n=6). pIR PY20 = tyrosine phosphorylation of IR, tIRβ = total insulin receptor β-subunit, pIRS-1 (PY20) = tyrosine phosphorylation of IRS-1 and tIRS-1 = total IRS-1, *p < 0.05 versus cells with insulin stimulation only, using Student's *t*-test. Figure 3.7(a) has been shown at Figure 3.5.

University of Cape Town

Based on these results, two possible hypotheses may be formulated:

1. the drug inhibits the insulin receptor kinase directly, or

2. the drug effects are indirect, and involve a regulator of tyrosine phosphorylation.

In order to test these hypotheses, the blots were stripped and reprobed with antibodies against regulatory proteins of insulin receptor signalling, such as serine 307 phosphorylated IRS-1, PTP1B, SOCS-1 and -3, SH2B and APS.

3.3.3 Effect of protease inhibitors on regulatory proteins in the insulin signalling pathway

There was a significant increase in the level of phosphorylated serine 307 on IRS-1 in both cell lines, CHO-IR cells ($p = 0.001$) (Figure 3.8(a)) and 3T3-L1 adipocytes ($p = 0.004$) (Figure 3.8(b)), treated with indinavir and then stimulated with insulin, compared to cells stimulated with insulin alone. These results were not accompanied by a change in the level of total IRS-1 (Figures 3.8(a) and 3.8(b)).

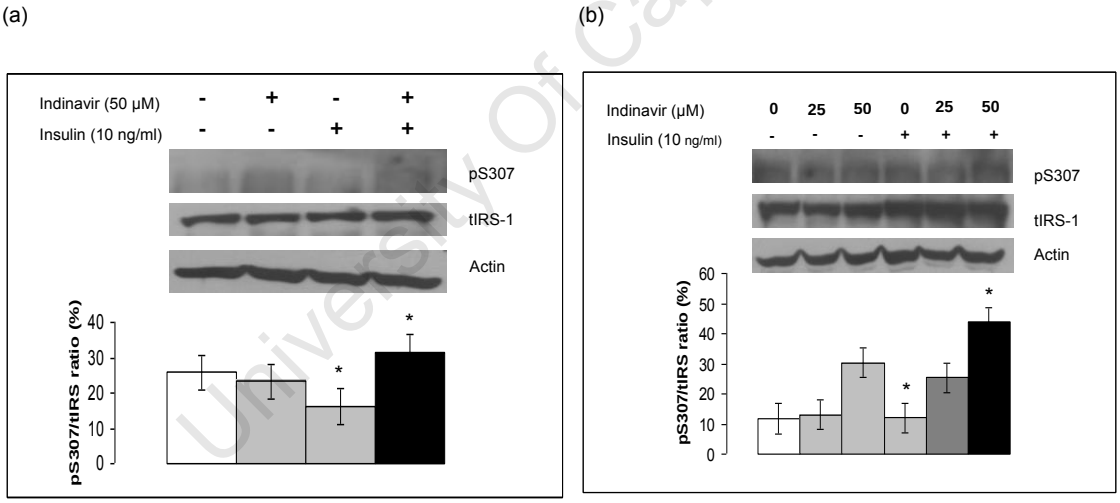

Figure 3.8: Effects of indinavir on serine 307 phosphorylation of IRS-1 in the insulin signalling pathway in (a) CHO-IR cells and (b) 3T3-L1 adipocytes. CHO-IR cells and 3T3-L1 adipocytes were treated with different concentrations of indinavir for 16 h, followed by insulin stimulation. The cells were then lysed and the lysates subjected to immunoblotting with an antibody against pS307 (upper panels). The blots were then stripped and reprobed with anti-IRS or anti-actin (lower panels). Bound antibodies were visualised by chemiluminescence. Chemiluminescence was quantified by realtime imaging. The band intensity of the proteins from three independent experiments was normalised to the band intensity of total IRS protein. Data are shown as the mean ± S.E.M. (n=3). pS307 = phosphorylated serine at residue 307, tIRS-1 = total IRS-1, *$p < 0.05$ versus cells with insulin stimulation only, using Student's *t*-test (Lord test).

University Of Cape Town

The expression levels of PTP1B, SOCS-1 and -3, and SH2B in CHO-IR cells after pre-treatment with indinavir were not significantly different (Figure 3.9(a, b, c, d)).

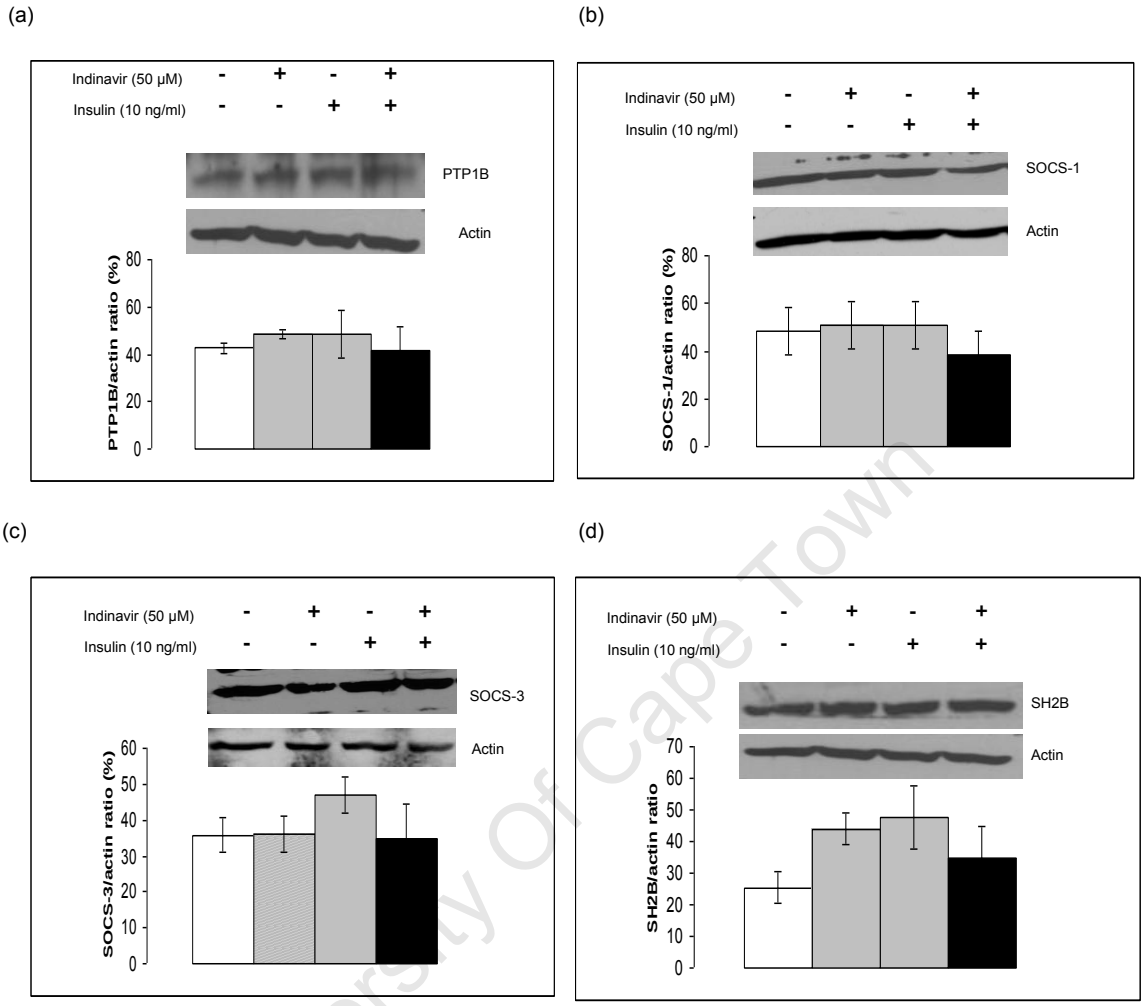

Figure 3.9: Effects of indinavir on regulatory proteins in the insulin signalling pathway in CHO-IR cells. CHO-IR cells were treated with indinavir (50 μM) for 16 h followed by insulin stimulation. The cells were then lysed and the lysates subjected to immunoblotting with antibodies against: (a) PTP1B (b) SOCS-1 (c) SOCS-3 (d) SH2B (upper panels). The blots were then stripped and reprobed with anti-actin (lower panels). Bound antibodies were visualised by chemiluminescence. Chemiluminescence was quantified by realtime imaging. The band intensity of the proteins from five independent experiments was normalised to the band intensity of actin. Data are shown as the mean ± S.E.M. (n=5). PTP1B = protein tyrosine phosphatase 1 B, SOCS-1 = suppressor of cytokines signalling 1, SOCS-3 = suppressor of cytokines signalling 3, SH2B = Src homology 2 B.

University Of Cape Town

In 3T3-L1 adipocytes, pre-treatment with indinavir did not significantly alter the expression levels of PTP1B, SOCS-1 and -3, SH2B1 and APS (Figure 3.10(a, b, c, d, e)).

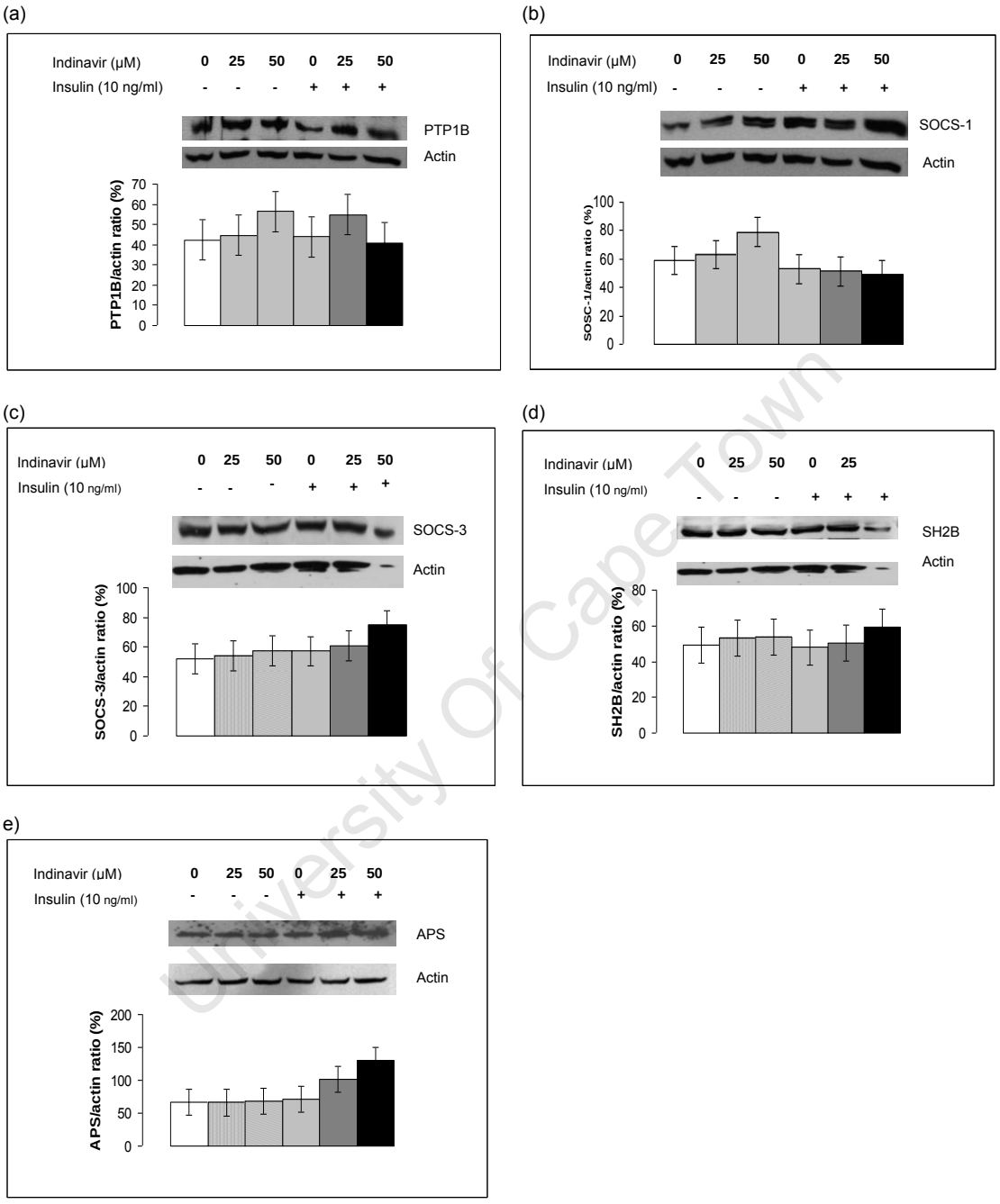

Figure 3.10: Effects of indinavir on regulatory proteins in the insulin signalling pathway in 3T3-L1 adipocytes. 3T3-L1 adipocytes were treated with different concentrations of indinavir for 16 h, followed by insulin stimulation. The cells were then lysed and the lysates subjected to immunoblotting with antibodies against: (a) PTP1B (b) SOCS-1 (c) SOCS-3 (d) SH2B (e) APS (upper panels). The blots were then stripped and reprobed with anti-actin (lower panels). Bound antibodies were visualised by chemiluminescence. Chemiluminescence was quantified by realtime imaging. The band intensity of the proteins from three to six independent experiments was normalised to the band intensity of actin. Data are shown as the mean ± S.E.M. (n=3 to 6). PTP1B = protein tyrosine phosphatase 1 B, SOCS-1 = suppressor of cytokines signalling 1, SOCS-3 = suppressor of cytokines signalling 3, SH2B = Src homology 2 B, APS = adapter protein with a pleckstrin homology domain and an SH2 domain.

University Of Cape Town

3.3.4 Effect of protease inhibitors after pre-treatment with sodium salicylate

CHO-IR cells were used to examine the effects of sodium salicylate on indinavir treatment, as the cells have a high level of insulin receptor expression, which facilitates more sensitive detection of changes in signalling proteins than is the case with 3T3-L1 adipocytes.

Cells pre-treated with sodium salicylate prior to treatment with indinavir showed a significant increase in insulin-stimulated tyrosine phosphorylation of the insulin receptor β-subunit ($p = 0.002$) (Figure 3.11(a)) when compared to cells treated with indinavir and insulin only. In fact, insulin-stimulated tyrosine phosphorylation was restored to the levels seen in the presence of insulin only, without indinavir. This indicates that sodium salicylate blocked the effects of indinavir to inhibit tyrosine phoshorylation of the insulin receptor β-subunit.

A slight, but statistically insignificant, increase in insulin-stimulated tyrosine phosphorylation of IRS-1 was also observed after salicylate treatment, when compared to cells treated with indinavir and insulin alone (Figure 3.11(b)). Sodium salicylate also decreased phosphorylation of IRS-1 at serine 307 twofold, although this was not statistically significant compared to cells treated with indinavir followed by insulin (Figure 3.11(c)).These results suggest that sodium salicylate treatment abrogated the effects of indinavir to inhibit tyrosine phosphorylation of the insulin receptor β-subunit and IRS-1 in parallel with a decrease in phosphorylation of IRS-1 at serine 307 (Figure 3.11(a, c)).

University of Cape Town

(a)

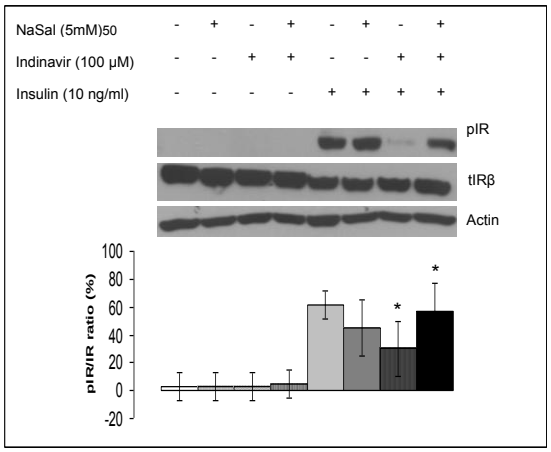

(b)

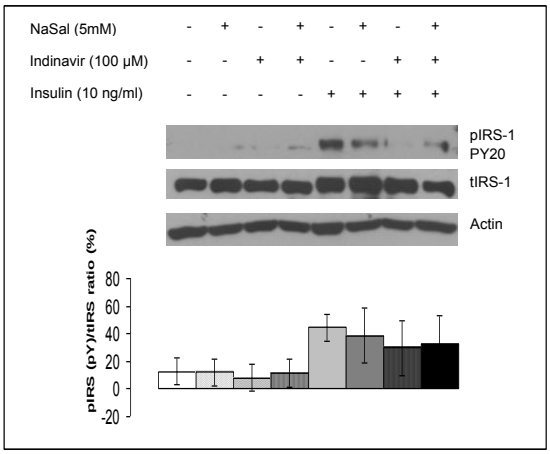

(c)

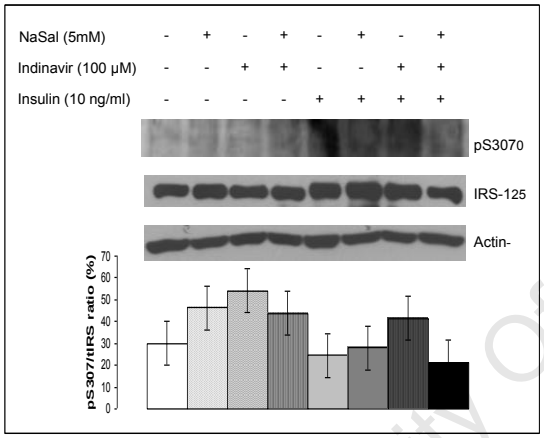

University Of Cape Town

Figure 3.11: Effects of indinavir in the insulin signalling pathway of CHO-IR cells after pre-treatment with sodium salicylate. CHO-IR cells were pre-treated with sodium salicylate (5 mM) for 1 h prior to treatment with indinavir (100 µM) for 16 h. The cells were stimulated with insulin for 5 min. The cells were then lysed and the lysates subjected to immunoblotting with antibodies against: (a) and (b) anti-phosphotyrosine PY20 antibody and (c) pS307 (upper panels). The blots were then stripped and reprobed with anti-IR, anti-IRS-1 and anti-actin (lower panels). Bound antibodies were visualised by chemiluminescence. Chemiluminescence was quantified by realtime imaging. The band intensity of the proteins from three independent experiments was normalised to the band intensity of total IR or IRS-1 protein. Data are shown as the mean ± S.E.M. (n=3). pIR PY20 = tyrosine phosphorylation of IR, pIRS-1 PY20 = tyrosine phosphorylation of IRS-1, tIRβ = total insulin receptor β-subunit, pS307 = phosphorylated serine at residue 307 of IRS-1, tIRS-1 = total IRS-1, *p< 0.05 versus cells treated with indinavir and stimulated with insulin, using factorial-ANOVA.

3.4 Discussion

The effects of antiretroviral protease inhibitors have been examined in numerous studies (for a review, see Ismail et al., 2009, and Chapter 1 of this study). The majority of studies have focused largely on downstream events in the insulin signalling pathway. Protease inhibitors, including saquinavir and indinavir, were found to inhibit glucose uptake by preventing the migration of GLUT4 from the

cytoplasm to the cell surface (Ben-Romano et al., 2003; Murata et al., 2002; Noor et al., 2002; Ranganathan and Kern, 2002). However, the underlying mechanism of this process has not yet been explained, and it is possible that these effects on glucose uptake may have resulted from inhibition at a proximal level. Few studies have examined proximal steps in the insulin signalling cascade. Areas still to be investigated include insulin binding to the receptor, and activation of intrinsic tyrosine kinase activity; and the subsequent tyrosine phosphorylation of substrate, where direct or indirect drug-induced inhibition may occur.

In this study, for the first time, CHO-IR cells were used to analyse the effects of protease inhibitors on the insulin receptor β-subunit phosphorylation and tyrosine kinase activation. Saquinavir inhibited tyrosine phosphorylation of the insulin receptor β-subunit in CHO-IR cells and 3T3-L1 adipocytes. The drug also decreased the expression levels of insulin receptor β-subunit and actin in both cell lines. It is possible that saquinavir is toxic at 20 μM concentration. In addition, using an inverted microscope, the cells observed did not show normal growth at this concentration. The finding of saquinavir toxicity is supported by a previous study using a cell proliferation assay to monitor cell viability of human fibroblasts, 3T3-L1 fibroblasts, L6 myoblasts and myotubes (Germinario and Colby-Germinario, 2003). However, indinavir was not toxic to the cells at the same concentration (Germinario and Colby-Germinario, 2003). Thus, indinavir was used to study the effects of protease inhibitors in the insulin signalling pathway in cell lines in the present study.

The results of this study reveal that CHO-IR cells treated with indinavir (50 μM) for 16 h, followed by insulin stimulation, inhibited tyrosine phosphorylation of the insulin receptor β-subunit and IRS-1. These are early events following the binding of insulin to the insulin receptor. The same effect was observed in 3T3-L1 adipocytes. In a prior study using HepG2 hepatoma cells, it was reported that indinavir (100 μM) treatment for 48 h decreased tyrosine phosphorylation of the IRS-1 protein, but not phosphorylation of the insulin receptor itself (Schutt et al., 2000). The effects of indinavir may differ in different cell lines, depending on the experimental model and the duration of the exposure (Ben-Romano et al., 2003; Kovsan et al., 2009; Noor et al., 2006).

The indinavir concentration used in this study was higher than previously reported plasma concentrations (11 μM) (Lin, 1999). A prior study reported that indinavir accumulates in adipose tissue (Vernochet et al., 2005). Therefore, *in vivo,* drug concentrations at plasma levels do not reflect the actual drug concentrations at tissue

University Of Cape Town

levels, which may be higher than the circulating plasma levels (Ranganathan and Kern, 2002). The effects of indinavir observed in the present study are unlikely to be due to cellular toxicity, as the drug inhibited tyrosine phosphorylation of the insulin receptor β-subunit without decreasing the expression levels of insulin receptor β-subunit and actin in CHO-IR cells and 3T3-L1 adipocytes. This finding is supported by an early study, using a cell viability test, which showed that indinavir was not toxic to a number of cells, even at concentrations of 100 μM (Germinario and Colby-Germinario, 2003). Therefore, the range of indinavir used in the present study was 0-100 μM.

In a cellular context, *ex vivo*, the effects of indinavir may only be apparent at submaximal insulin concentrations, which are more typical of physiological circulating insulin concentrations. For this reason, a submaximal concentration of 10 ng/ml (1.7 nM) insulin has been used to stimulate the cells, even though the maximal activation of the insulin receptor tyrosine phosphorylation is observed at levels approximately tenfold higher than 10 ng/ml, i.e. 100 ng/ml (17 nM). Therefore, even though the maximal activation of insulin receptor tyrosine phosphorylation is observed at much higher levels of insulin in CHO-IR cells, the effects of insulin used at pharmacological concentrations in a cell line that overexpresses insulin receptors at such a high level may mask the inhibitory effects of indinavir.

The inhibition of tyrosine phosphorylation of the insulin receptor kinase and its substrate, IRS-1, implies that indinavir interacts at a very proximal step in the insulin signalling pathway. There are two possible mechanisms that may explain this. The drug may act directly to inhibit the insulin receptor kinase, or the drug may affect other proteins that regulate intrinsic tyrosine kinase activity. In order to address this hypothesis, the blots were stripped and reprobed with antibodies against regulatory proteins of insulin receptor signalling, such as serine 307 phosphorylated IRS-1, PTP1B, SOCS-1 and -3, SH2B and APS.

The protein expression of PTP1B in CHO-IR cells and 3T3-L1 adipocytes after pre-treatment with indinavir was not significantly different compared to control. PTP1B, a tyrosine phosphatase, may negatively regulate insulin signalling by binding to the tyrosine phosphorylated proteins, insulin receptor β-subunit and IRS-1 (Cheng et al., 2002) and catalysing dephosphorylation. However, the effect of protease inhibitors on PTP1B expression *in vivo* and *in vitro* has not been investigated. In this study, it was found that indinavir did not affect the protein expression in either cell line.

University Of Cape Town

The protein expression of SOCS-1 and -3 in CHO-IR cells and 3T3-L1 adipocytes was again not significantly different after treatment with indinavir compared to control. SOCS-1 and -3 are adapter proteins that bind to the insulin receptor β-subunit or IRS-1 or IRS-2 to inhibit downstream signalling. Increased SOCS-1 and -3 expression has been reported to be increased after treatment with indinavir and this could induce insulin resistance by preventing tyrosine phosphorylation and subsequent activation of IRS-1 and -2 proteins (Carper et al., 2008). In addition, it has been reported that SOCS-1 and -3 negatively regulate the insulin signalling pathway, without modifying the insulin receptor tyrosine kinase activity (Emanuelli et al., 2001).

Furthermore, SOCS-1 and -3 expression can be induced by TNF-α (Emanuelli et al., 2001). TNF-α induces insulin resistance (Lee et al., 2009). However, this cytokine is released from immune cells and adipose tissue, and not from CHO-IR cells. Thus, there was no change in SOCS-1 and -3 protein expression in CHO-IR cells following treatment with indinavir. Similarly, the protein expression of SOCS-1 and -3 was not significantly altered in 3T3-L1 adipocytes treated with indinavir. Thus, the results of this study indicate that in CHO-IR cells and 3T3-L1 adipocytes, these proteins are not involved in decreasing phosphorylation of the insulin receptor β-subunit.

SH2B (aka SH2B1) is an adapter protein involved in the signalling pathway mediated by insulin tyrosine kinases and Janus kinase. Deletion of the adapter protein gene in mice results in severe obesity, infertility, and leptin and insulin resistance (Maures et al., 2007). This protein has also been shown to regulate the tyrosine phosphorylation state of the insulin receptor (Ahmed and Pillay, 2001). However, the expression of SH2B in CHO-IR cells and 3T3-L1 adipocytes was not significantly altered after treatment with indinavir.

The adapter protein, APS (aka SH2B2) has similar roles to SH2B protein in that both proteins delay dephosphorylation of the insulin receptor kinase and IRS-1 and -2 in the insulin signalling pathway (Ahmed and Pillay, 2001; Ahmed and Pillay, 2003). However, APS binds the insulin receptor with a higher affinity than SH2B (Ahmed and Pillay, 2001; Ahmed and Pillay, 2003). CHO-IR cells lack endogenous APS protein (Ahmed et al., 2000). Thus, in this study, only 3T3-L1 adipocytes were used to analyse this protein (Ahn et al., 2004). The protein expression of APS in 3T3-L1 adipocytes was not significantly different after treatment with indinavir compared to control.

University Of Cape Town

Indinavir treatment resulted in a significant increase in phosphorylation of IRS-1 at serine 307 in both CHO-IR cells and 3T3-L1 adipocytes. Serine phosphorylation of IRS-1 is known to inhibit phosphorylation of the insulin receptor. Indinavir may induce pro-inflammatory cytokines such as TNF-α or unknown cytokines in the cells, which activate IKKβ. IKKβ is a serine kinase that regulates the activation of NFκB, a critical activator of genes involved in inflammation and immunity. Prior to activation, NFκB is bound to the inhibitor κB (IκB). The activated IKKβ phosphorylates the NFκB-IκB complex, which stimulates conjugation of IκB with ubiquitin and the subsequent degradation of IκB protein in the proteasome, leading to the nuclear translocation of NFκB (Tergaonkar, 2006). Activation of IKKβ also induces serine phosphorylation of IRS-1, as IRS-1 is a substrate of IKKβ. This phosphorylation blocks interactions with the insulin receptor β-subunit, decreases tyrosine phosphorylation, and inhibits insulin action in the cells (Aguirre et al., 2002; Gao et al., 2003).

High doses of salicylate (4 to 10 g per day), including sodium salicylate and aspirin, are known to reduce blood glucose concentrations in diabetic patients via inhibition of NFκB and its upstream activator IKKβ (Yuan et al., 2001). In this study, sodium salicylate was used for the first time in the context of cells treated with protease inhibitors. In CHO-IR cells treated with protease inhibitors, the present findings revealed that salicylate inhibits the effects of indinavir on insulin receptor tyrosine phosphorylation, even at 100 μM concentration of indinavir, which was the concentration used to obtain the maximal effect of the drug on insulin receptor tyrosine phosphorylation. A significant increase of insulin-stimulated tyrosine phosphorylation of insulin receptor β-subunit in cells pre-treated with sodium salicylate (prior to treatment with protease inhibitor) was observed, and this is consistent with the known effects of sodium salicylate on the activation of IKKβ. Sodium salicylate also increased tyrosine phosphorylation of IRS-1 slightly, and decreased serine phosphorylation of IRS-1 twofold. This was associated with a decreased inhibition of tyrosine phosphorylation in response to indinavir i.e. a blockade of the effects of indinavir. Based on these results, the hypothesis of this study was that protease inhibitors may induce insulin resistance via the NFκB pathway.

3.5 Conclusion

The protease inhibitors saquinavir and indinavir inhibited insulin-stimulated tyrosine phosphorylation of the insulin receptor β-subunit in CHO-IR cells and 3T3-L1 adipocytes. The findings reveal for the first time that the blockade of IKKβ by sodium

University Of Cape Town

salicylate may abrogate the effect of indinavir on tyrosine phosphorylation of the insulin receptor β-subunit, by decreasing phosphorylation of IRS-1 at serine 307.

Therefore, in conclusion from these studies, HIV protease inhibitors appear to inhibit insulin receptor tyrosine phosphorylation indirectly via the NFκB pathway as a secondary effect involving a regulator of tyrosine phosphorylation, i.e. the level of phosphorylation of IRS-1 at serine 307. Salicylates may therefore provide a novel therapy for HIV protease inhibitor-induced insulin resistance and lipodystrophy. In addition, it was found that the other regulatory proteins investigated (PTP1B, SOCS-1 and -3, SH2B1 and APS) in the insulin signalling pathway were not altered after indinavir treatment, indicating that changes in the expression of these proteins are unlikely to play a role in the insulin resistance induced by antiretroviral protease inhibitors.

University Of Cape Town

CHAPTER 4: METABOLOMIC ANALYSIS OF CELL CULTURE SUPERNATANTS FROM 3T3-L1 ADIPOCYTES TREATED WITH HIV PROTEASE INHIBITORS

4.1 Introduction

Metabolism is an essential process for all organisms. It is necessary for the acquisition and utilisation of free energy for carrying out various functions in the biological system of an organism using specific metabolic pathways. Metabolic pathways are a series of consecutive enzymatic reactions that produce specific products or metabolites, including amino acids, organic acids and free fatty acids (FFA). A metabolite is a small molecule that is one of the ultimate products of gene, mRNA, and protein activity. Metabolites may be synthesised from either a catabolic (degradation) or an anabolic (biosynthesis) pathway (Arakaki et al., 2008).

Metabolomics is the study of metabolites (their characterisation, identification, and quantification) in a wide range of biochemical processes in living systems. It is beginning to emerge as a powerful tool for understanding the metabolic state of an organism (Arakaki et al., 2008; Koulman et al., 2009; Oresic, 2009).

Adipose tissue functions as a fat storage depot. It also plays a pivotal role as an endocrine organ that regulates and maintains not only the tissue itself, but whole-body metabolism, at the physiological level (Lee et al., 2009). Any dysfunctional alterations in metabolism in adipocytes may induce various side effects, such as insulin resistance and lipodystrophy. Insulin resistance may lead to type 2 diabetes. Thus, secreted metabolites from adipocytes act as biomarkers in indicating the metabolic state of adipocytes and potential disease conditions (Arakaki et al., 2008; Fonseca-Alaniz et al., 2007).

Protease inhibitors have been reported to impair insulin-regulated metabolism in adipose tissue, resulting in metabolic abnormalities such as insulin resistance and lipodystrophy (Gougeon et al., 2004). Previous studies have shown that protease inhibitors induce insulin resistance by inhibiting insulin-regulated GLUT4 translocation and glucose uptake (Murata et al., 2000; Rudich et al., 2001). Protease inhibitors have also been reported to inhibit lipogenesis, by impairing maturation of the sterol regulatory element-binding protein-1 (SREBP-1) and simultaneously inducing lipolysis in adipocytes (Carr, 2003; Lenhard et al., 2000). However, the precise molecular process by which protease inhibitors cause these effects is not clear (Gougeon et al., 2004).

University of Cape Town

In addition, protease inhibitor-treated patients with insulin resistance and lipodystrophy show increased FFA flux (Meininger et al., 2002). Since 40 years ago, FFAs (aka non-esterified fatty acids) have been known to play a role in glucose uptake (Randle et al., 1963). Increased FFA concentrations have been shown to lead directly to serine/threonine phosphorylation of IRS-1 and -2, thus reducing the ability of the IRS to activate PI3-K and GLUT4, and inducing insulin resistance (Lee et al., 2009; Meininger et al., 2002). Moreover, increased FFA levels have a similar role to TNF-α. Both activate inflammatory pathways such as c-Jun NH_2-terminal kinase (JNK) and IKKβ, which have been shown to inhibit insulin signalling in rodents (Lee et al., 2009). However, FFA levels in 3T3-L1 adipocytes treated with protease inhibitors have not been investigated.

Previous studies (Carr, 2003; Garg, 2006; Lee et al., 2009; Meininger et al., 2002; Murata et al., 2000; Rudich et al., 2001) indicate that protease inhibitors interfere in the metabolism of adipose tissue at multiple levels, thereby inducing various side-effects. We wanted to investigate the effects of antiretroviral protease inhibitors on adipocyte metabolism. Therefore, in this study, a metabolomic approach was used for the first time to investigate the effects of a protease inhibitor (indinavir) on 3T3-L1 adipocytes. This was performed in an attempt to clarify some of the side-effects on adipose tissue. Specifically, amino acid and organic acid metabolism in 3T3-L1 adipocytes was investigated by analysis of cell culture supernatants, using gas chromatography mass spectrometry (GC-MS). FFA levels in the supernatants of cells treated with the protease inhibitor were also analysed.

University Of Cape Town

4.2 Methods

4.2.1 Sample preparation

3T3-L1 pre-adipocyte fibroblasts were cultured using standard techniques, and differentiated as described in section 2.2.1 (Wilcox et al., 2004). Following differentiation, the cells were serum-starved for 16 h and stimulated with either or both of indinavir (50 μM) for 16 h and insulin (10 ng/ml) (1.7 nM) for 5 min. The four cell culture supernatants (i.e. untreated and treated with indinavir in a serum-free medium, with or without insulin stimulation) were harvested and stored at -80 °C for amino acid, organic acid and FFA analyses. Basal culture medium (serum-free medium) was used as a control, to compare the differences in the levels of amino acids, organic acids and FFAs in the untreated and treated cell culture supernatants, followed by insulin stimulation. For FFA analysis, 3T3-L1 adipocytes were also cultured in Medium 4 (see section 2.2.1) and treated with indinavir (50 μM) for 16 h.

The two cell culture supernatants (i.e. untreated, and treated with indinavir in Medium 4) were harvested and stored as above. Basal culture medium (adipocyte maintenance medium, viz. Medium 4) was used as a control in order to gauge the differences in the levels of FFAs in the untreated and treated cell culture supernatants.

4.2.2 GC-MS analysis

GC-MS analysis was perfomed at Red Cross Children's Hospital, Rondebosch, South Africa.

4.2.2.1 Amino acid analysis

Amino acids were analysed in 100 µl of untreated and indinavir-treated cell culture supernatants, with or without insulin stimulation, using GC-MS on an Agilent 7890A/5975C system (Agilent Technologies, CA, USA). The GC-MS detects amino acids at a minimum of 0.5 to 2 µM. Samples were prepared for analysis using a Phenomenex EZ-faast™ GC-MS kit (Phenomenex, CA, USA) (for cation exchange, extraction and derivation) to form a carbonyl hydrocarbon with the amino groups, and hydrocarbon esters with the carboxyl groups of amino acids. Amino acids in the basal culture medium were quantified as a control. After GC-MS analysis, the data were processed by Chemstation™ (Agilent Technologies, CA, USA) software. Amino acids were quantified using the nor-valine internal standard, and standard curves were generated from the kit calibrators. Amino acid concentrations in the cell culture supernatants were normalised to the total amount of cellular protein, assayed by protein assay, in each culture flask, as detailed in section 2.2.4.

4.2.2.2 Organic acid analysis

200 to 500 µl of cell culture supernatants (untreated and indinavir-treated, and then subjected to insulin stimulation) was analysed using GC-MS, to quantify organic acids. Organic acids in the basal culture medium were quantified as a control. The GC-MS detects organic acids at a minimum of 0.5 to 1 nM, to provide a detectable peak area to quantify. Organic acids are hydrocarbon carboxylic acids that are easily extracted from an aqueous medium by acidification and solvent extraction, using two different solvents (ethylacetate and diethyl-ether). Prior to extraction, a pentadecanoate (PDA) internal standard was added to each sample. The extracted acids were volatised by reaction with bis-(trimethylsilyl)trifluoroacetamide (BSTFA) to form trimethylsilyl (TMS) esters. The sample was injected into an Agilent

University of Cape Town

7890A/5975C system, and the chromatogram was analysed qualitatively and semi-quantitatively. Initial analysis identified the chromatogram using Chemstation™ software. Then, semi-quantitation was performed by comparing the ratio of integrated peak areas of individual compounds to the internal standard between samples. Standardisation of the semi-quantitative analysis was done by correcting the amount of PDA internal standard to the total amount of cellular protein present in each flask.

4.2.3 MetaboAnalyst web server

Metabolomic analysis of the data was performed using the MetaboAnalyst web server (http://metaboanalyst.ca) (Xia et al., 2009). This web server was developed using Java Server Faces, and its operation is based on microarray analysis. Briefly, the process is divided into six steps: data upload, processing, normalisation, statistical analysis, annotation and final report.

4.2.3.1 Data upload

Data were converted to CSV (comma separated values) format before being loaded onto the web server, accessed through http://metaboanalyst.ca. A data integrity check was performed automatically, and the data details were reported for the next steps.

4.2.3.2 Normalisation

There are two normalisation procedures in the web server process. Row-wise normalisation was performed to normalise each concentration of amino acid or peak area of organic acid in cell culture supernatants (untreated and treated with indinavir, with or without insulin stimulation) from three to five independent experiments (a row) to ensure they are comparable to each other. In this study, amino acids were normalised according to protein concentration in each sample, and organic acids were normalised according to protein concentration and PDA internal standard in each sample.

Column-wise normalisation (in the form of log normalisation) was performed to render all amino acids or organic acids (a column) in the untreated and drug-treated cell culture supernatants more comparable in magnitude to each other.

Statistical analysis was performed on the data to identify the most significantly different amino acids and organic acids in all cell culture supernatants (untreated or treated with indinavir, followed by insulin stimulation). These statistical analyses

University Of Cape Town

included volcano plot, partial-least squares discriminant analysis (PLS-DA) and significance analysis of microarrays (and metabolites) (SAM).

4.2.3.3 Volcano plot analysis

The volcano plot is a simple statistical analysis that is used initially to obtain an overview of the data before applying more sophisticated data analysis tools. It examines each variable separately without including the effect of multiple comparisons. This statistical analysis is used to compare the size of the fold change (FC) to the p-value from the Student's *t*-test. Fold change is a comparison of absolute value changes between mean concentrations of amino acids or peak areas of organic acids in untreated cell culture supernatants versus those treated with indinavir, with or without insulin stimulation. The Student's *t*-test was conducted to detect whether the concentrations of amino acids or peak areas of organic acids are significantly different between the untreated and drug-treated cell culture supernatants. The threshold of FC is 1.8 and the significance level (threshold) of the *t*-test is 90% ($\alpha = 0.1$). These values are suitable for the number of the samples in the study. The further away the amino acid position is (>75 %) from the origin (0.0) of the graph and the thresholds, the more significant is the change in the level of amino acid or organic acid in the untreated and drug-treated cell culture supernatants.

4.2.3.4 PLS-DA analysis

PLS-DA is a supervised method that can perform both classification and feature selection. The classification selection is a selection of amino acids or organic acids classified according to their samples or group, i.e. cell culture supernatants (untreated/treated with indinavir, followed by insulin stimulation). The feature selection is a selection of individual amino acids or organic acids in both the untreated and drug-treated cell culture supernatants, with or without insulin stimulation. This method uses a multiple linear regression technique to find the direction of maximum covariance between the individual amino acids or organic acids and the untreated and treated cell culture supernatants, with or without insulin stimulation.

There are two variable importance measures in PSL-DA: variable importance in projection (VIP) and the coefficient-based importance measure (CIM). VIP is a weighted sum of the squares of the PLS loadings. The weights are based on the amount of explained Y-variance; i.e. the variance in the concentration of amino acids

University Of Cape Town

or the peak area of organic acids in each dimension, being the untreated and drug-treated cell culture supernatants.

CIM is based on the weighted sum of PLS-regression coefficients; i.e. the regression coefficient in concentration of amino acids or the peak area of organic acids, which is a function of the reduction of the sums of the squares across the full number of PLS components, being the total number of amino acids and organic acids in the untreated and drug-treated cell culture supernatants.

The VIP scores tend to be 200 times larger than the CIM scores, but the relative ranking of significant metabolites is largely the same. After the VIP and CIM measurements, the identified amino acids and organic acids were used for further data analysis.

4.2.3.5 SAM analysis

SAM is designed to address False Discovery Rate (FDR) problems or errors when performing multiple tests on high-dimensional data. Firstly, it assigns a significance score to each variable of the amino acids or organic acids in cell culture supernatants (untreated/treated with indinavir, followed by insulin stimulation) based on its d-value, i.e. its change relative to the standard deviation of repeated measurements. Then, it chooses variables of amino acids and organic acids in the cell culture supernatants with scores below the lower (cutlow) threshold or greater than the upper (cutup) threshold and compares their relative difference to the distribution estimated by random permutations of the class labels ('observed=expected' line). For each threshold, a certain proportion of the variables in the permutation set will be found to be significant by chance. This number is used to calculate the FDR in the amino acid and organic acid analysis.

In order to control the FDR, the Delta value or threshold of false positive in the validated dataset has been specified as 0.1 in the analysis. The Delta value (0.1) has an FDR of 12 % and identifies approximately 10 significant compounds above the adjustable threshold. It is a compromise between the FDR and the number of amino acids and organic acids detected. The Delta value in SAM analysis is showed as lower and upper thresholds (cutlow and cutup) in order to measure the most significant amino acids or organic acids in the untreated and treated cell culture supernatants.

University of Cape Town

The cutlow is a lower or negative threshold where the significantly different amino acids or organic acids were measured, i.e. the mean concentration of amino acids or peak area of organic acids in 'untreated higher than those in treated' (negative) cell culture supernatants (untreated/treated with indinavir, followed by insulin stimulation). The cutup is an upper or positive threshold at which the significantly different amino acids or organic acids were measured, i.e. the mean concentration of amino acids (or peak area of organic acids) in the 'treated higher than those in untreated' (positive) cell culture supernatants. The lowest or greatest score of amino acid (or organic acid) from the thresholds (cutlow and cutup) indicates the most significantly different levels of amino acids (or organic acids) in the untreated-versus-treated cell culture supernatants.

In addition, the most significantly different amino acids (or organic acids) in the samples were also based on the lowest p-value (rawp), which was calculated automatically in the analysis. In this way, SAM is able to perform permutation testing which is not done in the *t*-test. The results of the SAM analysis are presented in the SAM graph and SAM results table for each of the significant compounds.

The amino acids and organic acids from the above analysis that showed the most significant changes between untreated and indinavir-treated cell culture supernatants (followed by insulin stimulation) were further analysed to investigate whether the amino acids or organic acids were synthesised or utilised compared with the basal culture medium (control).

The final reports are available to download in PDF format from the web server.

University of Cape Town

4.2.4 Free fatty acid (FFA) analysis

Levels of free fatty acids in untreated and indinavir-treated cell culture supernatants kept in a serum-free medium for 16 h (and then insulin-stimulated) were measured using a Free Fatty Acids Half-Micro Test Kit (Roche, Penzberg, Germany). The same analysis was performed on untreated and indinavir-treated cell culture supernatants in Medium 4 for 16 h, and on the basal culture media (serum-free medium and Medium 4) as controls.

This kit allows a small volume (20 µl) of sample to be assayed readily. 20 µl of the cell culture supernatants and the basal culture medium was added to 400 µl potassium phosphate buffer, pH 7.8, containing adenosine triphosphate, coenzyme A, acyl-CoA-synthetase (Acyl CS), peroxidase, ascorbate oxidase and 4-

aminoantipyrine. 20 µl of N-ethyl-maleimide solution was added. Blanks with deionised water and controls with 0.35 mM palmitic acid were prepared in the same way. The absorbance without enzyme was first measured using a spectrophotometer (Beckman Coulter, Cape Town, South Africa) at 546 nm. Subsequently, 20 µl of enzyme acyl-CoA-oxidase was added to the mixture (final volume 460 µl) and incubated for 15 min at room temperature before the second reading was taken.

The concentration of FFA in the untreated and indinavir-treated cell culture supernatants in the serum-free medium, Medium 4 and the basal culture media (serum-free medium and Medium 4) was measured after subtracting the absorbance of the samples from the blank using this standard formula:

$$\text{Concentration (mM/l)} = \frac{V}{v \times d \times \varepsilon} \times \Delta A$$

V = final volume (460 µl)
v = sample volume (20 µl)
d = light path (1 cm)
ε = absorbance coefficient of the dye at 546 nm: 19.3 (1 x mM^{-1} x cm^{-1})
∆A = absorbance of sample after subtraction from the blank

The kit uses Acyl CS and acyl-CoA-oxidase to convert FFA into enoyl-CoA and hydrogen peroxide. The hydrogen peroxide oxidises 4-amino-antipyrine, forming a red dye that absorbs at 546 nm. This method shows linearity up to a concentration of 1.5 mM.

University Of Cape Town

4.3 Results

Initially, the concentrations of amino acids and the peak areas under the curves of organic acids in untreated and indinavir-treated cell culture supernatants (followed by insulin stimulation) were compared to those in the basal culture medium (control). Changes in the amino acid and organic acid levels were analysed using the Student's *t*-test.

4.3.1 Amino acid analysis

A total of 27 amino acids and derivatives were detected in untreated and indinavir-treated cell culture supernatants (followed by insulin stimulation), and in the basal culture medium (control). There were significant increases in the levels of four amino acids in the untreated supernatants and none in the drug-treated supernatants (without insulin stimulation) compared to the control (Figure 4.1). With insulin stimulation, there were significant increases in the levels of 19 amino acids in the untreated supernatants, and 26 in the treated supernatants, compared to the control (Figure 4.1).

University Of Cape Town

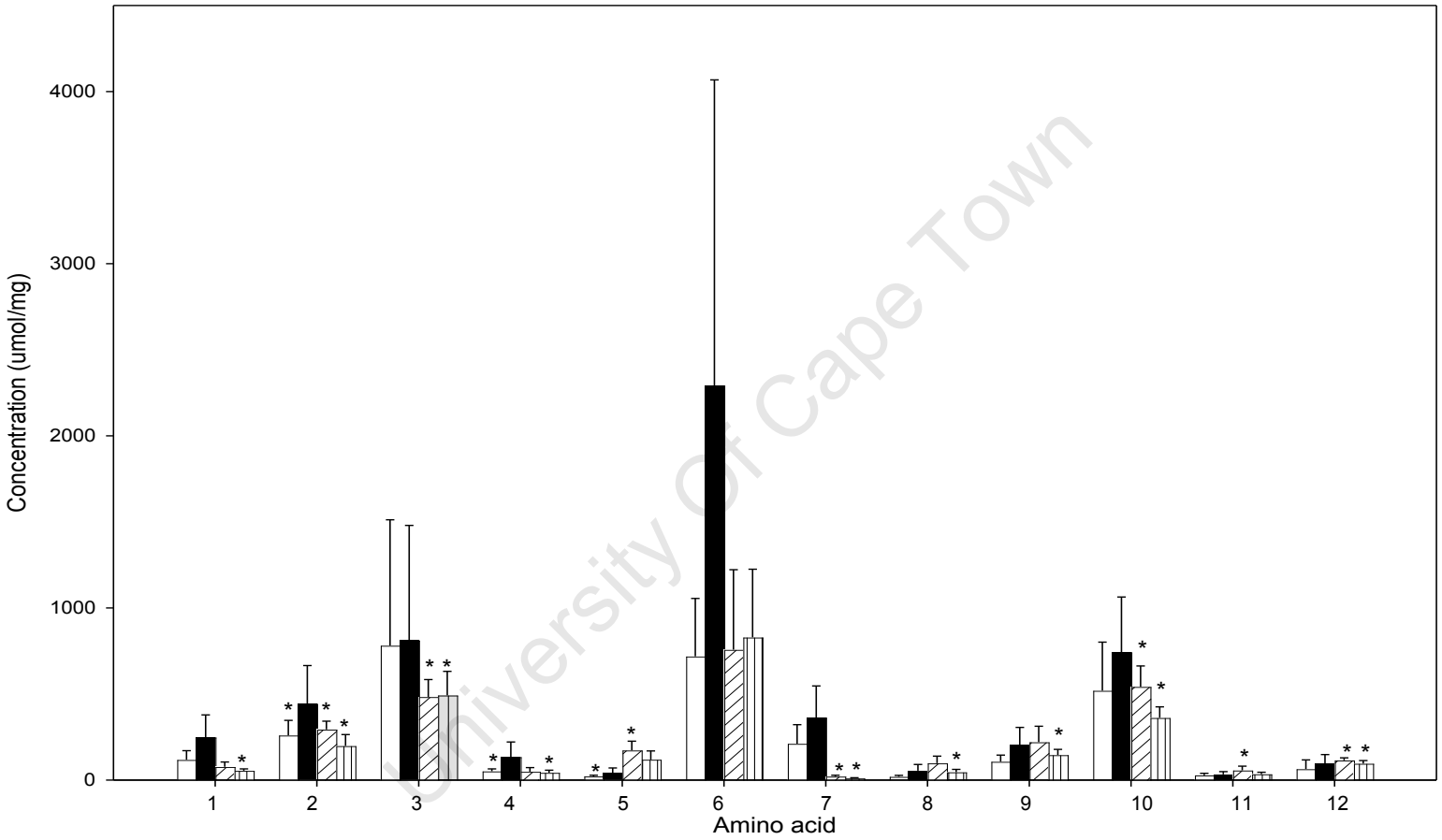

(a)

University Of Cape Town

See detail on pages 66

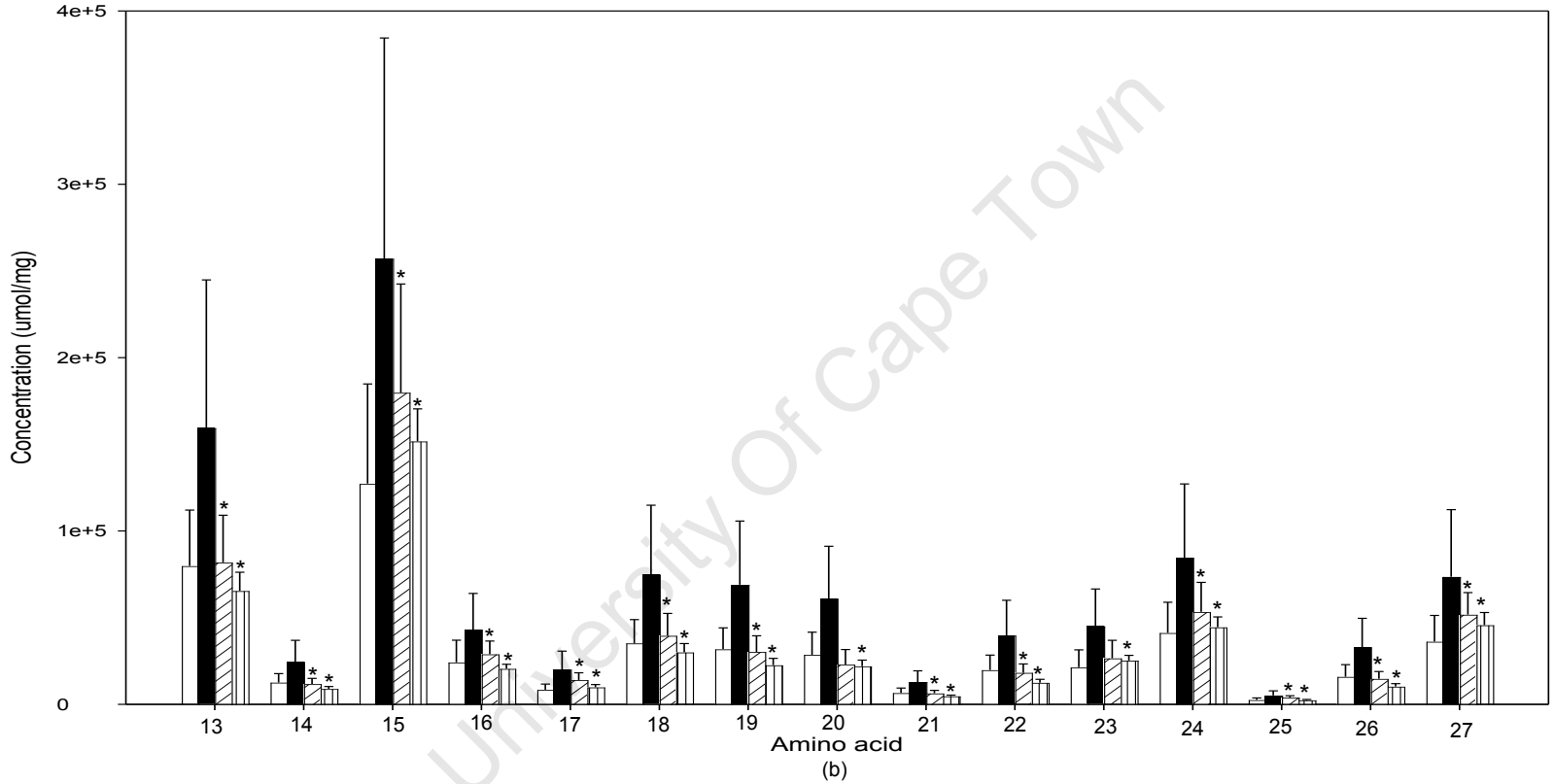

University Of Cape Town

Figure 4.1: Amino acid analysis of untreated (□) and drug-treated (■) without insulin stimulation, and untreated (▨) and drug-treated (▥) with insulin-stimulation of cell culture supernatants compared to the basal culture medium (control). (a) Concentration of amino acids 1-12: 0-4000 µmol/mg. (b) Concentration of amino acids 13-27: 0-4 x 10^5 µmol/mg. 3T3-L1 adipocytes were treated with indinavir (50 µM) for 16 h, followed by insulin stimulation. Cell culture supernatants were harvested for amino acid analysis using GC-MS. Concentrations of amino acids and derivatives in the untreated and treated cell culture supernatants were subtracted from those in the basal culture medium. Amino acid analysis is from three to five independent experiments. Data are shown as the mean and S.E.M. (n=3 to 5). *$p < 0.05$, using two-tailed Student's *t*-test, untreated or treated cell culture supernatants versus basal culture medium. 1= Alpha-amino-butyrate, 2 = Beta-amino-isobutyrate, 3 = Asparagine, 4 = Aspartate, 5 = Cystathionine, 6 = Glutamate, 7 = OH-Proline, 8 = Hydroxylysine, 9 = Ornithine, 10 = Proline, 11 = Thioproline, 12 = Beta-alanine, 13 = Alanine, 14 = Cystine, 15 = Glutamine, 16 = Glycine, 17 = Histidine, 18 = Isoleucine, 19 = Leucine, 20 = Lysine, 21 = Methionine, 22 = Phenylalanine, 23 = Serine, 24 = Threonine, 25 = Tryptophan, 26 = Tyrosine, 27 = Valine.

The MetaboAnalyst web server revealed two peaks (bimodal distribution) of amino acids revealed by normalisation, with or without stimulation with insulin (Figure 4.2, (a) and (b)).

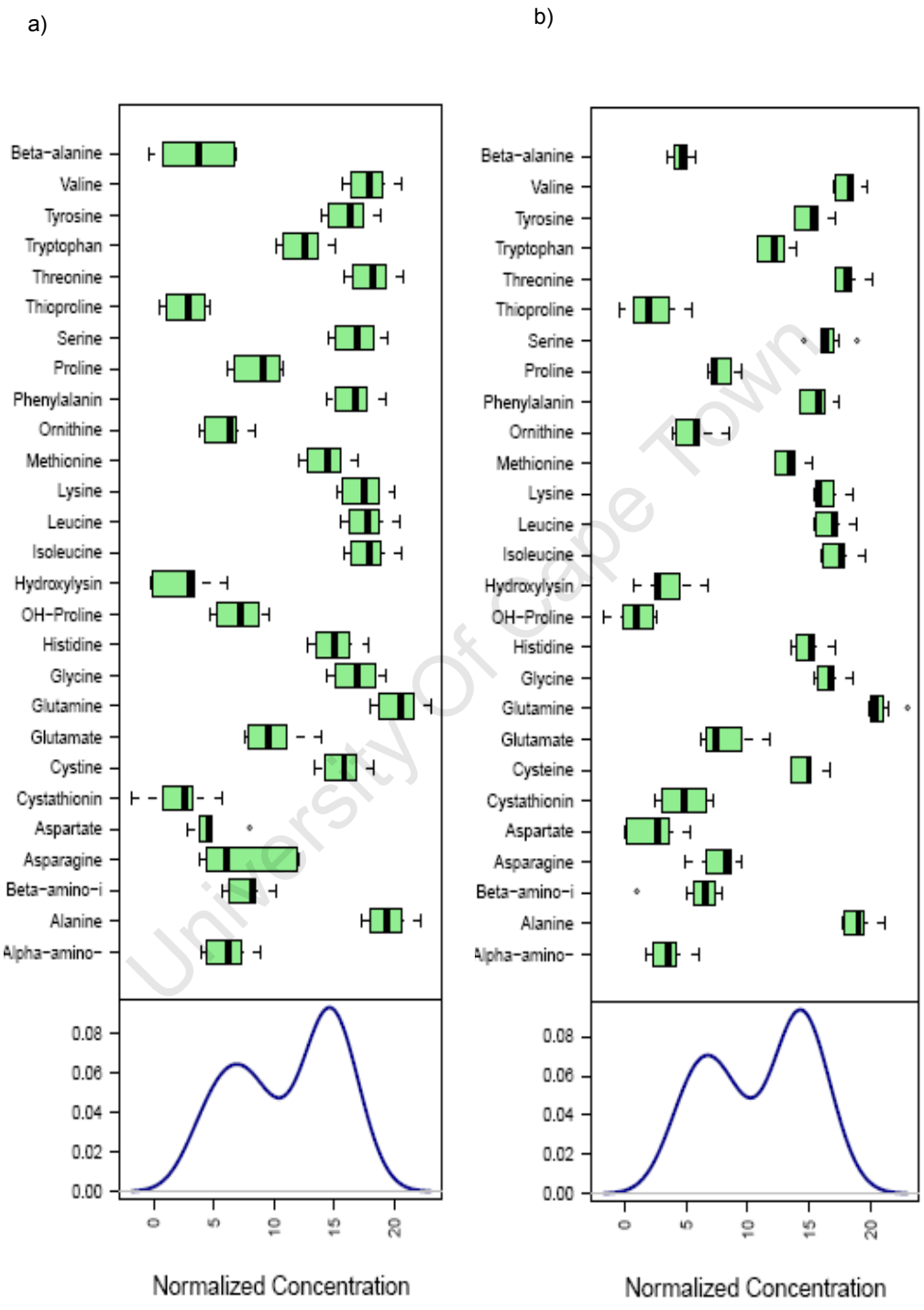

Figure 4.2: Box plots and kernel density plots of amino acids in the untreated and drug-treated cell culture supernatants (a) without and (b) with insulin stimulation after normalisation. 27 amino acids and derivatives were identified in supernatants of 3T3-L1 adipocytes before and after treatment with indinavir (50 μM) for 16 h followed by insulin stimulation using GC-MS.

University Of Cape Town

These data indicate that there were two separate groups of amino acids, based on their relative abundance. In addition, at a glance, amino acids in the untreated and indinavir-treated supernatants without insulin stimulation showed no difference compared to those with insulin stimulation. Thus, statistical analyses using volcano plot, PLS-DA and SAM were performed to measure the most significantly different levels of amino acids between the two groups, with or without insulin stimulation.

In the first analysis, statistical differences in amino acids in untreated and indinavir-treated supernatants of 3T3-L1 adipocytes (followed by insulin stimulation) were analysed using a volcano plot. No significantly different amino acids in the untreated versus indinavir-treated cell culture supernatants with or without insulin stimulation were identified (see Figure 4.3). All 27 amino acids were < 75 % from the origin (0.0) of the graph.

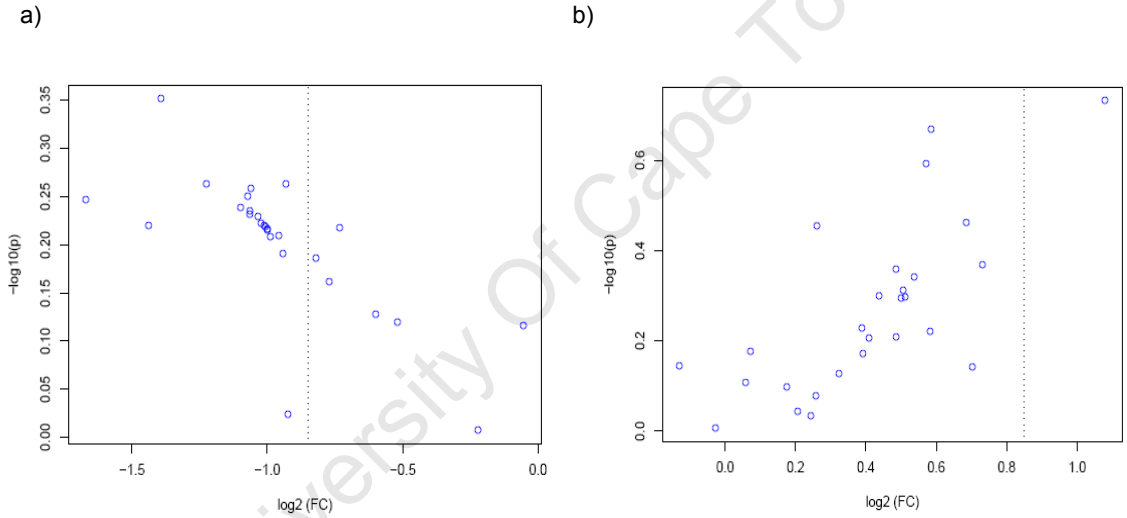

Figure 4.3: Volcano plot analysis of amino acids in the untreated and drug-treated cell culture supernatants a) without and b) with insulin stimulation. No significantly different amino acids in untreated cell culture supernatants versus those treated with indinavir (50 µM) for 16 h (followed by insulin stimulation) were identified in this plot. Circles represent 27 amino acids identified in the amino acid analysis using GC-MS. Both fold change and p-value were log-transformed to plot the amino acids in a symmetrical way. FC = fold change, p = p-value of Student's *t*-test.

In the PLS-DA analysis, VIP and CIM measurements were used to analyse the most significantly different amino acids between the untreated and drug-treated cell culture supernatants. In the cell culture supernatants tested without insulin stimulation, based on VIP (Figure 4.4(a)) and CIM (Figure 4.5(a)) measurements, glutamate, aspartate and hydroxylysine were the amino acids ranked as having the most significantly different levels between the two groups. For these amino acids, the VIP and CIM measurements were > 1.2 and 0.006, respectively.

University Of Cape Town

According to VIP measurement, beta-amino-isobutyrate, hydroxylysine, thioproline and glutamate were ranked as the amino acids having the most significantly different levels between the two groups with insulin stimulation (Figure 4.4(b)). For these amino acids, the VIP measurements were > 1.5. Using the CIM measurement, hydroxylysine and thioproline were ranked as the amino acids with the most significantly different levels between the untreated and treated cell culture supernatants (Figure 4.5(b)). The CIM measurements were > 0.1.

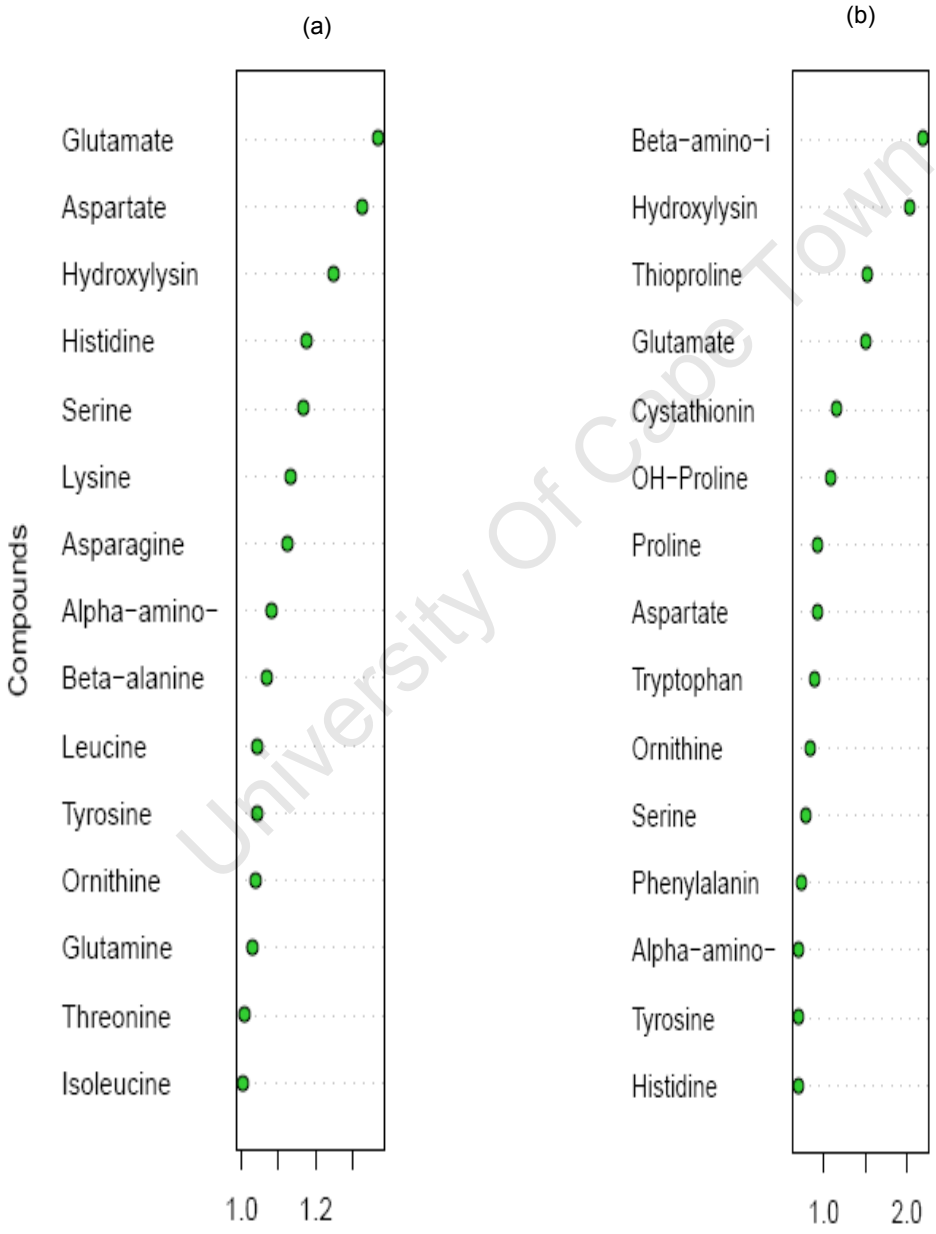

Figure 4.4: Partial-least squares discriminant analysis of amino acids in the untreated and drug-treated cell culture supernatants a) without and b) with insulin stimulation according to VIP (variable importance in projection) score.

University Of Cape Town

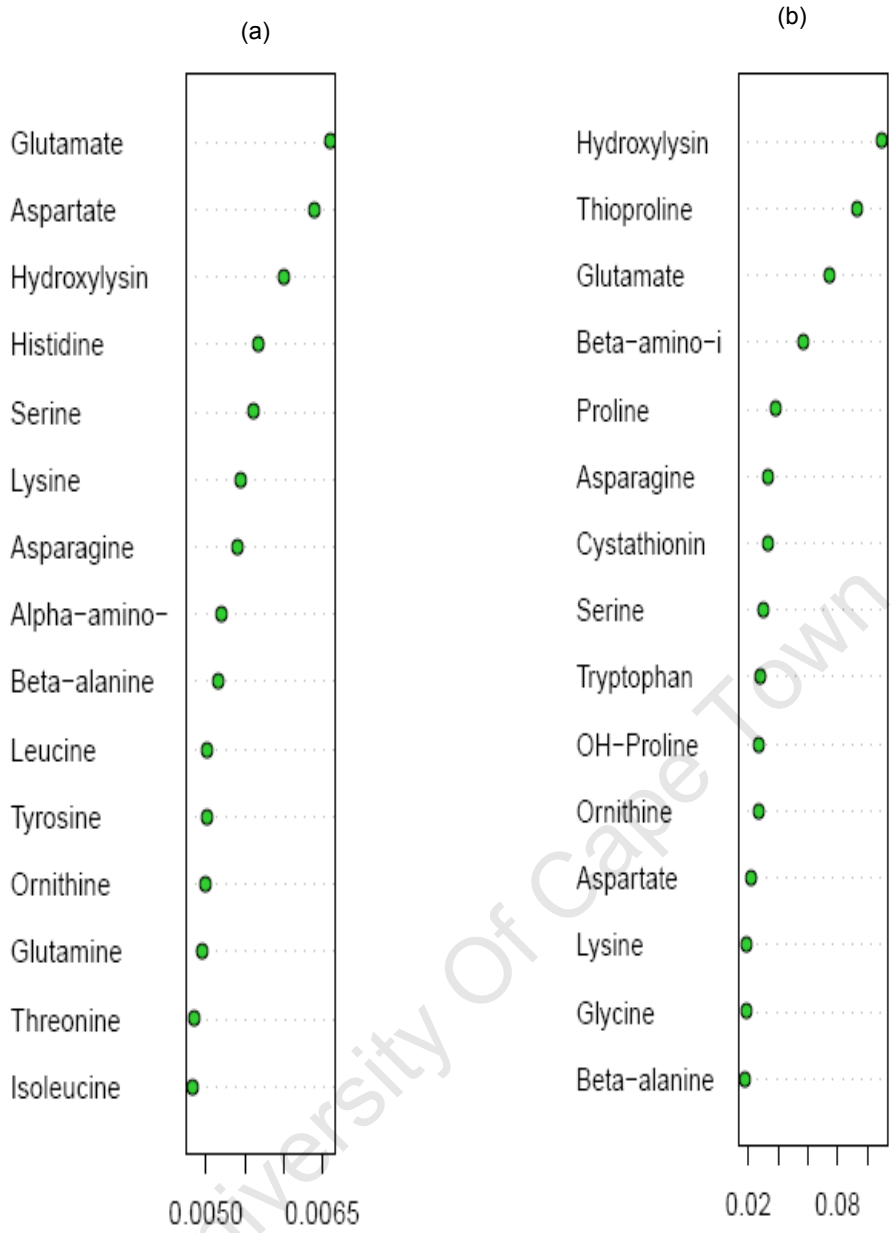

University Of Cape Town

Figure 4.5: Partial-least squares discriminant analysis of amino acids in the untreated and drug-treated cell culture supernatants a) without and b) with insulin stimulation according to CIM (coefficient-based importance measure) score.

In the final analysis, the differences in amino acids in untreated cell culture supernatants and those treated with indinavir (followed by insulin stimulation) were analysed using SAM analysis. Using a Delta value of 0.1, in the cell culture supernatants analysed without the insulin stimulation, the cutup was 0.574, while the cutlow of the graph was infinity (Figure 4.6). In total, there were significant differences in the levels of 14 amino acids in the drug-treated versus untreated supernatants located above the cutup threshold. Data from Table 4.1 indicated that aspartate had the greatest d-value (0.880) at the threshold, and the lowest p-value (rawp), of 0.426. Thus, aspartate was identified as the amino acid having the most

significantly different level in the untreated versus drug-treated cell culture supernatants without insulin stimulation.

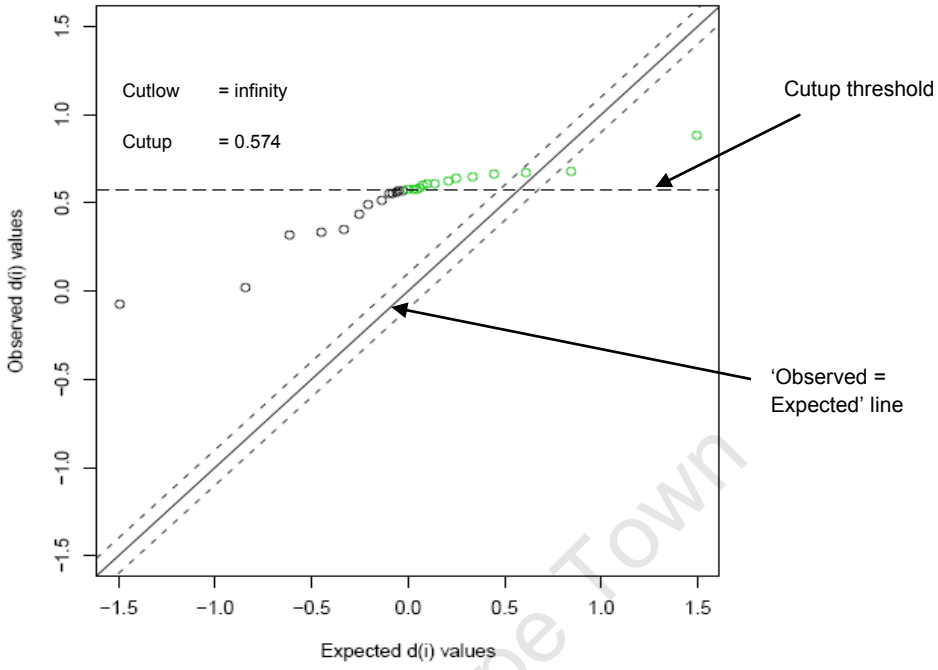

Figure 4.6: Significance analysis of microarrays (and metabolites) (SAM) of amino acids in the untreated and drug-treated cell culture supernatants without insulin stimulation. 27 amino acids in untreated cell culture supernatants versus those treated with indinavir (50 μM) for 16 h at the basal level were plotted on the graph based on the d-value (Table 4.1). The green circles represent significant differences in the levels of 14 amino acids (see Table 4.1) between the two groups (i.e. the levels of the amino acids were increased). FDR = false discovery rate.

Table 4.1: Significantly different amino acids in the untreated and drug-treated cell culture supernatants without insulin stimulation identified by SAM (from Figure 4.6). d-value = a 'score', i.e. concentration of amino acids which is changed relative to the standard deviation (stdev) of repeated measurements, stdev = standard deviation, rawp = raw p-value from Student's *t*-test.

Amino acids	d-value	stdev	rawp	Relative fold-effect	Changes
1. Aspartate	0.880	1.027	0.426	1.871	Increase
2. Histidine	0.682	1.175	0.481	1.743	Increase
3. Ornithine	0.667	1.059	0.493	1.632	Increase
4. Serine	0.661	1.200	0.504	1.733	Increase
5. Lysine	0.645	1.196	0.519	1.707	Increase
6. Glutamate	0.638	1.461	0.522	1.909	Increase
7. Leucine	0.625	1.136	0.533	1.635	Increase
8. Alpha-amino-butyrate	0.609	1.207	0.556	1.665	Increase
9. Isoleucine	0.607	1.124	0.563	1.605	Increase
10. Tyrosine	0.597	1.188	0.570	1.634	Increase
11. Threonine	0.583	1.178	0.581	1.609	Increase
12. Glutamine	0.576	1.215	0.593	1.625	Increase
13. Hydroxylysine	0.574	1.479	0.596	1.802	Increase
14. Valine	0.574	1.149	0.600	1.580	Increase

In the cell culture supernatants analysed with insulin stimulation, the cutup was infinity, while the cutlow of the graph was -0.517 (Figure 4.7). In total, there were significant differences in the levels of 16 amino acids in indinavir-treated versus

University of Cape Town

untreated supernatants located below the cutlow threshold. Data from Table 4.2 indicate that hydroxylysine had the greatest d-value (-1.454) at the threshold, with the lowest p-value (rawp) of 0.185. Thus, hydroxylysine was identified as the amino acid having the most significantly different levels in the untreated versus drug-treated cell culture supernatants with insulin stimulation.

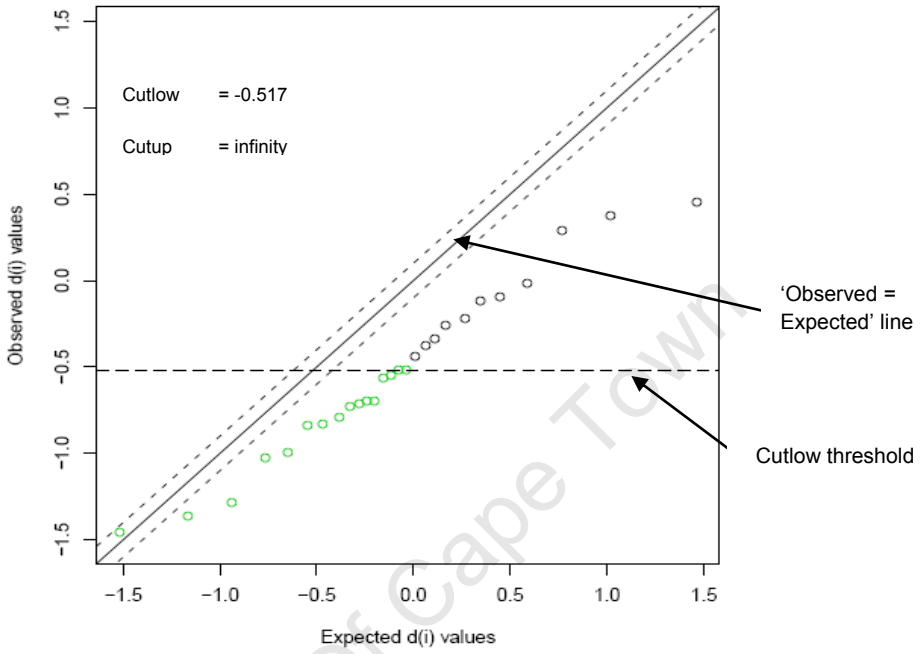

Figure 4.7: Significance analysis of microarrays (and metabolites) (SAM) of amino acids in the untreated and drug-treated cell culture supernatants with insulin stimulation. 27 amino acids in untreated cell culture supernatants versus those treated with indinavir (50 μM) for 16 h (followed by insulin stimulation) were plotted on the graph based on the d-value (Table 4.2). The green circles represent significant differences in the levels of 16 amino acids (see Table 4.2) between the two groups (i.e. the levels of the amino acids were decreased). FDR = false discovery rate.

Table 4.2: Significantly different amino acids in the untreated and drug-treated cell culture supernatants with insulin stimulation identified by SAM (from Figure 4.7). d-value = a score i.e. concentration of amino acid which is changed relative to the standard deviation (stdev) of repeated measurements, stdev = standard deviation, rawp = raw p-value from Student's *t*-test.

Amino acids	d-value	stdev	rawp	Relative fold-effect	Changes
1. Hydroxylysine	-1.454	0.662	0.185	0.513	Decrease
2. Proline	-1.365	0.378	0.227	0.699	Decrease
3. Beta-amino-isobutyrate	-1.288	0.811	0.258	0.485	Decrease
4. Tryptophan	-1.023	0.497	0.344	0.703	Decrease
5. Beta-alanine	-0.995	0.307	0.355	0.809	Decrease
6. Hydroxyproline	-0.841	0.661	0.404	0.680	Decrease
7. Glycine	-0.830	0.413	0.408	0.789	Decrease
8. Phenylalanine	-0.795	0.486	0.418	0.765	Decrease
9. Tyrosine	-0.733	0.484	0.456	0.782	Decrease
10. Methionine	-0.713	0.428	0.468	0.81	Decrease
11. Histidine	-0.700	0.486	0.477	0.790	Decrease
12. Cystathionine	-0.696	0.816	0.479	0.674	Decrease
13. Cysteine	-0.562	0.449	0.577	0.839	Decrease
14. Ornithine	-0.548	0.619	0.590	0.791	Decrease
15. Alpha-amino-butyrate	-0.520	0.554	0.618	0.819	Decrease
16. Leucine	-0.517	0.494	0.620	0.838	Decrease

University Of Cape Town

Without insulin stimulation, aspartate was noted to be significantly increased (i.e. synthesised more) in untreated cell culture supernatants, compared to the basal culture medium (control) (Figure 4.1). Results from PLS-DA and SAM analyses indicated that aspartate was the amino acid having the most significantly different level between the untreated versus indinavir-treated cell culture supernatants. In particular, in this study, synthesis of aspartate was found to be significantly increased in the drug-treated cell culture supernatants (Figure 4.8).

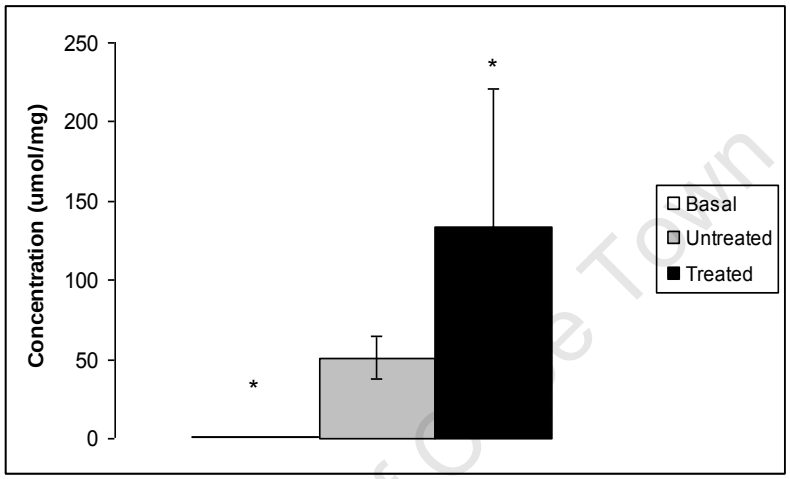

Figure 4.8: Synthesis of aspartate in the drug-treated cell culture supernatants without insulin stimulation based on PLS-DA and SAM analyses. 3T3-L1 adipocytes were untreated (□) and treated (■) with indinavir (50 μM) for 16 h at the basal level. Cell culture supernatants were harvested for amino acid analysis using GC-MS. Basal (□) culture medium was used as a control. Data are shown as the mean ± S.E.M. (n=3). *$p < 0.05$ versus basal culture medium (control).

With insulin stimulation, hydroxylysine was established to be significantly increased (i.e. synthesised more) in cell culture supernatants treated with indinavir, compared to the basal culture medium (control) (Figure 4.1). Results from PLS-DA and SAM analyses indicated that hydroxylysine was the amino acid having the most significantly different level between the drug-treated versus untreated cell culture supernatants. In particular, in this study, synthesis of hydroxylysine was found to be significantly decreased in the drug-treated versus untreated cell culture supernatants with insulin stimulation (Figure 4.9).

University Of Cape Town

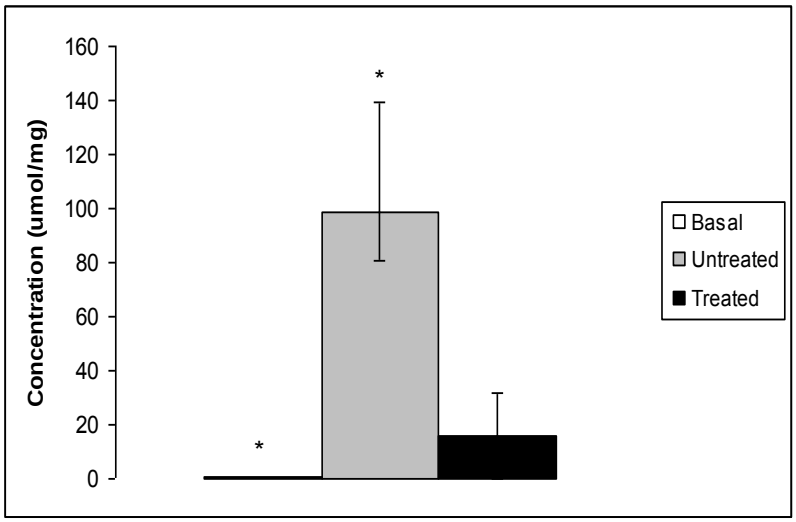

Figure 4.9: Synthesis of hydroxylysine in the drug-treated cell culture supernatants with insulin stimulation based on PLS-DA and SAM analyses. 3T3-L1 adipocytes were treated (■) with indinavir (50 µM) or untreated (▢) for 16 h, followed by insulin stimulation. Cell culture supernatants were harvested for amino acid analysis using GC-MS. Basal (□) culture medium was used as a control. Data are shown as the mean ± S.E.M. (n=5). $p < 0.05$ versus basal culture medium (control).

4.3.2 Organic acid analysis

A total of 60 organic acids and derivatives were identified in untreated cell culture supernatants and those treated with indinavir (followed by insulin stimulation), and in the basal culture medium (control). There were significant increases in the levels of 10 organic acids in the untreated supernatants (and of eight in the drug-treated supernatants) without insulin stimulation, compared to the control (Figure 4.10). With insulin stimulation, there were significant increases in the levels of 14 organic acids in the untreated supernatants (and 12 in the treated supernatants) compared to the control (Figure 4.10).

University of Cape Town

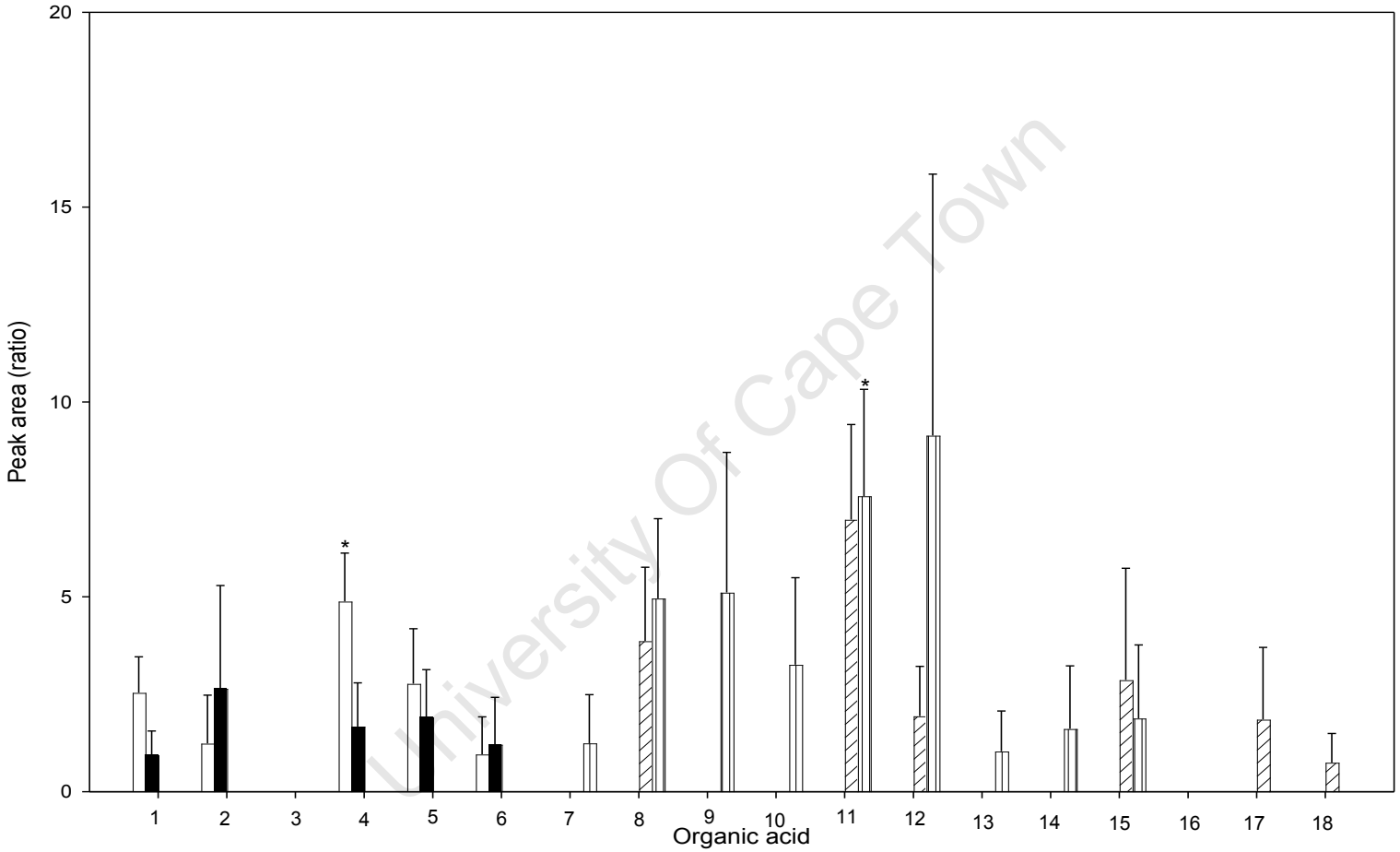

(a)

University Of Cape Town

See detail on pages 74 and 75.

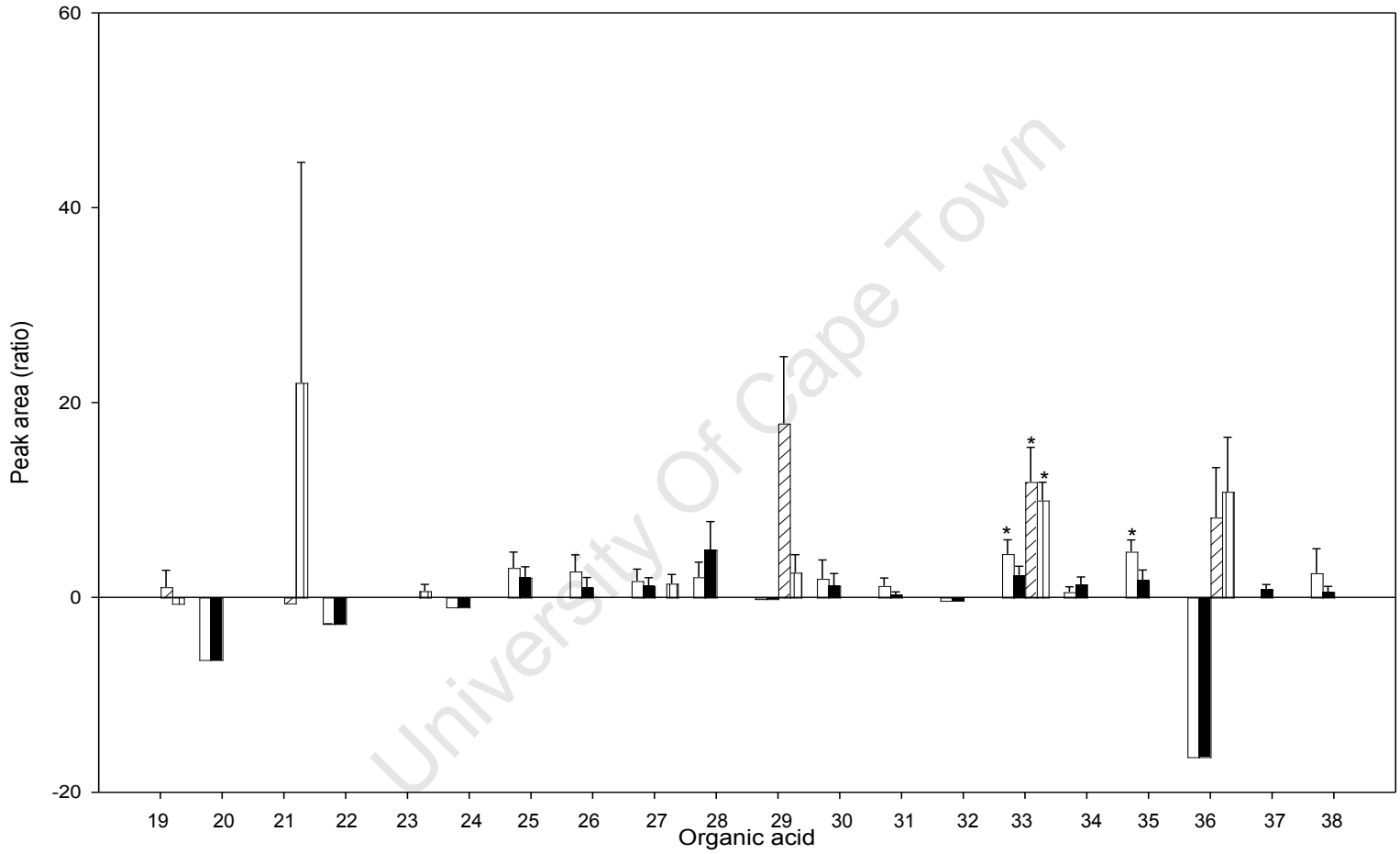

(b)

University Of Cape Town

See detail on pages 74 and 75.

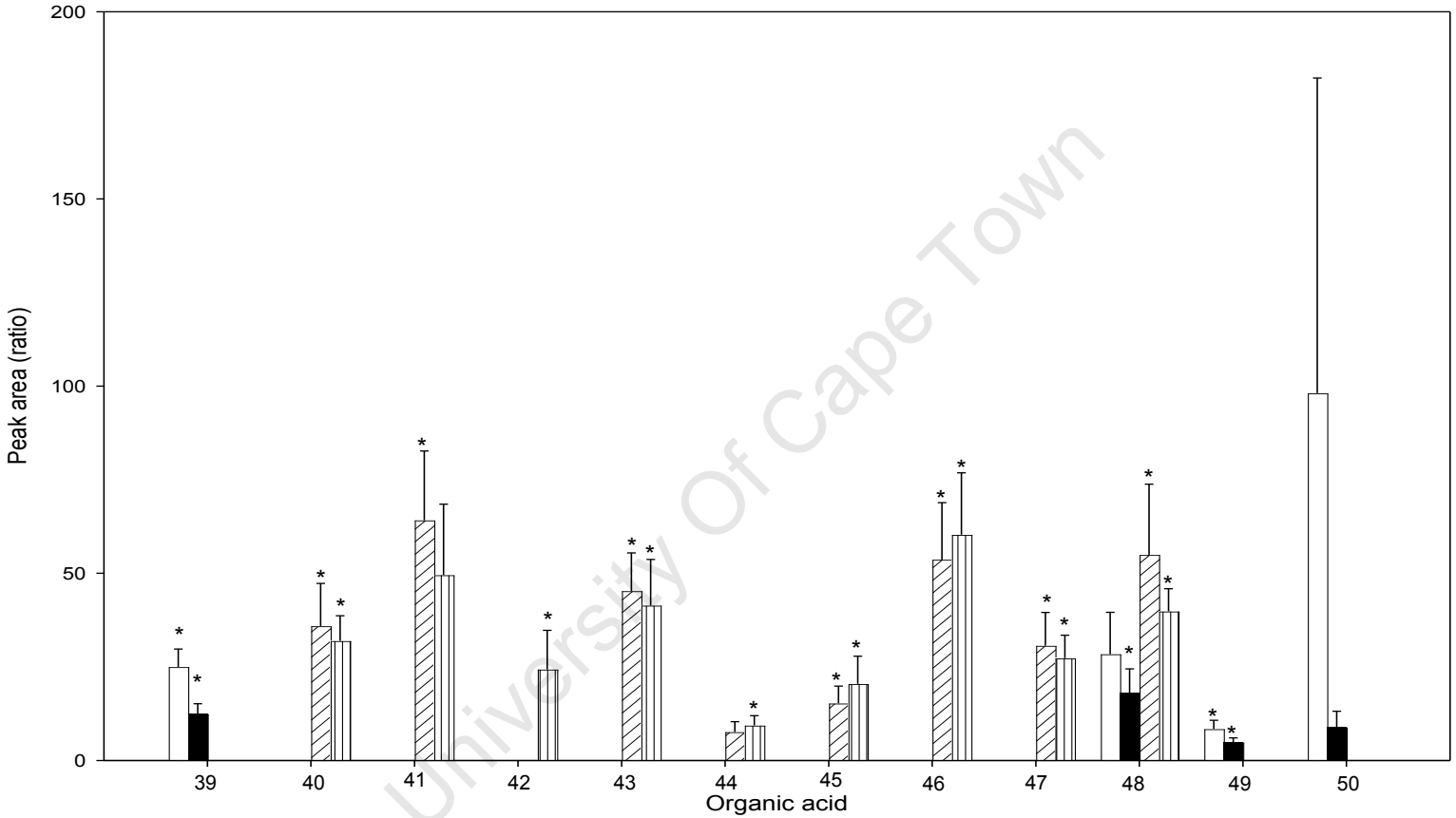

(c)

University Of Cape Town

See detail on pages 74 and 75.

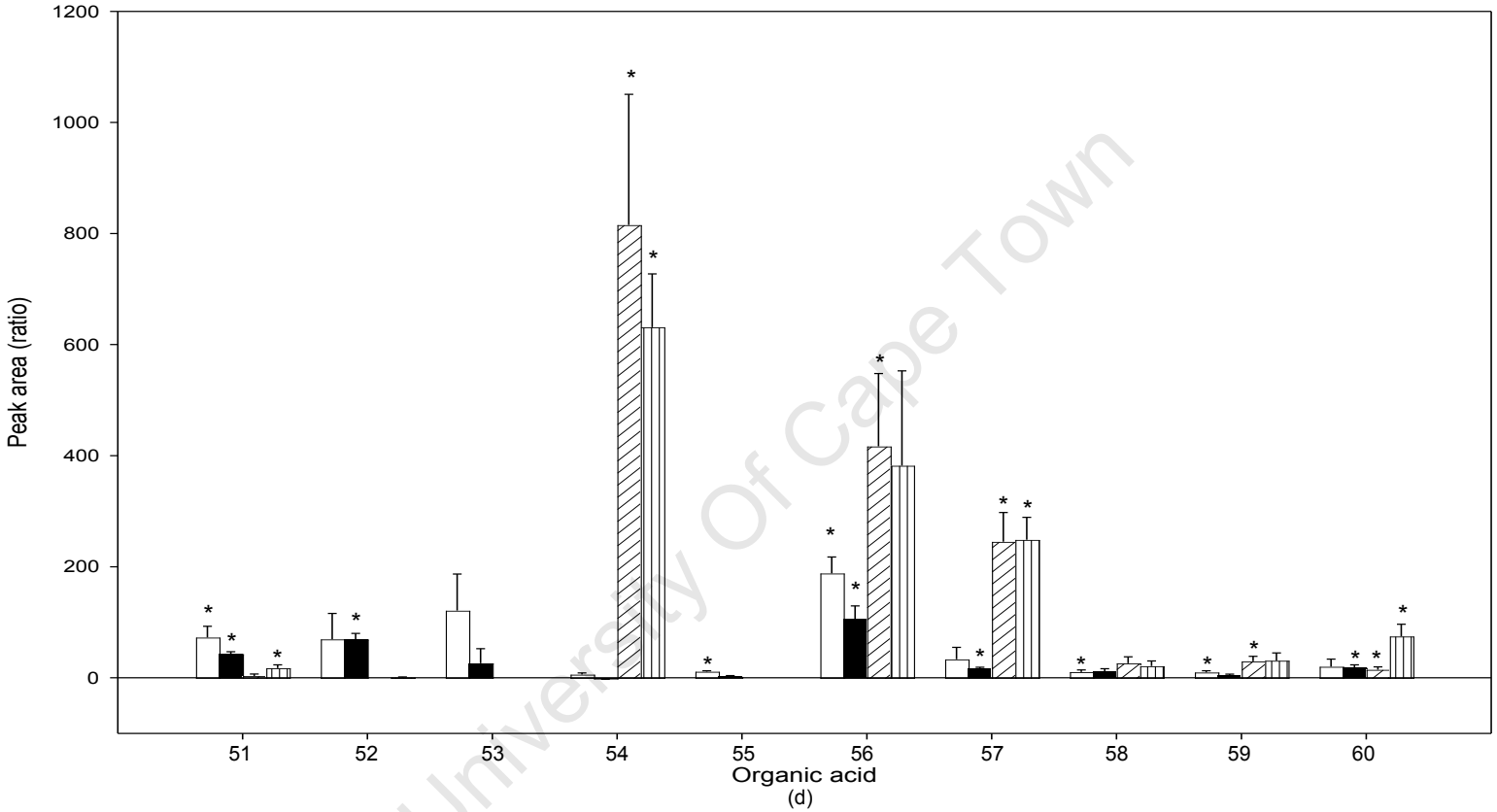

University Of Cape Town

Figure 4.10: Organic acid analysis of untreated (□) and drug-treated (■) without insulin stimulation, and untreated (▨) and drug-treated (▥) with insulin stimulation of cell culture supernatants compared to the basal culture medium (control). (a) Concentration of organic acids 1-18: 0-20 pear area (ratio). (b) Concentration of organic acids 19-38: -20 - 60 peak area (ratio). (c) Concentration of organic acids 39-50: 0-200 peak area (ratio). (d) Concentration of organic acids 51-60: 0 - 1200 peak area (ratio). 3T3-L1 adipocytes were treated with indinavir (50 μM) for 16 h followed by insulin stimulation. Cell culture supernatants were harvested for organic acid analysis using GC-MS. Peak areas of organic acids and derivatives in the untreated and treated cell culture supernatants were subtracted from those in the basal culture medium. Organic acid analysis is from five independent experiments. Data are shown as the mean and S.E.M. (n=5). *$p < 0.05$, using two-tailed Student's *t*-test, untreated or treated cell culture supernatants versus basal culture medium. For details of organic acids (1-60), please see Table 4.3.

Table 4.3: Organic acids identified in the drug-treated or untreated cell culture supernatants using GC-MS. 3T3-L1 adipocytes were left untreated or treated with indinavir (50 μM) for 16 h, followed by insulin stimulation.

No.	Organic acids	No.	Organic acids
1	Azelaic acid	31	Nonanoic acid
2	N-phenylacetylglycine	32	2-deoxytetronate
3	Myristate	33	(R*,S*)-3,4-dihydroxybutanoic acid
4	Pantothenic acid	34	2-methyl-1,3-bis(trimethylsilyloxy)butane
5	Palmitelaidic acid	35	L-proline
6	Glucopyranose	36	Pyroglutamate
7	2,4,6(1H,3H,5H)-pyrimidinetrione,5-(1-methylpropyl)-5-(2-propenyl)-1	37	Pentanedioicaid
8	Benzoic acid	38	Dodecanoic acid
9	Pentasiloxane,dodecamethyl	39	1,2,3-propanetricarboxylic acid
10	2-ethylhydracrylic acid	40	Palmitate
11	N,O-bis(trismethylsilyl)-L-phenylalanine	41	Sulphate
12	Homovanillate	42	Isovalerate
13	Oxacyclotetradec-5-yn	43	Propylene glycol
14	4-hydroxyphenyllactate	44	Phenyl acetic acid
15	Oleate	45	Phenylacetylglycine
16	Oleic acid	46	Citrate
17	Oleanitrile	47	Stearate
18	Dehydroabietic acid	48	Hexadecanoic acid
19	1,2-bis(trimethylsiloxy)ethane	49	Heptadecanoic acid
20	Acetamide	50	Octadecanoic acid
21	3-hydroxybutyrate	51	Butanoic acid, 3-(trimethylsiloxy)-,ethylester
22	Lactate	52	Trifluoromethyl-bis-(trimethyl)methylketone
23	Phosphorous acid	53	Carbamic acid
24	2-propanedioic acid	54	Benzene
25	2-ketoisocaproic acid	55	Butane
26	1-pentanethyldisilyloxybutane	56	Propanoic acid
27	Glycerol	57	Acetic acid
28	Butanedioic acid	58	Ethanedioic acid
29	Succinate	59	Butanoic acid, 4-(trimethylsiloxy)-,ethylester
30	Cyclohexasilaxane	60	D-erythro-pentonic acid

In addition, only one organic acid was exclusively identified in indinavir-treated supernatants without insulin stimulation, and eight in the drug-treated supernatants with insulin stimulation (Table 4.4).

University Of Cape Town

Table 4.4: Organic acids that were exclusively identified in cell culture supernatants treated with indinavir with or without insulin stimulation using GC-MS. 3T3-L1 adipocytes were left untreated or treated with indinavir (50 μM) for 16 h, followed by insulin stimulation.

Without insulin stimulation	With insulin stimulation
1. Pentanedioicaid	1. 3-hydroxybutyrate
	2. Phosphorous acid
	3. 2,4,6(1H,3H,5H)-primidinetrione,5-(1-methylpropyl)-5-(2-propenyl)-1
	4. Isovalerate
	5. Pentasiloxane,dodecamethyl
	6. 2-ethylhydracrylic acid
	7. Oxacyclotetradec-5-yn
	8. 4-hydroxyphenyllactate

Two peaks (bimodal distribution) of organic acids emerged after normalisation (Figure 4.11(a) and (b)) by the MetaboAnalyst web server.

These data indicate that there are two separate groups of organic acids, based on their relative abundance. In addition, organic acids in the untreated and indinavir-treated supernatants without insulin stimulation showed changes compared to those with insulin stimulation. Thus, statistical analyses using volcano plot, PLS-DA and SAM were performed to measure the most significantly different levels of organic acids between the two groups, with or without insulin stimulation.

University Of Cape Town

a) b)

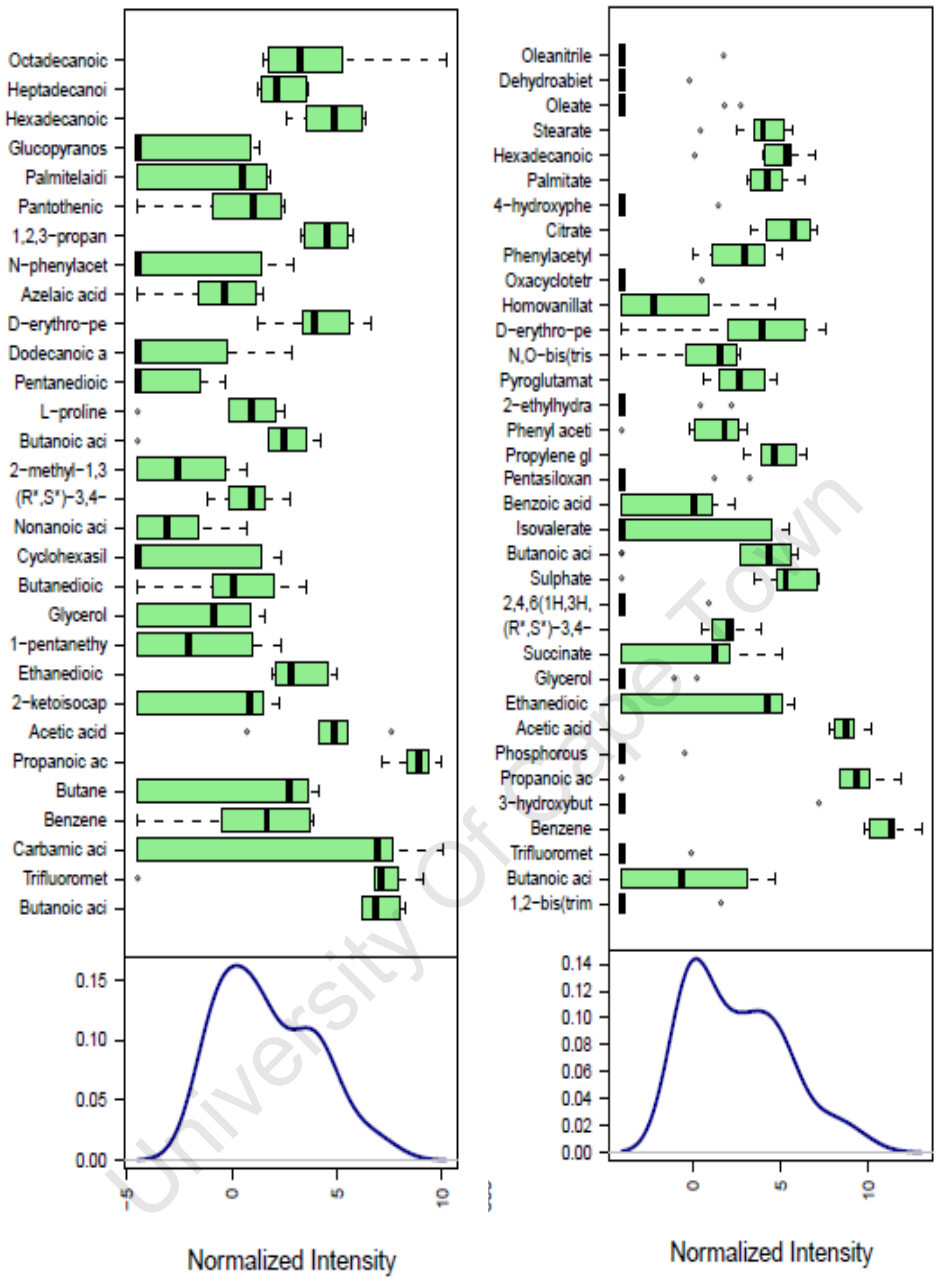

University Of Cape Town

Figure 4.11: Box plots and kernel density plots of organic acids in the untreated and drug-treated cell culture supernatants (a) without and (b) with insulin stimulation after normalisation. 60 organic acids and derivatives were identified in supernatants of 3T3-L1 adipocytes before and after treatment with indinavir (50 µM) for 16 h, followed by insulin stimulation using GC-MS.

In the first analysis, a volcano plot was used to obtain an overview of statistical differences of organic acids in untreated supernatants of 3T3-L1 adipocytes and those treated with indinavir (followed by insulin stimulation). 1,2,3-propanetricarboxylic acid (FC = 2.021, p = 0.078) (Figure 4.12(a)) was shown to be significantly different between the untreated and

drug-treated supernatants without insulin stimulation. With insulin stimulation, succinate (FC = 5.283, p = 0.016), butanoic acid 3-(trimethylsiloxy)-ethylester (FC = 0.221, p = 0.060) and isovalerate (FC = 0.026, p = 0.071) were shown to be significantly different between the untreated and drug-treated supernatants using the volcano plot analysis (Figure 4.12(b).

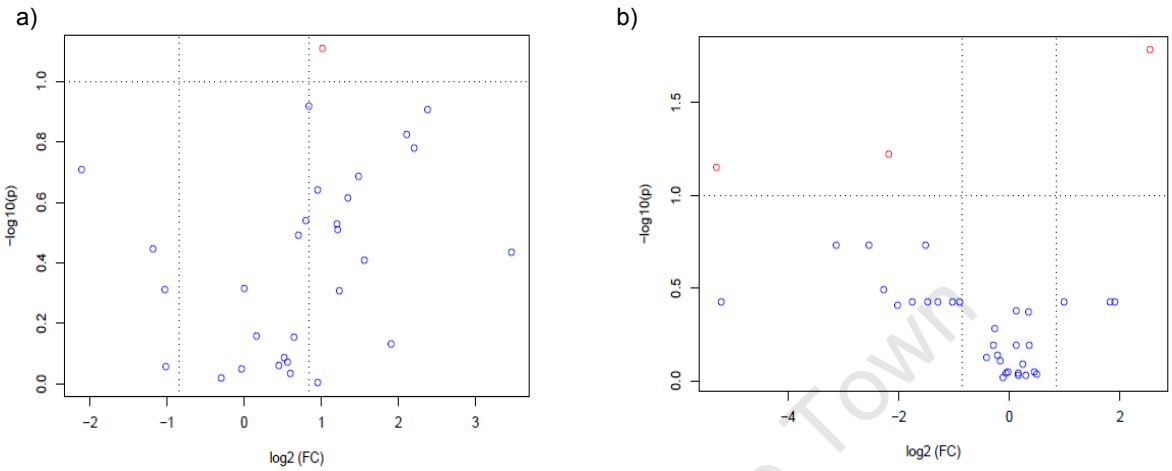

Figure 4.12: Volcano plot analysis of organic acids in the untreated and drug-treated cell culture supernatants a) without and b) with insulin stimulation. The red circles represent significantly different organic acids in untreated cell culture supernatants versus those treated with indinavir (50 µM) for 16 h (followed by insulin stimulation) that were identified in this plot. Circles represent 60 organic acids identified in the organic acid analysis using GC-MS. Both fold change and p-value were log-transformed to plot the organic acids in a symmetrical way. FC = fold change, p = p-value of Student's *t*-test.

Subsequently, organic acids were analysed using the PLS-DA analysis. In the case of cell culture supernatants without insulin stimulation, based on VIP (Figure 4.13(a)) and CIM (Figure 4.14(a)) measurements, carbamic acid and butane were ranked as having the most significantly different organic acid levels between the two groups. For these organic acids, the VIP and CIM measurements were > 2.0 and 0.02, respectively.

With insulin stimulation, according to VIP (Figure 4.13(b)) and CIM (Figure 4.14(b)) measurements, isovalerate, butanoic acid 3-(trimethylsiloxy)-ethylester and succinate were ranked as the most significantly different organic acid levels between the two groups. For these organic acids, the VIP and CIM measurements were > 2.0 and 0.04, respectively.

University of Cape Town

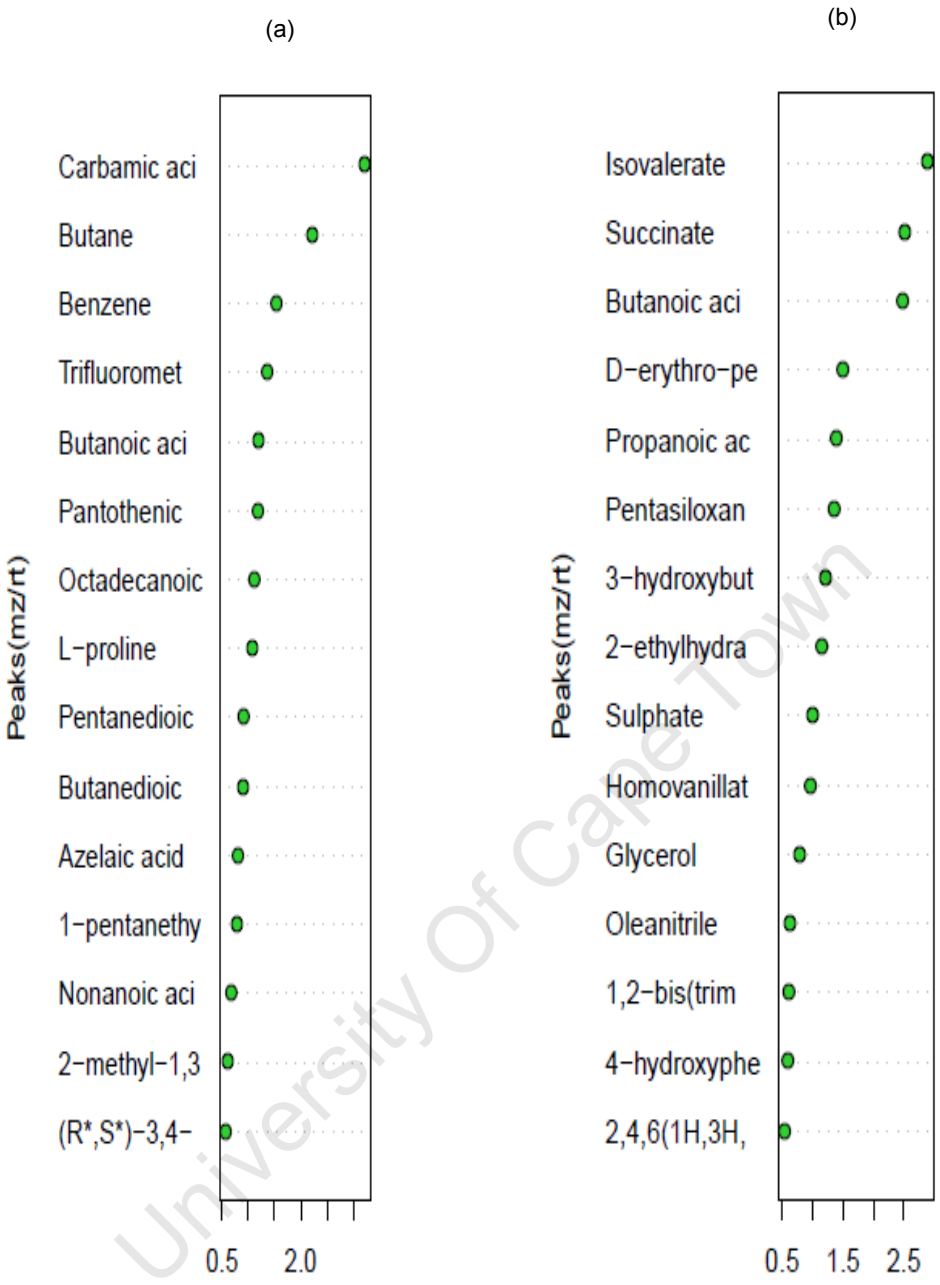

University Of Cape Town

Figure 4.13: Partial-least squares discriminant analysis of organic acids in the untreated and drug-treated cell culture supernatants a) without and b) with insulin stimulation according to VIP (variable importance in projection) score.

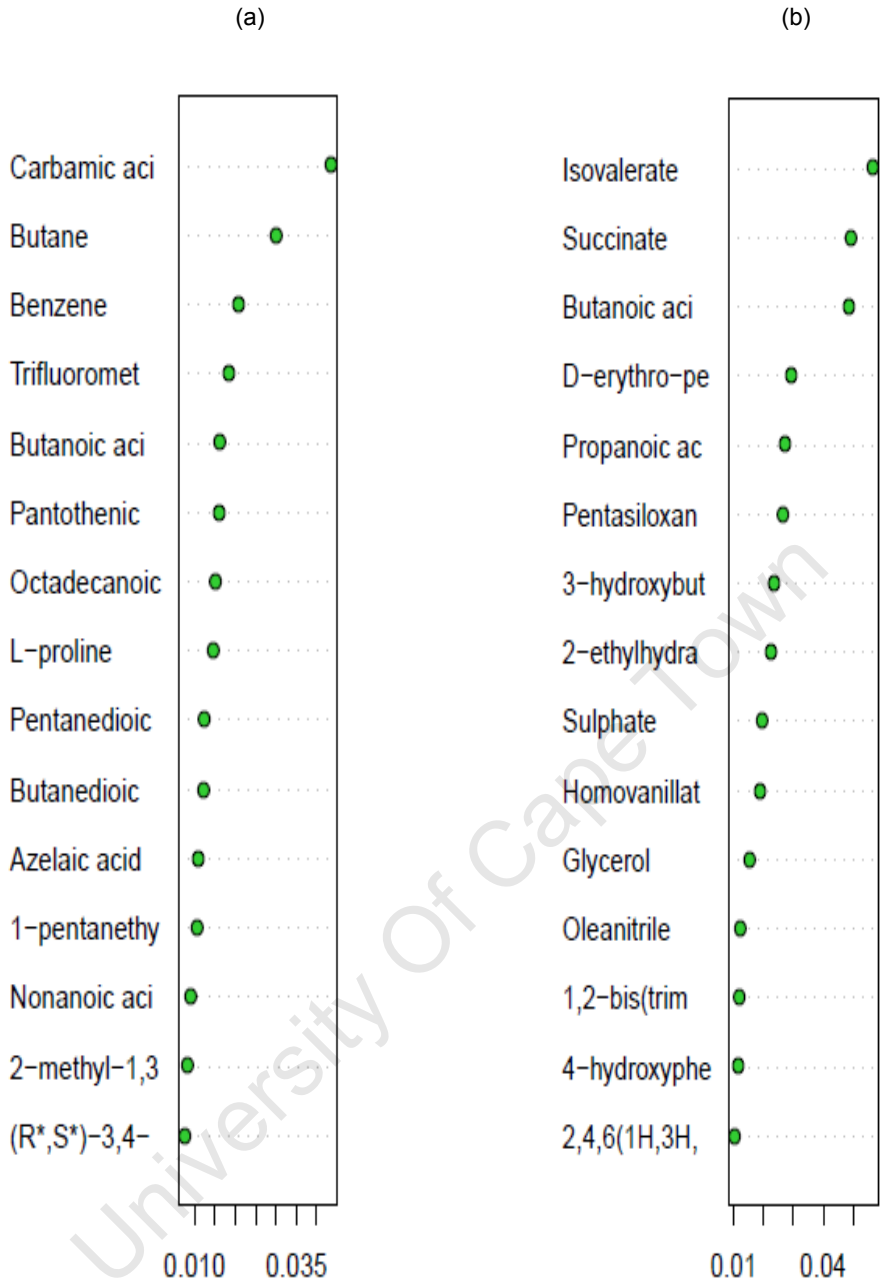

University Of Cape Town

Figure 4.14: Partial-least squares discriminant analysis of organic acids in the untreated and drug-treated cell culture supernatants a) without and b) with insulin stimulation according to CIM (coefficient-based importance measure) score.

In the final analysis using SAM, there were significant changes in the levels of 15 organic acids in untreated cell culture supernatants and those treated with indinavir, without insulin stimulation (Figure 4.15 and Table 4.5). Using a Delta value of 0.1, the cutlow was -0.753, while the cutup of the graph was infinity (Figure 4.15). Data from Table 4.5 indicate that butane, 1,2,3-propanetricarboxylic acid and propanoic acid have the greatest d-value (< -2) at the threshold, with the lowest p-value (rawp) of < 0.1. Thus, those organic acids were

identified as the organic acids with the most significantly different levels between the untreated and drug-treated cell culture supernatants without insulin stimulation.

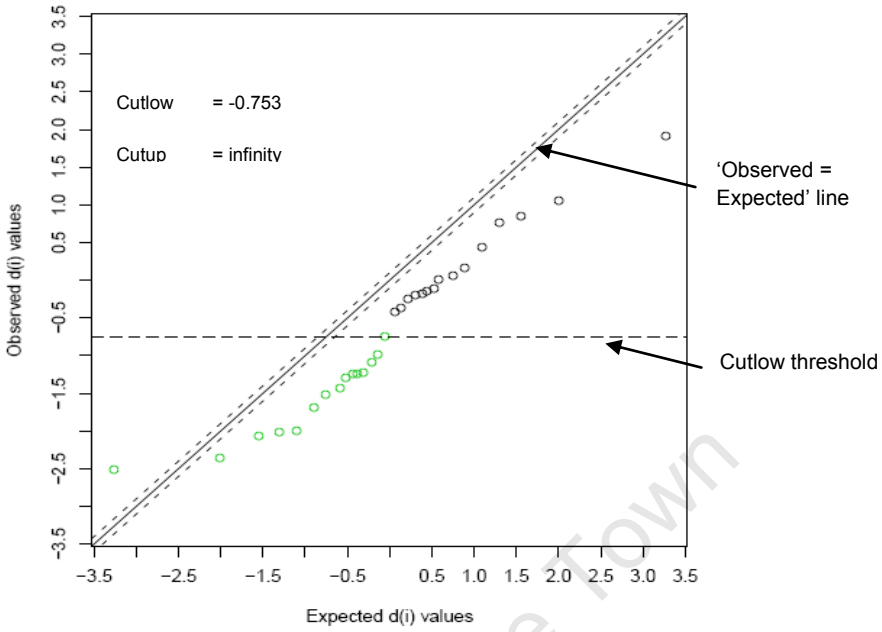

Figure 4.15: Significance analysis of microarrays (and metabolites) (SAM) of organic acids in the untreated and drug-treated cell culture supernatants without insulin stimulation. 60 organic acids in untreated cell culture supernatants versus those treated with indinavir (50 µM) for 16 h at the basal level were plotted on the graph based on the d-value (Table 4.5). The green circles represent significant differences in the levels of 15 organic acids (see Table 4.5) between the two groups (i.e. the levels of the organic acids were decreased). FDR = false discovery rate.

Table 4.5: Significantly different organic acids in the untreated and drug-treated cell culture supernatants without insulin stimulation, identified by SAM (from Figure 4.15). d-value = a score i.e. peak area of organic acids which is changed relative to the standard deviation (stdev) of repeated measurements, stdev = standard deviation, rawp = raw p-value from Student's *t*-test.

Organic acids	d-value	stdev	rawp	Relative fold-effect	Changes
1. Butane	-2.516	1.620	0.057	0.059	Decrease
2. 1,2,3-propanetricarboxylic acid	-2.359	0.433	0.067	0.493	Decrease
3. Propanoic acid	-2.073	0.431	0.097	0.538	Decrease
4. Carbamic acid	-2.015	2.934	0.100	0.017	Decrease
5. Benzene	-1.997	1.416	0.103	0.141	Decrease
6. Pantothenic acid	-1.692	1.288	0.200	0.221	Decrease
7. L-proline	-1.523	1.296	0.220	0.255	Decrease
8. (R*,S*)-3,4-dihydroxybutanoic acid	-1.432	0.720	0.237	0.489	Decrease
9. Butanoic acid, 4-(trimethylsiloxy)-ethylester	-1.294	1.694	0.267	0.219	Decrease
10. Heptadecanoic acid	-1.248	0.592	0.273	0.599	Decrease
11. Butanoic acid, 3-(trimethylsiloxy)-ethylester	-1.244	0.476	0.277	0.663	Decrease
12. Azelaic acid	-1.224	1.205	0.287	0.360	Decrease
13. Octadecanoic acid	-1.090	1.874	0.343	0.243	Decrease
14. Nonanoic acid	-0.981	1.252	0.387	0.427	Decrease
15. 1-pentanethyldisilyloxybutane	-0.753	1.911	0.500	0.369	Decrease

University Of Cape Town

In the cell culture supernatants analysed with insulin stimulation, the cutup was 0.335, while the cutlow of the graph was -3.200 (Figure 4.16). In total, there were significant differences in the levels of 18 organic acids in the drug-treated versus untreated supernatants (Figure 4.16 and Table 4.6). Data from Table 4.6 indicate that succinate, isovalerate and butanoic acid 3-(trimethylsiloxy)-ethylester had the lowest d-value (>-3.200) at the threshold, with the lowest p-value (rawp) of <0.1. Thus, succinate, isovalerate and butanoic acid 3-(trimethylsiloxy)-ethylester were identified as the organic acids having the most significantly different levels in the untreated versus drug-treated cell culture supernatants with insulin stimulation.

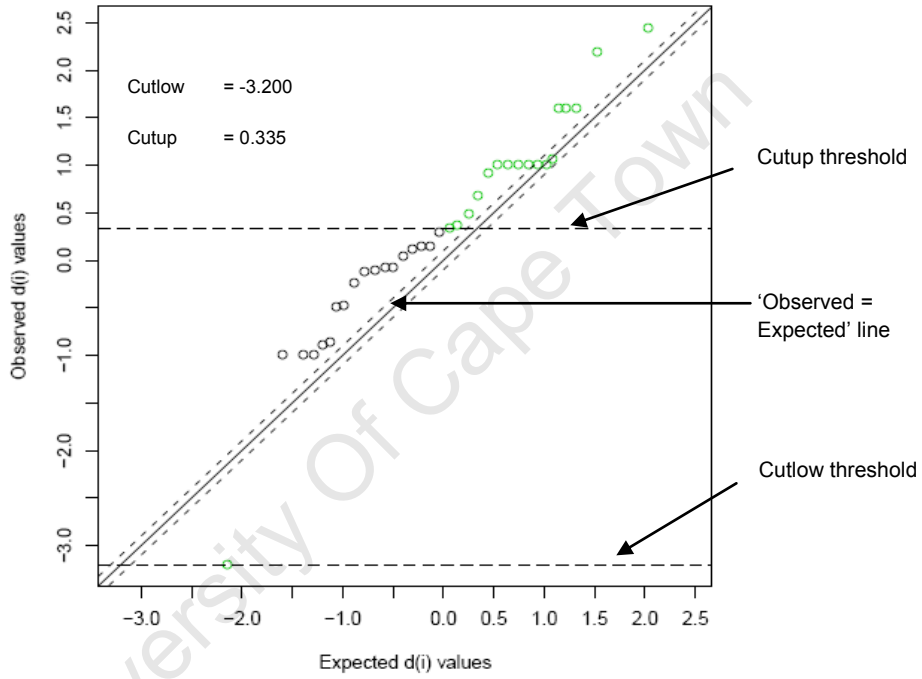

Figure 4.16: Significance analysis of microarrays (and metabolites) (SAM) of organic acids in the untreated and drug-treated cell culture supernatants with insulin stimulation. 60 organic acids in untreated cell culture supernatants versus those treated with indinavir (50 μM) for 16 h at the basal level were plotted on the graph based on the d-value (Table 4.6). The green circles represent significant differences in the levels of 18 organic acids (see Table 4.6) between the two groups (i.e. the levels of the organic acids were increased). FDR = false discovery rate.

Without insulin stimulation, butane was observed not to be statistically different in indinavir-treated supernatants versus the basal culture medium (control) (Figure 4.10). Results from PLS-DA and SAM analyses indicated that butane was the organic acid with the most significantly different levels between the drug-treated versus untreated cell culture supernatants. In particular, in this study, synthesis of butane was found to be significantly decreased in the drug-treated cell culture supernatants (Figure 4.17).

University Of Cape Town

Table 4.6: Significantly different organic acids in the untreated and drug-treated cell culture supernatants with insulin stimulation identified by SAM (from Figure 4.16). d-value = a score i.e. peak area of organic acids, which is changed relative to the standard deviation (stdev) of repeated measurements, stdev = standard deviation, rawp = raw p-value from Student's *t*-test.

Organic acids *	d-value	stdev	rawp	Relative fold-effect	Changes
1. Succinate	-3.200	0.978	0.006	0.114	Decrease
2. Isovalerate	2.443	1.470	0.022	12.047	Increase
3. Butanoic acid, 3-(trimethylsiloxy),-ethylester	2.194	1.404	0.035	8.461	Increase
4. Pentasiloxane, dodecamethyl	1.599	1.049	0.105	3.199	Increase
5. 2-ethylhydracrylic acid	1.596	0.897	0.12	2.697	Increase
6. Glycerol	1.591	0.612	0.138	1.963	Increase
7. D-erythro-pentonic acid	1.057	1.759	0.253	3.628	Increase
8. 2,4,6(1H,3H,5H)-pyrimidinetrione,5-(1-methylpopyl)	1.000	0.662	0.271	1.582	Increase
9. Oxacyclotetradec-5-yn	1.000	0.609	0.373	1.525	Increase
10. Trifluoromethyl-bis-(trimethyl)methylketone	1.000	0.526	0.373	1.440	Increase
11. 4-hydroxyphenyllactate	1.000	0.737	0.470	1.667	Increase
12. Phosphorous acid	1.000	0.481	0.470	1.396	Increase
13. 3-hydroxybutyrate	1.000	1.499	0.527	2.826	Increase
14. Homovanillate	0.909	1.315	0.551	2.290	Increase
15. Phenyl acetic acid	0.675	0.944	0.639	1.556	Increase
16. Benzoic acid	0.484	1.108	0.735	1.450	Increase
17. Pyroglutamate	0.362	0.669	0.792	1.183	Increase
18. Phenylacetylglycine	0.335	0.801	0.803	1.204	Increase

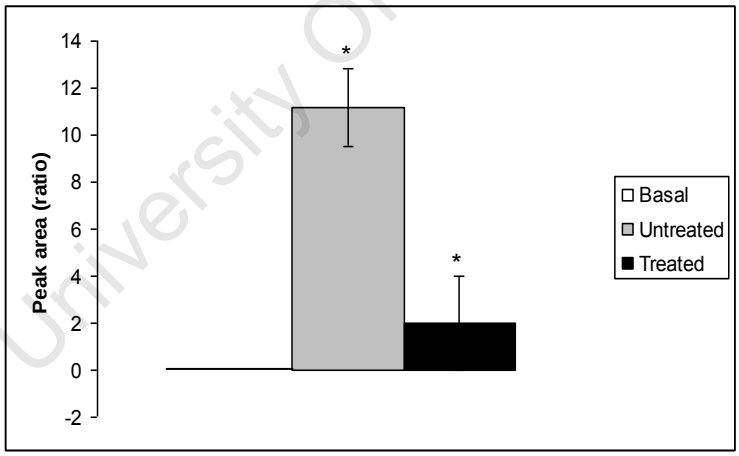

Figure 4.17: Synthesis of butane in the drug-treated cell culture supernatants without insulin stimulation based on PLS-DA and SAM analyses. 3T3-L1 adipocytes were left untreated ( ) and treated ( ) with indinavir (50 μM) for 16 h at the basal level. Cell culture supernatants were harvested for organic acid analysis using GC-MS. Basal ( ) culture medium was used as a control. Data are shown as the mean ± S.E.M. (n=3). $p < 0.05$ versus untreated cell culture supernatants.

University Of Cape Town

With insulin stimulation, butanoic acid 3-(trimethylsiloxy)-ethylester was revealed to be significantly increased (i.e. synthesised more) in cell culture supernatants treated with indinavir, followed by insulin stimulation, versus the basal culture medium (control) (Figure 4.10). Based on volcano plot, PLS-DA and SAM analyses, butanoic acid 3-(trimethylsiloxy)-ethylester was identified as among the most significantly different organic acids between untreated cell culture supernatants versus those treated with indinavir, followed by insulin stimulation. In particular, synthesis of butanoic acid 3-(trimethylsiloxy)-ethylester was significantly increased in the drug-treated versus untreated cell culture supernatants (Figure 4.18).

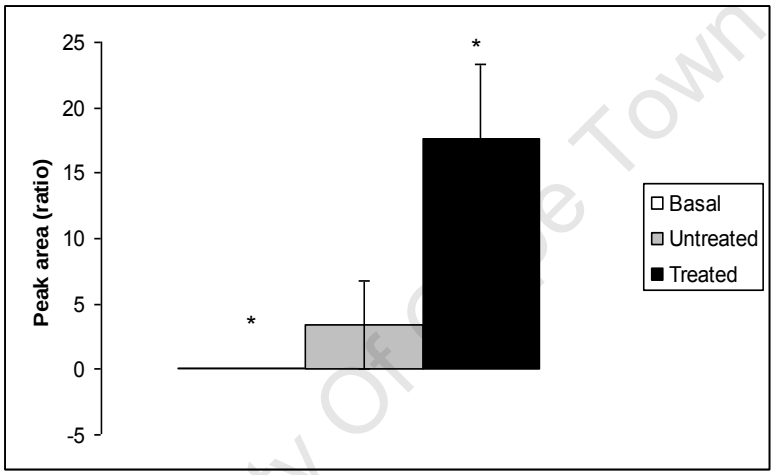

Figure 4.18: Synthesis of butanoic acid 3-(trimethylsiloxy)-ethylester in the drug-treated cell culture supernatants with insulin stimulation, based on PLS-DA and SAM analyses. 3T3-L1 adipocytes were left untreated (▢) or treated (■) with indinavir (50 μM) for 16 h with or without insulin stimulation. Cell culture supernatants were harvested for organic acid analysis using GC-MS. Basal (☐) culture medium was used as a control. Data are shown as the mean ± S.E.M. (n=5). $p < 0.05$ versus basal culture medium (control).

University Of Cape Town

Levels of succinate were not statistically different in untreated cell culture supernatants or those treated with indinavir (followed by insulin stimulation) versus the basal culture medium (control) (Figure 4.10). However, in the context of biology, the difference in succinate may be significant between the groups and the control. Volcano plot, PLS-DA and SAM analyses indicated that succinate was among the organic acids with most significantly different levels between untreated cell culture supernatants versus those treated with indinavir, followed by insulin stimulation. In particular, synthesis of succinate was significantly reduced in the drug-treated versus untreated cell culture supernatants (Figure 4.19).

Isovalerate was identified as exclusively significant, i.e. synthesised only in cell culture supernatants treated with indinavir, followed by insulin stimulation, using volcano plot, PLS-DA and SAM analyses.

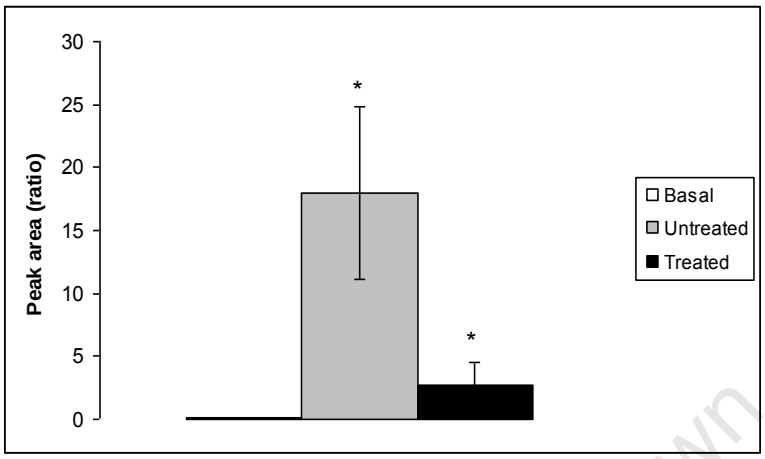

Figure 4.19: Synthesis of succinate in the drug-treated cell culture supernatants (with insulin stimulation) based on PLS-DA and SAM analyses. 3T3-L1 adipocytes were left untreated ( ) and treated ( ) with indinavir (50 µM) for 16 h followed by insulin stimulation. Cell culture supernatants were harvested for organic acid analysis using GC-MS. Basal ( ) culture medium was used as a control. Data are shown as the mean ± S.E.M. (n=5). $p < 0.05$ versus untreated cell culture supernatants.

University Of Cape Town

4.3.3 Free fatty acid analysis

FFA analysis was performed in untreated cell culture supernatants and those treated with indinavir for 16 h in a serum-free medium followed by insulin stimulation, and in Medium 4, using the Free Fatty Acids Half-Micro Test Kit. Results from the analysis indicate that there were no differences in the levels of FFAs in the untreated and drug-treated cell culture supernatants in the serum-free medium without (Figure 4.20(a)) and with (Figure 4.20(b)) insulin stimulation, compared to the basal serum-free medium.

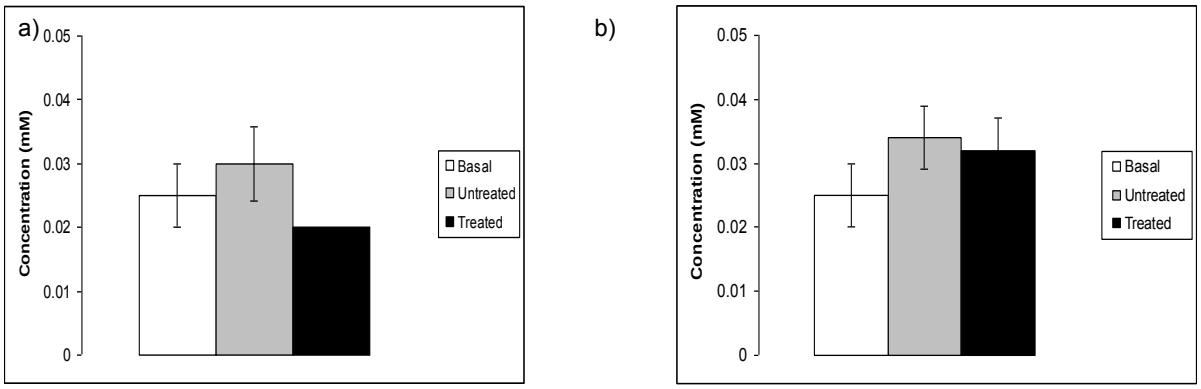

Figure 4.20: FFA analysis using the Free Fatty Acids Half-Micro Test Kit (Roche). 3T3-L1 adipocytes were serum-starved and treated with indinavir (50 µM) ( ) or left untreated ( ) for 16 h without (a) and with (b) insulin stimulation. Data are shown as the mean and S.E.M. (n=3). Basal ( ) = serum-free medium (control).

There was a significant decrease (p = 0.02) in the levels of FFAs in Medium 4 exposed to cells when compared to basal cell culture. However, this significant decrease in the levels of FFAs was not evident when cells were treated with indinavir (Figure 4.21).

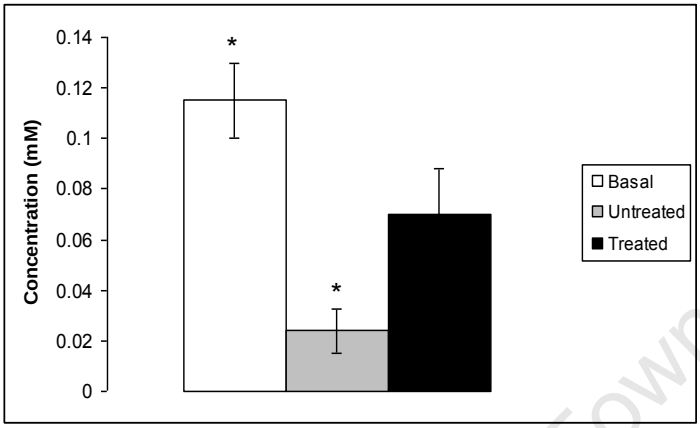

Figure 4.21: FFA analysis using the Free Fatty Acids Half-Micro Test Kit (Roche). 3T3-L1 adipocytes were cultured, and left untreated (▒) and treated (■) with indinavir (50 μM) in Medium 4 for 16 h. Data are shown as the mean and S.E.M. (n=3). *p < 0.05, using Student's *t*-test versus basal culture medium (control).
Basal (□) = Medium 4 (control).

University Of Cape Town

4.4 Discussion

Adipocyte metabolism is critical for the biological functions of multicellular organisms. Any alteration in adipocyte metabolism induced by protease inhibitors is likely to affect insulin action. For the first time the effect of indinavir on amino acid and organic acid metabolism in 3T3-L1 adipocytes was investigated using metabolomic analysis, by GC-MS. This is advantageous, as secreted metabolites from the cell culture supernatants are easier to measure than a complex cell lysate. Any perturbation in adipocyte metabolome may be easier to detect. Moreover, to date the number of systematic studies of metabolites from adipocytes treated with HIV protease inhibitors using these approaches has been limited.

Generally, the synthesis of amino acids without insulin stimulation was found to be higher in cell culture supernatants treated with indinavir versus untreated supernatants. However, with insulin stimulation, synthesis of amino acids was lower in the drug-treated than in the untreated supernatants. These findings show that antiretroviral drugs may interfere in insulin-mediated amino acid metabolism in the cells.

In the context of organic acids in untreated cell culture supernatants and in those treated with indinavir, several organic acids were exclusively synthesised at the basal level, while some were found only with insulin stimulation. In addition, some organic acids were found at

both levels. Most interestingly, there were several organic acids that were exclusively synthesised in drug-treated supernatants, with or without insulin stimulation. They may act as biomarkers in the study of insulin resistance induced by protease inhibitors.

The organic acids in untreated and drug-treated cell culture supernatants appeared higher with insulin stimulation. However, in general, with insulin stimulation the organic acid levels in the untreated supernatants were higher than in the drug-treated supernatants. It appears that HIV protease inhibitors alter the insulin-mediated metabolism of organic acids.

In order to find the most significantly different amino acid and organic acid levels in the cell culture supernatants, the data were analysed using the MetaboAnalyst web server (Xia et al., 2009). Access to this web server is free; it is easy to use; it is able to characterise a large number of metabolites; and it accepts a variety of input data, such as nuclear magnetic resonance peak list, binned spectra, mass spectrometry peak list, compound or concentration data, in a wide variety of formats, from GC-MS to liquid chromatography mass spectrometry (Xia et al., 2009). Thus, the web server is very useful, and suited to analysing the data from the present study.

In amino acid analysis, without insulin stimulation, aspartate was the amino acid found to have the most significantly different level between the untreated and indinavir-treated cell culture supernatants. This amino acid is the carboxylic acid analogue of asparagine. Aspartate is a nonessential amino acid which is made from glutamic acid by enzymes, using vitamin B6 (http://www.hmdb.ca/). It has important roles in the urea cycle and in DNA metabolism (http://www.hmdb.ca/). In addition, aspartate is a major excitatory neurotransmitter, which is sometimes found to be increased in epileptic and stroke patients (Rainesalo et al., 2004). However, the function of aspartate in insulin resistance is still unclear. In the present study, aspartate was found to have significantly higher levels in the drug-treated versus untreated cell culture supernatants. This result shows that the antiretroviral drug may alter aspartate metabolism in the cells and then induce insulin resistance.

Synthesis of hydroxylysine was significantly reduced in cell culture supernatants treated with indinavir versus untreated supernatants, with insulin stimulation. This amino acid derivative is hydroxylated from lysine and is involved in collagen synthesis (Rautavuoma et al., 2002). Adiponectin, an adipokine released by adipocytes, contains a collagenous domain with four lysine residues (68, 71, 80 and 104) (Fonseca-Alaniz et al., 2007). These four lysines have been reported to be hydroxylated to hydroxylysine, and subsequently glycosylated to modulate the insulin sensitivity of cells (Wang et al., 2002). A previous study noted that adiponectin levels were negatively correlated with insulin resistance and lipodystrophy

University Of Cape Town

induced by protease inhibitors (Gougeon et al., 2004). The low level of hydroxylysine synthesis observed in the present study may be correlated with a low level of adiponectin, which has induced insulin insensitivity in the cells.

Organic acid analysis of indinavir-treated cells revealed a significantly decreased level of butane in the treated versus untreated cell culture supernatants, without insulin stimulation. The significance of this finding, however, is unclear and requires further investigation.

With insulin stimulation, synthesis of succinate was significantly reduced in cell culture supernatants treated with indinavir versus untreated supernatants. Succinate is a Krebs cycle intermediate (http://www.hmdb.ca/) and has been observed at higher levels during differentiation of 3T3-F442A adipocytes (Lai and Goldman, 1992). A low level of succinate in the treated cell culture supernatants may indicate low activity of the Krebs cycle. In addition, extracellular glucose uptake, which is essential for the Krebs cycle, is inhibited during insulin resistance (Murata et al., 2002; Rudich et al., 2001). Therefore, it is possible that inhibition of glucose uptake decreased activity of the Krebs cycle and reduced synthesis of succinate.

Isovalerate was exclusively identified in cell culture supernatants treated with indinavir with insulin stimulation. This organic acid is derived from leucine catabolism (http://www.hmdb.ca/). Utilisation of leucine was higher in the treated cell culture supernatants, although this increase was not statistically different compared to the untreated cell culture supernatants. A high utilisation of leucine suggests an increase in synthesis of isovalerate in the treated cell culture supernatants. Though the function of isovalerate is still unclear, increased isovalerate has been observed to be associated with certain diseases such as Reye's syndrome (Trauner et al., 1975).

Synthesis of butanoic acid 3-(trimethylsiloxy)-ethylester was significantly increased in cell culture supernatants treated with indinavir versus untreated supernatants, followed by insulin stimulation. Butanoic acid 3-(trimethylsiloxy)-ethylester (aka butyric acid) is a fatty acid and a normal urinary metabolite (http://www.hmdb.ca/). Overproduction of this organic acid will produce ketone bodies and may induce ketosis and ketoacidosis. Overproduction of ketone bodies is associated with insulin deficiency in type 1 diabetes mellitus (Laffel, 1999). In this study, 3-hydroxybutyrate, a ketone body, was synthesised only in the treated cell culture supernatants, but the results were not statistically different compared to those of the untreated supernatants, based on volcano plot, PLS-DA and SAM analyses. Thus, butanoic acid 3-(trimethylsiloxy)-ethylester and ketone bodies are probably involved in the insulin resistance induced by protease inhibitors.

University of Cape Town

The levels of FFAs in untreated supernatants of 3T3-L1 adipocytes and those treated with HIV protease inhibitors were investigated for the first time. The levels of FFAs established were not statistically different in untreated cell culture supernatants and those treated with indinavir in a serum-free medium for 16 h (with or without insulin stimulation) to those of the control (basal serum-free medium).

The levels of FFAs were significantly increased in the basal culture Medium 4 (DMEM with 10 % FCS, 2 mM L- glutamine, 1 % of 100 x antibiotic/antimycotic and 0.1 % gentamicin) versus cell culture supernatants untreated with indinavir left in the medium for 16 h. The presence of FFAs probably reflects the contribution of serum.

The levels of FFAs were significantly decreased in the untreated cell culture supernatants versus the basal Medium 4. In particular, 3T3-L1 adipocytes untreated with indinavir utilised FFAs which were supplied in the medium. However, the levels of FFAs were not significantly decreased in the drug-treated cell culture supernatants versus the basal Medium 4. This finding indicates that the drug-treated cells used smaller amounts of FFAs in the culture medium than the cells untreated with indinavir. It appears that indinavir decreased the ability of the cells to utilise the FFAs in the medium. Thus, the levels of FFAs were higher (i.e. they had accumulated) in the drug-treated versus untreated cell culture supernatants. The high levels of FFAs may induce insulin resistance.

FFAs have been reported to play a role similar to TNF-α, which activates the inflammatory pathway of IKKβ and NFκB, and then phosphorylates serine 307 of IRS-1, thus inhibiting insulin signalling in rodent (Lee et al., 2009). This finding parallels the Western blot analysis (see Chapter 3), showing that the NFκB pathway may be involved in inducing insulin resistance in 3T3-L1 adipocytes treated with protease inhibitors. However, these findings are still unclear, as the levels of FFAs observed in the basal serum-free medium, and in the untreated cells and those treated with indinavir in serum-free medium followed by insulin stimulation, were not statistically different.

University Of Cape Town

4.5 Conclusion

Metabolomic analysis is emerging as a powerful tool for analysing disease conditions. The results from this study suggest that HIV protease inhibitors induce alterations in the metabolism of adipocytes. FFAs may play a role in inducing insulin resistance in 3T3-L1 adipocytes treated with protease inhibitors via the NFκB pathway. The alterations in the levels of aspartate, hydroxylysine, succinate, isovalerate and butanoic acid 3-(trimethylsiloxy)-ethylester may be a secondary effect and a marker of insulin insensitivity induced by a high level of FFAs. However, further studies are required to confirm these

findings. An understanding of the effects of protease inhibitors on adipocyte metabolism, particularly regarding the levels of amino acids, organic acids and FFAs, may shed new light on drug development.

University Of Cape Town

CHAPTER 5: EFFECT OF HIV PROTEASE INHIBITORS ON LIPOPROTEIN LIPASE ACTIVITY IN ADIPOCYTES

5.1 Introduction

Lipoprotein lipase (LPL) is an enzyme expressed in cardiac muscle, skeletal muscle and adipose tissue, and is located in the endothelial cells lining the capillaries. This insulin-regulated enzyme hydrolyses the lipids in lipoprotein to three free fatty acids and one glycerol molecule, and therefore has a function in the anabolic actions of insulin. Abnormalities in LPL function have been reported to be associated with a number of pathophysiological conditions, including atherosclerosis, chylomicronaemia, Alzheimer's disease and cancer, as well as lipodystrophy associated with insulin resistance and diabetes mellitus (Mead et al., 2002).

More than 60 % of HIV-positive patients treated with protease inhibitors develop lipodystrophy associated with insulin resistance (Barbaro and Barbarini, 2006; Gan et al., 2001). Lipodystrophy is a result of the abnormal hydrolysis and remobilisation of adipose tissue. It appears that protease inhibitors are the major antiretroviral drugs causing these abnormalities. However, the mechanisms responsible for these side effects have not been positively established. As alluded to above, LPL is known to play a role in lipid storage in adipose tissue, in response to insulin. Therefore, it is important to assess LPL activity in adipocytes after exposure to protease inhibitors.

LPL activity has been measured in 3T3-L1 adipocytes using several methods (Dousset et al., 1988; Nilsson-Ehle and Schotz, 1976; Shirai and Jackson, 1982; Trost et al., 2009; Vilaro et al., 1986). Traditional methods for LPL activity assay include: measurement of the hydrolysis of a radioactive substrate emulsion ([^{3}H]triolein (glycerol tri-[9,10(N)-^{3}H]oleate) (Nilsson-Ehle and Schotz, 1976), fluorescently labelled triacylglycerol as a substrate (Dousset et al., 1988), and a method which measures the clearing of Intralipid (Vilaro et al., 1986). A fluorescent LPL activity assay kit (Roar, NY, USA) has recently been developed to measure the activity of the enzyme (Yokota et al., 2009). This method uses a ready-made non-fluorescent substrate emulsion (propriety substrate) which becomes intensely fluorescent when it is hydrolysed by LPL.

However, these methods are either expensive, or laborious and cumbersome. By contrast, an earlier method for assaying LPL in milk established that LPL-catalysed hydrolysis of *p*-nitrophenyl butyrate (pNPB) could be measured relatively easily and cheaply using the appearance of *p*-nitrophenyl phosphate as an endproduct (Shirai and Jackson, 1982). This method has not been evaluated on adipocytes or *in vivo*.

University of Cape Town

The objective of this study was to establish a rapid and robust method for analysing LPL activity in supernatants from 3T3-L1 adipocytes, such that the effects of various protease inhibitors on LPL activity could be assessed.

5.2 Methods

5.2.1 Preparation of 3T3-L1 adipocytes for the assay of released LPL

3T3-L1 adipocytes were differentiated and serum-starved as described in sections 2.2.1 and 2.2.2 (Wilcox et al., 2004). The cells were rinsed with PBS (1 ml) twice, and bathed in an additional aliquot of fresh PBS (500 µl) containing insulin (100 ng/ml) (17 nM) for 1 h at 37 °C in an incubator, to stimulate LPL activity. After 1 h, heparin sodium-fresenius (final concentration 100 U/ml) was added for a further 20 min to release the enzyme from the cell surface (Knutson, 2000; Ong et al., 1988; Ranganathan and Kern, 2002; Stewart and Schotz, 1974). The cell culture supernatants were then harvested in order to assay LPL activity. The cells that remained were lysed with lysis buffer to measure protein concentration, as described in section 2.2.3.

5.2.2 Linearity tests

Part of the validation of the assay required assessment of the linearity of the assay methodology using pNPB as a substrate for the measurement of LPL activity. Linearity was assessed as a function of both time (measured in duplicate in six independent experiments) and LPL concentration (measured in duplicate in two independent experiments). For the former, LPL activity in 100 µl of the 500 µl cell culture supernatants harvested was measured continuously at specific time points (after 5, 10, 15, 30, 60, 120, 180 and 240 min) of incubation at 37 °C in a waterbath. The linearity of the assay in response to LPL concentration was measured using 100 µl cell culture supernatants diluted serially twofold stepwise in PBS.

The standard for the experiment was prepared from LPL derived from *Pseudomonas* sp. in a range of concentrations from 2.13 µU/mg to 213 U/mg. Enzyme activity was also measured after the addition of phenylmethylsulphonyl fluoride (PMSF) (1 mM) (measured in duplicate in two independent experiments), to confirm that the assessed enzyme activity belonged to the LPL, as PMSF is known to inhibit LPL activity (Quinn et al., 1983). PMSF (10 mM) was prepared in ethanol.

University Of Cape Town

5.2.3 **LPL activity assay**

The assay of LPL activity in supernatants from 3T3-L1 adipocytes was designed as follows (Shirai and Jackson, 1982):

900 µl buffer + 100 µl supernatants from 3T3-L1 adipocytes + 10 µl pNPB in acetonitrile Total volume = 1010 µl

Cell culture supernatants (100 µl) were mixed with 900 µl buffer (0.1 M sodium phosphate, monobasic, anhydrous, pH 7.2; 0.9 % sodium chloride; 0.5 % (v/v) Triton X-100 (900 µl)) (Quinn et al., 1982; Shirai and Jackson, 1982). pNPB (10 µl of 50 mM in acetonitrile at 1 % (v/v) final concentration) was then added. The reactions were incubated in cuvettes at 37 °C in a waterbath (Shirai and Jackson, 1982) for specific periods of time. Absorbance was then measured using spectrophotometry at 400 nm.

Enzyme activity was calculated using the following formula (Quinn et al., 1983):

$$\text{Units/ml enzyme} = \frac{(\Delta A_{400nm}/\text{min test} - (\Delta A_{400nm}/\text{min substrate blank}))\ (1.01)\ (df)}{(0.0148)(0.1)}$$

1.01 = volume (in ml) of incubation mixture

df = dilution factor (0.1)

0.0148 = µM extinction coefficient of *p*-nitrophenol at 400 nm

0.1 = volume (in ml) of enzyme used

$$\text{Units/mg protein} = \frac{\text{units/ml supernatant}}{\text{mg protein/ml supernatant}}$$

Unit definition:

One unit will release 1.0 nmole of *p*-nitrophenol phosphate per minute at pH 7.2 and 37° C, when using *p*-nitrophenyl butyrate as substrate.

University Of Cape Town

5.2.4 Effect of HIV protease inhibitors on LPL activity

3T3-L1 adipocytes were serum-starved and treated with HIV protease inhibitors for 16 h. The protease inhibitors used were at plasma concentrations determined *in vivo* or at experimental concentration as measured in Chapter 3. Plasma concentrations of darunavir (2 μM) and tipranavir (15 μM) have previously been reported (Martin et al., 2009). The experimental concentration of indinavir (50 μM) was previously determined (see Chapter 3). The cells were then stimulated with insulin to increase LPL activity and treated with heparin to release LPL, as described in section 5.2.1. The LPL activity in 100 μl of the cell culture supernatants was measured as described in section 5.2.3, after 10 min incubation in a waterbath at 37 °C and measured in duplicate in two independent experiments.

In addition to measuring whether these drugs interfere directly with LPL activity, quantities of the drugs (darunavir (2 μM), tipranavir (15 μM) and indinavir (50 μM)) were added directly to the assay reaction after recovering the untreated (no drug) cell culture supernatants from cells stimulated with both insulin and heparin. These were then incubated at 37 °C in a waterbath for 10 min. This experiment was also designed to reveal whether the drugs affected the spectral absorbance of the assay reaction. This experiment was conducted once.

5.3 Results

5.3.1 Optimisation procedures

The LPL-catalysed hydrolysis of pNPB was successfully measured in supernatants of 3T3-L1 adipocytes stimulated with both insulin and heparin (Figure 5.1). Cells which were stimulated with both insulin and heparin had significantly increased LPL activity, with detectable enzyme release from the cell surface from 5 min ($p = 0.0005$) up to 120 min ($p = 0.03$) incubation. The cells which were stimulated with heparin only also released LPL from the cell surface, and showed significantly increased LPL activity after 5 min ($p = 0.04$) up to 120 min ($p = 0.03$) incubation. However, the LPL activity in cell culture supernatants stimulated with heparin only was significantly lower after 5 min ($p = 0.002$) up to 60 min ($p = 0.02$) of incubation than the enzyme activity from the cells stimulated with both insulin and heparin.

University Of Cape Town

In 3T3-L1 adipocytes stimulated with both insulin and heparin, LPL activity reached a plateau at 60 min. However, in cells stimulated with heparin only, LPL activity reached a plateau at a later time point. This result indicates that LPL activity was higher (i.e. the total enzyme activity was higher) in the cell culture supernatants stimulated with both insulin and heparin, compared to the cell culture supernatants stimulated with heparin only. Thus, insulin significantly increased the level of enzyme activity.

LPL activity in 3T3-L1 adipocytes stimulated with insulin, but not heparin-treated, was not significantly different from the LPL activity of the cells in PBS (Figure 5.1). No LPL was released from unstimulated cells in PBS, or from cells stimulated with insulin without the addition of heparin.

The release of *p*-nitrophenol from supernatants of 3T3-L1 adipocytes stimulated with both insulin and heparin was linear for 15 min (Figure 5.1). Thus, 10 min of incubation was considered appropriate for future experimentation.

University Of Cape Town

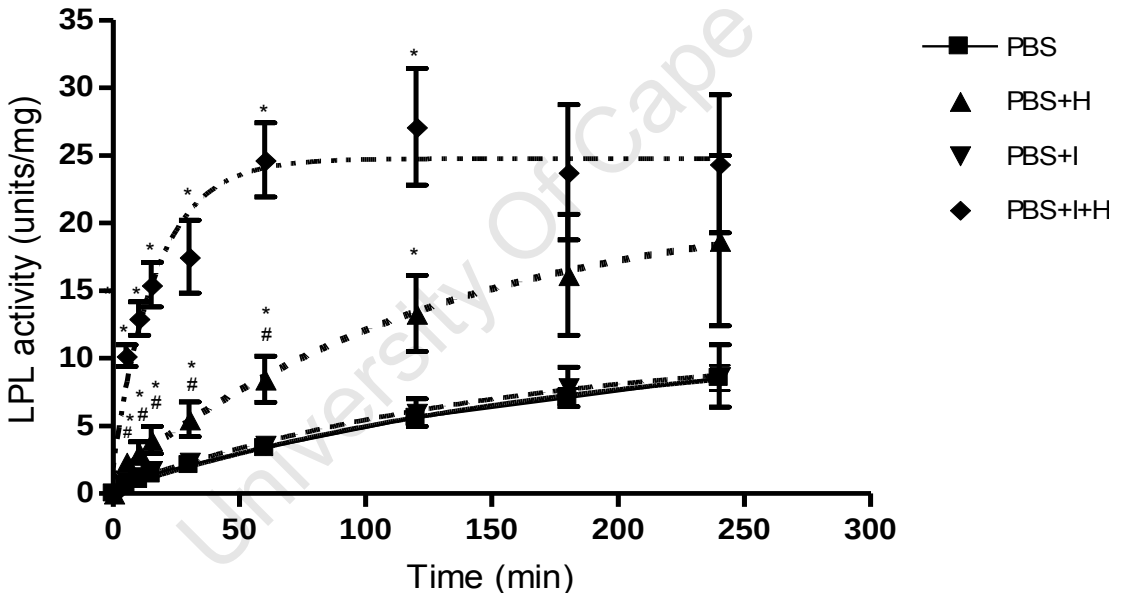

Figure 5.1: Time course of LPL activity in supernatants of 3T3-L1 adipocytes stimulated with insulin and heparin. 3T3-L1 adipocytes were stimulated with insulin for 1 h followed by the addition of heparin. Cell culture supernatants were harvested to measure LPL activity at indicated incubation periods using spectrophotometry (400 nm). LPL activity was measured in duplicate in six independent experiments. Data are shown as the mean and S.E.M. (n=6). * = PBS+I+H or PBS+H versus PBS, # = PBS+H versus PBS+I+H, $p<0.05$, using Student's *t*-test. PBS = phosphate buffered saline, H = heparin, I = insulin.

In the assessment of linearity with respect to LPL concentration, 100 µl and twofold serial dilutions of LPL from supernatants of 3T3-L1 adipocytes stimulated with both insulin and heparin were prepared in the assay reaction, and incubated for 10 min. The absorbance of the LPL activity assay showed linearity after the 10 min incubation (Figure 5.2).

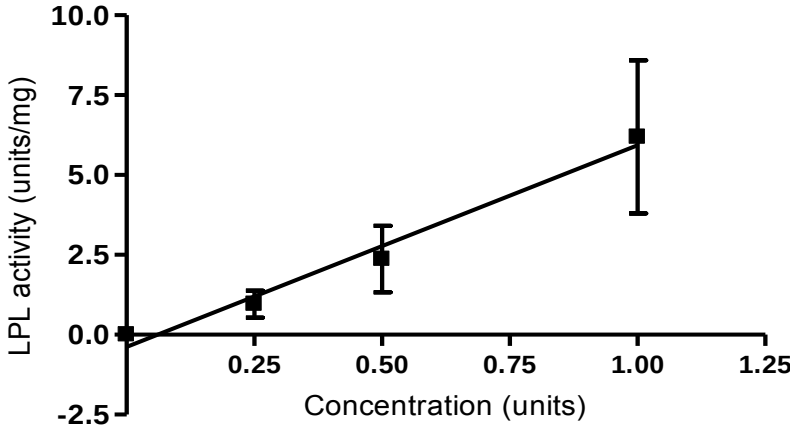

Figure 5.2: LPL activity in supernatants of 3T3-L1 adipocytes stimulated with both insulin and heparin, at different dilutions after 10 min incubation. 3T3-L1 adipocytes were stimulated with insulin for 1 h followed by the addition of heparin. Cell culture supernatants were harvested to measure LPL activity at different concentrations after 10 min incubation using spectrophotometry (400 nm). LPL activity was measured in duplicate in two independent experiments. Data are shown as the mean and S.E.M. (n=2).

LPL was assayed after the addition of PMSF for the different times indicated. The results showed significantly decreased LPL activity in 3T3-L1 adipocytes stimulated with both insulin and heparin after 10 min ($p = 0.04$) to 240 min ($p = 0.01$) incubation (Figure 5.3). The activity of LPL in cell culture supernatants in PBS with or without PMSF addition was not significantly different. These data indicate that PMSF inhibited enzyme activity, suggesting that the enzyme activity noted belonged to the LPL.

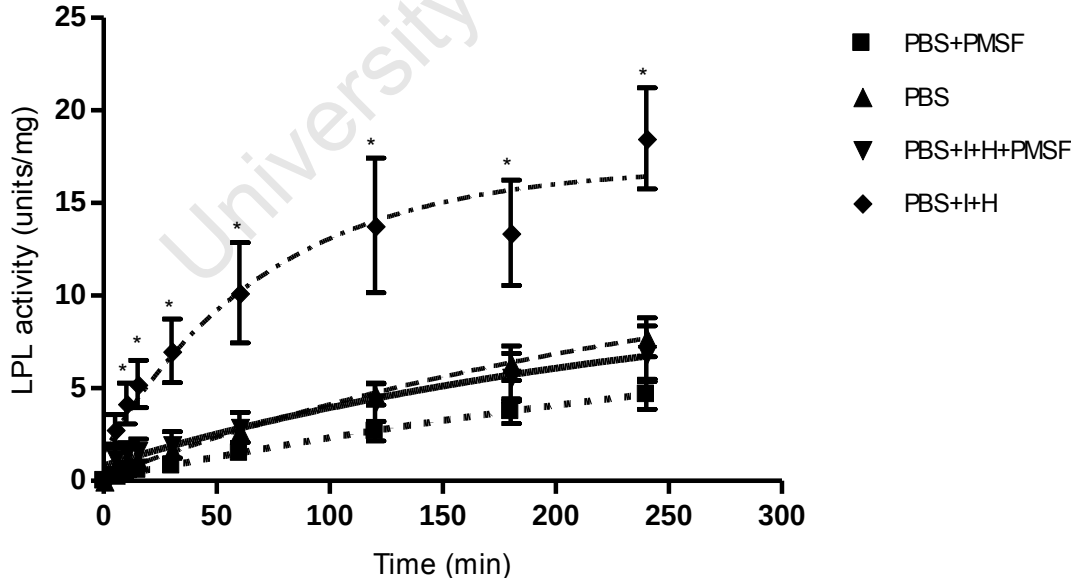

Figure 5.3: LPL activity terminated by PMSF. 3T3-L1 adipocytes were stimulated with insulin for 1 h followed by the addition of heparin. Cell culture supernatants were harvested and PMSF was then added prior to the indicated incubation periods to measure LPL activity using spectrophotometry (400 nm). LPL activity was measured in duplicate in two independent experiments. Data are shown as the mean and S.E.M. (n=2). * = PBS+I+H versus PBS+I+H+PMSF, $p<0.05$, using Student's *t*-test (Lord test). PBS = phosphate buffered saline, H = heparin, I = insulin, PMSF = phenylmethylsulphonyl fluoride.

University of Cape Town

5.3.2 Effect of HIV protease inhibitors on LPL activity

LPL activity was measured in 3T3-L1 adipocytes treated with darunavir, tipranavir and indinavir for 16 h using the optimised assay conditions. As observed previously, LPL activity was significantly increased ($p = 0.002$) when cells were exposed to both insulin and heparin, compared to the unstimulated cell culture supernatants (Figure 5.4). In addition, the results showed darunavir ($p = 0.002$) and indinavir ($p = 0.002$) significantly decreased LPL activity (Figure 5.4) compared to the enzyme activity in the untreated cells exposed to both insulin and heparin.

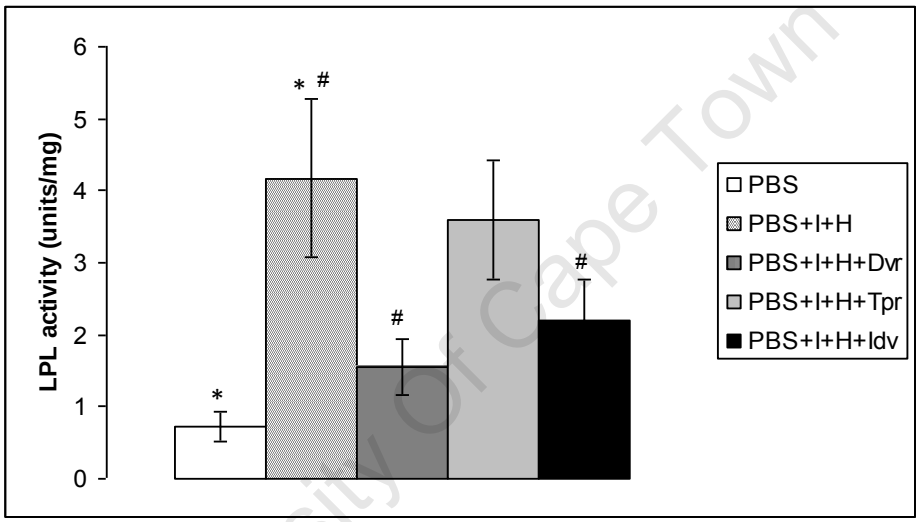

Figure 5.4: LPL activity in supernatants of 3T3-L1 adipocytes treated with darunavir, tipranavir and indinavir. 3T3-L1 adipocytes were treated with the protease inhibitors for 16 h in a serum-free medium, followed by exposure to both insulin and heparin. LPL activity was measured in duplicate in two independent experiments. Data are shown as the mean and S.E.M. (n=2). * = PBS versus PBS+I+H, # = PBS+I+H+Dvr or PBS+I+H+Idv versus PBS+I+H, $p < 0.05$, using Student's *t*-test (Lord test). PBS = phosphate buffered saline, H = heparin, I = insulin, Dvr = darunavir, Tpr = tipranavir, Idv = indinavir.

Protease inhibitors that were added directly to the assay reaction prior to incubation in a waterbath for 10 min did not decrease LPL activity (Figure 5.5). In contrast, LPL activity from cells treated with the protease inhibitors darunavir and indinavir showed decreased enzyme activity as observed above (Figure 5.4). In addition, it was found that the drugs did not interfere with the spectral absorbance of the assay reaction at the wavelength used.

University Of Cape Town

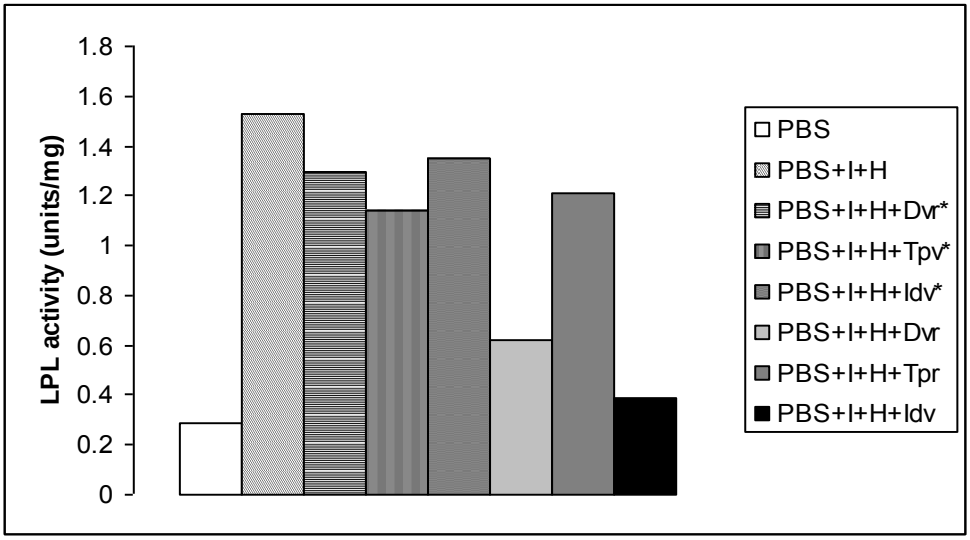

Figure 5.5: Effect of protease inhibitors on the catalytic activity of LPL as measured in the supernatant of adipocytes after prior exposure to protease inhibitors. 3T3-L1 adipocytes were treated with the protease inhibitors or left untreated for 16 h in a serum-free medium, followed by exposure to both insulin and heparin. LPL activity was measured singularly Thus, no statistical analysis was done for this experiment. PBS = phosphate buffered saline, H = heparin, I = insulin, Dvr = darunavir, Tpr = tipranavir, Idv = indinavir, Dvr*, Tpr* and Idv* = protease inhibitors were added directly to the assay reaction prior to 10 min incubation to determine if the protease inhibitors affected the catalytic activity of LPL directly.

University Of Cape Town

5.4 Discussion

This study shows that LPL release from 3T3-L1 adipocytes can be measured successfully in a colourimetric assay, using pNPB as substrate. pNPB was chosen as a substrate because LPL has been shown to catalyse the hydrolysis of short-chain fatty acyl esters such as tributyrin, p-nitrophenylacetate and pNPB *in vivo* (Shirai and Jackson, 1982). This substrate is more convenient to use than lipid-soluble substrates, as the product of LPL-catalysed hydrolysis of pNPB, *p*-nitrophenol, absorbs light strongly at 400 nm. It also allows the continuous monitoring of the reaction in the assay (Quinn et al., 1982).

In this study, 3T3-L1 adipocytes were incubated in 500 µl PBS, which was assessed to be the smallest volume that could cover the cells adequately and yet still obtain the highest concentration of enzyme from the cells. The results of the study revealed that 100 ng/ml (17 nM) insulin significantly stimulated LPL activity in the cells, while 100 U/ml heparin significantly released the enzyme from the cell surface. Heparin (100 U/ml) has been found to release 97 % of the enzyme from the cell surface (Knutson, 2000; Ong et al., 1988; Ranganathan and Kern, 2002; Stewart and Schotz, 1974). Thus, in this study, LPL activity in 3T3-L1 adipocytes was found to be stimulated by insulin and released by heparin.

LPL is a heparin-releasable enzyme. This enzyme binds to heparan sulphate-proteoglycans at the endothelial surface *in vivo* by ionic interactions (Mead et al., 2002). Heparin, a heparan sulphate, releases LPL from the cell surface and stabilises the purified enzyme (Jackson et al., 1980). In this study, supernatants of 3T3-L1 adipocytes treated with heparin showed measurable LPL activity. However, the activity was significantly lower than in cells stimulated with both heparin and insulin. These results showed that insulin stimulated LPL activity in the cells. Insulin stimulates LPL activity by increasing LPL mRNA, which leads to an increase in the synthetic rate of the LPL protein (Ong et al., 1988). However, insulin does not cause the release of LPL from the cell surface. Thus, cells stimulated with insulin only showed no increase in LPL activity in this study.

LPL activity was significantly inhibited by PMSF. This result suggested that the assessed enzyme activity belonged to the LPL. PMSF, a serine protease inhibitor, is one of the inhibitors known to inhibit LPL activity by binding to the active site of the enzyme (Mamputu et al., 2000; Quinn et al., 1983; Van Heusden, 1993). Other protease inhibitors such as phenyl-n-butylborinic acid also inhibit LPL activity (Van Heusden, 1993). However, this current study was focussed only on examining of the role of heparin-induced activity on pNPB hydrolysis. The effect of heparin is a characteristic property of LPL and therefore the heparin-induced hydrolysis of pNPB can be assumed to be directly due to LPL activity, rather than any other lipase.

Darunavir and tipranavir are relatively new protease inhibitor drugs. LPL activity of 3T3-L1 adipocytes treated with darunavir and tipranavir (at plasma concentrations) and indinavir (at experimental concentrations) have not been investigated previously. In the present study, it was shown for the first time that LPL activity in the cells was significantly decreased after treatment with darunavir and indinavir. This concurs with a previous study using a different method (Ranganathan and Kern, 2002). It was found that indinavir (11 μM) at therapeutically-measured plasma concentrations did not result in significant reduction of LPL activity in 3T3-F442A cell lines, assayed using an emulsified [^{3}H]-triolein substrate (Ranganathan and Kern, 2002). Tipranavir also reduced enzyme activity, but this was not statistically significant at the concentrations used. This finding suggests that protease inhibitors may play a role in inhibiting lipoprotein lipase activity *in vivo*, and may thereby induce metabolic disorders in HIV-positive patients being treated with protease inhibitors.

In addition, protease inhibitors were not found to decrease LPL activity directly when added to the assay reaction *in vitro*. This indicates that the drugs act intracellularly. The drugs may interfere with the enzyme activity either through inhibition of the synthesis of the LPL

University Of Cape Town

enzyme, or through the prevention of transport of LPL from the cytoplasm to the cell surface. It was also found that the drugs did not cause any spectral interference with the absorbance of the assay reaction.

Alteration of LPL activity affects lipid metabolism and induces metabolic disorders such as chylomicronaemia, atherosclerosis, cancer, and lipodystrophy associated with insulin resistance and diabetes mellitus. The hydrolysis and release of lipids for storage from triglyceride-rich lipoproteins such as chylomicrons and very low density lipoproteins, and their subsequent storage in adipose tissue, cannot take place without lipoprotein lipase. Therefore, inhibition of these activities could potentially lead to hypertriglyceridaemia, lipodystrophy and increased coronary artery disease (Mead et al., 2002).

5.5 Conclusion

This study revealed that LPL activity can be readily assayed in adipocytes using pNPB as a substrate. Furthermore, the assay can be used to assay the effects of drugs on adipocytes. This is the first study to report that darunavir and indinavir significantly decrease LPL activiy. Alteration of LPL activity in HIV-positive patients treated with protease inhibitors could potentially lead to hypertriglyceridaemia, and subsequent aberrant mobilisation and deposition of lipids.

University Of Cape Town

CHAPTER 6: GENERAL DISCUSSION AND CONCLUSION

6.1 General discussion

Protease inhibitors have been observed to play a leading role in inducing insulin resistance in HIV-positive patients (Ismail et al., 2009). However, details of the mechanistic basis of insulin resistance induced by protease inhibitors are largely unknown, and may be related to the general insulin resistance found in type 2 diabetes and obesity.

Previous studies have shown that protease inhibitors inhibit insulin-stimulated glucose uptake in the insulin signalling pathway (Murata et al., 2002; Rudich et al., 2005). Most of the early studies focused on the distal steps of the insulin signalling pathway; but the inhibition of glucose uptake may occur at a proximal step, which has been observed in cases of insulin resistance in type 2 diabetes and obesity (Arner et al., 1987; Caro et al., 1987; Meyer et al., 2002; Nolan et al., 1994). However, only a few studies have shown that protease inhibitors decrease insulin-stimulated tyrosine phosphorylation of IRS-1 (Cammalleri and Germinario, 2003; Schutt et al., 2000). The effect of protease inhibitors on tyrosine phosphorylation of the insulin receptor β-subunit has previously been unclear, and this study reveals new insights.

Using cells transfected with high levels of insulin receptor, CHO-IR cells, and 3T3-L1 adipocytes, the effects of protease inhibitors on insulin-stimulated tyrosine phosphorylation of insulin receptor β-subunit and tyrosine kinase activation were investigated. CHO-IR cells were used for the first time to study the effects of protease inhibitors on the insulin signalling pathways. These cells have a high level of insulin receptor expression, which facilitates more sensitive detection of changes in signalling proteins than is the case in 3T3-L1 adipocytes. This may have facilitated easier analysis of changes in the insulin receptor β-subunit than has been possible previously.

In both CHO-IR cells and 3T3-L1 adipocytes, treatment with the protease inhibitor indinavir significantly decreased insulin-stimulated tyrosine phosphorylation of the insulin receptor β-subunit and IRS-1. The treatment also significantly increased phosphorylation of serine 307 on IRS-1. However, pre-treatment with sodium salicylate blocked the effects of indinavir, i.e. decreased serine 307 phosphorylation of IRS-1 and increased insulin-stimulated tyrosine phosphorylation of the insulin receptor β-subunit and IRS-1. These findings suggest that protease inhibitors induce insulin resistance via the NFκB pathway, similar to salicylate action in reducing blood glucose concentrations in diabetic patients (Yuan et al., 2001).

Using the metabolomic approach, amino acids, organic acids and FFA in supernatants of 3T3-L1 adipocytes treated with indinavir were analysed for the first time. In the analysis of

University of Cape Town

amino acids, it was found that aspartate and hydroxylysine were significantly decreased in cell culture supernatants treated with indinavir versus untreated supernatants, with or without insulin stimulation, respectively. A high level of aspartate was noted in the drug-treated supernatants without insulin stimulation. It has been reported that a high level of aspartate may be associated with several diseases (Rainesalo et al., 2004). However, the function of the amino acid in insulin resistance has not yet been established and may merely be a function of the general disturbance of metabolism in the adipocytes.

A low level of hydroxylysine was established in the drug-treated supernatants in cells stimulated with insulin. This may be correlated with a low level of adiponectin secreted by the adipocytes. A decrease in adiponectin will cause insulin resistance. This finding of decreased hydroxylysine is worthy of further investigation.

Organic acid analysis of drug-treated cells revealed significantly less butane in the treated cell culture supernatants without insulin stimulation. High levels of butane may be a result of exposure to serum-free medium. Succinate synthesis was decreased in indinavir-treated cell culture supernatants compared to untreated cells (insulin-stimulated), indicating low activity of the Krebs cycle. Succinate is usually found in high levels in differentiated adipocytes (Lai and Goldman, 1992). The decreased level of succinate found may be a result of the decreased tyrosine phosphorylation in the insulin receptor β-subunit and IRS-1, as observed above. This decreased activity of the tyrosine kinase may decrease glucose uptake (which is essential for the Krebs cycle) and therefore less succinate may be produced in the treated supernatants. However, further investigation is required.

In contrast, butanoic acid 3-(trimethylsiloxy)-ethylester was synthesised significantly more in the treated versus untreated cell culture supernatants with insulin stimulation. Overproduction of this organic acid may relate to the production of ketone bodies concomitant with the low activity of the Krebs cycle. Ketone bodies are known to be associated with insulin deficiency, for example in type 1 diabetes mellitus (Laffel, 1999).

In addition, isovalerate was synthesised exclusively in the treated cell culture supernatants with insulin stimulation. A high level of isovalerate is also associated with several diseases (Trauner et al., 1975). However, the effects of this synthesis of isovalerate, and its relationship to insulin resistance induced by protease inhibitors, are still unclear.

The levels of FFAs were high in the cell culture supernatants treated with indinavir. This suggests that the drug inhibits the utilisation of FFAs via FFA uptake. This could potentially result in high levels of circulating FFAs. FFAs may play a role in inducing insulin resistance. High levels of FFAs are known to stimulate phosphorylation of serine 307 on IRS-1, and

University of Cape Town

induce insulin resistance via the NFκB pathway (Lee et al., 2009). This finding parallels the results of indinavir treatment, which significantly increased phosphorylation of serine 307 on IRS-1 in the present study. It is important to compare the effects of other HIV protease inhibitors on the release of FFAs from adipocytes.

Treatment with protease inhibitors also reduced LPL activity in 3T3-L1 adipocytes. Low LPL activity may affect lipid metabolism which could potentially lead to insulin resistance, hypertriglyceridaemia, lipodystrophy and increased coronary artery disease (Mead et al., 2002). There were differences in the effects of the individual protease inhibitors on LPL activity. Thus, this assay could potentially be used to evaluate protease inhibitors for effects on LPL, and this could provide information on the propensity of the drug to cause increased FFA levels *in vivo*. The availability of this novel high-throughput method would facilitate the analysis of newly developed protease inhibitors, other novel antiretroviral drugs and for clinical studies. Although other lipases act on pNPB, only LPL is released by heparin indication that the activity measured after heparin is specific for LPL.

6.2 Future work

Sodium salicylate may provide a novel therapy for HIV protease inhibitor-induced insulin resistance and lipodystrophy. However, it has been reported to inhibit NFκB and induce apoptosis in rats (Kiss et al., 2004). Therefore, observation of the effects of sodium salicylate on apoptosis via the caspase-3 protein in CHO-IR cells and 3T3-L1 adipocytes treated with protease inhibitors is suggested for future study. In addition, signals obtained with phosphospecific antibodies tend to be of low intensity and significant optimisation is required before higher intensity signals can be obtained.

The present study suggests that protease inhibitors induce insulin resistance via the NFκB pathway. In order to confirm this finding, the effects of protease inhibitors should be investigated in NFκB-knockout cells.

In addition, as the present study showed, it would be useful to perform metabolomic analysis of other protease inhibitors such as ritonavir and liponavir for the purposes of a comparison study. The results may shed new light on drug development in insulin resistance induced by protease inhibitors.

Furthermore, it would be interesting to expand the established method of LPL assay from 3T3-L1 adipocytes to human serum in clinical study.

University Of Cape Town

6.3 Conclusion

In conclusion, this study suggests that treatment of CHO-IR cells and 3T3-L1 adipocytes with protease inhibitors inhibits LPL activity and increases FFA. The high levels of FFAs stimulate the NFκB pathway, which increases serine 307 phosphorylation of IRS-1, and then decreases insulin-stimulated tyrosine phosphorylation of IRS-1 and the insulin receptor β-subunit to induce insulin resistance. Low levels of hydroxylysine and succinate, and high levels of aspartate, butanoic acid 3-(trimethylsiloxy)-ethylester and isovalerate may be a secondary effect of insulin resistance induced by protease inhibitors.

In the context of adipocytes, NFκB induced by TNF-α has been observed to inhibit adipogenesis (Berg et al., 2004). Protease inhibitors may activate TNF-α or other inflammatory cytokines to induce the NFκB pathway of adipocytes in HIV-positive patients. This mechanism may affect the insulin signalling pathway, FFA, amino acids, organic acids and LPL activity as discussed above.

University Of Cape Town

REFERENCES

Aguirre, V., Werner, E. D., Giraud, J., Lee, Y. H., Shoelson, S. E., and White, M. F. (2002). Phosphorylation of Ser307 in insulin receptor substrate-1 blocks interactions with the insulin receptor and inhibits insulin action. J Biol Chem *277*, 1531-1537.

Ahmed, Z., and Pillay, T. S. (2001). Functional effects of APS and SH2-B on insulin receptor signalling. Biochem Soc Trans *29*, 529-534.

Ahmed, Z., and Pillay, T. S. (2003). Adapter protein with a pleckstrin homology (PH) and an Src homology 2 (SH2) domain (APS) and SH2-B enhance insulin-receptor autophosphorylation, extracellular-signal-regulated kinase and phosphoinositide 3-kinase-dependent signalling. Biochem J *371*, 405-412.

Ahmed, Z., Smith, B. J., and Pillay, T. S. (2000). The APS adapter protein couples the insulin receptor to the phosphorylation of c-Cbl and facilitates ligand-stimulated ubiquitination of the insulin receptor. FEBS Lett *475*, 31-34.

Ahn, M. Y., Katsanakis, K. D., Bheda, F., and Pillay, T. S. (2004). Primary and essential role of the adaptor protein APS for recruitment of both c-Cbl and its associated protein CAP in insulin signaling. J Biol Chem *279*, 21526-21532.

Arakaki, A. K., Skolnick, J., and McDonald, J. F. (2008). Marker metabolites can be therapeutic targets as well. Nature *456*, 443.

Arkan, M. C., Hevener, A. L., Greten, F. R., Maeda, S., Li, Z. W., Long, J. M., Wynshaw-Boris, A., Poli, G., Olefsky, J., and Karin, M. (2005). IKK-beta links inflammation to obesity-induced insulin resistance. Nat Med *11*, 191-198.

Arner, P., Pollare, T., Lithell, H., and Livingston, J. N. (1987). Defective insulin receptor tyrosine kinase in human skeletal muscle in obesity and type 2 (non-insulin-dependent) diabetes mellitus. Diabetologia *30*, 437-440.

Bailey, A. C., and Fisher, M. (2008). Current use of antiretroviral treatment. Br Med Bull *87*, 175-192.

Barbaro, G. (2002). HIV infection, antiretroviral therapy and cardiovascular risk. J Cardiovasc Risk *9*, 295-300.

Barbaro, G., and Barbarini, G. (2006). Highly active antiretroviral therapy-associated metabolic syndrome and cardiovascular risk. Chemotherapy *52*, 161-165.

Ben-Romano, R., Rudich, A., Etzion, S., Potashnik, R., Kagan, E., Greenbaum, U., and Bashan, N. (2006). Nelfinavir induces adipocyte insulin resistance through the induction of oxidative stress: differential protective effect of antioxidant agents. Antivir Ther *11*, 1051-1060.

Ben-Romano, R., Rudich, A., Tirosh, A., Potashnik, R., Sasaoka, T., Riesenberg, K., Schlaeffer, F., and Bashan, N. (2004). Nelfinavir-induced insulin resistance is associated with impaired plasma membrane recruitment of the PI 3-kinase effectors Akt/PKB and PKC-zeta. Diabetologia *47*, 1107-1117.

Ben-Romano, R., Rudich, A., Torok, D., Vanounou, S., Riesenberg, K., Schlaeffer, F., Klip, A., and Bashan, N. (2003). Agent and cell-type specificity in the induction of insulin resistance by HIV protease inhibitors. Aids *17*, 23-32.

University Of Cape Town

Berg, A. H., Lin, Y., Lisanti, M. P., and Scherer, P. E. (2004). Adipocyte differentiation induces dynamic changes in NF-kappaB expression and activity. Am J Physiol Endocrinol Metab *287*, E1178-1188.

Bernasconi, E. (1999). Metabolic effects of protease inhibitor therapy. AIDS Read *9*, 254-256, 259-260, 266-259.

Beyrer, C. (2007). HIV epidemiology update and transmission factors: risks and risk contexts--16th International AIDS Conference epidemiology plenary. Clin Infect Dis *44*, 981-987.

Bhattacharya, S., Dey, D., and Roy, S. S. (2007). Molecular mechanism of insulin resistance. J Biosci *32*, 405-413.

Bozkurt, B. (2004). Cardiovascular toxicity with highly active antiretroviral therapy: review of clinical studies. Cardiovasc Toxicol *4*, 243-260.

Bradford, M. M. (1976). A rapid and sensitive method for the quantitation of microgram quantities of protein utilizing the principle of protein-dye binding. Anal Biochem *72*, 248-254.

Cai, D., Yuan, M., Frantz, D. F., Melendez, P. A., Hansen, L., Lee, J., and Shoelson, S. E. (2005). Local and systemic insulin resistance resulting from hepatic activation of IKK-beta and NF-kappaB. Nat Med *11*, 183-190.

Cammalleri, C., and Germinario, R. J. (2003). The effects of protease inhibitors on basal and insulin-stimulated lipid metabolism, insulin binding, and signaling. J Lipid Res *44*, 103-108.

Capanni, C., Mattioli, E., Columbaro, M., Lucarelli, E., Parnaik, V. K., Novelli, G., Wehnert, M., Cenni, V., Maraldi, N. M., Squarzoni, S., and Lattanzi, G. (2005). Altered pre-lamin A processing is a common mechanism leading to lipodystrophy. Hum Mol Genet *14*, 1489-1502.

Caro, J. F., Sinha, M. K., Raju, S. M., Ittoop, O., Pories, W. J., Flickinger, E. G., Meelheim, D., and Dohm, G. L. (1987). Insulin receptor kinase in human skeletal muscle from obese subjects with and without noninsulin dependent diabetes. J Clin Invest *79*, 1330-1337.

Carper, M. J., Cade, W. T., Cam, M., Zhang, S., Shalev, A., Yarasheski, K. E., and Ramanadham, S. (2008). HIV-protease inhibitors induce expression of suppressor of cytokine signaling-1 in insulin-sensitive tissues and promote insulin resistance and type 2 diabetes mellitus. Am J Physiol Endocrinol Metab *294*, E558-567.

Carr, A. (2000). HIV protease inhibitor-related lipodystrophy syndrome. Clin Infect Dis *30 Suppl 2*, S135-142.

Carr, A. (2003). HIV lipodystrophy: risk factors, pathogenesis, diagnosis and management. Aids *17 Suppl 1*, S141-148.

Carr, A., Samaras, K., Burton, S., Law, M., Freund, J., Chisholm, D. J., and Cooper, D. A. (1998). A syndrome of peripheral lipodystrophy, hyperlipidaemia and insulin resistance in patients receiving HIV protease inhibitors. Aids *12*, F51-58.

Chandra, S., Mondal, D., and Agrawal, K. C. (2009). HIV-1 protease inhibitor induced oxidative stress suppresses glucose stimulated insulin release: protection with thymoquinone. Exp Biol Med (Maywood) *234*, 442-453.

University of Cape Town

Chaparro, J., Reeds, D. N., Wen, W., Xueping, E., Klein, S., Semenkovich, C. F., Bae, K. T., Quirk, E. K., Powderly, W. G., Yarasheski, K. E., and Li, E. (2005). Alterations in thigh subcutaneous adipose tissue gene expression in protease inhibitor-based highly active antiretroviral therapy. Metabolism *54*, 561-567.

Cheng, A., Dube, N., Gu, F., and Tremblay, M. L. (2002). Coordinated action of protein tyrosine phosphatases in insulin signal transduction. Eur J Biochem *269*, 1050-1059.

Djedaini, M., Peraldi, P., Drici, M. D., Darini, C., Saint-Marc, P., Dani, C., and Ladoux, A. (2009). Lopinavir co-induces insulin resistance and ER stress in human adipocytes. Biochem Biophys Res Commun *386*, 96-100.

Dousset, N., Negre, A., Salvayre, R., Rogalle, P., Dang, Q. Q., and Douste-Blazy, L. (1988). Use of a fluorescent radiolabeled triacylglycerol as a substrate for lipoprotein lipase and hepatic triglyceride lipase. Lipids *23*, 605-608.

Dunaif, A., Xia, J., Book, C. B., Schenker, E., and Tang, Z. (1995). Excessive insulin receptor serine phosphorylation in cultured fibroblasts and in skeletal muscle. A potential mechanism for insulin resistance in the polycystic ovary syndrome. J Clin Invest *96*, 801-810.

Emanuelli, B., Peraldi, P., Filloux, C., Chavey, C., Freidinger, K., Hilton, D. J., Hotamisligil, G. S., and Van Obberghen, E. (2001). SOCS-3 inhibits insulin signaling and is up-regulated in response to tumor necrosis factor-alpha in the adipose tissue of obese mice. J Biol Chem *276*, 47944-47949.

Emanuelli, B., Peraldi, P., Filloux, C., Sawka-Verhelle, D., Hilton, D., and Van Obberghen, E. (2000). SOCS-3 is an insulin-induced negative regulator of insulin signaling. J Biol Chem *275*, 15985-15991.

Esser, S., Helbig, D., Hillen, U., Dissemond, J., and Grabbe, S. (2007). Side effects of HIV therapy. J Dtsch Dermatol Ges *5*, 745-754.

Evans, J. L., Maddux, B. A., and Goldfine, I. D. (2005). The molecular basis for oxidative stress-induced insulin resistance. Antioxid Redox Signal *7*, 1040-1052.

Fenkci, V., Fenkci, S., Yilmazer, M., and Serteser, M. (2003). Decreased total antioxidant status and increased oxidative stress in women with polycystic ovary syndrome may contribute to the risk of cardiovascular disease. Fertil Steril *80*, 123-127.

Filippini, P., Scolastico, C., Battaglia, M., Nacca, C., Coppola, N., Rossi, G., Pisapia, R., Martini, S., Imparato, M., Sagnelli, C*., et al.* (2006). Lipodystrophy and serum lipid abnormalities in HIV-positive sub-Saharan population on ART. J Infect *53*, e29-33.

Fleischman, A., Shoelson, S. E., Bernier, R., and Goldfine, A. B. (2008). Salsalate improves glycemia and inflammatory parameters in obese young adults. Diabetes Care *31*, 289-294.

Flexner, C. (1998). HIV-protease inhibitors. N Engl J Med *338*, 1281-1292.

Florescu, D., and Kotler, D. P. (2007). Insulin resistance, glucose intolerance and diabetes mellitus in HIV-infected patients. Antivir Ther *12*, 149-162.

Fonseca-Alaniz, M. H., Takada, J., Alonso-Vale, M. I., and Lima, F. B. (2007). Adipose tissue as an endocrine organ: from theory to practice. J Pediatr (Rio J) *83*, S192-203.

University Of Cape Town

Friedl, A. C., Attenhofer Jost, C. H., Schalcher, C., Amann, F. W., Flepp, M., Jenni, R., Linka, A., and Weber, R. (2000). Acceleration of confirmed coronary artery disease among HIV-infected patients on potent antiretroviral therapy. Aids *14*, 2790-2792.

Gallo, R. C., and Reitz, M. S., Jr. (1985). The first human retroviruses: are there others? Microbiol Sci *2*, 97-98, 101-104.

Gan, S. K., Samaras, K., Carr, A., and Chisholm, D. (2001). Anti-retroviral therapy, insulin resistance and lipodystrophy. Diabetes Obes Metab *3*, 67-71.

Gao, Z., Zhang, X., Zuberi, A., Hwang, D., Quon, M. J., Lefevre, M., and Ye, J. (2004). Inhibition of insulin sensitivity by free fatty acids requires activation of multiple serine kinases in 3T3-L1 adipocytes. Mol Endocrinol *18*, 2024-2034.

Gao, Z., Zuberi, A., Quon, M. J., Dong, Z., and Ye, J. (2003). Aspirin inhibits serine phosphorylation of insulin receptor substrate 1 in tumor necrosis factor-treated cells through targeting multiple serine kinases. J Biol Chem *278*, 24944-24950.

Garg, A. (2006). Adipose tissue dysfunction in obesity and lipodystrophy. Clin Cornerstone *8 Suppl 4*, S7-S13.

Germinario, R. J., and Colby-Germinario, S. P. (2003). The effect of human immunodeficiency virus-1 protease inhibitors on the toxicity of a variety of cells. In Vitro Cell Dev Biol Anim *39*, 275-279.

Glenn, K. C., Shieh, J. J., and Laird, D. M. (1992). Characterization of 3T3-L1 storage lipid metabolism: effect of somatotropin and insulin on specific pathways. Endocrinology *131*, 1115-1124.

Gougeon, M. L., Penicaud, L., Fromenty, B., Leclercq, P., Viard, J. P., and Capeau, J. (2004). Adipocytes targets and actors in the pathogenesis of HIV-associated lipodystrophy and metabolic alterations. Antivir Ther *9*, 161-177.

Goulbourne, C. N., and Vaux, D. J. (2010) HIV protease inhibitors inhibit FACE1/ZMPSTE24: a mechanism for acquired lipodystrophy in patients on highly active antiretroviral therapy? Biochem Soc Trans *38*, 292-296.

Hadigan, C., Rabe, J., Meininger, G., Aliabadi, N., Breu, J., and Grinspoon, S. (2003). Inhibition of lipolysis improves insulin sensitivity in protease inhibitor-treated HIV-infected men with fat redistribution. Am J Clin Nutr *77*, 490-494.

Hammer, S. M., Squires, K. E., Hughes, M. D., Grimes, J. M., Demeter, L. M., Currier, J. S., Eron, J. J., Jr., Feinberg, J. E., Balfour, H. H., Jr., Deyton, L. R.*, et al.* (1997). A controlled trial of two nucleoside analogues plus indinavir in persons with human immunodeficiency virus infection and CD4 cell counts of 200 per cubic millimeter or less. AIDS Clinical Trials Group 320 Study Team. N Engl J Med *337*, 725-733.

Hara, K., Horikoshi, M., Yamauchi, T., Yago, H., Miyazaki, O., Ebinuma, H., Imai, Y., Nagai, R., and Kadowaki, T. (2006). Measurement of the high-molecular weight form of adiponectin in plasma is useful for the prediction of insulin resistance and metabolic syndrome. Diabetes Care *29*, 1357-1362.

Hertel, J., Struthers, H., Horj, C. B., and Hruz, P. W. (2004). A structural basis for the acute effects of HIV protease inhibitors on GLUT4 intrinsic activity. J Biol Chem *279*, 55147-55152.

University Of CapeTown

Hirosumi, J., Tuncman, G., Chang, L., Gorgun, C. Z., Uysal, K. T., Maeda, K., Karin, M., and Hotamisligil, G. S. (2002). A central role for JNK in obesity and insulin resistance. Nature *420*, 333-336.

Hotamisligil, G. S., Shargill, N. S., and Spiegelman, B. M. (1993). Adipose expression of tumor necrosis factor-alpha: direct role in obesity-linked insulin resistance. Science *259*, 87-91.

Hruz, P. W., Murata, H., Qiu, H., and Mueckler, M. (2002). Indinavir induces acute and reversible peripheral insulin resistance in rats. Diabetes *51*, 937-942.

Hui, D. Y. (2003). Effects of HIV protease inhibitor therapy on lipid metabolism. Prog Lipid Res *42*, 81-92.

Ikeda, Y., Olsen, G. S., Ziv, E., Hansen, L. L., Busch, A. K., Hansen, B. F., Shafrir, E., and Mosthaf-Seedorf, L. (2001). Cellular mechanism of nutritionally induced insulin resistance in Psammomys obesus: overexpression of protein kinase Cepsilon in skeletal muscle precedes the onset of hyperinsulinemia and hyperglycemia. Diabetes *50*, 584-592.

Ismail, W. I. W., King, J., and Pillay, T. S. (2009). Insulin resistance induced by antiretroviral drugs: Current understanding of molecular mechanisms. JEMDSA *14(3)*, 129-132.

Itani, S. I., Ruderman, N. B., Schmieder, F., and Boden, G. (2002). Lipid-induced insulin resistance in human muscle is associated with changes in diacylglycerol, protein kinase C, and IkappaB-alpha. Diabetes *51*, 2005-2011.

Jackson, R. L., Pattus, F., and de Haas, G. (1980). Mechanism of action of milk lipoprotein lipase at substrate interfaces: effects of apolipoproteins. Biochemistry *19*, 373-378.

Jones, S. P., Waitt, C., Sutton, R., Back, D. J., and Pirmohamed, M. (2008). Effect of atazanavir and ritonavir on the differentiation and adipokine secretion of human subcutaneous and omental preadipocytes. Aids *22*, 1293-1298.

Kachko, I., Maissel, A., Mazor, L., Ben-Romano, R., Watson, R. T., Hou, J. C., Pessin, J. E., Bashan, N., and Rudich, A. (2009). Postreceptoral adipocyte insulin resistance induced by nelfinavir is caused by insensitivity of PKB/Akt to phosphatidylinositol-3,4,5-trisphosphate. Endocrinology *150*, 2618-2626.

Kadowaki, T., Yamauchi, T., Kubota, N., Hara, K., Ueki, K., and Tobe, K. (2006). Adiponectin and adiponectin receptors in insulin resistance, diabetes, and the metabolic syndrome. J Clin Invest *116*, 1784-1792.

Kern, P. A., Di Gregorio, G. B., Lu, T., Rassouli, N., and Ranganathan, G. (2003). Adiponectin expression from human adipose tissue: relation to obesity, insulin resistance, and tumor necrosis factor-alpha expression. Diabetes *52*, 1779-1785.

Kim, J. K., Fillmore, J. J., Sunshine, M. J., Albrecht, B., Higashimori, T., Kim, D. W., Liu, Z. X., Soos, T. J., Cline, G. W., O'Brien, W. R., *et al.* (2004). PKC-theta knockout mice are protected from fat-induced insulin resistance. J Clin Invest *114*, 823-827.

Kiss, K., Kiss, J., Rudolf, E., Cervinka, M., and Szeberenyi, J. (2004). J Biochem Biophys Methods *61*, 229-240.

Knutson, V. P. (2000). The release of lipoprotein lipase from 3T3-L1 adipocytes is regulated by microvessel endothelial cells in an insulin-dependent manner. Endocrinology *141*, 693-701.

University of Cape Town

Koska, J., Ortega, E., Bunt, J. C., Gasser, A., Impson, J., Hanson, R. L., Forbes, J., de Courten, B., and Krakoff, J. (2009). The effect of salsalate on insulin action and glucose tolerance in obese non-diabetic patients: results of a randomised double-blind placebo-controlled study. Diabetologia *52*, 385-393.

Kotani, K., Wilden, P., and Pillay, T. S. (1998). SH2-Balpha is an insulin-receptor adapter protein and substrate that interacts with the activation loop of the insulin-receptor kinase. Biochem J *335 (Pt 1)*, 103-109.

Koulman, A., Lane, G. A., Harrison, S. J., and Volmer, D. A. (2009). From differentiating metabolites to biomarkers. Anal Bioanal Chem *394*, 663-670.

Kovsan, J., Osnis, A., Maissel, A., Mazor, L., Tarnovscki, T., Hollander, L., Ovadia, S., Meier, B., Klein, J., Bashan, N., and Rudich, A. (2009). Depot-specific adipocyte cell lines reveal differential drug-induced responses of white adipocytes--relevance for partial lipodystrophy. Am J Physiol Endocrinol Metab *296*, E315-322.

Laffel, L. (1999). Ketone bodies: a review of physiology, pathophysiology and application of monitoring to diabetes. Diabetes Metab Res Rev *15*, 412-426.

Lagathu, C., Eustace, B., Prot, M., Frantz, D., Gu, Y., Bastard, J. P., Maachi, M., Azoulay, S., Briggs, M., Caron, M., and Capeau, J. (2007). Some HIV antiretrovirals increase oxidative stress and alter chemokine, cytokine or adiponectin production in human adipocytes and macrophages. Antivir Ther *12*, 489-500.

Lai, R. K., and Goldman, P. (1992). Organic acid profiling in adipocyte differentiation of 3T3-F442A cells: increased production of Krebs cycle acid metabolites. Metabolism *41*, 545-547.

Larmarange, J. (2009). [HIV prevalence in sub-Saharan Africa: background of an estimation]. Med Sci (Paris) *25*, 87-92.

Lee, D. E., Kehlenbrink, S., Lee, H., Hawkins, M., and Yudkin, J. S. (2009). Getting the message across: mechanisms of physiological cross talk by adipose tissue. Am J Physiol Endocrinol Metab *296*, E1210-1229.

Lee, G. A., Rao, M., Mulligan, K., Lo, J. C., Aweeka, F., Schwarz, J. M., Schambelan, M., and Grunfeld, C. (2007). Effects of ritonavir and amprenavir on insulin sensitivity in healthy volunteers. Aids *21*, 2183-2190.

Leitges, M., Gimborn, K., Elis, W., Kalesnikoff, J., Hughes, M. R., Krystal, G., and Huber, M. (2002). Protein kinase C-delta is a negative regulator of antigen-induced mast cell degranulation. Mol Cell Biol *22*, 3970-3980.

Lenhard, J. M., Furfine, E. S., Jain, R. G., Ittoop, O., Orband-Miller, L. A., Blanchard, S. G., Paulik, M. A., and Weiel, J. E. (2000). HIV protease inhibitors block adipogenesis and increase lipolysis in vitro. Antiviral Res *47*, 121-129.

Lijnen, H. R. (2005). Pleiotropic functions of plasminogen activator inhibitor-1. J Thromb Haemost *3*, 35-45.

Lim, J. H., Lee, H. J., Ho Jung, M., and Song, J. (2009). Coupling mitochondrial dysfunction to endoplasmic reticulum stress response: a molecular mechanism leading to hepatic insulin resistance. Cell Signal *21*, 169-177.

University Of Cape Town

Lin, J. H. (1999). Role of pharmacokinetics in the discovery and development of indinavir. Adv Drug Deliv Rev *39*, 33-49.

Mamputu, J. C., Levesque, L., and Renier, G. (2000). Proliferative effect of lipoprotein lipase on human vascular smooth muscle cells. Arterioscler Thromb Vasc Biol *20*, 2212-2219.

Maraldi, N. M., Capanni, C., Mattioli, E., Columbaro, M., Squarzoni, S., Parnaik, W. K., Wehnert, M., and Lattanzi, G. (2007). A pathogenic mechanism leading to partial lipodistrophy and prospects for pharmacological treatment of insulin resistance syndrome. Acta Biomed *78 Suppl 1*, 207-215.

Martin, J., Deslandes, G., Dailly, E., Renaud, C., Reliquet, V., Raffi, F., and Jolliet, P. (2009). A liquid chromatography-tandem mass spectrometry assay for quantification of nevirapine, indinavir, atazanavir, amprenavir, saquinavir, ritonavir, lopinavir, efavirenz, tipranavir, darunavir and maraviroc in the plasma of patients infected with HIV. J Chromatogr B Analyt Technol Biomed Life Sci *877*, 3072-3082.

Maures, T. J., Kurzer, J. H., and Carter-Su, C. (2007). SH2B1 (SH2-B) and JAK2: a multifunctional adaptor protein and kinase made for each other. Trends Endocrinol Metab *18*, 38-45.

Mead, J. R., Irvine, S. A., and Ramji, D. P. (2002). Lipoprotein lipase: structure, function, regulation, and role in disease. J Mol Med *80*, 753-769.

Mehra, A., Macdonald, I., and Pillay, T. S. (2007). Variability in 3T3-L1 adipocyte differentiation depending on cell culture dish. Anal Biochem *362*, 281-283.

Meininger, G., Hadigan, C., Laposata, M., Brown, J., Rabe, J., Louca, J., Aliabadi, N., and Grinspoon, S. (2002). Elevated concentrations of free fatty acids are associated with increased insulin response to standard glucose challenge in human immunodeficiency virus-infected subjects with fat redistribution. Metabolism *51*, 260-266.

Meyer, M. M., Levin, K., Grimmsmann, T., Beck-Nielsen, H., and Klein, H. H. (2002). Insulin signalling in skeletal muscle of subjects with or without Type II-diabetes and first degree relatives of patients with the disease. Diabetologia *45*, 813-822.

Monier, P. L., and Wilcox, R. (2004). Metabolic complications associated with the use of highly active antiretroviral therapy in HIV-1-infected adults. Am J Med Sci *328*, 48-56.

Morino, K., Petersen, K. F., and Shulman, G. I. (2006). Molecular mechanisms of insulin resistance in humans and their potential links with mitochondrial dysfunction. Diabetes *55 Suppl 2*, S9-S15.

Moyle, G. (2007). Metabolic issues associated with protease inhibitors. J Acquir Immune Defic Syndr *45 Suppl 1*, S19-26.

Mueckler, M. (2001). Insulin resistance and the disruption of Glut4 trafficking in skeletal muscle. J Clin Invest *107*, 1211-1213.

Murata, H., Hruz, P. W., and Mueckler, M. (2000). The mechanism of insulin resistance caused by HIV protease inhibitor therapy. J Biol Chem *275*, 20251-20254.

Murata, H., Hruz, P. W., and Mueckler, M. (2002). Indinavir inhibits the glucose transporter isoform Glut4 at physiologic concentrations. Aids *16*, 859-863.

University of Cape Town

Nilsson-Ehle, P., and Schotz, M. C. (1976). A stable, radioactive substrate emulsion for assay of lipoprotein lipase. J Lipid Res *17*, 536-541.

Nolan, J. J., Freidenberg, G., Henry, R., Reichart, D., and Olefsky, J. M. (1994). Role of human skeletal muscle insulin receptor kinase in the in vivo insulin resistance of noninsulin-dependent diabetes mellitus and obesity. J Clin Endocrinol Metab *78*, 471-477.

Noor, M. A., Flint, O. P., Maa, J. F., and Parker, R. A. (2006). Effects of atazanavir/ritonavir and lopinavir/ritonavir on glucose uptake and insulin sensitivity: demonstrable differences in vitro and clinically. Aids *20*, 1813-1821.

Noor, M. A., Lo, J. C., Mulligan, K., Schwarz, J. M., Halvorsen, R. A., Schambelan, M., and Grunfeld, C. (2001). Metabolic effects of indinavir in healthy HIV-seronegative men. Aids *15*, F11-18.

Noor, M. A., Seneviratne, T., Aweeka, F. T., Lo, J. C., Schwarz, J. M., Mulligan, K., Schambelan, M., and Grunfeld, C. (2002). Indinavir acutely inhibits insulin-stimulated glucose disposal in humans: a randomized, placebo-controlled study. Aids *16*, F1-8.

Ong, J. M., Kirchgessner, T. G., Schotz, M. C., and Kern, P. A. (1988). Insulin increases the synthetic rate and messenger RNA level of lipoprotein lipase in isolated rat adipocytes. J Biol Chem *263*, 12933-12938.

Oresic, M. (2009). Metabolomics, a novel tool for studies of nutrition, metabolism and lipid dysfunction. Nutr Metab Cardiovasc Dis *19*, 816-824.

Palella, F. J., Jr., Delaney, K. M., Moorman, A. C., Loveless, M. O., Fuhrer, J., Satten, G. A., Aschman, D. J., and Holmberg, S. D. (1998). Declining morbidity and mortality among patients with advanced human immunodeficiency virus infection. HIV Outpatient Study Investigators. N Engl J Med *338*, 853-860.

Pandey, M., Loskutoff, D. J., and Samad, F. (2005). Molecular mechanisms of tumor necrosis factor-alpha-mediated plasminogen activator inhibitor-1 expression in adipocytes. Faseb J *19*, 1317-1319.

Perseghin, G., Petersen, K., and Shulman, G. I. (2003). Cellular mechanism of insulin resistance: potential links with inflammation. Int J Obes Relat Metab Disord *27 Suppl 3*, S6-11.

Piacenti, F. J. (2006). An update and review of antiretroviral therapy. Pharmacotherapy *26*, 1111-1133.

Quinn, D., Shirai, K., and Jackson, R. L. (1983). Lipoprotein lipase: mechanism of action and role in lipoprotein metabolism. Prog Lipid Res *22*, 35-78.

Quinn, D. M., Shirai, K., Jackson, R. L., and Harmony, J. A. (1982). Lipoprotein lipase catalyzed hydrolysis of water-soluble p-nitrophenyl esters. Inhibition by apolipoprotein C-II. Biochemistry *21*, 6872-6879.

Quinn, T. C. (2008). HIV epidemiology and the effects of antiviral therapy on long-term consequences. Aids *22 Suppl 3*, S7-12.

Rainesalo, S., Keranen, T., Palmio, J., Peltola, J., Oja, S. S., and Saransaari, P. (2004). Plasma and cerebrospinal fluid amino acids in epileptic patients. Neurochem Res *29*, 319-324.

University Of Cape Town

Randle, P. J., Garland, P. B., Hales, C. N., and Newsholme, E. A. (1963). The glucose fatty-acid cycle. Its role in insulin sensitivity and the metabolic disturbances of diabetes mellitus. Lancet *1*, 785-789.

Ranganathan, S., and Kern, P. A. (2002). The HIV protease inhibitor saquinavir impairs lipid metabolism and glucose transport in cultured adipocytes. J Endocrinol *172*, 155-162.

Rautavuoma, K., Takaluoma, K., Passoja, K., Pirskanen, A., Kvist, A. P., Kivirikko, K. I., and Myllyharju, J. (2002). Characterization of three fragments that constitute the monomers of the human lysyl hydroxylase isoenzymes 1-3. The 30-kDa N-terminal fragment is not required for lysyl hydroxylase activity. J Biol Chem *277*, 23084-23091.

Richman, D. D. (2001). HIV chemotherapy. Nature *410*, 995-1001.

Rose, R. B., Craik, C. S., and Stroud, R. M. (1998). Domain flexibility in retroviral proteases: Structural implications for drug resistant mutations. Biochem J *37*, 2607-2621.

Rudich, A., Ben-Romano, R., Etzion, S., and Bashan, N. (2005). Cellular mechanisms of insulin resistance, lipodystrophy and atherosclerosis induced by HIV protease inhibitors. Acta Physiol Scand *183*, 75-88.

Rudich, A., Vanounou, S., Riesenberg, K., Porat, M., Tirosh, A., Harman-Boehm, I., Greenberg, A. S., Schlaeffer, F., and Bashan, N. (2001). The HIV protease inhibitor nelfinavir induces insulin resistance and increases basal lipolysis in 3T3-L1 adipocytes. Diabetes *50*, 1425-1431.

Ryo, M., Nakamura, T., Kihara, S., Kumada, M., Shibazaki, S., Takahashi, M., Nagai, M., Matsuzawa, Y., and Funahashi, T. (2004). Adiponectin as a biomarker of the metabolic syndrome. Circ J *68*, 975-981.

Samuel, V. T., Liu, Z. X., Wang, A., Beddow, S. A., Geisler, J. G., Kahn, M., Zhang, X. M., Monia, B. P., Bhanot, S., and Shulman, G. I. (2007). Inhibition of protein kinase Cepsilon prevents hepatic insulin resistance in nonalcoholic fatty liver disease. J Clin Invest *117*, 739-745.

Savage, D. B., Petersen, K. F., and Shulman, G. I. (2005). Mechanisms of insulin resistance in humans and possible links with inflammation. Hypertension *45*, 828-833.

Schmidtke, G., Holzhutter, H. G., Bogyo, M., Kairies, N., Groll, M., de Giuli, R., Emch, S., and Groettrup, M. (1999). How an inhibitor of the HIV-I protease modulates proteasome activity. J Biol Chem *274*, 35734-35740.

Schutt, M., Meier, M., Meyer, M., Klein, J., Aries, S. P., and Klein, H. H. (2000). The HIV-1 protease inhibitor indinavir impairs insulin signalling in HepG2 hepatoma cells. Diabetologia *43*, 1145-1148.

Shirai, K., and Jackson, R. L. (1982). Lipoprotein lipase-catalyzed hydrolysis of p-nitrophenyl butyrate. Interfacial activation by phospholipid vesicles. J Biol Chem *257*, 1253-1258.

Sierra, S., Kupfer, B., and Kaiser, R. (2005). Basics of the virology of HIV-1 and its replication. J Clin Virol *34*, 233-244.

Stein, J. H. (2007). Cardiovascular risks of antiretroviral therapy. N Engl J Med *356*, 1773-1775.

University Of Cape Town

Stewart, J. E., and Schotz, M. C. (1974). Release of lipoprotein lipase activity from isolated fat cells. II. Effect of heparin. J Biol Chem *249*, 904-907.

Temesgen, Z., Warnke, D., and Kasten, M. J. (2006). Current status of antiretroviral therapy. Expert Opin Pharmacother *7*, 1541-1554.

Tergaonkar, V. (2006). NFkappaB pathway: a good signaling paradigm and therapeutic target. Int J Biochem Cell Biol *38*, 1647-1653.

Trauner, D. A., Nyhan, W. L., and Sweetman, L. (1975). Short-chain organic acidemia and Reye's syndrome. Neurology *25*, 296-298.

Trost, Z., Sok, M., Marc, J., and Cerne, D. (2009). Increased lipoprotein lipase activity in non-small cell lung cancer tissue predicts shorter patient survival. Arch Med Res *40*, 364-368.

Turner, B. G., and Summers, M. F. (1999). Structural biology of HIV. J Mol Biol *285*, 1-32.

Ueki, K., Kondo, T., and Kahn, C. R. (2004). Suppressor of cytokine signaling 1 (SOCS-1) and SOCS-3 cause insulin resistance through inhibition of tyrosine phosphorylation of insulin receptor substrate proteins by discrete mechanisms. Mol Cell Biol *24*, 5434-5446.

Um, S. H., D'Alessio, D., and Thomas, G. (2006). Nutrient overload, insulin resistance, and ribosomal protein S6 kinase 1, S6K1. Cell Metab *3*, 393-402.

van den Ouweland, J. M., Lemkes, H. H., Ruitenbeek, W., Sandkuijl, L. A., de Vijlder, M. F., Struyvenberg, P. A., van de Kamp, J. J., and Maassen, J. A. (1992). Mutation in mitochondrial tRNA(Leu)(UUR) gene in a large pedigree with maternally transmitted type II diabetes mellitus and deafness. Nat Genet *1*, 368-371.

Van Heusden, M. C. (1993). Characterization and identification of a lipoprotein lipase from Manduca sexta flight muscle. Insect Biochem Mol Biol *23*, 785-792.

Vernochet, C., Azoulay, S., Duval, D., Guedj, R., Cottrez, F., Vidal, H., Ailhaud, G., and Dani, C. (2005). Human immunodeficiency virus protease inhibitors accumulate into cultured human adipocytes and alter expression of adipocytokines. J Biol Chem *280*, 2238-2243.

Vigouroux, C., Maachi, M., Nguyen, T. H., Coussieu, C., Gharakhanian, S., Funahashi, T., Matsuzawa, Y., Shimomura, I., Rozenbaum, W., Capeau, J., and Bastard, J. P. (2003). Serum adipocytokines are related to lipodystrophy and metabolic disorders in HIV-infected men under antiretroviral therapy. Aids *17*, 1503-1511.

Vilaro, S., Reina, M., Ramirez, I., and Llobera, M. (1986). Intralipid administration induces a lipoprotein lipase-like activity in the livers of starved adult rats. Biochem J *236*, 273-278.

Vodenik, B., Rovira, J., and Campistol, J. M. (2009). Mammalian target of rapamycin and diabetes: what does the current evidence tell us? Transplant Proc *41*, S31-38.

Wang, Y., Xu, A., Knight, C., Xu, L. Y., and Cooper, G. J. (2002). Hydroxylation and glycosylation of the four conserved lysine residues in the collagenous domain of adiponectin. Potential role in the modulation of its insulin-sensitizing activity. J Biol Chem *277*, 19521-19529.

Waraich, R. S., Weigert, C., Kalbacher, H., Hennige, A. M., Lutz, S. Z., Haring, H. U., Schleicher, E. D., Voelter, W., and Lehmann, R. (2008). Phosphorylation of Ser357 of rat

University Of Cape Town

insulin receptor substrate-1 mediates adverse effects of protein kinase C-delta on insulin action in skeletal muscle cells. J Biol Chem *283*, 11226-11233.

Weiss, R. A. (2008). Special anniversary review: twenty-five years of human immunodeficiency virus research: successes and challenges. Clin Exp Immunol *152*, 201-210.

White, M. F. (2002). IRS proteins and the common path to diabetes. Am J Physiol Endocrinol Metab *283*, E413-422.

Wilcox, A., Katsanakis, K. D., Bheda, F., and Pillay, T. S. (2004). Asb6, an adipocyte-specific ankyrin and SOCS box protein, interacts with APS to enable recruitment of elongins B and C to the insulin receptor signaling complex. J Biol Chem *279*, 38881-38888.

Woerle, H. J., Mariuz, P. R., Meyer, C., Reichman, R. C., Popa, E. M., Dostou, J. M., Welle, S. L., and Gerich, J. E. (2003). Mechanisms for the deterioration in glucose tolerance associated with HIV protease inhibitor regimens. Diabetes *52*, 918-925.

Wouters, E., van Rensburg, H., and Meulemans, H. (2009). The National Strategic Plan of South Africa: what are the prospects of success after the repeated failure of previous AIDS policy? Health Policy Plan.

Xia, J., Psychogios, N., Young, N., and Wishart, D. S. (2009). MetaboAnalyst: a web server for metabolomic data analysis and interpretation. Nucleic Acids Res *37*, W652-660.

Yokota, T., Nagashima, M., Ghazizadeh, M., and Kawanami, O. (2009). Increased effect of fucoidan on lipoprotein lipase secretion in adipocytes. Life Sci *84*, 523-529.

Young, J., Weber, R., Rickenbach, M., Furrer, H., Bernasconi, E., Hirschel, B., Tarr, P. E., Vernazza, P., Battegay, M., and Bucher, H. C. (2005). Lipid profiles for antiretroviral-naive patients starting PI- and NNRTI-based therapy in the Swiss HIV cohort study. Antivir Ther *10*, 585-591.

Youngren, J. F. (2007). Regulation of insulin receptor function. Cell Mol Life Sci *64*, 873-891.

Yuan, M., Konstantopoulos, N., Lee, J., Hansen, L., Li, Z. W., Karin, M., and Shoelson, S. E. (2001). Reversal of obesity- and diet-induced insulin resistance with salicylates or targeted disruption of Ikkbeta. Science *293*, 1673-1677.

Zhang, Z. Y., Zhou, B., and Xie, L. (2002). Modulation of protein kinase signaling by protein phosphatases and inhibitors. Pharmacol Ther *93*, 307-317.

Zu, L., Jiang, H., He, J., Xu, C., Pu, S., Liu, M., and Xu, G. (2008). Salicylate blocks lipolytic actions of tumor necrosis factor-alpha in primary rat adipocytes. Mol Pharmacol *73*, 215-223.

University of Cape Town

APPENDICES

Appendix 1: Materials

1) Antibodies	Supplier
Actin goat polyclonal IgG (SC1615)[6]	Santa Cruz Biotechnology, CA, USA
APS rabbit polyclonal IgG ((#4832)	Cell Signaling, MA, USA
Goat anti-mouse horseradish peroxidase-conjugated (HRP) (#31430)	Pierce, IL, USA
Goat anti-rabbit HRP (SC2004)	Santa Cruz Biotechnology, CA, USA
IR β-subunit rabbit polyclonal IgG (SC711)	Santa Cruz Biotechnology, CA, USA
Total IRS-1 rabbit polyclonal IgG (#2382)	Cell Signaling, MA, USA
Mouse anti-goat HRP (#314000)	Pierce, IL, USA
pS307 rabbit polyclonal IgG (#2381S)	Cell Signaling, MA, USA
PTP1B rabbit polyclonal IgG (SC4021)	Santa Cruz Biotechnology, CA, USA
Mouse monoclonal IgG of PY20 (610000)	BD Transduction Laboratories, NJ, USA
SH2B rabbit polyclonal IgG	(Kotani et al., 1998)
SOCS-1 rabbit polyclonal IgG (SC9021)	Santa Cruz Biotechnology, CA, USA
SOCS-3 rabbit polyclonal IgG (SC9023)	Santa Cruz Biotechnology, CA, USA
2) Cell lines	
CHO-IR cells	Dr. Gus Gustafson, University of Maryland, USA (Wilcox et al., 2004)
3T3-L1 murine adipocytes	Prof. Peter Shepherd, University College London, UK (Wilcox et al., 2004)
3) Chemicals/Reagents	
Acetic acid (2789)	Merck, Darmstadt, Germany
Acetonitrile (2567064)	Merck, Darmstadt, Germany
Acrylamide/bis (A3449)	Sigma, MO, USA
Antibiotic/antimycotic solution (A5955)	Sigma, MO, USA
Ammonium persulphate (APS) (A9164)	Sigma, MO, USA

[6] Catalogue number

University Of Cape Town

Bromophenol blue (B5525)	Sigma, MO, USA
Bovine serum albumin (BSA) (A3059)	Sigma, MO, USA
Chemiluminescent reagent (34080)	Pierce, IL, USA
Dexamethasone (D1756)	Sigma, MO, USA
Dulbecco's modified Eagle's medium (DMEM) (D5671)	Sigma, MO, USA
Dimethyl sulphoxide (DMSO) (D2650)	Sigma, MO, USA
Ethanol	Kimix, Cape Town, South Africa
Foetal calf serum (FCS) (DE14-801FI)	Lonza, MA, USA
Film developer (83052-50)	Ilford, Cheshire, UK
Film fixer (83060-10)	Ilford, Cheshire, UK
Free fatty acid (FFA) kit (11383175001)	Roche, Basel, Switzerland
G418-sulphate (11811-03)	Gibco, CA, USA
Gas chromatography mass spectrometry (GC-MS) kit (KGO-7165)	Phenomenex, CA, USA
Gentamicin (G1272)	Sigma, MO, USA
Glycerol (G8773)	Sigma, MO, USA
Glycine	Kimix, Cape Town, South Africa
Ham's F12 medium (12-615F)	Lonza, MA, USA
Heparin sodium-fresenius 5000 i.u/ml	Bodene, Port Elizabeth, South Africa
4-(2-hydroxyethyl)-1-piperazineethanesulfonic acid (HEPES) (H3375)	Sigma, MO, USA
3-isobutyl-1-methyl-xanthine (IBMX) (I7018)	Sigma, MO, USA
Insulin from bovine pancreas (I5500)	Sigma, MO, USA
Isopropanol (1219)	Merck, Darmstadt, Germany
L-glutamine (17-605E)	Lonza, MA, USA
Lipoprotein lipase (LPL) from *Pseudomonas* sp. (62336)	Fluka, Buschs, Switzerland
Methanol	Kimix, Cape Town, South Africa
Newborn calf serum (NCS) (N4762)	Lonza, MA, USA
Phosphate buffered saline (PBS) (BR0014G)	Oxoid, Cambridge, UK

University Of Cape Town

Phenoxylpolyethoxylethanol (Tergitol) (NP40)	Sigma, MO, USA
Phosphatase inhibitors for cell culture (04906837001)	Roche, Basel, Switzerland
Protein assay (500-0006)	Bio-Rad, CA, USA
Protease inhibitors (indinavir, darunavir, tipranavir)	Merck, Darmstadt, Germany and NIH, MD, USA
Ponceau S (27195)	Sigma, MO, USA
Precision plus protein dual colour standard (marker) (161-0374)	Bio-Rad, CA, USA
Protease inhibitors for cell culture (04693124001)	Roche, Basel, Switzerland
Skimmed milk powder (92964)	Marvel, London, UK
Sodium dodecyl sulphate (SDS) (161-0301)	Bio-Rad, California, USA
Sodium chloride (71378)	Fluka, Buschs, Switzerland
Sodium phosphate, monobasic, anhydrous (6346)	Merck, Darmstadt, Germany
Sodium salicylate (S2679)	Sigma, MO, USA
N, N, N', N',-tetra-methyl-ethylenediamine (TEMED) (161-0801)	Bio-Rad, CA, USA
Tris base	Kimix, Cape Town, South Africa
Tris-HCl	Promega, WI, USA
Triton x-100 (T8787)	Sigma, MO, USA
Trypsin-ethylenediaminetetraacetic acid (trypsin-EDTA) (T3924)	Sigma, MO, USA
Tween 20 (P1379)	Sigma, MO, USA
2-mercaptoethanol (805740)	Merck, Darmstadt, Germany
p-nitrophenyl butyrate (*p*NPB) (N9876)	Sigma, MO, USA
4) Consumables	
6-well plate (140675)	Amersham Biosciences, NJ, USA
20 ml universal bottle (128B)	Sterilin, London, UK
25 cm^2 flask (430639)	Corning, NY, USA
3.5 cm dish (150318)	Amersham Biosciences, NJ, USA
50 ml centrifuge tube	Corning, NY, USA
75 cm^2 flask (156499)	Amersham Biosciences, NJ, USA

University Of Cape Town

Cryotube	Nalgene, NY, USA
Disposable counting chamber	ISL, Paignton, UK
Disposable cuvette	Lasec, Cape Town, South Africa
Filter paper (3030-861)	Whatman, Kent, UK
Medical X-ray film (LEEBN000)	Agfa, Mortsel, Belgium
Mirocentrifuge tubes and tips	QSP, CA, USA
Nitrocellulose membrane (RPN303P)	Amersham Biosciences, NJ, USA
Syringe	Pall, NY, USA
Syringe filter (0.2 µm)	Pall, NY, USA
5) Software and web server	
ChemiImager (Fluorchem 5500 Programme)	Alpha Innotech Corporation, CA, USA
Chemstation	Agilent Technologies, CA, USA
GraphPad Prism	GraphPad Software, CA, USA
MetaboAnalyst	University of Alberta, Alberta, Canada
Statistica 8	StatSoft, OK, USA
Sigmaplot 8	Aspire Software International, VA, USA

University Of Cape Town

Appendix 2: Cell culture reagent

1) Ham's F12 mixture culture medium

Reagents	Volume (ml)	Final concentration
a) Ham's F12 medium	500	
b) Foetal calf serum (FCS)	50	10 %
c) 200 mM Glutamine	5	2 mM
d) 100 x Antibiotic/antimycotic solution	5	1%
e) Gentamicin	2.5	0.5 %
f) G418	0.5	400 µg/ml
Total volume	563	

0.4 g G418-sulphate powder was dissolved in 1 ml dH_2O and filtered using a 0.2 µM syringe filter.

2) Medium 1

Reagents	Volume (ml)	Final concentration
a) Dulbecco's modified Eagle's medium (DMEM)	500	
b) Newborn calf serum	50	10 %
c) 200 mM Glutamine	5	2 mM
d) 100 x Antibiotic/antimycotic solution	5	1 %
e) Gentamicin	2.5	0.5 %
Total volume	562.5	

3) Medium 2

Reagents	Volume (ml)	Final concentration
a) DMEM	500	
b) FCS	50	10 %
c) 200 mM Glutamine	5	2 mM
d) 100 x Antibiotic/antimycotic solution	5	1 %
e) Gentamicin	2.5	0.5 %
f) 0.125 mM Dexamethasone	1	0.25 µM
g) 0.25 M IBMX	1	0.5 mM
h) 1 mg/ml Insulin	0.5	166 nM
Total volume	565	

0.125 mM dexamethasone was prepared in ethanol and 0.25 M IBMX was prepared in 1 M NaOH. Insulin (1mg/ml) (0.17 mM) was prepared in 1 % acetic acid. The solutions were filtered using a 0.2 µM syringe filter prior to use.

University Of Cape Town

4) Medium 3

Reagents	Volume (ml)	Final concentration
a) DMEM	500	
b) FCS	50	10 %
c) 200 mM Glutamine	5	2 mM
d) 100 x Antibiotic/antimycotic solution	5	1 %
e) Gentamicin	2.5	0.5 %
f) 1 mg/ml Insulin	0.5	166 nM
Total volume	563	

5) Medium 4

Reagents	Volume (ml)	Final concentration
a) DMEM	500	
b) FCS	50	10 %
c) 200 mM Glutamine	5	2 mM
d) 100 x Antibiotic/antimycotic solution	5	1 %
e) Gentamicin	2.5	0.5 %
Total volume	562.5	

6) Serum-free medium

Reagents	Volume (ml)	Final concentration
a) DMEM	500	
c) 200 mM Glutamine	5	2 mM
d) 100 x Antibiotic/antimycotic solution	5	1 %
e) Gentamicin	2.5	0.5 %
Total volume	512.5	

7) 10 x Lysis buffer stock solution

Reagents	Volume	Final concentration
a) 4-(2-hydroxyethyl)-1-piperazineethanesulfonic acid (HEPES), pH 7.5	445 ml	50 mM
b) Phenoxylpolyethoxyethanol (NP40)	5 ml	1 %
c) Glycerol	50 ml	10 %
d) Sodium chloride (NaCl)	1.461 g	50 mM
Total volume	500 ml	

8) 1 x Lysis buffer solution

The lysis buffer was prepared with 1 tablet of protease inhibitor and 1 tablet of phosphatase inhibitor in 10 ml of 10 x lysis buffer stock solution.

University Of Cape Town

9) 5 x Laemmli buffer

Reagents	Volume	Final concentration
a) 1 M Tris, pH 6.8	1.25 ml	25 nM
b) Sodium dodecyl sulphate (SDS)	1 g	2 %
c) 1 % Bromophenol blue	0.33 ml	0.002 %
d) Glycerol	5 ml	10 %
e) 2-Mercaptoethanol	2.5 ml	5 %
f) Water	1.25 ml	
Total volume	10.33 ml	

10) Freezing solution for CHO-IR cells

Reagents	Volume (ml)	Final concentration
a) Dimethyl sulphoxide (DMSO)	10	10 %
b) FCS	40	
Total volume	50	

11) Freezing solution for 3T3-L1 pre-adipocytes

Reagents	Volume (ml)	Final concentration
a) DMSO	10	10 %
b) Newborn calf serum	40	
Total volume	50	

12) Phosphate buffered saline (PBS)

1 tablet of PBS was dissolved in 100 ml dH_2O and the mixture was filtered sterile with a syringe filter.

13) Insulin stimulation

Insulin was prepared in 100 mM acetic acid + 0.1% bovine serum albumin (BSA)

i. 100 mM acetic acid
    a. 0.294 ml 17 M acetic acid + 49.706 ml dH_2O
ii. 0.1% BSA
    a. Add 0.05 g BSA into 50 ml acetic acid to become 0.1% BSA

5 mg insulin was dissolved in 5 ml of 100 mM acetic acid + 0.1% BSA = 1 mg/ml

100 ng/ml (17 nM) insulin = 10 µl + 990 µl PBS

10 ng/ml (1.7 nM) insulin = 100 µl of 100 ng/ml (17 nM) insulin + 900 µl PBS

University Of Cape Town

14) Drugs stock solutions

Drugs were prepared using a standard formula:

Mass drug (g) = concentration (M) x molecular weight (MW) x volume (L)

a) 5 mM indinavir, MW = 711.88

b) 5 mM saquinavir, MW = 670.85

c) 0.2 mM darunavir, MW = 593.73

d) 1.5 mM tipranavir, MW = 602.70

e) 50 mM sodium salicylate, MW = 160.10

15) Calculation of cell number

CHO-IR cells were counted using a haemocytometer to determine the total number of cells in the original flask. Then, 10 µl cell medium solution was loaded into the haemocytometer. The number of cells in 5 of 10 of the 0.1 mm^3 blocks was counted as follows:

$$\text{Cells } cm^{-3} = \frac{\text{Number of cells counted}}{\text{Number of squares counted}} \times \text{conversion factor (1000)}$$

100 000 cells per well of each 6-well plate was required to achieve 70-85 % confluence on day 2/3.

University Of Cape Town

Appendix 3: Electrophoresis and Western blot analysis

1) 1.5 M Tris-HCl, pH 8.8, for 500 ml

Using an Henderson–Hasselbalch equation:

$$pH = pHa + \log \frac{(Base)\ B}{(Acid)\ A}$$

Tris-HCl (A) = 0.113 g

Tris-Base (B) = 0.276 g

2) 0.5 M Tris-HCl, pH 6.8, for 500 ml

Tris-HCl (A) = 0.153 g

Tris-Base (B) = 0.004 g

3) 10 % Ammonium persulphate (APS)

0.1 g APS was dissolved in 1 ml dH_2O

4) 10 % SDS

5 g SDS was dissolved in 50 ml dH_2O

5) 4 % Stacking gel

Reagents	Volume (ml)	Final concentration
a) 0.5 M Tris-HCl, pH 6.8	1.260	0.126 M
b) 30 % Acrylamide/bis (19:1)	0.660	4 %
c) dH_2O	3.000	
d) 10 % SDS	0.500	0.1 %
e) 10 % APS	0.250	0.05 %
f) TEMED	0.005	0.1 %
Total volume	5.675	

6) 7.5 % Resolving gels

Reagents	Volume (ml)	Final concentration
a) 1.5 M Tris-HCl, pH 8.8	2.500	0.375 M
b) 30 % Acrylamide/bis (19:1)	2.500	7.5 %
c) dH_2O	4.850	
d) 10 % SDS	0.100	0.1 %
e) 10 % APS	0.050	0.05 %
f) TEMED	0.005	0.05 %
Total volume	10.005	

University Of Cape Town

7) 10 x Running buffer

Reagents	Volume	Final concentration
a) Tris base	14.41 g	0.025 M
b) Glycine	3 g	0.192 M
c) SDS	1 g	0.1 %
d) dH_2O	1 l	
Total volume	1 l	

8) 1 x Running buffer

100 ml 10 x stock solution was added to 900 ml deionised water.

9) 10 x Transfer buffer

Reagents	Volume	Final concentration
a) Tris base	30.28 g	0.025 M
b) glycine	144.13g	0.192 M
c) dH_2O	800 ml	
Total volume	800 l	

10) 1 x Transfer buffer

80 ml 10 x stock solution was added to 720 ml deionised water and 200 ml methanol.

5) Tris buffered saline + 0.1% Tween 20 (TBST), pH 7.4

Reagents	Volume	Final concentration
a) Tris-HCl	6.8 g	0.05 M
b) Tris base	0.82 g	
c) NaCl	8.77 g	0.150 M
d) Tween 20	5 ml	0.1 %
e) dH_2O	1 l	
Total volume	1 l	

11) 0.1 % Ponceau S solution

0.1 g Ponceau was dissolved in 100 ml of 5 % acetic acid.

12) 3 % BSA

1.5 g BSA was dissolved in 50 ml TBST.

13) 5 % Milk solution

2.5 g skimmed milk powder was dissolved in 50 ml TBST.

University Of Cape Town

14) Stripping solution

Reagents	Volume (ml)	Final concentration
a) 1 M Tris-HCl, pH 6.8	1.56	0.063M
b) 10 % SDS	5	2 %
c) 2-mercaptoethanol	0.175	0.1 M
d) dH_2O	18.27	
Total volume	25	

University Of Cape Town

Appendix 4: Metabolomic analysis

1) Amino acid analysis (summarised from Phenomenex EZ-faast™ kit: user's manual)

a) 100 µl of nor-valine internal standard (Reagent 1) was pipetted into tubes.
b) 100 µl of sample was added to each tube and mixed.
c) The mixture was slowly drawn up into a sorbent tip. Avoid air-bubble.
d) The sorbent tip was left in a new tube and washed with washing solution (Reagent 2) (200 µl).
e) Elution fluid (Reagent 3) (200 µl) was then pipetted into the tube.
f) The elution fluid was drawn up and expelled twice until all the resin in the sorbent tip had been removed from the tip.
g) Reagent 4 (50 µl) was added into each tube using a glass Hamilton syringe.
h) The mixture was vortexed for 5 sec and let stand for 1 min, twice.
i) Reagent 5 (100 µl) was added to each tube using a glass Hamilton syringe and vortexed for 5 sec.
j) The mixture was centrifuged at 2300 rpm for 1 min.
k) Top layer of the mixture was transferred into a vial using a glass Pasteur pipette.
l) The top layer was dried down under nitrogen for 10 min.
m) The dried sample was then resuspended with reagent 6 (100 µl) and vortexed for 5 sec.
n) The entire sample was transferred into an insert using a glass Pasteur pipette prior to performing GC-MS analysis.

University Of Cape Town

2) Organic acid analysis (Procedure of organic acid extraction)

a) Samples (200-500 µl) were pipetted into tubes (Tube 1) and were made up to 2 ml with dH_2O.
b) Six drops of 5 M HCl were added to each tube (pH < 2).
c) 5 µl of pentadecanoate (PDA) was added to each tube.
d) Approximately 1 g of NaCl was added to saturate the samples, and the mixture was vortexed.
e) The mixture was transferred to a tube (Tube 2) in a fume cupboard.
f) 2 ml ethyl acetate was added to each tube.
g) The tubes were capped and placed on a mixer for 2 min.
h) The mixture was centrifuged for 3 min at 1000 rpm using Mistral 6L Centrifuge. The temperature was set to 10 °C.
i) Top layer was transferred to another tube using a glass Pasteur pipette.
j) Steps f) to i) were repeated.
k) Steps f) to i) were repeated using 2 ml diethyl ether.
l) The extract was dried by adding approximately 2 g anhydrous sodium sulphate.
m) The dry extract was transferred to another tube (Tube 3).
n) The dry extract was evaporated under nitrogen at 37 °C using a heating block.
o) Bis-(trimethylsilyl)trifluoroacetamide (BSTFA) (75 µl) and pyridine (20 µl) were added to each tube in a fume cupboard. The tubes were capped and vortexed.
p) The tubes were placed in a heating block at 80 °C for 30 min.
q) The tubes were allowed to cool to room temperature prior to GCMS analysis.

University Of Cape Town

3) Free fatty acid analysis

For life science research only. Not for use in diagnostic procedures.
FOR *IN VITRO* USE ONLY.

Free fatty acids, Half-micro test

Optimized enzymatic colorimetric assay for the determination of free fatty acids (= Non-Esterified Fatty Acids, NEFA) in research samples from serum or plasma.

Cat. No. 11 383 175 001

Test-Combination for approx. 5 × 10 determinations

Version June 2004

Store at 2-8° C

Product overview

Contents

Bottle	Contents
1	• 5 x 11 ml • each of potassium phosphate buffer, pH 7.8
2	• 5 tablets • each tablet contains: ATP, coenzyme A, acyl-CoA-synthetase (Acyl CS), peroxidase, ascorbate oxidase, 4-aminoantipyrine and stabilizers.
3	• 3 ml • ready-to-use! • aqueous N-ethyl-maleinimide solution with stabilizers. ***Note:*** The presence of N-ethyl-maleinimide in the test is necessary for the removal of an existing surplus of CoA before the oxidation of the activated fatty acids by ACOD.
4	• 5 x approx. 0.6 ml • each of ACOD dilution solution and stabilizers.
5	• 5 tablets • each tablet contains: acyl-CoA-oxidase (ACOD) and stabilizers

Test principle

In the presence of the enzyme acyl-CoA synthetase (Acyl CS) and adenosine-5'-triphosphate (ATP), free fatty acids are converted into acyl-coenzyme A (acyl-CoA), adenosine-5'-monophosphate (AMP), and pyrophosphate.

Acyl-CoA reacts with oxygen (O_2) in the presence of acyl-CoA oxidase (ACOD) to form 2,3-enoyl-coenzyme A (enoyl-CoA).

The resulting hydrogen peroxide (H_2O_2) converts 2,4,6-tribromo-3-hydroxy-benzoic acid (TBHB) and 4-aminoantipyrine (4-AA) to a red dye in the presence of peroxidase (POD).

The dye is measured in the visible wavelength range at 546 nm.

$$\text{Free fatty acids} + \text{CoA} + \text{ATP} \xrightarrow{\text{Acyl CS}} \text{acyl-CoA} + \text{AM P} + \text{pyrophosphate}$$

$$\text{Acyl-CoA} + O_2 \xrightarrow{\text{ACOD}} \text{enoyl-CoA} + H_2O_2$$

$$H_2O_2 + \text{4-AA} + \text{TBHB} \xrightarrow{\text{POD}} \text{red dye} + 2\,H_2O + \text{HBr}$$

Application

Determination of free fatty acids (non-esterified fatty acids, NEFA) in serum and plasma in life science research applications.

Interference

Hemoglobin, bilirubin and ascorbic acid do not interfere with the assay if they are present in the normal range.

Storage and stability

The reagents in the unopened bottles are stable at 2-8°C until the expiration date printed on the label.

Note: Reaction mixtures A and B are stable for 5 days at 2-8°C or for 8 h at 15-25°C stored protected from light.

Procedure

Handling instructions

For use with instruments (like Hitachi 704) N-ethyl-maleinimide solution (bottle 3) and Reaction mix B should be mixed at equal volumes. For the assay 0.1 ml of this mixture should be used.

Working solutions

For preparation and stability of working solutions refer to the table below.

Note: Use forceps for taking the tablets out of bottle 2 and 5

.

Solution	Preparation	Stability
Reaction mixture A	Dissolve one tablet of bottle 2 in one bottle 1, sufficient for 10 assays.	Stable for • 5 days at 2-8°C • 8 hrs at 15-25°C if stored protected from light
Reaction mixture B	Dissolve one tablet of bottle 5 in one bottle 4, sufficient for 10 assays.	

Sample preparation

- Collect blood from a non-congested vein into a test tube containing EDTA (plasma).
- Prepare serum in the usual way.

Note: Stability of the free fatty acids in serum or plasma: 7 days at 2-8°C or 2 days at 20-25°C.

Assay conditions

Measurement against air (without a cuvette in the light path) or against water.

Note: If desired, commercially available disposable cuvettes may be used instead of glass cuvettes.

Wavelength	546 nm (Hg)
Half micro glass cuvette	1 cm light path
Temperature	25°C ± 1°C
Assay volume	1.15 ml

University Of Cape Town

0604.11412 221®

Roche

Protocol

Please refer to the following table.

Note: We recommend to mix the reagents in the cuvettes *e.g.* with a plastic spatula or by gentle swirling after closing the cuvettes, *e.g.* with Parafilm [1].

Step	Action
1	Pipette into cuvettes: **Reagent** / **Blank** / **Sample** Reaction mix A / 1.00 ml / 1.00 ml Sample / - / 0.05 ml Double dist. water / 0.05 ml / - ***Note:*** Rinse the enzyme pipette or pipette tip of the piston pipette with the sample solution before use.
2	• Mix the reagents and bring to 25°C • Keep at this temperature for approx. 10 min.
3	• To each cuvette add 0.05 ml ready-to-use N-ethyl-maleinimide-solution (bottle 3). • Mix and read absorbances of the solutions (A_1).
4	• Start reaction by adding 0.05 ml of Reaction mix B to each cuvette and mix. • Wait for the end of the reaction at 25°C (approx. 15 min) and read absorbances of the solutions (A_2).

Calculation

Calculate the absorbance differences ($A_2 - A_1$) for both blank and sample. Subtract the absorbance difference of the blank (ΔA_b) from the absorbance difference of the sample (ΔA_s).

This gives ΔA.

$$\Delta A = \Delta A_S - \Delta A_b .$$

Reference values

In serum obtained from up to 3 days old children values between 0.3 and 0.8 mM have been found (2).

Palmitic acid standard solution

If checking the assay by using a standard solution, this may be prepared as follows.

Additional reagents required

- Triton [2] X-100 (Cat. No. 789 704)
- Ethanol, absolute
- Palmitic acid (available from *e.g.* Fa. Sigma, P0500)

Preparation of solutions

Please refer to the following table.

Solution	Preparation/Composition
1	Dissolve 6.0 g of Triton X-100 in about 80 ml of double dist.water (30°-40°C), allow to cool to 15-25°C and make up to 100 ml in a measuring cylinder.
2	Weigh 9 mg of palmitic acid into a 100 ml beaker and dissolve in about 6 ml of warm ethanol (about 35-40°C). Immediately seal the beaker with Parafilm and allow to cool to 15-25°C.

Preparation of standard solution

- Add about 80 ml of solution 1 to solution 2, stirring slowly to avoid the formation of microcrystals at the point of entry.
- Stir using a magnetic stirrer for a further 30 min, transfer quantitatively to a 100 ml volumetric flask and make up to the mark with solution 1.

Note: Stable for 3 days when stored at 4-8°C (refrigerator). The standard has a concentration of 0.35 mM.

Calculation of the concentration

According to the general formula for calculating the concentration, the equation is:

$$c = \frac{V}{\epsilon \times d \times v} \times \Delta A \text{ [mM sample solution]}$$, where:

V = final volume (ml)

v = sample volume (ml)

d = light path (cm)

ε = absorption coefficient of the dye at 546 nm:

19.3 [l × mmol^{-1} × cm^{-1}]

Note: The absorbance coefficient of the dye depends on the type of buffer, the pH of the assay system and the purity of TBHB. Under the assay conditions stated above, it varies between 19.1 and 19.5 [l ×mmol^{-1} × cm^{-1}].

It follows for free fatty acids:

$$c = \frac{1.15}{19.3 \times 1 \times 0.05} \times \Delta A = 1.192 \times \Delta A \text{ [mM free fatty acids/serum, plasma]}$$

Note: If checking the assay by using a standard solution, pipette 0.05 ml of standard into the cuvette instead of the sample (serum) as shown in the pipetting scheme.

If deproteinized serum is used in the test, the test volume V in the equation must be corrected by multiplying by the factor F = 0.948.

Dilution factor

The dilution factor is calculated from the specific gravity of the serum or plasma (ρ = 1.03 g/ml) and from the liquid fraction of the serum or plasma (92% = 0.92); F = 1.03 × 0.92 = 0.948.

Dilution limit

The method shows linearity up to a concentration of 1.5 mM free fatty acids/sample (serum, plasma).

References

1 Shimizu, S. et al. (1980) *Anal. Biochem.* **107**, 193-198.
2 Harris, R. J. (1974)). *Pediatr.* **84**, 578-584.

*available from Roche Applied Science

[1] Parafilm is a trademark of the American Can Company, Greenwich, Ct., USA.
[2] Triton is a trademark of Rohm & Haas, Philadelphia, PA, USA.

How to contact Roche Applied Science:

www.roche-applied-science.com

- to place your order
- find product information
- for answers to technical queries, or,
- contact your local sales representative.

www.roche-applied-science.com/pack-insert/11383175001a.pdf

Please visit our new Online Technical Support Site under
www.roche-applied-science.com/support

Roche Diagnostics GmbH
Roche Applied Science
Nonnenwald 2
82372 Penzberg
Germany

University Of Calgary

4) Normalisation

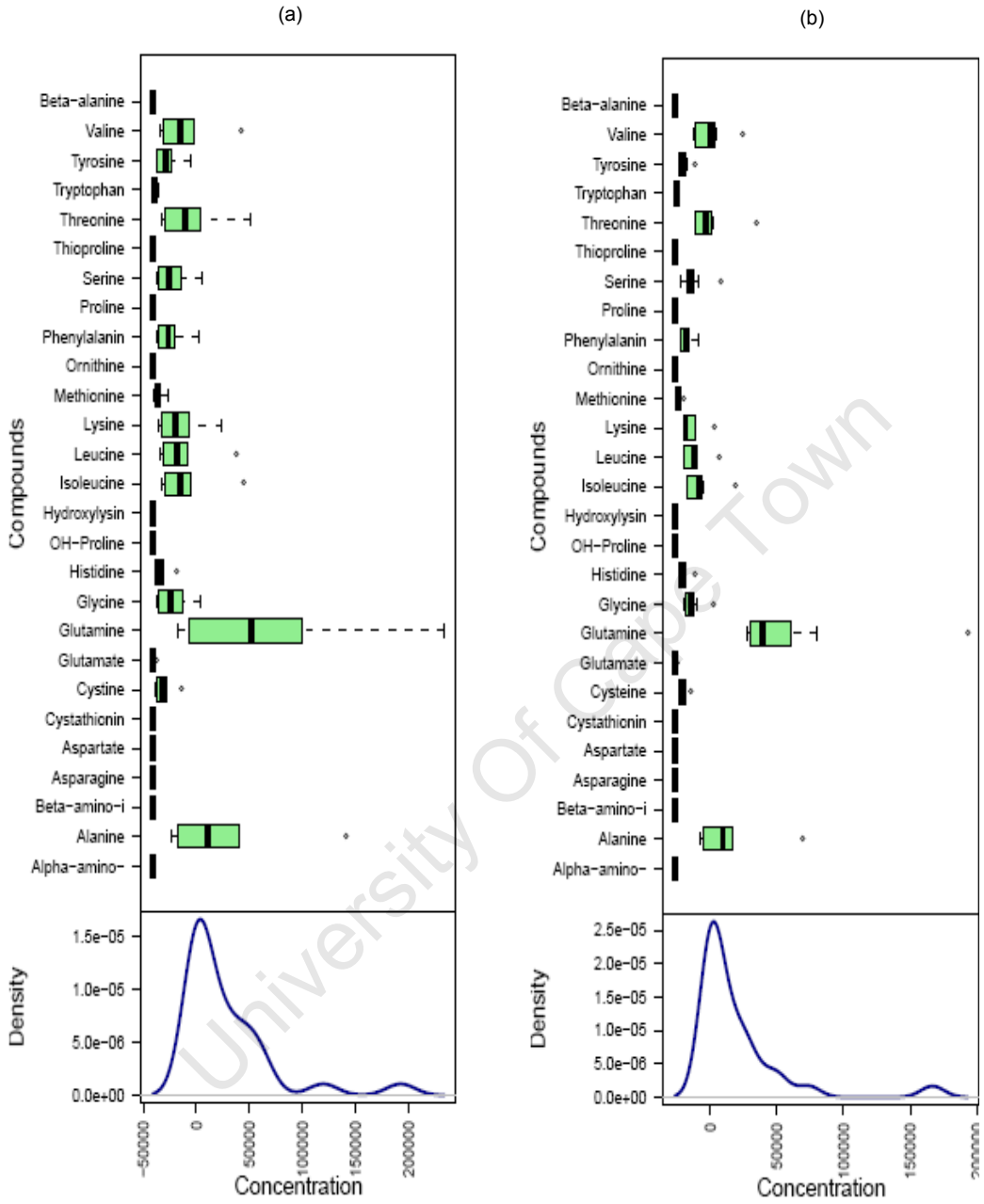

Box plots and kernel density plots of amino acids in the untreated and drug-treated cell culture supernatants (a) without and (b) with insulin stimulation: before normalisation. 27 amino acids and derivatives were identified in supernatants of 3T3-L1 adipocytes before and after treatment with indinavir (50 μM) for 16 h followed by insulin stimulation using GC-MS.

University Of Cape Town

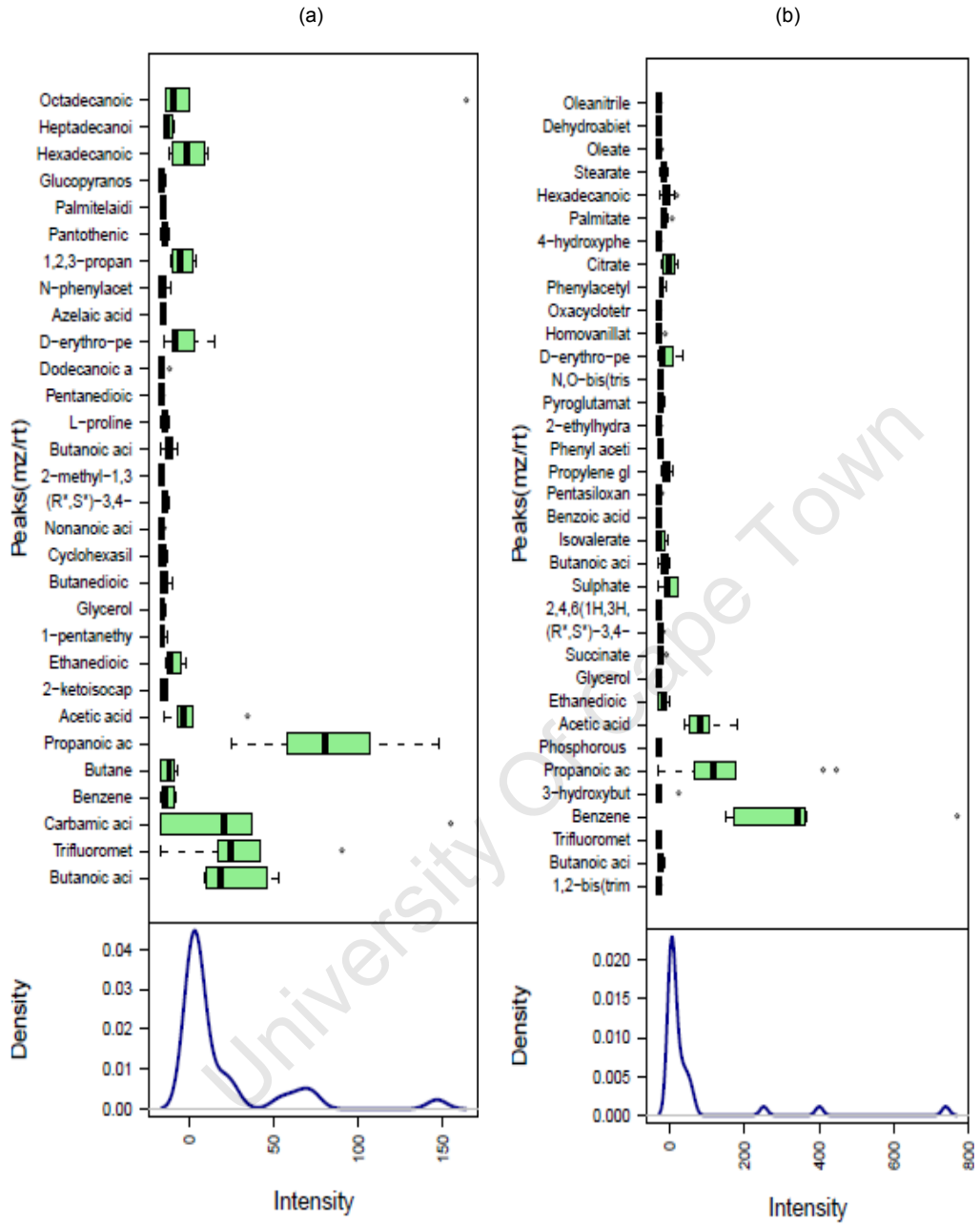

Box plots and kernel density plots of organic acids in the untreated and drug-treated cell culture supernatants (a) without and (b) with insulin stimulation: before normalisation. 60 organic acids and derivatives were identified in supernatants of 3T3-L1 adipocytes before and after treatment with indinavir (50 μM) for 16 h, followed by insulin stimulation using GC-MS.

University of Cape Town

Organic acids that were exclusively identified in cell culture supernatants (drug-treated, untreated or both) with or without insulin stimulation using GC-MS. 3T3-L1 adipocytes were left untreated or treated with indinavir (50 μM) for 16 h, followed by insulin stimulation.

Before insulin stimulation		After insulin stimulation		Untreated and drug-treated supernatants with or without insulin simulation
Untreated supernatants	Drug-treated supernatants	Untreated supernatants	Drug-treated supernatants	
1. Carbamic acid	1. Carbamic acid	1. Succinate	1. Succinate	1. Butanoic acid,3-(trimethylsilyloxy)-ethylester
2. Butane	2. Butane	2. Sulphate	2. Sulphate	2. Benzene
3. 2-ketoisocaproic acid	3. 2-ketoisocaproic acid	3. Pyroglumate	3. Pyroglumate	3. Propanoic acid
4. 1-pentanethyldisilyloxybutane	4. 1-pentanethyldisilyloxybutane	4. Palmitate	4. Palmitate	4. Ethanedioic acid
5. Butanedioic acid	5. Butanedioic acid	5. Stearate	5. Stearate	5. (RxSx)-3,4-dihydroxybutanoic acid
6. Cyclohexasilaxane	6. Cyclohexasilaxane	6. Benzoic acid	6. Benzoic acid	6. Butanoic acid,4-(trimethylsilyloxy)-,ethylester
7. Nonanoic acid	7. Nonanoic acid	7. Propylene glycol	7. Propylene glycol	7. D-erythro-pentonic acid
8. 2-methyl-1,3-bis(trimethylsilyloxy)butane	8. 2-methyl-1,3-bis(trimethylsilyloxy)butane	8. Phenylacetylglycine	8. Phenylacetylglycine	8. Hexanedoic acid
9. L-proline	9. L-proline	9. N,O-bis(trismethylsilyl)-L-phenylalanine	9. N,O-bis(trismethylsilyl)-L-phenylalanine	9. Acetic acid
10. Dodecanoic acid	10. Dodecanoic acid	10. Homovanillate	10. Homovanillate	
11. Azelaic acid	11. Azelaic acid	11. Citrate	11. Citrate	
12. 1,2,3-propanetricarboxylic acid	12. 1,2,3-propanetricarboxylic acid	12. Oleate	12. Oleate	
13. Pantothenic acid	13. Pantothenic acid	13. Phenyl acetic acid	13. Phenyl acetic acid	
14. Palmitelaidic acid	14. Palmitelaidic acid	14. 1,2-bis(trimethylsiloxy)ethane	14. 3-hydroxybutyrate	
15. Glucopyranose	15. Glucopyranose	15. Oleanitrile	15. Phosphorous acid	
16. Heptadecanoic acid	16. Heptadecanoic acid	16. Dehydroabietic acid	16. 2,4,6(1H,3H,5H)-primidinetrione,5-(1-methylpropyl)-5-(2-propenyl)-1	
17. Octadecanoic acid	17. Octadecanoic acid		17. Isovalerate	
	18. Pentanedioicaid		18. Pentasiloxane,dodecamethyl	
			19. 2-ethylhydracrylic acid	
			19. Oxacyclotetradec-5-yn	
			20. 4-hydroxyphenyllactate	

University of Cape Town

Appendix 5: Lipoprotein lipase assay

1) Measurement of protein concentration using Bradford protein assay

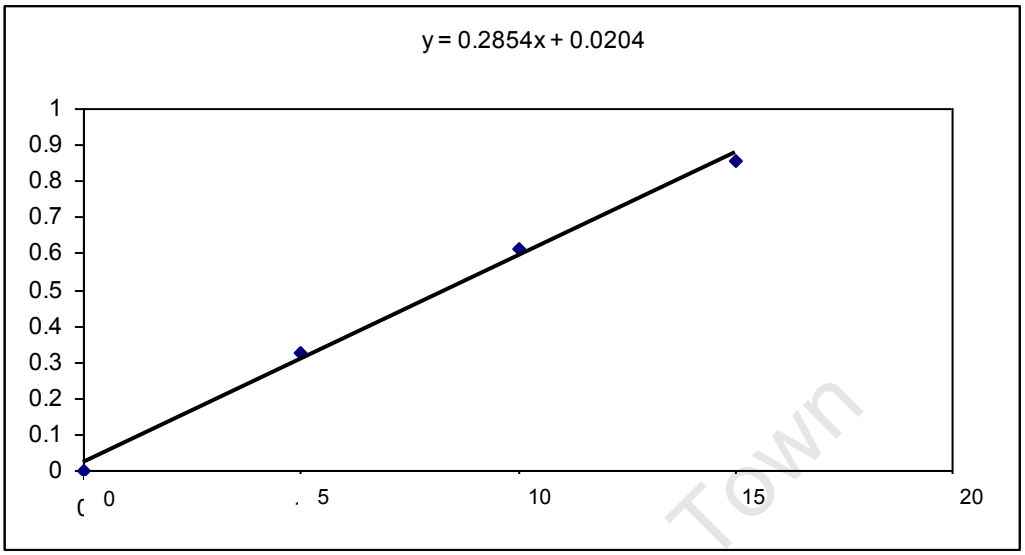

Bovine serum albumin (µg/ml)	Absorbance at 595 nm
0	0
5	0.326
10	0.612
15	0.856

University Of Cape Town

2) Absorbance of assay reagent of LPL activity assay in cuvettes at 400 nm after 10 min incubation at 37 ºC in a waterbath

No.	Assays	Absorbance (nm) at 400nm
1	Buffer + (PBS) + pNPB	0.12
2	Buffer + (PBS + H) + pNPB	0.12
3	Buffer + (PBS + I) + pNPB	0.13
4	Buffer + (PBS + I + H) + pNPB	0.12
5	Buffer + (PBS) + acetonitrile	0
6	Buffer + (PBS + H) + acetonitrile	0
7	Buffer + (PBS + I) + acetonitrile	0
8	Buffer + (PBS + I + H) + acetonitrile	0
9	Buffer + (Cell culture supernatants in PBS) + acetonitrile	0
10	Buffer + (Cell culture supernatants in PBS + H) + acetonitrile	0
11	Buffer + (Cell culture supernatants in PBS + I) + acetonitrile	0
12	Buffer + (Cell culture supernatants in PBS + I + H) + acetonitrile	0
13	Buffer + (Cell culture supernatants in PBS) + pNPB	0.14
14	Buffer + (Cell culture supernatants in PBS + H) + pNPB	0.18
15	Buffer + (Cell culture supernatants in PBS+I) + pNPB	0.16
16	Buffer + (Cell culture supernatants in PBS+I+H) + pNPB	0.58
17	Buffer + (PBS) + pNPB	0.12
18	Standard LPL enzyme from *Pseudomonas* sp. (E)1 (213 U/mg)	3.04
19	E1/100 (2.13 U/mg)	2.46
20	E1/100000 (2.13 mU/mg)	1.48
21	E1/1000000000 (2.13 µU/mg)	0.45

Buffer = 0.1 M sodium phosphate, monobasic, anhydrous, pH 7.2; 0.9 % sodium chloride; 0.5 % (v/v) Triton X-100

PBS = phosphate buffered saline

pNPB = *para*-nitrophenyl butyrate was prepared in acetonitrile

I = insulin (100 ng/ml) (17 nM)

H = heparin (100 U/ml)

LPL = lipoprotein lipase

E = standard LPL enzyme from *Pseudomonas* sp.

University Of The Western Cape Town

JEMDSA

Review Article: Insulin resistance induced by antiretroviral drugs: Current understanding of molecular mechanisms

Insulin resistance induced by antiretroviral drugs: Current understanding of molecular mechanisms

Ismail WIW, BSc (Hons), MSc **King JA,** BSc(Hons), MSc, PhD **Pillay TS,** MBChB (Natal), PhD (Cantab), FRCPath(UK), FCPath(SA)
Division of Chemical Pathology, Department of Clinical Laboratory Sciences, University of Cape Town and National Health Laboratory Service, Groote Schuur Hospital, Cape Town
Correspondence to: Prof. T.S. Pillay, email:profts.pillay@uct.ac.za
Keywords: HIV protease inhibitors; insulin resistance; insulin signalling pathway

Abstract

The increase in incidence of HIV infection continues to be a major public health problem across the world, but more especially in sub-Saharan Africa. Treatment with highly active antiretroviral therapy (HAART) has improved the prognosis of patients with AIDS, but it has also increased the incidence of various metabolic disorders, in particular insulin resistance accompanied by dyslipidaemia, hyperglycaemia and lipodystrophy. This is often accompanied by frank type 2 diabetes and increased mortality from cardiovascular disease. It is important to understand the mechanistic basis for these side-effects as the incidence of these is likely to increase as the rollout of antiretroviral drugs continues.

Peer reviewed. (Submitted: 2009-10-31, Accepted: 2009-11-13) JEMDSA 2009;14(3):129-132

University Of Cape Town

Introduction

Twenty-six years after the acquired immune deficiency syndrome (AIDS) was first reported, human immunodeficiency virus (HIV) infection still remains a major global challenge, especially in the southern part of sub-Saharan Africa. In South Africa, there were six million people infected, and more than 400 000 had died from AIDS by 2007.[1-3]

Currently, the most potent treatment for HIV infection is highly active antiretroviral therapy (HAART). This therapy is a combination of two or more antiretroviral drugs. These drugs work as inhibitors which contain five classes including entry inhibitors (EIs), nucleoside or nucleotide reverse transcriptase inhibitors (NRTIs), non-nucleotide reverse transcriptase inhibitors (NNRTIs), integrase inhibitors (IIs) and HIV protease inhibitors (HPIs). This treatment can extend the lifespan of HIV-infected patients by suppressing HIV viral load, increasing CD4+ T-cell[a] counts,[b] and reducing opportunistic infections associated with AIDS.[4,5]

Unfortunately, besides improving patient prognosis, these drugs also result in metabolic abnormalities, in particular insulin resistance accompanied by dyslipidaemia,[c] hyperglycaemia and lipodystrophy.[6,7] Consequently, patients are also at high risk of developing premature cardiovascular morbidity and type 2 diabetes mellitus.[8-11]

A substantial number of clinical and epidemiological studies have shown that HPIs play a major role in inducing metabolic disorders in HAART-treated patients.[6,12,13] It appears that HPIs impair insulin-mediated metabolism in adipose tissue and result in insulin resistance.[14] However, the mechanisms for these side-effects are largely unknown. It is important to understand the mechanistic basis for these side-effects as the incidence of these is likely to increase as the rollout of antiretroviral drugs continues.

The insulin signalling pathway (see Figure 1)

Signalling through the insulin receptor pathway is critical for the regulation of blood glucose levels by insulin.[15] In the post-prandial phase, in response to glucose, the pancreas releases insulin into the bloodstream. Insulin then binds to its receptor. The heterotetrameric (2 α- and 2 β-subunits) receptor is a ligand-activated tyrosine kinase. The binding of insulin leads to autophosphorylation of the receptor β-subunit on tyrosine residues. This then activates the intrinsic tyrosine kinase domain and leads to tyrosine phosphorylation of its substrate, insulin receptor substrate-1 (IRS-1). Typically, phosphotyrosine residues interact with a particular type of protein domain, Src homology 2 (SH2) domain with high specificity and affinity. The tyrosine phosphorylated IRS-1 binds to the SH2 domain of phosphoinositide 3-kinase (PI3-K) leading to activation of this enzyme and conversion of phosphatidylinositol 4,5-biphosphate (PIP_2) into phosphatidylinositol 3,4,5-triphosphate (PIP_3). The bound PIP_3 causes translocation of both PIP_3-dependent protein kinase (PDK) and PKB, also known as Akt. This then allows PDK to phosphorylate and then activate (PKB). The activation of PKB/Akt is necessary for the final steps leading to glucose transport. This then results in the migration of glucose transporter 4 (GLUT4) from the cytoplasm to the cell membrane to facilitate the uptake of extracellular glucose. Some of the detailed final steps leading to the translocation of GLUT4 are still unclear and is still the subject of intensive research.

[a] T cell or T helper cell is a subgroup of lymphocytes; a type of white cell which functions to activate other immune cells and express surface protein CD4
[b] This method is to detect HIV infection as HIV targets cells that express CD4+ T cells and reduces the circulating levels
[c] Dyslipidaemia usually manifests as elevated triglycerides and cholesterol

Figure 1: Insulin signalling pathway

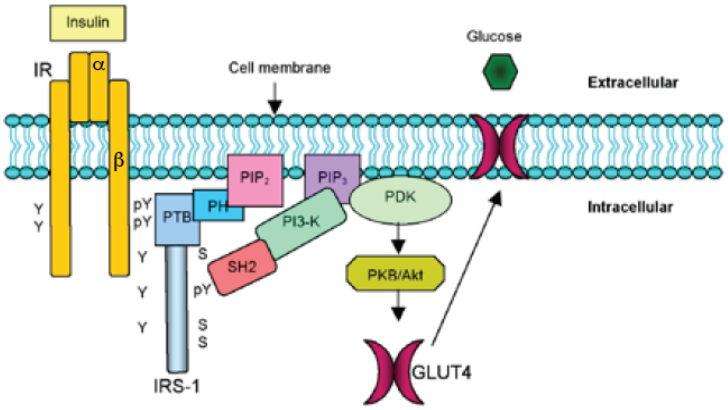

Insulin resistance and HIV protease inhibitors (HPIs)

The mechanism of insulin resistance induced by antiretroviral drugs is not well-understood. Insulin resistance occurs when normal insulin levels are inadequate to stimulate glucose uptake in the insulin signalling pathway in insulin-sensitive tissues such as liver, muscle and subcutaneous adipose tissue. The insulin resistance manifests as hyperinsulinaemia, hyperglycaemia and dyslipidaemia (hypertriglyceridaemia).

It has emerged that one class of the antiretroviral drugs, the HPIs, plays a critical role in inducing the side-effects. HPIs are potent competitive inhibitors of HIV aspartyl endopeptidase, an enzyme required for producing a mature HIV virion, such as saquinavir, indinavir, ritonavir, nelfinavir, amprenavir, lopinavir/ritonavir (Kaletra), fosamprenavir, atazanavir, tipranavir and darunavir.[16]

A clinical report revealed glucose intolerance and insulin resistance in HIV-positive patients treated with HPIs.[17] Moreover, the incidence of insulin resistance in HIV-positive patients is significantly higher in HPI-treated patients than in patients treated with NRTIs or NNRTIs,[18] even when one considers related factors such as demography and virology.[19] Furthermore, HPIs have been shown to induce insulin resistance in seronegative patients and in animal models,[20-23] implying a clear link between HPI use and insulin resistance. However, the underlying precise mechanisms have yet to be elucidated. The purpose of this review is to analyse the possible molecular mechanisms for the effects of the HPIs on the insulin signalling pathway.

HPIs impair the distal steps in the insulin signalling pathway

Initial studies examined the effects of antiretrovirals on both glucose transport and translocation of the intracellular glucose transporter, GLUT4. An early study of insulin resistance induced by HPIs demonstrated that the drug inhibits glucose uptake (measured by radioactive glucose uptake) without affecting GLUT4 translocation (assessed by immunostaining).[24] GLUT4 is considered to be the major transporter responsible for insulin-stimulated glucose disposal into adipose tissue, cardiac and skeletal muscle, and plays a critical role in whole-body glucose homeostasis.[25] In this particular study, it was reported that 3T3-L1 adipocytes treated with indinavir, an HPI, at 100 µM for 4 h displayed decreased glucose uptake. There was no evidence for any effects on early insulin signalling events such as insulin receptor and IRS-1 tyrosine phosphorylation or on the translocation of GLUT4 to the cell surface.[24] In addition, indinavir did not have any effect on the activation of PKB/Akt. The effect of indinavir on glucose uptake was rapid and did not change even when indinavir was added 20 min after insulin stimulation indicating that the drug acted at a site distal to GLUT4 translocation.[24] Similar effects on glucose uptake were reported in rats and in HIV-negative patients treated with HPIs.[20,21,23]

However, in a subsequent study, it was reported that prolonged treatment (18 h) of 3T3-L1 adipocytes with nelfinavir, an HPI, at plasma concentrations (10 µM) impaired both GLUT4 translocation and glucose uptake.[26] Nelfinavir appeared to induce insulin resistance by inhibiting the stimulation of PKB/Akt serine 473 phosphorylation without any effect on the tyrosine phosphorylation of IRS-1. Nelfinavir also decreased expression of the lipolysis regulator, perilipin.[26] These effects of nelfinavir to impair PKB/Akt activation, GLUT4 translocation and glucose uptake were confirmed in a subsequent study. In this particular study, nelfinavir at 30 µM induced insulin resistance in 3T3-L1 adipocytes by inhibiting recruitment and activation of PI3-K, leading to impaired GLUT4 translocation and thus preventing insulin-stimulated glucose uptake.[27,28] These effects were not accompanied by changes in insulin receptor expression or insulin receptor tyrosine phosphorylation.[27] More recently, the effects of nelfinavir were studied in 3T3-L1 adipocytes expressing a GLUT4-green fluorescent protein (GFP) fusion protein to analyse transporter movement. Fusion of GLUT4 to GFP allows real time visualisation of glucose transporter movement under a fluorescent microscope. The authors of this study maintained that PKB/Akt activation was affected (i.e. inhibited) after insulin-stimulated generation of PIP_3, leading to impaired GLUT4 translocation because even when cellular levels of PIP_3 were raised artificially by using a constitutively activated PI3-K, thus bypassing the requirement for normal insulin stimulation, nelfinavir inhibited GLUT4 translocation.[29] When a membrane targeted constitutively active PKB is expressed, in the presence of nelfinavir, PKB is phosphorylated normally by PDK and is able to induce GLUT4 translocation. The authors concluded that nelfinavir interfered with the "sensing" of PIP_3 by PKB/Akt or the PIP_3-induced translocation of PKB/Akt based on the fact that even in cells expressing a constitutively activated PI3-K, nelfinavir was still able to block the activation of PKB/Akt.

University of Cape Town

Taken together, the results imply that nelfinavir has more profound effects on insulin signalling than indinavir. Indinavir inhibits glucose transport without affecting translocation, while nelfinavir inhibits both translocation and uptake, possibly at the level of PKB/Akt. The differences in the studies reviewed above may therefore have arisen from differences in the HPIs used or from the experimental methodology used to quantify GLUT4 translocation, which is often semi-quantitative and subjective, as compared to the measurement of glucose uptake.

The notion that nelfinavir has more profound effects is supported by studies on adipocytes that show that it induces oxidative stress.[30] Oxidative stress induces insulin resistance by activating serine kinases that lead to serine phosphorylation of IRS-1 and also by disrupting the subcellular distribution of PI3 kinase (i.e. decreased membrane localisation). This would in turn lead to decreased tyrosine phosphorylation of IRS-1 and consequently reduced PKB/Akt activation and hence decreased GLUT4 translocation.

Do HPIs impair the proximal steps of the insulin signalling pathway?

The studies reviewed above suggest that the effects of HPI occur downstream in the insulin signalling pathway in 3T3-L1 adipocytes, in rats and humans,[21,22,24] possibly at the level of PKB/Akt activation and beyond. However, there is evidence that HPIs possibly act at a more proximal level of the insulin signalling pathway. For example, in HepG2 hepatoma cells exposed to 100 μM indinavir for 48 h there was a 30–60% decrease in the insulin-stimulated tyrosine phosphorylation of IRS-1 and this was associated with decreased PI3-K activation and no change in insulin binding.[31] In a subsequent study, it was found that ritonavir at 10 μM decreased insulin receptor numbers in 3T3-L1 pre-adipocytes without any effect on binding affinity. This was accompanied by decreased IRS-1 tyrosine phosphorylation in response to insulin. [32]

A more recent study suggested that lopinavir, an HPI, inhibited IRS-1 phosphorylation in human adipocytes and resulted in a concentration-dependent decrease in glucose uptake.[33] It was proposed that the drug decreased the phosphorylation of IRS-1 directly since there was no effect observed on the phosphorylation of the insulin receptor β-subunit i.e. the decrease in IRS-1 phosphorylation was primary, rather than secondary to a change in receptor activation. Taken together, these data imply that some of the HPIs may impair the earlier steps in the insulin signalling pathway.

The differences in the studies reviewed above are likely to be due to differences in experimental design, cell types, types of HPIs used and durations of exposure. It is possible that, differences between the various drugs on protein and gene expression in cells are more likely to be unmasked after prolonged exposure, hence resulting in different final observations in the various studies. These differences will be exaggerated further when different cell lines are used. Overall, however, it appears that the final common pathway is an effect on glucose transport and that all of the HPIs reviewed above display some effect at one or more steps in the insulin signalling pathway.

Other factors involved in the insulin resistance induced by HPIs: oxidative stress, adapter proteins and adipokines

As mentioned above, some of the HPIs may increase oxidative stress.[30,34] HPIs may also alter chemokines, cytokines or adiponectin production in human adipocytes and macrophages.[35] The induction of oxidative stress is known to cause insulin resistance.

Changes in the expression of regulatory proteins could also potentially explain the effects of HPIs. Suppressor of cytokine signalling-1 (SOCS-1) is one example of a known inducer of insulin resistance. SOCS-1 and the related protein suppressor of cytokine signalling-3 (SOCS-3) bind to the insulin receptor following activation and impair the ability of the insulin receptor to phosphorylate downstream substrates. In addition, SOCS proteins are able to target IRS-1 for degradation. In essence, increased expression of SOCS proteins will interfere with the signalling functions of the insulin receptor and IRS-1. In addition to the previously described effects on the signalling proteins in the early part of the insulin signalling pathway, it has also been shown that the expression of SOCS-1 was increased in rats exposed to indinavir for seven weeks.[36] In this study, chronic HPI exposure induced SOCS-1 expression in muscle, liver and adipose tissue. This was associated with an increase in the expression of tumour necrosis factor-α (TNF-α) and the downstream target sterol regulatory element-binding protein-1 (SREBP-1) along with decreased expression of insulin receptor substrate-2 (IRS-2). IRS-2 is another major substrate that mediates insulin action in the insulin signalling pathway.

TNF-α induces insulin resistance primarily by affecting the function of IRS proteins. It can also induce the expression of SOCS-1. As discussed above, the association of increased TNF-α in animals exposed to indinavir may have arisen from the induction by TNF-α or by another unknown mechanism.

In relation to IRS-1, TNF-α induces the activation of several serine kinases (c-Jun N-terminal kinase (JNK); inhibitor κB kinase (IKK)) leading to increased serine phosphorylation of IRS-1. Increased serine phosphorylation of IRS-1 converts it into an inhibitory protein of the insulin receptor, leading to insulin resistance. Therefore, in summary, TNF-α can induce insulin resistance by affecting IRS-1 function directly or by inducing the expression of SOCS-1.

HPIs have also been found to alter adipose tissue gene expression *in vivo*.[37] The mRNA expression levels of the CCAAT/enhancer-binding protein α, leptin, and adiponectin in HIV-positive patients treated with HPIs have been found to be significantly lower than in HPI-naive patients.[37] Since adiponectin levels are important in the whole body response to insulin, a lowering of adiponectin would affect glucose homeostasis adversely and oppose the actions of insulin.

Summary (see Table I)

The individual differences in the effects of HPIs observed in the different studies may be attributed to the different HPI drugs used in the studies and in experimental design. HPIs induce different effects on different cell lines.[38,39] Additionally, several HPIs demonstrate different results *in vitro* and *in vivo*.[40] The most consistent phenomenon observed has been the effect on glucose uptake, the most obvious physiological end result of insulin. Whether these phenomena arise primarily from effects on early steps in the insulin signalling pathway is not entirely clear. Recent studies[29,33] support the idea that HPIs affect a more proximal level of the insulin signalling pathway, in particular tyrosine phosphorylation of the insulin receptor and its substrate, IRS-1. This then leads to the secondary inhibition of downstream events in the insulin signalling

University of Cape Town

Table I: Summary of the effect of HPIs in the insulin signalling pathway

HPI Effects	References	Drug	Experimental model	Observations
1) The distal steps in the insulin signalling pathway	Murata et al (2000)[24]	Indinavir (100 µM) for 4 h	3T3-L1 adipocytes	Decreased glucose uptake
	Rudich et al (2001)[26]	Nelfinavir (10 µM) for 18 h	3T3-L1 adipocytes	Impaired GLUT4 translocation and glucose uptake by inhibiting stimulation of PKB serine 473 phosphorylation
	Ben-Romano et al (2004)[27] and Rudich et al (2005)[28]	Nelfinavir (30 µM) for 18 h	3T3-L1 adipocytes	Inhibited recruitment and activation of PI3-K, impaired GLUT4 translocation and glucose uptake
	Kachko et al (2009)[29]	Nelfinavir (30 µM) for 18 h	3T3-L1 adipocytes used a GLUT4-GFP chimeric construct	Interfered with the sensing of PIP3 by PKB/Akt and inhibited GLUT4 translocation
2) The proximal steps in the insulin signalling pathway	Schutt et al (2000)[31]	Indinavir (100 µM) for 48 h	HepG2 hepatoma cells	Decreased tyrosine phosphorylation of IRS-1 and PI3-K activation
	Cammalleri and Germinario (2003)32	Ritonavir (10 µM) for 11 days	3T3-L1 pre-adipocytes	Decreased insulin receptor expression and tyrosine phosphorylation of IRS-1
	Djedaini et al (2009)[33]	Lopinavir (10 µg/ml) for 48 h	Human adipocytes	Decreased tyrosine phosphorylation of IRS-1 and glucose uptake
3) Other factors	Ben-Romano et al (2006)[30]	Nelfinavir (30 µM) for 18 h	3T3-L1 adipocytes	Induced oxidative stress
	Lagathu et al (2007)[35]	Indinavir, amprenavir, lopinavir, ritonavir (10 µmol/l), atazanavir (4 µmol/l), nelfinavir (5 µmol/l) for 24 and 48 h	Human adipocytes and macrophages	Induced oxidative stress and altered chemokines, cytokines or adiponectin production
	Carper et al (2008)[36]	Indinavir (20 µM) for 7 weeks	Rats	Increased SOCS-1, TNF-α and SREBP-1 expression
	Chapparo et al (2005)[37]	Indinavir, nelfinavir, liponavir/ritonavir, ritonavir and saquinavir	Human adipose tissue biopsies	Altered adipose tissue gene expression

cascade, in particular, extracellular glucose uptake by GLUT4. With the exception of the studies cited, there is a paucity of studies that have examined the proximal steps in the insulin receptor signalling cascade, particularly at the early steps in the activation of the insulin receptor tyrosine kinase.

Conclusion

Insulin resistance is a major complication of treatment with antiretroviral drugs. With the increased longevity of patients following antiretroviral treatment, the incidence of these complications is likely to increase. An understanding of the molecular basis of these complications could lead to the development of diagnostic tests to predict the onset of the side-effects or alternatively to rational drug design. In conclusion, the studies reviewed above suggest that the manifestation of insulin resistance due to HPI treatment is likely to be associated with dysregulation of several cellular factors, specifically in the early steps in the pathway of insulin receptor signalling, in addition to alterations in GLUT4 transporter function. Alternatively, the perturbation of glucose transport may be secondary to inhibition of critical steps early in the signalling pathway.

References

1. Beyrer C. HIV epidemiology update and transmission factors: risks and risk contexts –16th International AIDS Conference epidemiology plenary. Clin Infect Dis 2007;44(7):981–7.
2. Weiss RA. Special anniversary review: twenty-five years of human immunodeficiency virus research: successes and challenges. Clin Exp Immunol 2008;152(2):201–10.
3. Larmarange J. [HIV prevalence in sub-Saharan Africa: background of an estimation]. Med Sci (Paris) 2009;25(1):87–92.
4. Hammer SM, Squires KE, Hughes MD, et al. A controlled trial of two nucleoside analogues plus indinavir in persons with human immunodeficiency virus infection and CD4 cell counts of 200 per cubic millimeter or less. AIDS Clinical Trials Group 320 Study Team. N Engl J Med 1997;337(11):725–33.
5. Placenti FJ. An update and review of antiretroviral therapy. Pharmacotherapy 2006;26(8):1111–33.
6. Bernasconi E. Metabolic effects of protease inhibitor therapy. AIDS Read 1999;9(4):254–6, 259–60, 266–9.
7. Esser S, Helbig D, Hillen U, Dissemond J, Grabbe S. Side effects of HIV therapy. J Dtsch Dermatol Ges 2007;5(9):745–54.
8. Friedl AC, Attenhofer Jost CH, Schalcher C, et al. Acceleration of confirmed coronary artery disease among HIV-infected patients on potent antiretroviral therapy. Aids 2000;14(17):2790–2.
9. Bozkurt B. Cardiovascular toxicity with highly active antiretroviral therapy: review of clinical studies. Cardiovasc Toxicol 2004;4(3):243–60.
10. Florescu D, Kotler DP. Insulin resistance, glucose intolerance and diabetes mellitus in HIV-infected patients. Antivir Ther 2007;12(2):149–62.
11. Stein JH. Cardiovascular risks of antiretroviral therapy. N Engl J Med. 2007;356(17):1773–5.
12. Carr A. HIV protease inhibitor-related lipodystrophy syndrome. Clin Infect Dis 2000;30 Suppl 2:S135–42.
13. Hui DY. Effects of HIV protease inhibitor therapy on lipid metabolism. Prog Lipid Res 2003;42(2):81–92.
14. Gougeon ML, Penicaud L, Fromenty B, Leclercq P, Viard JP, Capeau J. Adipocytes targets and actors in the pathogenesis of HIV-associated lipodystrophy and metabolic alterations. Antivir Ther 2004;9(2):161–77.
15. Youngren JF. Regulation of insulin receptor function. Cell Mol Life Sci 2007;64(7–8):873–91.
16. Temesgen Z, Warnke D, Kasten MJ. Current status of antiretroviral therapy. Expert Opin Pharmacother 2006;7(12):1541–54.
17. Monier PL, Wilcox R. Metabolic complications associated with the use of highly active antiretroviral therapy in HIV-1-infected adults. Am J Med Sci 2004;328(1):48–56.
18. Woerle HJ, Mariuz PR, Meyer C, et al. Mechanisms for the deterioration in glucose tolerance associated with HIV protease inhibitor regimens. Diabetes 2003;52(4):918–25.
19. Palella FJ, Jr, Delaney KM, Moorman AC, et al. Declining morbidity and mortality among patients with advanced human immunodeficiency virus infection. HIV Outpatient Study Investigators. N Engl J Med 1998;338(13):853–60.
20. Noor MA, Lo JC, Mulligan K, et al. Metabolic effects of indinavir in healthy HIV-seronegative men. Aids 2001;15(7):F11–18.
21. Hruz PW, Murata H, Qiu H, Mueckler M. Indinavir induces acute and reversible peripheral insulin resistance in rats. Diabetes 2002;51(4):937–42.
22. Noor MA, Seneviratne T, Aweeka FT, et al. Indinavir acutely inhibits insulin-stimulated glucose disposal in humans: a randomized, placebo-controlled study. Aids 2002;16(5):F1–8.
23. Lee GA, Rao M, Mulligan K, et al. Effects of ritonavir and amprenavir on insulin sensitivity in healthy volunteers. Aids 2007;21(16):2183–90.
24. Murata H, Hruz PW, Mueckler M. The mechanism of insulin resistance caused by HIV protease inhibitor therapy. J Biol Chem 2000;275(27):20251–4.
25. Mueckler M. Insulin resistance and the disruption of Glut4 trafficking in skeletal muscle. J Clin Invest 2001;107(10):1211–13.
26. Rudich A, Vanounou S, Riesenberg K, et al. The HIV protease inhibitor nelfinavir induces insulin resistance and increases basal lipolysis in 3T3-L1 adipocytes. Diabetes 2001;50(6):1425–31.
27. Ben-Romano R, Rudich A, Tirosh A, et al. Nelfinavir-induced insulin resistance is associated with impaired plasma membrane recruitment of the PI 3-kinase effectors Akt/PKB and PKC-zeta. Diabetologia 2004;47(6):1107–17.
28. Rudich A, Ben-Romano R, Etzion S, Bashan N. Cellular mechanisms of insulin resistance, lipodystrophy and atherosclerosis induced by HIV protease inhibitors. Acta Physiol Scand 2005;183(1):75–88.
29. Kachko I, Maissel A, Mazor L, et al. Postreceptoral adipocyte insulin resistance induced by nelfinavir is caused by insensitivity of PKB/Akt to phosphatidylinositol-3,4,5-trisphosphate. Endocrinology 2009;150(6):2618–26.
30. Ben-Romano R, Rudich A, Etzion S, et al. Nelfinavir induces adipocyte insulin resistance through the induction of oxidative stress: differential protective effect of antioxidant agents. Antivir Ther 2006;11(8):1051–60.
31. Schutt M, Meier M, Meyer M, Klein J, Aries SP, Klein HH. The HIV-1 protease inhibitor indinavir impairs insulin signalling in HepG2 hepatoma cells. Diabetologia 2000;43(9):1145–8.
32. Cammalleri C, Germinario RJ. The effects of protease inhibitors on basal and insulin-stimulated lipid metabolism, insulin binding, and signaling. J Lipid Res 2003;44(1):103–8.
33. Djedaini M, Peraldi P, Drici MD, et al. Lopinavir co-induces insulin resistance and ER stress in human adipocytes. Biochem Biophys Res Commun 2009;386(1):96–100.
34. Chandra S, Mondal D, Agrawal KC. HIV-1 protease inhibitor induced oxidative stress suppresses glucose stimulated insulin release: protection with thymoquinone. Exp Biol Med (Maywood) 2009;234(4):442–53.
35. Lagathu C, Eustace B, Prot M, et al. Some HIV antiretrovirals increase oxidative stress and alter chemokine, cytokine or adiponectin production in human adipocytes and macrophages. Antivir Ther 2007;12(4):489–500.
36. Carper MJ, Cade WT, Cam M, et al. HIV-protease inhibitors induce expression of suppressor of cytokine signaling-1 in insulin-sensitive tissues and promote insulin resistance and type 2 diabetes mellitus. Am J Physiol Endocrinol Metab 2008;294(3):E558–67.
37. Chaparro J, Reeds DN, Wen W, et al. Alterations in thigh subcutaneous adipose tissue gene expression in protease inhibitor-based highly active antiretroviral therapy. Metabolism 2005;54(5):561–67.
38. Ben-Romano R, Rudich A, Torok D, et al. Agent and cell-type specificity in the induction of insulin resistance by HIV protease inhibitors. Aids 2003;17(1):23–32.
39. Kovsan J, Osnis A, Maissel A, et al. Depot-specific adipocyte cell lines reveal differential drug-induced responses of white adipocytes – relevance for partial lipodystrophy. Am J Physiol Endocrinol Metab 2009;296(2):E315–22.
40. Noor MA, Flint OP, Maa JF, Parker RA. Effects of atazanavir/ritonavir and lopinavir/ritonavir on glucose uptake and insulin sensitivity: demonstrable differences in vitro and clinically. Aids 2006;20(14):1813–21.

University Of Cape Town

Abstract 1: 1st Medical Research Centre (MRC) Research Day, Cape Town, South Africa (18th October 2007)

Inhibition of the insulin receptor kinase by antiretroviral protease inhibitors

Wan Iryani Wan Ismail and Tahir S. Pillay

Division of Chemical Pathology, Department of Clinical Laboratory Sciences, Faculty of Health Sciences, University of Cape Town, South Africa

Human immunodeficiency virus (HIV) protease inhibitors (HPIs) are potent antiretroviral agents. Recently, a substantial number of clinical and epidemiological studies have shown that HPIs play a major role in inducing insulin resistance and lipodystrophy in highly active antiretroviral therapy (HAART)-treated patients. In this study, we assessed the effect of saquinavir on the insulin signalling pathway in Chinese Hamster Ovary (CHO) cells and differentiated 3T3-L1 adipocytes. A 17-h exposure to saquinavir resulted in impaired phosphorylation of the insulin receptor (IR) and insulin receptor substrate 1 (IRS-1) in CHO cells and 3T3-L1 adipocytes. A dose-dependent decrease in the phosphorylation of the IR and IRS-1 in CHO cells and 3T3-L1 adipocytes was observed with saquinavir (0.5-50 μM) following immunoblotting analysis using anti-phosphotyrosine antibody. In time-course studies, IR and IRS-1 phosphorylation in both cell lines declined slowly with increasing exposure to 50 μM of saquinavir over 17 hours. This study demonstrates that saquinavir induces insulin resistance in both CHO cells and 3T3-L1 adipocytes by inhibiting the early steps of the insulin signalling cascade.

Keywords: Saquinavir, CHO cells, 3T3-L1, Insulin Receptor, Insulin Receptor Substrate

University Of Cape Town

Abstract 2: 9th Annual Astra Zeneca Medical Research Day, University of Cape Town (UCT), Cape Town, South Africa (14th February 2008)

Effects of antiretroviral protease Inhibitors on the insulin receptor kinase *in vitro*

Wan Iryani Wan Ismail and Tahir S. Pillay

Division of Chemical Pathology, Department of Clinical Laboratory Sciences, Faculty of Health Sciences, University of Cape Town, South Africa

Human immunodeficiency virus (HIV) therapy using anti-retroviral protease inhibitors can increase lifetime of HIV infected patients. Unfortunately, the treatment has been reported to cause metabolic abnormalities such as insulin resistance, lipodystrohy, hyperglycemia, and type 2 diabetes. The molecular mechanisms of these side effects are still unknown and only small studies have been conducted to understand this pathway. In order to analyse the complications, cell culture study using Chinese Hamster Ovary transfected with high level of human insulin receptor (CHO-IR) cells and differentiated 3T3-L1 murine adipocytes were treated with various dose responses of saquinavir and indinavir for 16-h following immunoblotting analysis using anti-phosphotyrosine antibody. Saquinavir appeared to impair phosphorylation of the insulin receptor (IR) and insulin receptor substrate 1 (IRS-1) in CHO-IR cells and 3T3-L1 adipocytes at the basal level and insulin stimulation level. While indinavir inhibited the phosphorylation of the IR and IRS in CHO cells and 3T3-L1 adipocytes only at the basal level with the similar concentration. Saquinavir appeared to be more potent to cause the side effects compared to indinavir.

University Of Cape Town

Abstract 3: 43rd Society for Endocrinology, Metabolism and Diabetes of South Africa (SEMDSA) Meeting, Cape Town, South Africa (12-15th April 2008)

INHIBITION OF THE INSULIN RECEPTOR KINASE BY ANTIRETROVIRAL PROTEASE INHIBITORS

W. I. W. Ismail and T. S. Pillay

Division of Chemical Pathology, Department of Clinical Laboratory Sciences, Faculty of Health Sciences, University of Cape Town, Private Bag X3, Observatory, Cape Town, 7935

Human immunodeficiency virus protease inhibitors (HPIs) are potent antiretroviral agents. Unfortunately, prolonged use of the drugs has caused many complications among patients, including insulin resistance, lipodystrophy, hyperglycaemia, and type 2 diabetes mellitus. The molecular basis for these drug-induced metabolic syndromes is still unknown. Few studies have addressed the molecular pathways involved. Thus, this study was designed to elucidate how HPIs may affect the insulin signalling pathway in Chinese Hamster Ovary cells transfected with high levels of human insulin receptor (CHO-IR cells) and in differentiated 3T3-L1 murine adipocytes. We have also examined the effects of these drugs on lipoprotein lipase in the adipocytes. Cells were treated with a range of doses of HPIs (saquinavir and indinavir) for 16 h and then stimulated with insulin. Insulin-stimulated tyrosine phosphorylation was analyzed by immunoblotting with anti-phosphotyrosine antibody. Saquinavir (30-40 μM) displayed potent inhibition of the tyrosine phosphorylation of the insulin receptor □-subunit and IRS proteins in both cell types. In contrast, indinavir (60 μM) had mild effects on insulin signalling. Thus both drugs display differences in their effects on insulin signalling and this may influence the propensity to cause the side effect of insulin resistance seen in patients on the drugs. We postulate that the inhibition of the insulin receptor kinase may occur because of direct effects on the kinase domain or because of changes in the level or activity of tyrosine phosphatases.

University of Cape Town

Abstract 4: 3rd Faculty of Health Sciences Research Day, UCT, Cape Town, South Africa (3rd September 2008)

INHIBITION OF THE INSULIN RECEPTOR KINASE BY ANTIRETROVIRAL PROTEASE INHIBITORS

Wan Iryani Wan Ismail, Tahir Pillay

Division of Chemical Pathology, Department of Clinical Laboratory Sciences, Faculty of Health Sciences, University of Cape Town.

Human immunodeficiency virus protease inhibitors (HPIs) are potent antiretroviral agents. Unfortunately, prolonged use of these drugs causes many complications among patients, including insulin resistance, lipodystrophy, hyperglycaemia, and type 2 diabetes mellitus and the incidence of these is increasing as patients with HIV infection and on treatment experience prolonged lifespans. The molecular basis for these drug-induced metabolic syndromes is still unknown and few studies have attempted to address this. In this study we have sought to elucidate how HPIs may affect the insulin signalling pathway in Chinese Hamster Ovary cells transfected with high levels of human insulin receptor (CHO-IR cells) and in differentiated 3T3-L1 murine adipocytes. We have also examined the effects of these drugs on lipoprotein lipase (LPL) in the adipocytes as LPL levels have been found altered in patients treated with HPIs who later develop lipodystrophy. We investigated the effects of HPIs on cells were treated with saquinavir and indinavir for 16 h and then stimulated with insulin. Insulin-stimulated tyrosine phosphorylation was analyzed by immunoblotting with anti-phosphotyrosine antibody. We found that saquinavir (30-40 μM) displayed potent inhibition of the tyrosine phosphorylation of the insulin receptor □-subunit and IRS proteins in both cell types. Indinavir (50 μM) had similar effects on insulin signalling but with a different dose-response profile. Thus both drugs display potency differences in their effects on insulin signalling and this may influence the propensity to cause the side effect of insulin resistance seen in patients. The inhibition of insulin signalling appears to be at a proximal level and involves a direct effect on the insulin receptor. We postulated that the inhibition of the insulin receptor kinase may occur because of changes in the level or activity of tyrosine phosphatases and suppressor of cytokine signaling 1 (SOCS-1). However, we found that PTP1B and anti-SOCS-1 levels were not altered. We conclude that the effects of HPIs to cause insulin resistance does not involve PTP1B or SOCS-1 protein but may involve other regulatory proteins.

University of Cape Town

Abstract 5: 2nd MRC Research Day, Cape Town, South Africa (16-17th October 2008)

MOLECULAR BASIS OF INSULIN RESISTANCE INDUCED BY ANTIRETROVIRAL PROTEASE INHIBITORS

WIW Ismail, TS Pillay

Division of Chemical Pathology, Department of Clinical Laboratory Sciences, Faculty of Health Sciences, University of Cape Town, South Africa

BACKGROUND

Prolonged use of human immunodeficiency virus protease inhibitors (HPIs) has been reported to cause insulin resistance which is accompanied by dyslipidaemia, lipodystrophy, and atherosclerosis in patients. The incidence of these complications is increasing in patients as antiretroviral treatment is used increasingly. The mechanism of these adverse effects is not fully understood. Therefore, this study has attempted to identify possible mechanisms.

METHODS

Chinese hamster ovary cells transfected with high levels of human insulin receptor (CHO-IR cells) and differentiated 3T3-L1 murine adipocytes were serum-starved and treated with several concentrations of saquinavir or indinavir for 16 h followed by insulin stimulation for 5 min. The cells were lysed for immunoblotting using anti-phosphotyrosine antibody, anti-insulin receptor antibody, anti-protein tyrosine phosphatase 1B (PTP1B), and anti-suppressor of cytokine signaling 1 antibody (SOCS-1).

RESULTS

We found that saquinavir (30-40 μM) displayed potent inhibition of the tyrosine phosphorylation of the insulin receptor β-subunit and IRS proteins in both cell types. Indinavir (50 μM) had similar effects on insulin signalling but with a different dose-response profile. Thus both drugs display potency differences in their effects on insulin signalling and this may influence the propensity to cause the side effect of insulin resistance seen in patients. The inhibition of insulin signalling appears to be at a proximal level and involves a direct effect on the insulin receptor. We postulated that the inhibition of the insulin receptor kinase may occur because of changes in the level or activity of tyrosine phosphatases and SOCS-1. However, we found that PTP1B and anti-SOCS-1 levels were not altered.

CONCLUSION

We conclude that the effects of HPIs to cause insulin resistance do not involve PTP1B or SOCS-1 protein but may involve other regulatory proteins in the insulin signalling pathway.

Key words: CHO-IR cells, 3T3-L1 adipocytes, saquinavir, indinavir, phosphorylation, insulin receptor kinase

University Of Cape Town

Abstract 6: 10th International Workshop Adverse Drug Reactions and Lipodystrophy in HIV, London, United Kingdom (6-8th November 2008)

Inhibition of the Insulin Receptor Kinase by Antiretroviral Protease Inhibitors

WIW Ismail, TS Pillay

Division of Chemical Pathology, Department of Clinical Laboratory Sciences, Faculty of Health Sciences, University of Cape Town, South Africa

Human immunodeficiency virus protease inhibitors (HPIs) are potent antiretroviral agents. Unfortunately, prolonged use of these drugs causes many complications among patients, including insulin resistance, lipodystrophy, hyperglycaemia, and type 2 diabetes mellitus and the incidence of these is increasing as patients with HIV infection and on treatment experience prolonged lifespans. The molecular basis for these drug-induced metabolic syndromes is still unknown and few studies have attempted to address this.

Objectives: In this study we have sought to elucidate how HPIs may affect the insulin signalling pathway in Chinese Hamster Ovary cells transfected with high levels of human insulin receptor (CHO-IR cells) and in differentiated 3T3-L1 murine adipocytes. We have also examined the effects of these drugs on lipoprotein lipase (LPL) in the adipocytes as LPL levels have been found altered in patients treated with HPIs who later develop lipodystrophy.

Methods: We investigated the effects of HPIs on cells were treated with saquinavir and indinavir for 16 h and then stimulated with insulin. Insulin-stimulated tyrosine phosphorylation was analyzed by immunoblotting with anti-phosphotyrosine antibody.

Results: We found that saquinavir (30-40 μM) displayed potent inhibition of the tyrosine phosphorylation of the insulin receptor β-subunit and IRS proteins in both cell types. Indinavir (50 μM) had similar effects on insulin signalling but with a different dose-response profile. Thus both drugs display potency differences in their effects on insulin signalling and this may influence the propensity to cause the side effect of insulin resistance seen in patients. The inhibition of insulin signalling appears to be at a proximal level and involves a direct effect on the insulin receptor. We postulated that the inhibition of the insulin receptor kinase may occur because of changes in the level or activity of tyrosine phosphatases and suppressor of cytokine signaling 1 (SOCS-1). However, we found that PTP1B and anti-SOCS-1 levels were not altered.

Conclusion: We conclude that the effects of HPIs to cause insulin resistance does not involve PTP1B or SOCS-1 protein but may involve other regulatory proteins.

University of Cape Town

Abstract 7: 2nd Pfizer-College of Health Sciences National Young Health Scientists Research Symposium, University of Kwazulu-Natal, Durban, South Africa (21st October 2009)

HIV PROTEASE INHIBITORS INDUCE INSULIN RESISTANCE VIA THE NFκB PATHWAY

Ismail W.I.W., King J.A. and Pillay T.S.

Division of Chemical Pathology, University of Cape Town and National Health Laboratory Service, Groote Schuur Hospital, Cape Town, 7925, South Africa

Aim

The aim of this study was to elucidate the molecular basis of insulin resistance induced by HIV protease inhibitors (HPIs) using Chinese hamster ovary cells transfected with high levels of human insulin receptor (CHO-IR).

Methods

CHO-IR cells were treated with indinavir for 16 h followed by insulin stimulation for 5 min, and then lysed and analysed by immunoblotting using antibodies against phosphotyrosine, insulin receptor β-subunit, protein tyrosine phosphatase 1B (PTP1B), suppressor of cytokines signalling-1,-3 (SOCS-1,-3), insulin receptor substrate 1 (IRS-1), phosphoIRS-1 serine residue 307 (S307), Src homology 2B (SH2B) and actin. Cells were also pre-treated with sodium salicylate (NaSal) (5mM) for 1h to inhibit nuclear factor kappa B (NFκB).

Results

Indinavir inhibited tyrosine phosphorylation of the insulin receptor β-subunit and increased phosphorylation of IRS-1 on S307. PTP1B, SOCS-1,3 and SH2B levels were not altered. NaSal treatment blocked the effects of indinavir on the tyrosine phosphorylation of the insulin receptor and phosphorylation of IRS-1 at S307.

Discussion and Conclusion

Sodium salicylate inhibits the upstream activator of NFκB, the IκB kinase β (IKKβ), resulting in decreased phosphorylation of IRS-1 on S307. Serine phosphorylated IRS-1 acts to inhibit phosphorylation of the insulin receptor. We show for the first time that blockade of IKKβ by NaSal abrogates the effect of indinavir on the tyrosine phosphorylation of the insulin receptor by decreasing phosphoIRS-1 S307. We conclude, therefore, that protease inhibitors act via the NFκB pathway to induce insulin resistance *in vivo*. Salicylates may provide a novel therapy for HIV protease inhibitor-induced lipodystrophy.

University Of Cape Town